

## 6 DISRUPTIVE CONSEQUENCE ANALYSIS<sup>1</sup>

### 6.1 Overall Approaches for Treating Consequences of Disruptive Events

The performance of the undisturbed geologic repository may be modified by a number of disruptive events, as discussed in Chapter 3. Those considered in Iterative Performance Assessment (IPA) Phase 2 were: climate change (pluvial scenario); human intrusion (including exploratory drilling—drilling scenario); seismic shaking (seismic scenario); and magmatic eruption (volcanic scenario). These events, individually and in combination, have the potential to alter repository performance in several different ways. They may result in direct releases of radionuclides to the surface in the form of contaminated drill cuttings, or indirect releases, by way of the liquid or gas pathway, augmented by premature failure of waste packages.<sup>2</sup>

The approach employed in developing the disruptive models was to use the undisturbed system models, or “base case,” to the extent practicable, to assume a “reference biosphere”<sup>3</sup> for computing doses, and to use the least aggressive approach feasible. This involved generally altering the input data to the computational modules to simulate a disrupted condition (e.g., earlier failure of the waste package to simulated drilling, seismic or volcanic failures, or increased infiltration to simulate a pluvial climate). However, there were several modules developed specifically to simulate the time and extent of the drilling, seismic, and volcanic failures.

Each scenario class is denoted by a four-tuple ( $a_1 a_2 a_3 a_4$ ), with  $a_1, 2, 3, 4$  corresponding to the letter  $c, s, d$  and  $v$ , respectively, referring to the four disruptive events, or the letter  $o$ , to denote that the particular disruptive event is absent. There are a maximum of  $2^4 = 16$  distinct scenario classes that are possible. For example, the base case is denoted by  $oooo$ , and the fully disturbed by  $csdv$ . In

addition to the base case ( $o$ ), the four categories of fundamental causative events from which scenario classes are formed for Phase 2 are: climate change ( $c$ ); drilling ( $d$ ); seismic ( $s$ ); and volcanic ( $v$ ).

- Climate change is represented by change in the infiltration rate at the surface of the mountain and in the height of the water table. The infiltration rate is treated as a sampled parameter, where its value is determined using Latin Hypercube Sampling (LHS) (described in Section 2.1.3). The height of the water table is increased by 100 meters, compared with the base case in the climate scenario model. Climate change can only indirectly affect release of radionuclides from the repository.
- Human intrusion into the repository is considered to occur by exploratory drilling. Drilling is considered to cause both a direct and indirect release of radionuclides to the surface. Indirect release is caused by drilling-initiated failure of waste packages, which determines the source term. In computing the direct release of radionuclides from drilling, removal of radionuclides from the engineered barrier system (EBS) and rock column, by liquid and gaseous pathways, up to the time of drilling, are taken into account.
- Seismic events are assumed only to lead to premature failure of waste packages, affecting only indirectly the release of radionuclides from the repository. The model does not allow the alteration of site hydraulic properties, because of fault movement along the linear segment representing the fault. Because there are numerous faults and fractures intersecting the repository perimeter and its surroundings, it is expected that movement along existing faults will change the hydraulic characteristics of the site to a minimal degree.
- Magmatism is modeled as both intrusive and extrusive magmatic events. Intrusive magmatism is modeled as a linear dike in the plane of the repository and results in an indirect release of radionuclides. Extrusive magmatism is modeled as a volcanic eruption of ash

<sup>1</sup>The figures shown in this chapter present the results from a demonstration of staff capability to review a performance assessment. These figures, like the demonstration, are limited by the use of many simplifying assumptions and sparse data.

<sup>2</sup>The term “waste package” is used here synonymously with “container” and “canister.”

<sup>3</sup>Defined in Section 7.2.1.

## 6. Disruptive Consequences

flow extending from the basement. This event is assumed to result in a direct release of radionuclides. Coupling among magmatism and other release mechanisms are not considered. For example, the removal of radionuclides from the EBS and rock column by magmatic events is not taken into account in computing the release of radionuclides by liquid and gaseous pathways, and vice versa.

The models of disruptive events for early failure of the waste packages work in conjunction with *SOTEC* (Source Term Code), described in Chapter 5 (and in Sagar *et al.* (1992)). *SOTEC* considers only one representative waste package per repository sub-area, but is invoked three times to include: (1) initial failures (e.g., manufacturing defects); (2) failures from corrosion; and (3) failures by scenarios (i.e., drilling, seismic, or volcanism). For scenario classes with drilling-only (*oodo*) or drilling combined with pluvial climate (*codoo*), a direct hit from drilling will fail only a single waste package within the repository sub-area (unless it has already failed from corrosion). However the version of *SOTEC* used in the Phase 2 analyses cannot distinguish between types of scenario failures, so the analysis incorporates the most conservative assumption about the number of failed waste packages and the time of failures: the number of failures is the sum of the failures from drilling, seismicity, and volcanism, but the failure time is the shortest of the three failure times.

In IPA Phase 2, the consequences from disruptive events are treated by adjusting submodel parameters, introducing LHS parameters, or through additional dependent or independent calculations. A summary of the disruptive events, the names of the parameters, and their respective release modes is presented in Table 6-1. The LHS parameters (including those associated with the base case) are itemized in Appendix A.

The choice of LHS parameters was determined by the individual investigators responsible for the disruptive scenario modules, based where available from data on Yucca Mountain site or similar rocks. Parameter choices are discussed further in individual sections and in Appendix A. A detailed description of methods for computing consequences of disruptive scenarios is provided in the following sections.

## 6.2 Treatment of Climate

The climate at Yucca Mountain for the past approximately 50,000 years was assumed to characterize future climates at the proposed repository site. Variation in precipitation and temperature in the Yucca Mountain vicinity was no more than a few degrees Celsius ( $^{\circ}\text{C}$ ) decrease in temperature, accompanied by an up to 40 percent higher than present (ca. 150 millimeters annually) precipitation. To ensure a conservative analysis in IPA Phase 2, pluvial scenarios were incorporated by assuming an increase in infiltration from the possible wetter climatic conditions associated with likely cooler temperatures in the next 10,000 years. The conservative increase in infiltration was modeled by assuming a higher range for infiltration (5.0 to 10.0 millimeters/year in future scenarios, versus 0.01 to 5.0 millimeters/year for the base case (*oooo*)). Associated with the increase in infiltration was a rise of 100 meters in the water table, resulting in a decrease in the thickness of the unsaturated zone. The increased infiltration values and associated rise in the water table were within the values espoused in Czarnecki (1985). Thus, the approach to treating climate change in the development of performance assessment scenarios in IPA Phase 2 was essentially the same as that used in IPA Phase 1 (see Codell *et al.*, 1992; p. 57). Further discussion of the treatment of climate change within the modeling effort can be found in Chapter 4.

## 6.3 Improved Drilling Model and Code

### 6.3.1 Introduction

The techniques used in the Phase 2 drilling modules differ from those used in IPA Phase 1. The releases in IPA Phase 2, resulting from drilling, are determined using a series of geometric arguments and radionuclide inventories in the waste packages within each region of the repository and the rock columns encompassing the repository and extending down to the water table. The number of drilling events for each trial was sampled from a normal distribution as an approximation to a Poisson distribution. Each event was assumed to occur independently of any other drilling events and to occur randomly in time and space.

## 6. Disruptive Consequences

Table 6-2 The Distribution of Waste Packages by Repository Sub-Area

Repository Sub-Area	Surface Area (km <sup>2</sup> )	Number of Waste Packages
1	0.31	2335
2	1.40	6150
3	1.10	4875
4	0.66	3675
5	0.26	1275
6	1.20	5625
7	0.20	1073
Total	5.13	25,008

present in the rock column at the time of the drilling event,  $I_{i,k,RC}(t_b)$ , times the ratio of the borehole cross-sectional area  $A_b$  to that of the rock column  $A_{k,RC}$  and can be written as:

$$I_{i,k,RC}^R = \frac{A_b I_{i,k,RC}(t_b)}{A_{k,RC}}, \quad (6-1)$$

where  $I_{i,k,RC}^R(t_b)$  is the total inventory released from the rock column through the drilling event that occurred at time  $t_b$ , and  $N$  is the number of radionuclides.

For instance, where the borehole intersects a waste package, the inventory released includes radionuclides from the EBS and from the rock column. As a conservatism, any direct hit of a waste package assume that the entire borehole intersects that package. The amount released for each repository sub-area through a drilling event that intersects a waste package can be expressed as:

$$\begin{aligned} I_i^R &= I_{i,k,WP}^R + I_{i,k,RC}^R \\ &= \frac{A_b I_{i,k,WP}(t_b)}{A_{WP}} + \frac{A_b I_{i,k,RC}(t_b)}{A_{k,RC}}, \end{aligned} \quad (6-2)$$

where  $I_i^R$  is the inventory of radionuclide  $i$  released,  $I_{i,k,WP}^R$  is the amount of radionuclide  $i$

released from the waste package,  $A_{WP}$  is the cross-sectional area of the top of the waste package, and  $I_{i,k,WP}(t_b)$  is the inventory of nuclide  $i$  in a waste package, within region  $k$  of the repository at time ( $t_b$ ).

### 6.3.3 Consequences

The drill hole, itself, does not establish any new pathways either to the atmosphere or the water table; the only effect of drilling on liquid and gaseous releases would be through the premature failure of the waste package. However, the drilling model does consider the direct release of contaminated rock at the surface of the earth, contributing to the cumulative release at the accessible environment. Additionally, the model takes into account the assumption that a fraction of the radionuclides in the drill cuttings is capable of becoming airborne and respirable, which has been conservatively estimated to be about 4 percent of that brought to the surface. These respirable releases are factored into the dose model described in Chapter 7. The drilling events are still modeled somewhat simplistically and, as such, may not be fully conservative.

The probability of drilling incursions into the repository was estimated to be 0.0003 boreholes/square kilometer/year, and was based on the guidelines outlined by the U.S. Environmental Protection Agency (EPA) (see Appendix B in EPA, 1985). This translates into approximately 15.4 events within the repository horizon in 10,000 years (the period of regulatory concern). A

Poisson distribution of drilling events, approximated for convenience by a Gaussian normal distribution with  $\sigma = 3.88$  and  $m = 15.5$ , was used in the analysis and can be expressed as:

$$P(Z) = \frac{e^{-\frac{|Z-m|^2}{2\sigma^2}}}{\sigma\sqrt{2\pi}} \quad (6-3)$$

### 6.3.4 Hit Probability

The consequences also depend on whether the borehole intersects a waste package. The radii of the boreholes were held constant over a given realization and were sampled from a uniform distribution between 0.02 and 0.1 meters. The incident region was determined for each borehole by weighting the probability of penetrating a given region by its relative size. The time of occurrence was uniformly distributed over a range of 100 to 9900 years, for each borehole. The stated range includes the effects of drilling up to 10,000 years, and a nominal period of 100 years for active control over the site. The chance of striking a waste package in region  $k$  of the repository, assuming that no waste package is within  $2r_b$  from another, can be expressed as:

$$P_k(\text{hit}) = \frac{n\pi [(r_b + r_{WP})]^2}{A_{k,RC}}, \quad (6-4)$$

where  $P_k(\text{hit})$  is the probability of a hit,  $n$  is the number of waste packages within the region, and  $r_b$  and  $r_{WP}$  are the radii of the borehole and the waste package, respectively. The values of  $n$  are given in Table 6-2. If a uniformly sampled parameter,  $[0,1]$ , is within the range of  $[0, P_k(\text{hit})]$ , then the borehole intersects a waste package.

### 6.3.5 Radionuclide Inventory Determination

The inventory of radionuclides in the rock in each of the seven repository sub-areas depends on the initial inventory, radioactive decay, and the transport out of the area by water and gas flows. The inventory of radionuclides in the intact waste packages can be determined easily by considering initial inventory and radioactive decay, alone. *SOTEC* also keeps a running inventory of the radionuclides, for failed waste packages, considering transport by diffusion and flow. The

inventory of radionuclides in the rock column is more problematic, however, because there is incomplete information on radionuclide releases from *SOTEC* available to the drilling module. One approach to modeling the inventory is to develop a series of differential equations and to allow continuous and arbitrary time functions for the addition and the removal of mass from the rock columns.

The approach that was used in IPA Phase 2 is better suited for use, and simpler to integrate, with the limited information available from *SOTEC*. The differential equation for the inventory  $I_i$  in the rock column is:

$$\frac{dI_i}{dt} = -\lambda_i I_i + \lambda_{i-1} I_{i-1} + M_i(t), \quad (6-5)$$

where  $\lambda_i$  is the decay constant for nuclide  $i$ , and  $M_i(t)$  is the rate of mass injection or removal of nuclide  $i$  from the rock column.

Given initial concentrations of each nuclide and no injection or removal of nuclides (i.e.,  $I_i(t=0) = I_{i0}$  and  $M_i(t) = 0$ ), then this equation simplifies to a series of coupled, linear, ordinary differential equations, generally known as the Bateman equations. Letting  $B_i$  designate the solution of the Bateman equation for nuclide  $i$ , the inventory  $I_i$  can be written as:

$$I_i(t) = B_i(t, \lambda_i, I_{i0}). \quad (6-6)$$

Knowledge of the initial inventory of a given nuclide,  $I_{i0}$ , and its parent nuclides allows the inventory of nuclide  $I_i$  to be found at any time  $t$ . It is much more difficult to solve Equation (6-5) when mass is added to or withdrawn from the compartment. *SOTEC* calculates and outputs information on the rate of nuclide release from the EBS into the geosphere as a function of time. These values can be used to represent  $M_i(t)$  for the EBS and will contribute to the  $M_i(t)$  for the RC. The  $M_i(t)$  for the RC is further complicated by the loss of mass to the accessible environment.

Let the rate of release of radionuclide  $i$ , from the EBS into the RC, be denoted by  $f_i(t)$ . *SOTEC* will output discrete values of  $f_i(t)$  at times  $t_j$ , which may not be uniformly spaced. Let  $F_{ij}$  be defined

## 6. Disruptive Consequences

as  $f_i(t_j)$ , and it will be assumed that  $F_{i0} = 0$  for all  $i$ .

There are several options to represent the release rate  $f_i(t)$  from the point estimates  $F_{ij}$ . One option is to determine a curve fit to  $F_{ij}$ , which would require assumptions of linearity and continuity of the release rate from the *SOTEC* output. A second option would be to represent the source terms with a series of steps centered about the points  $f_i(t)$ . However, the method adopted for IPA Phase 2 simplifies the solution of the equations. This formulation adds and removes mass in instantaneous pulses, using the Dirac delta function. This technique avoids the introduction of new recursive relationships:

$$t_{L,j} = \frac{(t_j + t_{j-1})}{2}, \quad (6-7)$$

$$t_{L,j+1} = \frac{(t_{j+1} + t_j)}{2}. \quad (6-8)$$

Considering, for the time being, only mass withdrawal, which applies to the inventories in the waste packages, let:

$$\Delta t_{L,j} = t_{L,j+1} - t_{L,j}, \quad (6-9)$$

$$M_i(t) = -f_i(t) = -\sum_{j=1}^J \delta(t-t_j) \Delta t_j F_{ij}, \quad (6-10)$$

where  $\delta(t-t_j)$  is the Dirac delta function and  $J$  is the total number of time steps.

This representation of the source term by a delta function makes the mass removal term zero for all  $t \neq t_j$ . The mass removal rate at  $t = t_j$  is infinite. The integral of the constant rate,  $F_{ij}$ , over the interval  $\Delta t_j$ , is, however,  $F_{ij} \Delta t_j$ .

Consider a 2-member decay chain, where:

$$M_1(t) = -\sum \delta(t-t_j) F_{1j}, \quad (6-11)$$

$$M_2(t) = -\sum \delta(t-t_j) F_{2j}. \quad (6-12)$$

Using Laplace transformations, the solutions for the inventory of each radionuclide at an arbitrary time  $t$ , can be found:

$$I_1(t) = I_{10} e^{-\lambda_1 t} - \sum_{j=1}^J [H(t-t_j)] F_{1j} [e^{-\lambda_1(t-t_j)}], \quad (6-13)$$

$$I_2(t) = I_{20} e^{-\lambda_2 t} + \frac{I_{10} \lambda_1}{(\lambda_1 - \lambda_2)} [e^{-\lambda_2 t} - e^{-\lambda_1 t}] - \sum_{j=1}^J [H(t-t_j)] F_{2j} \Delta t_j (e^{-\lambda_2(t-t_j)}) - \sum_{j=1}^J [H(t-t_j)] F_{1j} \Delta t_j \left[ \frac{\lambda_1 (e^{-\lambda_2(t-t_j)} - e^{-\lambda_1(t-t_j)})}{(\lambda_1 - \lambda_2)} \right] \quad (6-14)$$

where  $H(t-t_j)$  is the Heaviside step function at time  $t_j$ . It may be noted that for the  $I_2$  solution, in this instance, that the relationships between the second and first terms are congruent to those of the fourth and third terms. Therefore, by superposition, the solution to the chain decay problem is given by:

$$I_l(t) = B_l(t, I_{l0}, \lambda_l), \quad (6-15)$$

where  $l = 1, \dots, i$ .

The solution to this problem is given by:

$$I_1 = B_i(t, I_{l0}, \lambda_l) - \sum_{j=1}^J [H(t-t_j)] B_i([t-t_j], \Delta t_j, F_{lj}, \lambda_l), \quad (6-16)$$

where  $l = 1, \dots, i$ .

Modifying the theoretical development now to include mass being added and withdrawn from the compartment, requires modification to Equation (6-15) to:

$$M_i(t) = \sum \delta(t-t_j)[F_{ij} - G_{ij}] , \quad (6-16)$$

where  $F_{ij}$  is the amount of mass added to the rock column, equal and opposite to the amount withdrawn from the EBS, and  $G_{ij}$  is the amount lost to the accessible environment. The solution for the inventory of nuclide  $i$  in the rock column is:

$$I_i = \sum_{j=1}^l [H(t-t_j)] B_i([t-t_j], \delta t_j [F_{ij} - G_{ij}] \lambda_i) , \quad (6-17)$$

where  $l = 1, \dots, i$ .

### 6.3.6 Overview

The present formulation of the drilling consequences offers a limited degree of sophistication. It does not, nor does it intend to, consider the full range of expected consequences of a drilling event. The effect of drilling fluid has, for example, been neglected throughout the analysis, which introduces an element of non-conservatism into the analysis. Furthermore, the model assumes that the process of drilling does not create any additional pathways for liquid or gaseous releases. The conceptual models of the drilling events were selected, in part, to allow effective use of, and integration with, the other IPA Phase 2 models, and to avoid unnecessary complexity. In light of the uncertainties in other parts of the IPA Phase 2 analyses, and the relatively minor contribution of drilling to either cumulative releases or doses, the drilling model appears to have received an appropriate level of attention.

## 6.4 Improved Seismic Scenarios Model and Code

### 6.4.1 Introduction

The physical integrity of the waste package is modeled, for the case of no seismicity, as if corrosion will proceed until the thickness of the waste package material reaches a critical value. With seismicity, a presumably lesser degree of corrosion can cause waste package failure. Since all waste packages are considered to be identical in each repository sub-area, all of them would fail at a time earlier than the time of corrosion-induced

collapse. The seismic analysis, therefore, calculates the time of failure for all the packages in the repository sub-area, which is less than the failure time of corrosion-induced failure. The critical thickness is calculated from models of pitting, crevice, and uniform corrosion, choosing the greatest corrosion depth from among the three without regard to the obvious differences in the likely effect of these processes on the mechanical strength of the waste packages.

The seismic analysis is embodied in the computer code *SEISMO* (see Freitas *et al.*, 1994). The seismic failure analysis relies on *SOTEC* for the depth of pitting and crevice corrosion. Premature failures of the waste packages are communicated back to the *SOTEC* code, to allow the release of radionuclides to commence sooner.

The *SEISMO* code determines the time step(s) during which waste package failure occurs. The probability that a seismic event of sufficient magnitude to cause waste package failure occurs (failure probability) is compared to an event indicator. If the event indicator, a random number ranging from zero to unity, is less than the failure probability, then it is assumed that seismicity during the time step is sufficient to cause premature waste package failure. The details of the calculation are presented in the succeeding sections. (See Table 6-3 for a description of the parameters used in the *SEISMO* code.)

### 6.4.2 Response of Waste Package to Seismic Shaking

The waste package is considered to be a hollow, slender, elastic cylinder of length  $L$  standing vertically, and attached at the bottom to the ground, as illustrated in Figure 6-1.

The moment of inertia of the cylinder,  $I$ , given by:

$$I = \frac{\pi}{4} [R^4 - (R-d)^4] \approx \pi R^3 d , \quad (6-18)$$

where  $R$  = outer radius of cylindrical waste package, and  $d$  = thickness of cylinder walls.

The spring constant  $K$  is given by:

$$K = \frac{3EI}{L^3} , \quad (6-19)$$

6. Disruptive Consequences

Table 6-3 Parameters Used in the *SEISMO* Code

<i>Parameter Name</i>	<i>Symbol</i>	<i>Description</i>	<i>Nominal Value and Units</i>
pac leng	$L$	package length	4.7625 m
pac rad	$R$	package radius	0.3302 m
pac thik	$d$	package thickness	0.01 m
damp fac	$\xi$	damping factor	0.03
elas mod	$E$	modulus of elasticity of package material	$2.0 \times 10^{11}$ N/m <sup>2</sup>
dens ss	$\rho_{ss}$	density of stainless steel	$7.75 \times 10^3$ kg/m <sup>3</sup>
wmass	$M_w$	mass of waste per package	$6.4 \times 10^3$ kg
freq acc	$\omega_a$	seismic wave frequency	5 hertz
width ag	$w_{ag}$	size of the air gap	0.0381 m

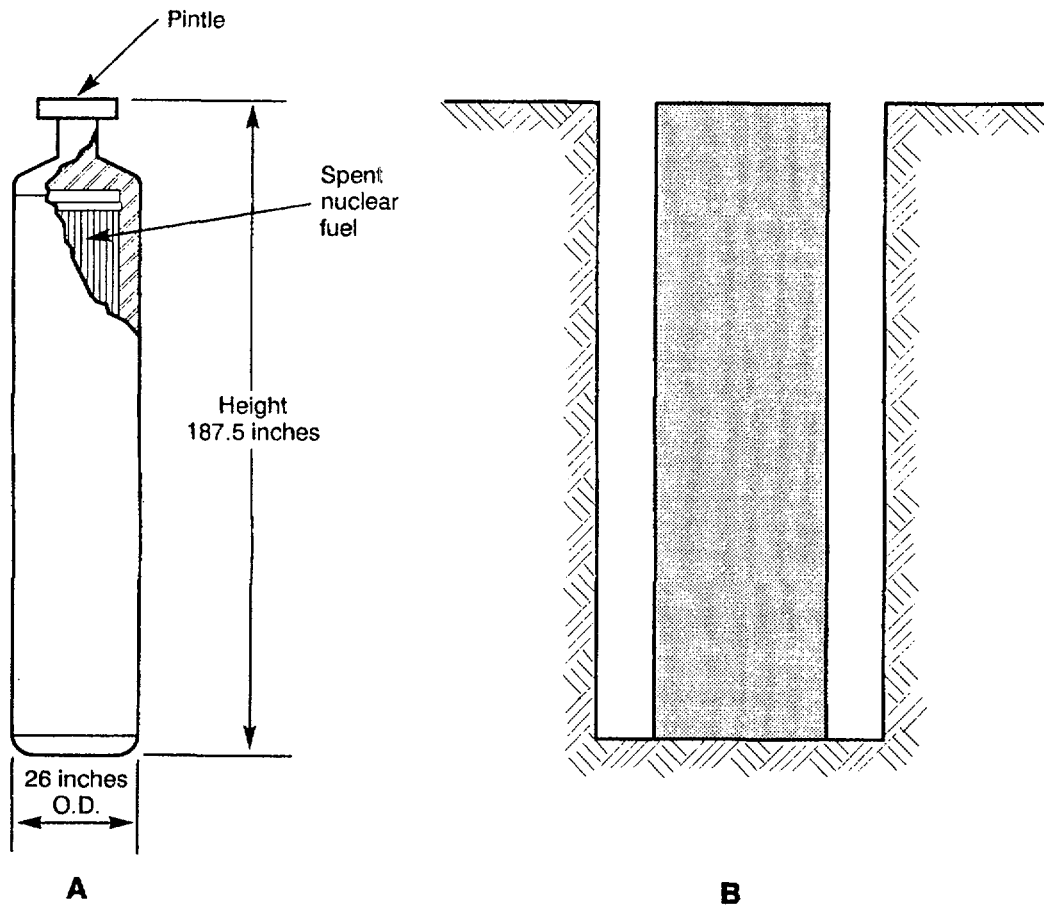


Figure 6-1 Representation of waste package canister for improved seismic scenarios model ((a) SCP disposal container concept for spent fuel (from DOE, 1988; p. 50). (b) IPA Phase 2 waste package representation.)

where  $E$  = elastic modulus and  $L$  = length of waste package.

Assuming that the cylinder is thin-walled, the volume of metal in the top or bottom ends of the waste package  $V_e$  is given by the expression:

$$V_e = \pi R^2 d. \quad (6-20)$$

The volume of the side  $V_s$  is given by:

$$V_s = \pi [R^2 - (R - d)^2] L. \quad (6-21)$$

The total volume  $V_T$  is given by:

$$V_T = 2 V_e + V_s. \quad (6-22)$$

The mass of the waste package is therefore:

$$M_p = V_T \rho_{ss}, \quad (6-23)$$

where  $\rho_{ss}$  = density of stainless steel.

The total mass is the sum of the waste package mass and the waste mass,

$$M_T = M_w + M_p. \quad (6-24)$$

The natural frequency of the undamped system is:

$$\omega_n = \left[ \frac{K}{M_T/2} \right]^{1/2}. \quad (6-25)$$

Half the total mass is used in this calculation, because a simple lumped-system model of the waste package and its contents would be for half the total mass at the end of the cantilever and half at the bottom. The mass at the bottom is assumed to travel with the ground, so it does not enter into the calculation.

The excitation frequency (i.e., the frequency of the ground motion) is an input parameter chosen for this seismic analysis to be similar to the resonant frequency of the object involved; in this case, the excitation frequency was chosen to be 5 hertz. The amplitude of the ground motion is a function of the excitation frequency, and, for the present analysis, has been taken from regional seismic data in the vicinity of Yucca Mountain (URS/Blume, 1986). The ratio of the excitation frequency to the resonant frequency is defined:

$$\Omega = \omega_a / \omega_n. \quad (6-26)$$

For the nominal waste package parameters, the natural frequency of the waste package will start off much higher than the excitation frequency, but declines as the metal thickness is reduced by corrosion. As an added conservatism in the model, the natural frequency is not permitted to decrease below the excitation frequency (i.e.,  $\Omega > 1$ ).

Let the displacement of the center of the mass be denoted by  $x(t)$ , the motion of the ground by  $x_g(t)$ , and the relative motion of the mass with respect to the ground (and the emplacement hole) by  $x_r(t)$ . Then,

$$x_r(t) = x(t) - x_g(t). \quad (6-27)$$

Further, since the analysis was interested in the harmonic motion solution, these functions are written in the form:

$$x_g(t) = A_g \sin(\omega_a t), \quad (6-28)$$

$$x_r(t) = A_r \sin(\omega_a t - \phi), \quad (6-29)$$

where  $A_g$  and  $A_r$  equal the amplitude of the ground and waste package displacement, respectively, and  $\phi$  is the phase difference between ground and waste package movement.

For a simple spring mass system with damping associated with the velocity term, we find that:

$$\frac{A_r}{A_g} = \frac{\Omega^2}{[(1 - \Omega^2)^2 + (2\xi\Omega)^2]^{1/2}}, \quad (6-30)$$

where  $\xi$  is the damping factor accounting for frictional forces opposite the direction of motion of the center of mass.

Since we are assuming sinusoidal motion, we obtain, by differentiating Equation (6-28) twice:

$$\ddot{x}_g(t) = -\omega_a^2 x_g(t) = -\omega_a^2 A_g \sin(\omega_a t). \quad (6-31)$$

Further, we may take the peak ground acceleration  $a$  to be equal to the amplitude of the acceleration of the seismic wave, that is:

$$a = \omega_a^2 A_g. \quad (6-32)$$

## 6. Disruptive Consequences

Then, the maximum displacement  $A_r$  is:

$$A_r = \frac{a}{\omega_a^2} \frac{\Omega^2}{[(1 - \Omega^2)^2 + (2\xi\Omega)^2]^{\frac{1}{2}}} \quad (6-33)$$

### 6.4.3 Waste Package Fragility

The waste package canister is assumed to fail if one of the following conditions occurs:

- The stress at the base exceeds the yield strength of the waste package material (Mode 1 failure), or;
- The motion induced in the end of the waste package is great enough to impinge on the side of the emplacement hole, thereby buckling the waste package (Mode 2 failure).

#### Failure by Mode 1.

Failure by Mode 1 is induced when the magnitude of the vibration of the waste package becomes so great that the stress at the base (which is assumed to be a cantilever support—hence stress is greatest at the base) exceeds the yield strength of the waste package material. Consider the forces at the base of the spring-mass system used to represent the waste package. The force  $F_M$  exerted by the movement of the mass at the free end of the cantilever beam can be derived from the definition of the spring constant:

$$F_M = -K x_r, \quad (6-34)$$

where  $x_r$  = deflection.

Then by using the formula for the spring constant, Equation (6-19), the moment  $M_A$  at the base is given by:

$$M_A = LF_M = -\frac{3EIx_r}{L^2}, \quad (6-35)$$

and the stress at the base is given by:

$$\sigma_A = M_A \frac{L}{I} = -\frac{3Ex_r}{L} \quad (6-36)$$

Since we are interested in the maximum stress, hence the maximum deflection, we can replace  $x_r$  with  $A_r$ , to obtain:

$$\sigma_A = 3 \frac{EA_r}{L} \quad (6-37)$$

A failure will occur if  $\sigma_A \geq \sigma_Y$ , that is:

$$A_r \geq \frac{L\sigma_Y}{3E}, \quad (6-38)$$

where  $\sigma_Y$  is the stress at the yield point.

#### Failure by Mode 2.

Failure by Mode 2 is induced when the motion of the end of the waste package is so great that it impinges on the side of the emplacement hole, thereby buckling the waste package. For failure to occur by this mechanism, two conditions must be met:

- (1) The displacement of the end of the waste package must be large enough so that the package hits the side of the emplacement hole; and
- (2) The force induced by this impact is great enough to buckle the side of the waste package.

For Condition (1) we can merely compare the amplitude of the displacement, given by Equation (6-33) with the magnitude of the air gap,  $w_{ag}$ , which is read in as data. The 1988 Site Characterization Plan design calls for a 3.81 centimeter-air gap all around the package (see DOE, 1988). Thus,

$$A_r \geq w_{ag} \quad (6-39)$$

implies a failure could take place by this mechanism. For the IPA Phase 2 version of the model, the staff conservatively assumed that any contact of the waste package with the side of the borehole will lead to failure.

### 6.4.4 Computational Algorithm for Seismic Failure of Waste Packages

At each time step, input on the corroded thickness of the waste package is supplied by SOTEC.

The thickness of the waste package metal is chosen from the largest corrosion depth calculated from models for pitting, crevice, or general corrosion. The strength of the remaining material, however, is conservatively calculated, assuming that the entire surface corrodes uniformly to the calculated depth, irrespective of which model (pitting, crevice, or general corrosion) gave the greatest depth of corrosion.

Given the thickness of the metal and the parameters presented in Table 6-3, the critical displacement of the waste package  $A_{rc}$  is calculated for Mode 1 or Mode 2 failure mechanisms, Equations (6-33) or (6-39), respectively. The smaller of the two amplitudes is then used to determine at what acceleration the waste package would fail.

The fragility  $f$  corresponds to the acceleration in  $g$ 's needed for the smaller amplitude:

$$f = A_{rc} \frac{\omega_a^2 [(1 - \Omega^2)^2 + (2\xi\Omega)^2]^{\frac{1}{2}}}{9.81 \Omega^2} \quad (6-40)$$

The fragility  $f$  has a corresponding annual rate of recurrence  $r_a$ , derived from a curve fit to a published relationship at Yucca Mountain (URS/Blume, 1986), that includes all events sufficient to cause displacements equal to or greater than the critical displacement. The fragility can be expressed as follows—

for  $f < 0.1 g$ :

$$r_a = 0.01 [\text{occurrences/year}], \quad (6-41a)$$

for  $0.1 < f < 4$ :

$$\log_{10}(r_a) = a_0 + a_1 l + a_2 l^2 + a_3 l^3 + a_4 l^4 + a_5 l^5 + a_6 l^6, \quad (6-41b)$$

where  $l = \log_{10}(f)$ :

$$a_0 = -4.67174, a_1 = -4.16482, a_2 = 1.91376, \\ a_3 = 3.75132, a_4 = -3.06375, a_5 = -2.04791, \\ a_6 = 1.65667,$$

for  $f > 4$ :

$$r_a = 0 [\text{occurrences/year}]. \quad (6-41c)$$

An approximation of the probability that the failure occurs within the time step  $t$  to  $t + \Delta t$  is approximated from the annual rate of recurrence  $r_a$  to be:

$$p\Delta t = 1 - (1 - r_a)^{\Delta t}, \quad (6-42)$$

where  $\Delta t$  is number of years in the time step.

Whether or not the failure occurs during a particular time step is a matter of chance. In the present model, the failure probability  $\{p\Delta t\}$  is compared with a number  $U$  between zero and unity, selected randomly from a uniform distribution. If the random number is less than  $\{p\Delta t\}$ , the waste package is assumed to fail. The random number is sampled once per vector from the main sampling routine, to keep all randomness in the control of the system-level program. Although it would appear that the random number  $U$  should be sampled for each time step within the vector, numerical experiments with the model indicate that the results are about the same statistically for either case, given a sufficiently large number of vectors.

#### 6.4.5 Estimating Probability of Seismic Failure Scenario

The task of this section is to define an acceleration and its probability below which there would be no perceptible difference between failure and no-failure by seismic forces.

Since the system code calculations are discretized in time, anything happening in less than one time step is below our ability to discern its cause. The curve of waste package thickness vs. time from the corrosion model is very steep and fairly insensitive to the environmental conditions, once corrosion commences. Figure 6-2 is a typical set of curves describing the decrease in metal thickness, with time, for the seven repository sub-areas. The thickness  $\theta_f$  for six of the repository sub-areas is  $9.8 \times 10^{-4}$  meters, 50 years before failure.

The natural frequency  $\omega_n$  at failure, can be calculated from Equations (6-18), (6-19), and (6-25), by

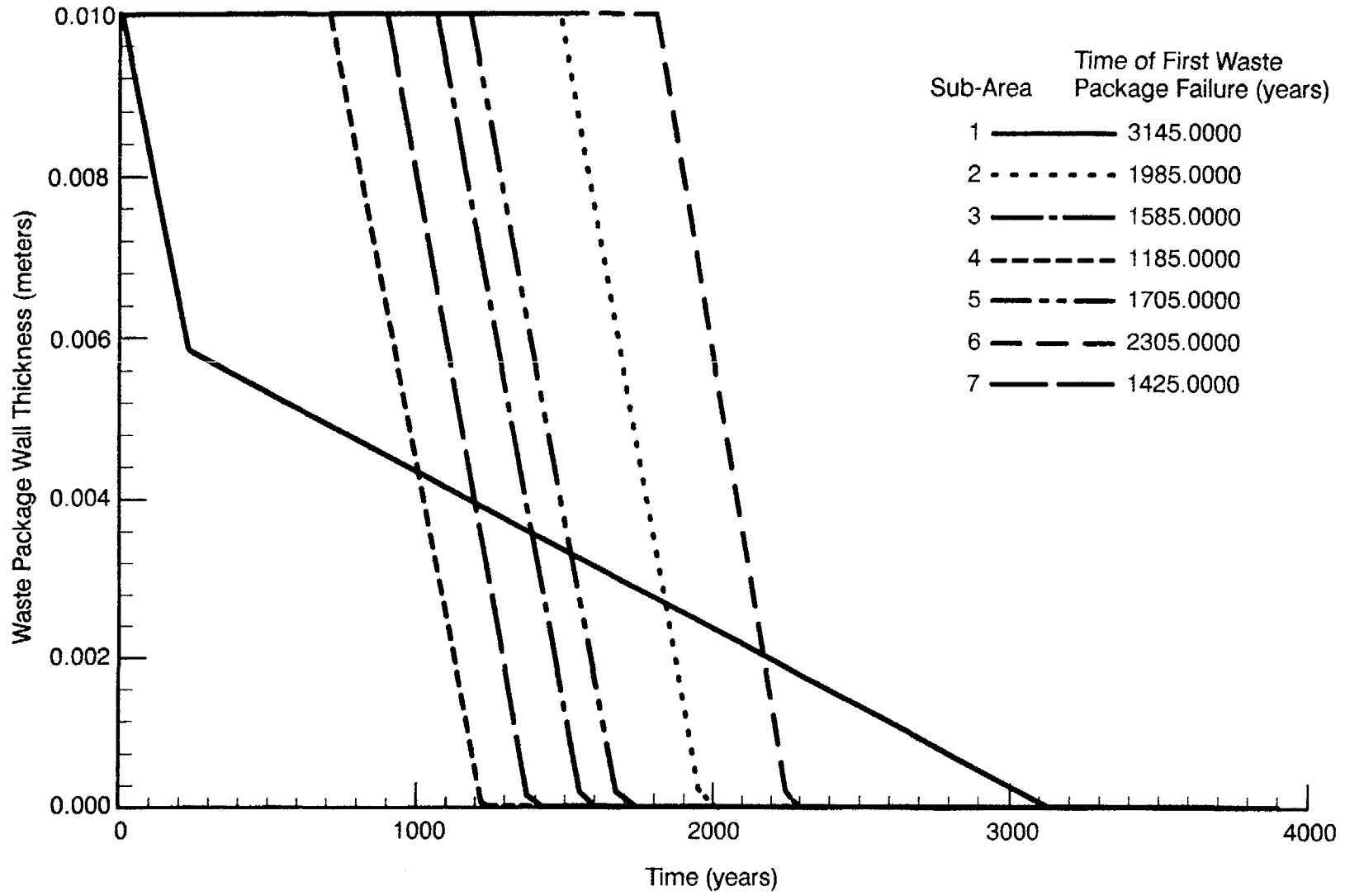


Figure 6-2 Waste package canister thickness versus time for seven repository sub-areas for the base case (0000) scenario

substituting  $\theta_f$  for  $d$ . For the assumed model parameters of  $R = 0.33$  meters;  $L = 4.7$  meters,  $\omega_a = 5$  hertz;  $E = 2 \times 10^{11}$  Newtons/square meter;  $\sigma_a = 2.067 \times 10^8$  Newtons/square meter; the mass of the fuel plus waste package  $M_f = 2925$  kilograms; thickness  $\theta_f$  (50 years before failure) =  $9.8 \times 10^{-4}$  meters; and the natural frequency from Equation (6-25) = 13.9 hertz, or  $\Omega = \omega_a/\omega_n = 0.36$ .

In most cases, the waste package fails first by failure Mode 1, so one can write:

$$A_r = \frac{\sigma_a L}{3E} = \frac{a}{\omega_a^2} \left[ \frac{\Omega^2}{[(1 - \Omega^2)^2 + (2\xi\Omega)^2]^{1/2}} \right] \quad (6-43)$$

The acceleration needed for the waste package to fail is:

$$a_f = \frac{\sigma_a L \omega_a^2}{3E} \frac{[(1 - \Omega^2)^2 + (2\xi\Omega)^2]^{1/2}}{\Omega^2} \quad (6-44)$$

Evaluating Equation (6-44) for the resonance  $\xi$  and  $\xi = 0.03$  gives an acceleration of only 0.028 g. Earthquakes of this magnitude would be expected to be very frequent. Equation (6-41) gives a default annual recurrence rate of 0.01/year. Conversely, the expectation of no earthquakes of this magnitude in 10,000 years would be vanishingly small:

$$\begin{aligned} \{p\Delta t\}_{(no\ seismic\ failure)} &= (1 - 0.01)^{10,000} \\ &= 2 \times 10^{-44} \quad (6-45) \end{aligned}$$

## 6.5 Improved Magmatic Scenarios Model and Code

### 6.5.1 Introduction

This section describes models and codes that have been used to simulate magmatic activity for the IPA Phase 2 consequence analysis. Magmatic scenarios are important for performance assessment because some repository material may be ejected onto the earth's surface if a magmatic event penetrates the repository during a volcanic eruption

(Valentine *et al.*, 1992). Even in the absence of actual eruption of waste, subsurface magmatic effects may also affect repository performance. In the case of intrusive events that occur within the repository area, dikes emplaced through and above the repository may damage the waste packages. In addition, dikes or sills below or in the repository horizon could affect the repository by producing hydrothermal processes or altering hydrology. The effects of intrusive dikes on the regional hydrology are presented in Appendix E. For the parameters chosen in the model, the model predicts a potential water table rise of over 100 meters for the case of two perpendicular dikes. The main effect of the intrusions would be to decrease the distance between the repository and the water table, but increase the travel time in the saturated zone. Hydrothermal processes could cause rapid corrosion of waste packages. As a result, radionuclides could be transported to the accessible environment by either ground-water flow or gaseous release. The hydrologic properties of the dike itself may produce important changes in the long-term flow of ground water.

Two areas of current investigation that are critical to consequence models are: (i) the mechanics of cinder cone eruptions, the duration of these eruptions, and the areal distribution of vents at active cinder cones, and; (ii) the secondary effects of volcanism, including the effects of diffuse degassing and thermal loading on waste package performance, geochemical transport, and ground-water movement. Many of these volcanic processes are incompletely characterized. For example, recent studies at historically active cinder cones indicate that these eruptions are, under some circumstances, considerably more energetic than normally inferred. During the 1992 eruption of Cerro Negro, Nicaragua, volcanic ash rose to much higher altitudes and was dispersed over a greater area than is typical for mafic eruptions. Although this volcano is in a magmatic arc, the rheological properties of its magmas are similar to those of Lathrop Wells (Connor and Hill, 1993). These data suggest that cinder cone eruption mechanics and their impact on waste entrainment and dispersal must be investigated more fully. The secondary effects of degassing and cooling of cinder cones are long-term processes, and their impact on repository performance also will need to be more fully integrated into future IPA models, as studies progress.

## 6. Disruptive Consequences

Two approaches have been used previously to model volcanism consequences related to damage of the repository and release of waste (Crowe *et al.*, 1983; Valentine *et al.*, 1992; Sheridan, 1992; and Margulies *et al.*, 1992). The first method involves development of a geometric model to estimate the amount of waste entrained in an ascending dike during both intrusive and extrusive events (Sheridan, 1992; and Margulies *et al.*, 1992). In this model it is assumed that the amount of waste entrained is directly proportional to the size of the dike. In the second approach, the likely amount of waste entrainment is estimated by considering the abundance of shallow crustal xenoliths identified at volcanoes near the repository site and at other cinder cones in the Great Basin (Crowe *et al.*, 1983). The basic premise in this approach is that the amount of waste entrained should be proportional to the lithic fraction in scoria cones, should a basaltic eruption occur through the repository. For IPA Phase 2, the geometric approach was adapted to develop the magmatic consequence model and code.

In the magmatic consequence model, the number of waste packages damaged is computed from the area of the repository intercepted by the ascending magma. Only one igneous event, either an intrusive (modeled as a dike only) or an extrusive event (modeled as a coincident dike and cone), is assumed to occur during each simulation run. It was assumed that all radioactive waste affected by the dike is released to the surface of the earth through the cinder cone, for extrusive events. For intrusive events, the magma is assumed to compromise the intercepted waste packages, leading to early failure, but not providing additional gas or liquid pathways for radioactive release.

### 6.5.2 Relevant Literature

The volcanic release probability at Yucca Mountain region during the period of regulatory concern for a potential repository has been studied by Crowe *et al.* (1982; 1983; 1992). The volcanic release probability was examined in these studies as the product of three factors: (i) the probability that a volcanic event will affect the repository site; (ii) the temporal probability of a volcanic event; and (iii) the probable amount of release of radionuclides because of a volcanic event. However, these studies underestimated some param-

eters in the consequence analysis, such as erosive depth, conduit shape, speed of entrainment, and total lithic fraction.

The effects of volcanism on performance of the potential Yucca Mountain radioactive waste repository were studied by Crowe *et al.* (1983) and Valentine *et al.* (1992). They adapted the implicit assumption of the geometric model that the amount of waste entrained is directly proportional to the size of the dike. Valentine *et al.*, then estimated the amount of waste entrained from the total volume of erupted lithics and the volume of repository intercepted by the dike.

Sheridan (1992) used Monte Carlo simulation to estimate the probability of occurrence of future volcanic dikes in the vicinity of Yucca Mountain. His model incorporates the geometric approach and addresses only the spatial probability of the various volcanic scenarios. In this model, the volcanic field defining the area in which dikes can occur is approximated by an elliptical outline. The centers of the dikes are distributed according to a bivariate Gaussian distribution centered in the middle of the volcanic field. The geometric parameters of dikes are specified by a mean value and a standard deviation. After each dike is located, the length and orientation are chosen from the Gaussian distributions specified by the mean and standard deviation. Because the location of dike centers and the dike geometry are generated independently, it is possible to have a dike field oriented in a different direction away from the orientation of the elongated volcanic field. This study sets upper bounds on the probability of intersection of dikes with the repository. Using this technique, Sheridan estimated that the worst-case probability of a volcanic dike intersection with the repository in the next 10,000 years is between 0.001 and 0.01.

Using a Monte Carlo simulation approach, Margulies *et al.* (1992) estimated the areal extent that a basaltic dike or volcanic cone intercepts the repository, by assuming the occurrence of magmatic activity in the region near the repository. The magmatic events modeled were represented by planar geometrical figures. Cones were represented as disks, and dikes were represented as rectangles. The repository area and borders were represented realistically in the simulations. Based only on geometry, Margulies *et al.* obtained the estimates of radionuclide release by assuming that

any radioactive waste intercepted by the magma would result in release of radionuclides to the accessible environment.

Margulies *et al.* (1992) assume an inhomogeneous Poisson model for the occurrence of a magmatic event. The probability of magmatism was uniform within simulation regions, but could vary between regions in their study. Similarly, the rate of occurrence of magmatic events was allowed to vary discretely in time. The vent distribution in the Yucca Mountain area indicates a clustering of vents (Connor and Hill, 1993). From geologic evidence and theory, the probability of magmatism is not likely to be constant in time in the vicinity of Yucca Mountain (Trapp and Justus, 1992). Important geological information, such as the temporal and spatial variation in the rate of magmatism, therefore, remains to be incorporated into the geometric approach of simulating magmatic events in the repository site.

### 6.5.3 Description of Modeling Approach

#### 6.5.3.1 Introduction

The geometric approach used is an extension of the work by Margulies *et al.* (1992). In the geometric approach, Monte Carlo sampling was used to estimate the areal extent that a basaltic dike or a volcanic cone intercepts the repository. From a probabilistic point of view, magmatic events are distributed in both space and time. For the purposes of IPA Phase 2, an estimate of the probability of magmatism in the Yucca Mountain repository (over the next 10,000 years) is needed.

#### 6.5.3.2 Simulation Procedure

In the Monte Carlo simulation, the staff considered a rectangular region surrounding the repository horizon. As shown in the simulation configuration of the repository (Figure 6-3), the repository is represented by a total of 17 rectangles. To obtain the simulation configuration of the repository, the outline of the perimeter of the proposed Yucca Mountain repository has been traced from actual drawings. The rectangles are further grouped into seven areas, also shown in Figure 6-3.

The simulation generates a volcanic event randomly in the simulated region. The volcanic event occurrence time is chosen randomly within the

specified time period. The simulation chooses an intrusive magma event (with only a dike) with a probability 10 times that of an extrusive event (with a feeder dike and a cone) (Crisp, 1984). Cones are represented as circular disks, whereas dikes are represented as narrow rectangles. The dimensions of cones and dikes are selected by a random sampling procedure. The Monte Carlo simulation procedure for estimating the occurrence and consequences of a magmatic event is described below:

- Locate the centerpoint of a dike event or an extrusive event by random sampling.
- Determine geometry parameters (e.g., length, width, radius) by random sampling.
- Calculate the overlapped area in each repository cell and convert the area to number of waste packages, if a dike or a cone intercepts the repository.
- In the case of cones, calculate and output the radioactive release amount in this trial. For dikes, report number of affected waste packages to *SOTEC*.

In the procedure of determining geometry parameters, parameters are chosen randomly from a range of values, based on the available data. Margulies *et al.* (1992) assumed that the length of the rectangular dike ranges between 1000 and 4000 meters, and the dike width ranges between 1 and 10 meters. Therefore, the area of the rectangular dike varies between 1000 and 40,000 square meters. The area of the rectangular dike is chosen at random, in the code, as given by the following expression (*op cit.*):

$$A = a^{(1-\mu)} b^{\mu} \quad , \quad (6-46)$$

where  $a = 1000$  square meters is the minimum area,  $b = 40,000$  square meters is the maximum area, and  $\mu$  is a random number chosen uniformly between 0 and 1. The probability density function of  $A$  for uniformly distributed  $\mu$  is skewed toward the smaller areas.

After the dike area is chosen, the length is chosen at random between  $\max\{c, A/f\}$  and  $\min\{A/e, d\}$ , with equal probability. The corresponding width

6. Disruptive Consequences

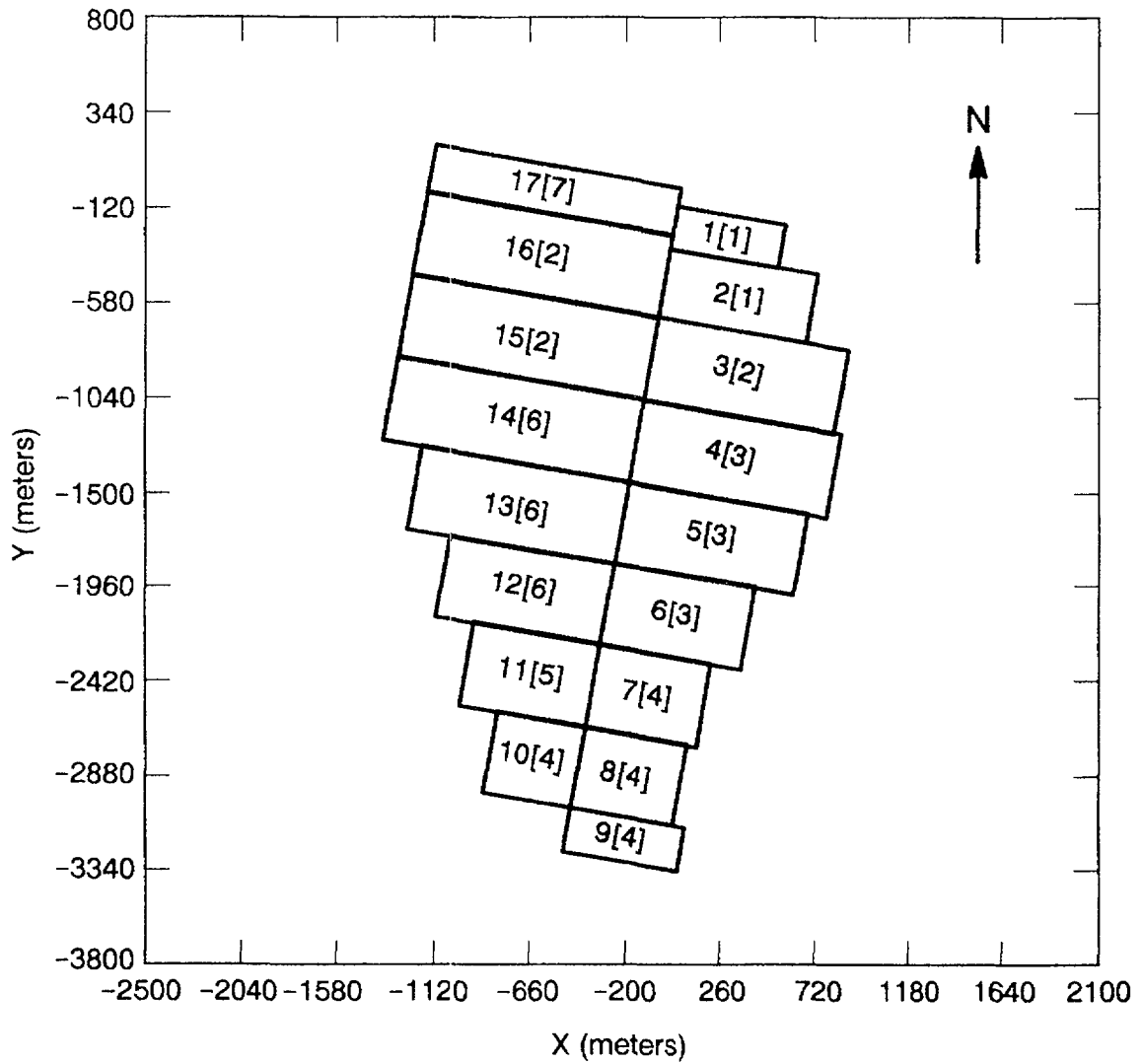


**Figure 6-3 Configuration of the geologic repository in the magmatic scenarios simulation** (The repository is divided into seven sub-areas with a total of 17 rectangular panels. The number inside the brackets represents the sub-area number, and the number outside the brackets gives the panel number.)

of the rectangular dike  $W$  is then determined from the area  $A$  and length  $L$ , as  $W = A/L$ . Here the parameters  $c$  and  $d$  define the minimum and maximum length, respectively, whereas the parameters  $e$  and  $f$  define the minimum and maximum width, respectively. The values of these parameters in the code are:

$$\begin{aligned} c &= 1000 \text{ meters (minimum length);} \\ d &= 4000 \text{ meters (maximum length);} \\ e &= 1 \text{ meter (minimum width); and} \\ f &= 10 \text{ meters (maximum width).} \end{aligned}$$

This randomly generated rectangular dike has an angle of orientation that is chosen at random with equal probability between two angles specified in the input. Typically, the input parameters for the angles are chosen to be  $75^\circ$  and  $90^\circ$  counterclockwise from the horizontal axis, corresponding to the dike orientations ranging from due north/south to north 15 degrees east. However, this distribution of dike orientation is based on a postulate by Smith *et al.* (1990), Ho (1990), and Ho *et al.* (1991), that there is a NE-trending structural control on vent distribution within the "area of most recent volcanism" (AMRV). Crowe and Perry (1989) have delineated a different area, the "crater flat volcanic zone" (CFVZ), that extends north-northwest from the buried Amorgosa Valley vents, located about 35 kilometers south of Yucca Mountain, to those at Sleeping Butte, about 65 kilometers northwest of the site.

To simulate the formation of volcanic cones through extrusion events, circular areas are used to represent cones. Since we are interested in the effect of the volcano on the subsurface repository, these circular areas more properly represent the stem-like conduit of magma feeding the volcanic eruption, which may intersect the repository. The cone radius then corresponds approximately to the radius of the approximately vertical, nearly circular magma conduit. The radius of the volcanic cones is chosen uniformly at random between two input parameters, the minimum and maximum cone radii. Margulies *et al.* (1992) have chosen the minimum and maximum radii to be 25 and 100 meters, respectively. Currently the simulation adapts the parameters chosen by Margulies *et al.* However, the minimum and maximum radii chosen in the simulation appear to be unrealistically small. The smallest cones in the Yucca Moun-

tain area have basal radii varying from 250 meters for Lathrop Wells and Little Black Peak, to 300 meters for Hidden Cone (e.g., Crowe *et al.* 1983). Future simulations should address more realistic values for the cone radii.

The program calculates the area of intersection between the dike and the repository by strictly geometrical computations. For an extrusive event, it also calculates the area of intersection between the cone and the repository. The predicted area of interception from the simulations is used to estimate the number of waste packages damaged, assuming a uniform distribution of waste packages within each repository cell. For extrusive events, upper bound and conservative estimates of radionuclide release into the atmosphere are calculated by assuming that the radioactive material damaged by the dike has been transported to the cone and a fraction of the transported material, 4 percent, released into the air. The amount of radionuclides released into the air is considered to be zero for intrusive events.

The simulation estimates the amount of release  $Q_k$  of radionuclide  $k$  to the atmosphere, for the extrusive event, by summing over the radioactive inventory at the time of the event,

$$Q_k = \sum_{j=1}^n N_j I_{jk}(t) \quad , \quad (6-47)$$

$$I_k(t) = I_k(0) \exp(-0.693t/t_k) \quad , \quad (6-48)$$

where  $N_j$  is the number of the damaged waste packages in area  $j$ , and  $I_{jk}$  is the inventory of  $k^{\text{th}}$  radionuclide in each waste package at time  $t$  in area  $j$ . This approach neglects the generation of radioactive progeny, which is non-conservative. The amount of radioactivity release for each radionuclide is used as input by the AIRCOM program, to calculate dose by the DITTY code (Dose Integrated over Ten Thousand Years). In addition, the number of damaged waste packages predicted by the Monte Carlo simulation is used by the SOTEC program to determine the release of waste in air and water. (See Section 2.1.3 for a description of these other total-system performance assessment (TPA) computer code modules.)

## 6. Disruptive Consequences

### 6.5.3.3 Assumptions and Limitations

Several assumptions are implied, in applying the geometric approach, to estimate the amount of waste entrained in an ascending dike, as discussed in Valentine *et al.* (1992). The Monte Carlo simulation model of basaltic igneous activity assumes: (i) any magma that intrudes into the repository will have a low volatile content; (ii) any igneous event will involve the intrusion of a single igneous dike; (iii) the repository itself will not affect magma flow or eruption dynamics; (iv) magmatic events are of relatively short duration; (v) ground water, possibly derived from a perched water table, will not interact with magma; and (vi) the probability of an intrusive event is 10 times that of an extrusive event. As the code is developed further, these assumptions will be explored in more detail.

The basic assumption that the amount of waste entrained in an ascending dike is determined by the dike size is justified if the magma intruding the repository has a low volatile content. High-volatile content magmas will likely erode wallrock during the eruption and thus entrain a larger volume of waste than what is calculated using a standard dike width.

The simulation results for magmatic activity are normalized according to the magma scenario probability and the area of the simulation region. The magma scenario probability, an input parameter to the TPA computer code, was determined from the work of Connor *et al.* (1993) and Connor and Hill (1993) (see Section 3.3.2.2 (A) for detailed discussion). They used a nonhomogeneous Poisson model calculated by near-neighbor methods to estimate the probability of volcanic disruption of a repository-sized area in the Yucca Mountain area over the next 10,000 years.

The simulation region used in the *VOLCANO* code (Lin *et al.*, 1993) is an assumed area of 12-by-12-square kilometers around the repository. The origin of the simulation region is the upper right corner of Area 7. In the simulation system, the *x* coordinate ranges from -6000 meters to 6000 meters, and the *y* coordinate from -7500 meters to 4500 meters. Because the maximum length of a dike is assumed to be 4000 meters, this simulation system is sufficiently large to ensure that it will

include any magmatic events intercepting the repository.

The current simulation model has several limitations. At present, effects of faults on magma activity are not considered in the *VOLCANO* code. At least two faults are known to be located in the area: the Ghost Dance fault passing through the repository and the Solitario Canyon fault west of the repository. Faults may localize magma ascent in the shallow crust if fault orientation corresponds to the current orientation of principal crustal stress (Nakamura, 1977). All these faults could localize magmatism and may influence dike occurrence in the repository area. The *VOLCANO* code needs to be improved by including magma events related to these faults. The model also considers only radioactivity release for intrusive and extrusive events. The consequence analysis has not taken into account the interaction between intruding magma and a perched body of water around the repository. However, Appendix E discusses an auxiliary analysis that considers the effect on saturated ground-water flow and water table elevation, at the regional scale resulting from intrusive dikes. Finally, the simulation model has not included the possibility of multiple eruptions. There is evidence of multiple eruptions (polycyclic activity) at some of the Quaternary-age cinder cones in the Yucca Mountain area (e.g., Crowe *et al.*, 1992). The effects of this type of igneous activity remain to be included in the model.

### 6.5.3.4 Summary

A geometric simulation approach has been used to model the consequence of volcanism in the proposed repository. The model *VOLCANO* obtains the area of intersection between the repository and the area of an intrusive magma event occurring randomly in a region encompassing the repository. The actual geometry of the proposed Yucca Mountain repository is used as input to the model. Using the repository initial inventory as input, the area of interception is converted into the number of waste packages damaged from which the amount of radioactivity released into the atmosphere is calculated. The predictions of the *VOLCANO* model are used as input by the *AIRCOM* and *SOTEC* modules in the TPA computer code. The number of waste packages damaged by magma activity is used in computing the source term in the *SOTEC* module. The

results of the radionuclide release calculations are used in *AIRCOM* (described in Section 2.1.3) to calculate human dose, and in the *TPA executive module* (Sagar and Janetzke, 1993), to calculate the total release. A detailed description of the *VOLCANO* code and its output is given in the *VOLCANO* User Guide (Lin *et al.*, 1993).

## 6.6 Overall Conclusions and Suggestions for Further Work

A number of conclusions were drawn from the disruptive consequence analyses. These conclusions are summarized here, with specific recommendations for improvement during the next phase of IPA:

### 1—*Improve model for climate change.*

The current implementation for climate change is very simplistic, and should be updated. Currently, climate change is modeled as a change in the infiltration rate. The relationship between infiltration and increased precipitation should be investigated. In particular, DeWispelare *et al.* (1993) have compiled an expert elicitation about future climate at Yucca Mountain that may be used to improve the model. It is recommended that the climate change scenario take into account the most recent understanding of climate at Yucca Mountain and how climate relates to infiltration.

### 2—*Drilling model: Consolidate calculations of radionuclide inventory.*

The drilling code calculates inventory, using the Bateman equations, and determines the inventory for the time of the earliest drilling event. Greater efficiency may have been attainable by calculating the evolution of the inventory one time only. The calculated inventory could be used by the source term, drilling, seismic, and volcanic models, rather than being repeated in several different modules.

### 3—*Drilling model: Allow multiple waste package failure times.*

The effect of drilling is predicted to be small relative to the other releases calculated in IPA Phase 2, in part because drilling affects only a small number of waste packages. However, for cases where there is both drilling combined with volcanism or seismicity, the source term model

predicts all failures occur at the earliest time for any event. This simplifying modeling assumption could lead to predictions of earlier and larger total releases when a later disruption (volcanic or seismic event) causes widespread failure of waste packages. The drilling code and source term code should be modified to allow multiple waste package failures at different times within the same run.

### 4—*Drilling model: Reduce number of parameters and tie sampled parameters to the extent of drilling activity.*

The drilling model uses a total of 92 sampled parameters, to determine mainly the time of the drilling event, the repository area in which the drilling occurs, and whether or not the drill hole intersected a waste package. The purpose for generating these parameters in the main sampling procedure was to avoid the necessity for generating random variables at the level of a consequence module, and to maintaining tight control over all sampled parameters, for further statistical analysis. Unlike most of the other variables sampled by the LHS procedure, the parameters used in the drilling model have little physical significance. Including these parameters in the statistical correlations did not yield meaningful results, and may have detracted from the correlations between performance and other sampled parameters. Possible alternatives to the present sampling of the drilling parameters might be to have the random sampling built into the drilling module, but relying on a random seed passed to the module as a sampled parameter generated from the system-level LHS routine. Alternatively, some of the analyses in the drilling code presently done in a Monte-Carlo fashion could be reduced to closed-form statistical formulae.

### 5—*Seismic model: Improve waste package failure model for mechanical and seismic input.*

The mechanisms for failure of waste packages from seismic shaking and buckling used in IPA Phase 2 were highly simplified, and design-dependent. The model was based on the response of a flexible beam rigidly attached to the ground and oscillating at a single frequency. Failure was caused by either contact of the waste package with the wall, or exceedance of stress at the point of attachment. A more mechanistic model of seismic failure would take into account a number of additional factors, including: (1) a realistic

## 6. Disruptive Consequences

mechanical model of the waste package and its contact with the ground; (2) a spectrum of frequencies of ground motion; (3) the reduction in strength of the waste package walls predicted by realistic models for pitting, crevice, and general corrosion; (4) the mechanical contact between the waste package, rock, and backfill; (5) repeated mechanical response of the waste package to oscillatory forces; and (6) failure caused by the repeated responsive motion, including the degradation of the metal by fatigue, heat, and radiation. Seismic failure models for future iterations must, of course, take into account the most recent design of the waste package.

### ***6—Improve volcanism model in regard to probability and volcanic processes.***

As discussed in Section 6.5.3.3, the volcanism model presented is preliminary. Some assumptions inherent in the *VOLCANO* code can be improved on through additional research. For example, the near-neighbor nonhomogeneous Poisson model used to generate the probability of magmatic activity for IPA Phase 2 is one example of a spatial model that accounts for cinder cone clustering in the region. Other models, such as Neymann-Scott and Poisson cluster models, should be explored, possibly as auxiliary analyses, with an emphasis on how they would be implemented in the future IPAs. Additional geologic information, including the role of volatiles in driving magma ascent, the importance of multiple dike intrusions, and the role of pre-existing structure, also needs to be incorporated. Effects of

uncertainty in geochronological data, and related factors, need to be explored. Future models should incorporate these kinds of analyses to provide a robust and defensible estimate of the probability and effects of volcanic disruption.

### ***7—Improve volcanism model in regard to magma interaction with waste.***

In the *VOLCANO* module, only direct effects of magma interacting with the radioactive waste are considered. It is recognized that magma may have a number of indirect effects, such as changing the groundwater conditions, and accelerating the corrosion of nearby waste packages. It is recommended that the scope of consequence analyses be expanded to include indirect effects of a nearby volcanic event.

### ***8—Improve tracking of radioactive inventory in the VOLCANO module.***

The present version of *VOLCANO* keeps track of the radionuclide inventory by considering only simple decay of radionuclides present in the waste packages, with no generation of radioactive progeny. It does not keep track of radionuclides that have left the repository sub-area by the liquid or gaseous pathway. Although the latter assumption is conservative, ignoring the ingrowth of radioactive progeny of chain decay could underestimate radioactive releases of several radionuclides. *VOLCANO* should be updated to include the ingrowth of radioactive progeny in the source term.

## 7 DOSE-ASSESSMENT MODULE

### 7.1 Background

A major difference between the Iterative Performance Assessment (IPA) Phase 1 and IPA Phase 2 studies was the incorporation of a dose-assessment capability into the total-system performance assessment (TPA) computer code in IPA Phase 2. A dose assessment for the proposed repository at Yucca Mountain was not included in IPA Phase 1 for the following reasons. First, the U.S. Environmental Protection Agency (EPA) adopted, as its primary criterion for compliance with the containment regulations in 40 CFR 191.13<sup>1</sup> (*Code of Federal Regulations*, Title 40, "Protection of Environment") a restriction on the quantity of any radionuclide that could be **released** to the accessible environment for 10,000 years after permanent closure, not on the exposures of individuals or populations that might result from these releases. Second, it appeared there was little likelihood of any non-compliance with the individual dose provisions in 40 CFR 191.15, "Individual Protection Requirements" (and therefore little need for a dose assessment capability) because EPA calculations showed that radionuclides released from a geologic repository located in volcanic tuff would not reasonably be expected to expose any human being for at least 1000 years after disposal. Section 191.15 restricts the annual dose to any individual only during the first 1000 years after permanent closure of the geologic repository operations area (GROA). Third, the staff believed that, if needed, existing computer codes for dose assessment could readily be assimilated into the TPA computer code.

In its original form, the criteria to be used for licensing a geologic repository were published in

---

<sup>1</sup>Currently, a revised set of standards specific to the Yucca Mountain site is being developed in accordance with the provisions of the Energy Policy Act of 1992. The Energy Policy Act of 1992 (Public Law 102-486), approved October 24, 1992, directs NRC to promulgate a rule, modifying 10 CFR Part 60 of its regulations, so that these regulations are consistent with EPA's public health and safety standards for protection of the public from releases to the accessible environment from radioactive materials stored or disposed of at Yucca Mountain, Nevada, consistent with the findings and recommendations made by the National Academy of Sciences (NAS), to EPA, on issues relating to the environmental standards governing the Yucca Mountain repository. It is assumed that the revised EPA standards for the Yucca Mountain site will not be substantially different from those currently contained in 40 CFR Part 191, particularly as they pertain to the need to conduct a quantitative performance assessment as the means to estimate postclosure performance of the repository system.

1985 by EPA as: "Environmental Standards for the Management and Disposal of Spent Nuclear Fuel, High-Level and Transuranic Radioactive Wastes; Final Rule," 40 CFR Part 191 (EPA, 1985; 50 *FR* 38066). On July 17, 1987, the U.S. Court of Appeals for the First Circuit in Boston vacated Subpart B of this 1985 version of 40 CFR Part 191 and remanded the rule to the EPA for further consideration (see EPA, 1993; 58 *FR* 7924).

In response to this action by the court, EPA published a final revision to 40 CFR Part 191 on December 20, 1993 (EPA, 1993; 58 *FR* 66398). The revised dose provisions included an extension of the period that applied to individual dose, from 1000 to 10,000 years after disposal. This proposal would significantly increase the probability for a subsequent exposure of a member of the public to releases of radionuclides from the geologic repository. Under the Waste Isolation Pilot Project Land Withdrawal Act (Public Law 102-579) and the Energy Policy Act of 1992, this revision is not applicable to a potential Yucca Mountain repository. However, since the Energy Policy Act of 1992 directed the EPA to evaluate a health-based standard based on doses to individuals, the staff believed that addition of a dose-assessment capability in the TPA computer code for a potential Yucca Mountain site would be prudent.

### 7.2 Basis for the Calculation of Human Exposures in IPA Phase 2

#### 7.2.1 Concept of the "Reference Biosphere"

The NRC staff adopted a concept of a stable, or reference biosphere for its studies in IPA Phase 2 (see Federline, 1993<sup>2</sup>). A reference biosphere will provide a basis for quantification of dose. This "reference biosphere" implies that the locations, lifestyles, and physiology of persons who live and work in the vicinity of Yucca Mountain over the future periods of interest (up to 10,000 years and beyond) are difficult to predict. The environmental pathways that could result in human exposure to ionizing radiation will remain unchanged from those that exist in today's biosphere. In IPA Phase

---

<sup>2</sup>Federline, M.V., "U.S. Nuclear Regulatory Commission Staff Views on Environmental Standards for Disposal of High-Level Wastes," Unpublished Presentation to the NAS Committee on Technical Bases for Yucca Mountain Standards, Washington, D.C., May 27, 1993.

## 7. Dose Assessment

2, scenarios that impacted the geosphere at Yucca Mountain were assumed not to disrupt this reference biosphere.

### 7.2.2 Similarity to Assumptions in 40 CFR Part 191

The use of a "reference biosphere" in NRC's approach to dose assessment is similar to that taken by EPA during the development of the background information for 40 CFR Part 191 (see EPA, 1985; p. 7-1). EPA's approach to dose assessment for the final rule contained the following caveat: "... it is pointless to try to make precise projections of the actual risks due to radionuclide releases from repositories. Population distributions, food chains, living habits, and technological capabilities will undoubtedly change in major ways over 10,000 years. Unlike geological processes, they can be realistically predicted only for relatively short times ...." (*op cit.*) The conceptual model for the human physiology adopted by EPA included the concept of a present-day "reference man" (see International Commission on Radiological Protection (ICRP), 1975).

EPA also proposed a definition for a "reference population" as another draft revision to 40 CFR Part 191 (see EPA, 1993). The "reference population" was defined as the entity of persons that, for 10,000 years after disposal, has the following features: (a) major population relocations or emergencies have not occurred; (b) the size of the (world) population is 10 billion; and (c) characteristics and behavior affecting estimates of radiation exposure and its effects are assumed to be as today; this includes level of knowledge, technical capability, human physiology, nutritional needs, societal structure, and access to pathways of exposure."

### 7.2.3 Similarity to the Approach Taken by BIOMOVS

The use of a "reference biosphere" in NRC's approach to dose assessment is also similar to that taken by a working group in BIOMOVS, the **Biospheric Model Validation Study**. BIOMOVS is a cooperative effort by the selected members of the international nuclear community to develop and test models that were designed to quantify the transfer and bio-accumulation of radionuclides in the environment (see BIOMOVS, 1992).

BIOMOVS recommends that long-term assessments of dose be based on the conceptual model of a "reference biosphere," that is analogous to the "reference-man" concept developed by the ICRP. The participants in BIOMOVS believe that it is impossible to predict all the possible **future** evolutions (future states) of the biosphere. However, they believe it may be possible to identify a comprehensive list of important features, events, and processes that are essential for safe disposal of high-level radioactive waste (HLW) in a geologic repository sited in the **present-day** environments. The range of present-day environments is expected to bound the biospheres expected in the various future states. (Because of the diversity of nature, BIOMOVS recognizes that it may be necessary to define a number of different "reference biospheres".) NRC staff is currently considering this concept.

## 7.3 Computer Code Selected for Dose Assessment

Human exposures in the IPA Phase 2 study were evaluated by *DITTY* (Dose Integrated for Ten Thousand Years) (see Napier *et al.*, 1988a; pp. 3-16—3-18), a new module added to the version of the TPA computer code. *DITTY* was selected for IPA Phase 2 because: (a) it could be used to calculate the relative variation in doses for the various scenarios used in Phase 2 (it does not predict the absolute doses for comparison with other performance-assessment studies); (b) it was easily interfaced to the outputs of other consequence modules used in the TPA computer code; (c) it could calculate population doses over durations of 10,000 years or more; and (d) it was available and could be executed with little further development.

### 7.3.1 Overview of DITTY

*DITTY* estimates the time integral of collective dose over a 10,000-year duration for releases of radionuclides to the accessible environment. *DITTY* can treat both chronic and acute releases of radionuclides. Only a few input parameters to *DITTY* can be entered as input variables at various times during the 10,000-year period. These include:

- Annual releases of radioactivity to air and water;

- The number of persons in the exposed regional population; and
- The dispersion factors in the terrestrial and aquatic environments.

*DITTY* breaks the 10,000-year duration into 143 periods of 70 years (each period is considered to be the length of a human lifetime), and the total population dose is determined for each of the 143 periods. The radioactivity present during any 70-year period is the sum of the activity in the nuclides released during that period and the residual radioactivity in the environment caused by releases in previous periods.

In IPA Phase 2, the exposure pathways to the accessible environment that were of interest are illustrated in Figure 7-1. These include: the atmosphere, land surfaces, the top 15 centimeters of surface soil, vegetation, animal products (milk, beef), and drinking water. Aquatic pathways were not considered in this study because they are not credible pathways near Yucca Mountain. The quantities of radionuclides released from the repository that move into the environmental media along these pathways are used to calculate concentrations and dose in the reference biosphere. *DITTY* cannot calculate concentrations of radionuclides in the lithosphere or the ground water contained therein.

For IPA Phase 2, the annual releases to the air or water pathways at selected times, during the 10,000-year period of regulatory interest (the source terms), were provided as input to *DITTY* by other TPA computer code modules in the form of average annual concentrations. Up to 450 of these paired values can be entered as an input file (e.g., as curies per year/time or curies per volume/time). The values for these concentration-time pairs were obtained as outputs directly from the *NEFTRAN* module, or indirectly, from the *C14*, *DRILL02*, and *VOLCANO* modules (see Figure 2-1).

*DITTY* calculates the downwind regional air concentrations as the product of the release rate of radionuclide (from the ground surfaces above the geologic repository into the atmosphere) and a dispersion factor, commonly designated as  $X/Q$ . For waterborne releases, in addition to the calcu-

lation of collective doses, *DITTY* will identify that 70-year period when the individual lifetime (70-year) dose is highest.

### 7.3.2 General Approach to Dose Calculations in *DITTY*

A calculation of internal dose to a human-body organ in *DITTY* can be visualized as the product of four parameters, so that for any single radionuclide:

$$D = C \times FTC \times U \times DCF ,$$

where  $D$  is the dose to a body organ from the radionuclide per year of intake;  $C$  is the concentration of radionuclide in a specific media (e.g., curies per kilogram of pasture grass eaten by beef cattle);  $FTC$ , is identified in *DITTY* as the food-transfer coefficient, is a dimensionless factor that expresses the distribution ratio of a radionuclide between two media at steady-state (e.g., the ratio of the steady-state concentration in the edible tissues of the beef cattle to the steady-state concentration in pasture grass);  $U$  is the human- or animal-use factor (e.g., kilograms of beef eaten per year) for the media; and  $DCF$  (dose conversion factor) is the quantity that will convert radioactivity ingested or inhaled into dose (e.g., rem/curie). The  $DCF$  values and the  $FTC$  values used in this study, which are described in Section 7.7, are different from values in the original *DITTY* databases.

### 7.3.3 Calculation of Total Dose in *DITTY*

The total population dose is expressed in terms of an *Effective Dose Equivalent* (EDE). This dose is the sum (over all organs) of internal and external doses that result from direct radiation or uptakes of radionuclides into the human body along the pathways illustrated in Figure 7-1.

Internal doses to body organs can result from the inhalation of airborne radioactivity or from the ingestion of radionuclides in contaminated food and water. In *DITTY*, these organ doses are multiplied by a risk-based weighting factor to give "effective" organ doses (i.e., committed EDE). The values used for these organ-weighting factors in *DITTY* are the same as those given in ICRP-26 (ICRP, 1977). All internal doses are integrated over the 50-year period that follows an intake of

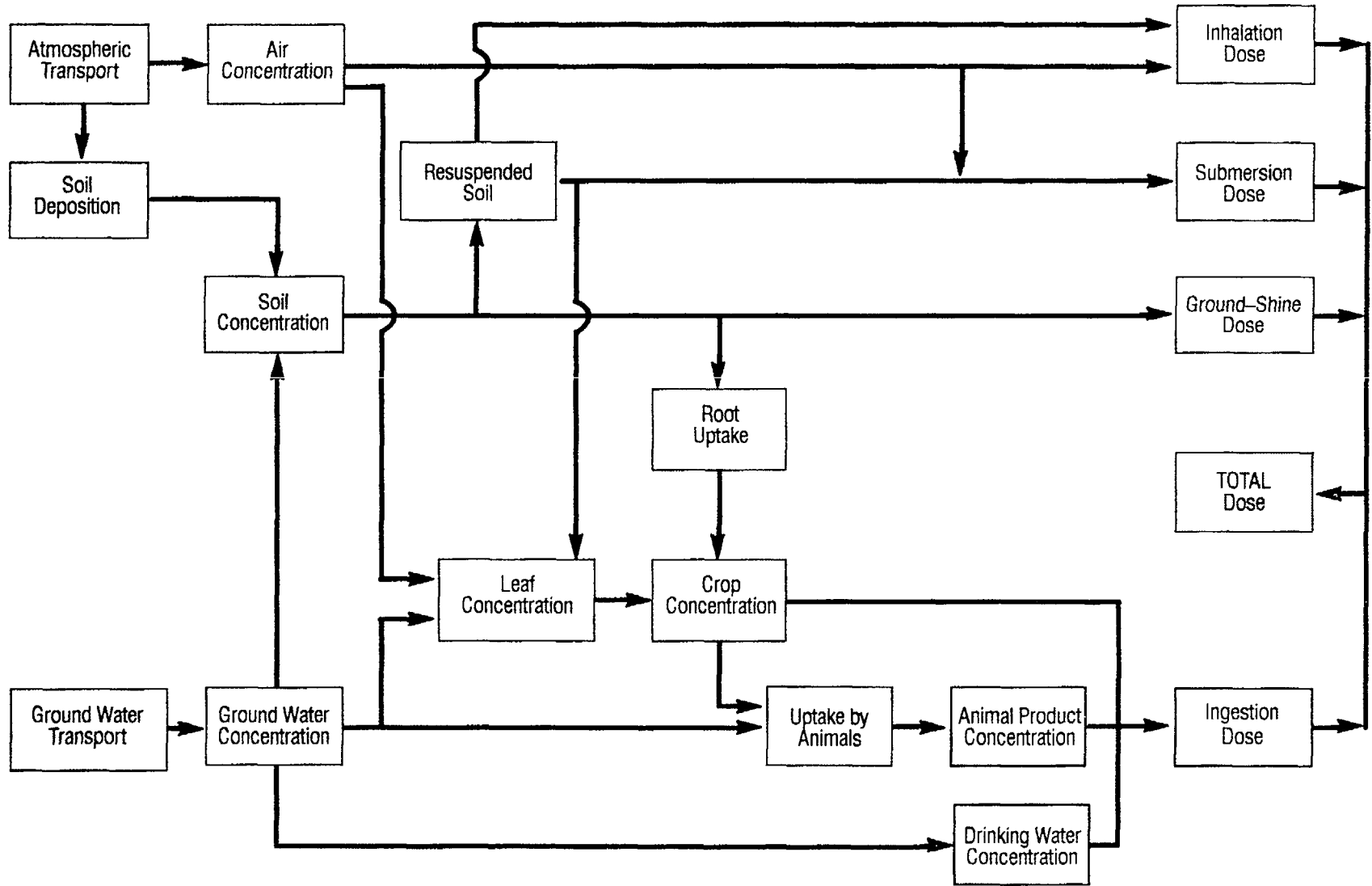


Figure 7-1 Human exposure pathways in the accessible environment, as calculated by the *DITTY* computer code

radionuclides (i.e., for a dose-commitment period of 50 years in the human body). The integrated dose is formed from the sum of the doses to six designated body organs and to the five remaining organs with the highest doses.

External exposures can result either from submersion of the human body in airborne radioactivity or from exposure to direct radiation (ground shine) that emanates from the surface of contaminated soil. In *DITTY*, organ doses caused by external exposures are expressed in terms of the EDE, instead of the more common dose equivalent quantities. A special energy-dependent dose factor (rem/rad) is used in *DITTY* to convert external doses to the body surfaces to deep organ-doses (Kocher, 1981). The use of these conversion factors in *DITTY* has preceded any guidance by the Commission on acceptable methods for calculation of EDE from external photon and particulate radiation.

### 7.3.4 Selection of *DITTY* Model Parameters

For IPA Phase 2, default values for the model parameters from *DITTY* were used in the dose-assessment models unless indicated otherwise. Probability density functions were not defined, and Latin Hypercube Sampling (LHS—discussed in Chapter 2, “Total-System Performance Assessment Computer Code”) was not attempted for any parameter used in the dose-assessment models. This was done intentionally to focus attention on the magnitude of the uncertainties introduced into the resulting doses by the collective uncertainties associated with the source term and geosphere models used in IPA Phase 2. In the future, it will be necessary to estimate site-specific values for the *DITTY* model parameters to make the most meaningful calculations of dose. In many cases, a literature study should be sufficient to select these values. However, for those radionuclides that are major contributors to the dose, laboratory and field studies may also be desirable. Sensitivity studies, similar to those conducted in other IPA Phase 2 modules (see Chapter 9, “Sensitivity and Uncertainty Analysis”), should also be carried out for parameters in the biosphere models. In this way, the parameters that significantly influence the magnitude of the doses and that may require further study in the field may be identified.

## 7.4 Differences From Internal Dosimetry Models in ICRP-30

The major differences of the biokinetic models in *DITTY* from those in ICRP-30—“Limits for Intakes of Radionuclides by Workers” (ICRP, 1979)—are found in the computer program *GENMOD*. *GENMOD* (Johnson and Carver, 1981), which was adapted directly from ICRP-30, incorporates additional models other than those developed by the ICRP (such as the alkaline earth model, the *MIRD* iron model, and the  $^{14}\text{C}$  model). *GENMOD* was used to generate databases that include values for the following metabolic parameters for each radionuclide used in *DITTY*: organ uptake, transfer coefficients from compartment to compartment, and elimination rates from compartments. The metabolic models for carbon assume it is inhaled as carbon dioxide gas, and that ingested carbon is in the form of carbohydrates that are readily absorbed through the gut and rapidly distributed throughout the body.

Although metabolic parameters for various ages, sexes, and ethnic groups were not available when this study was undertaken, they may require further consideration when guidance for members of the public becomes available. A rough estimate of the variation of lifetime dose with the age of initial exposure may be inferred from the Statement of Considerations for the final rule for 10 CFR Part 20 (*Code of Federal Regulations*, Title 10, “Energy”) which notes that “... those organs for which age dependency is important, such as the thyroid gland, are of lesser importance because of the lower  $w_T$  values [risk-weighting factors] ... used to calculate the effective dose. A factor of 2 is included ... which, in part, accounts for age dependency ...” (NRC, 1991; 56 *FR* 23390). This appears to be a reasonable assumption, given the observation recently made by Charles and Smith (1991, p. 10) that “... the generally higher committed doses per unit intakes for non-adult age groups are in the main cancelled by the lower consumption of foodstuffs ....”

## 7.5 Selection of DCFs for this Study

### 7.5.1 DCFs for Ingestion and Inhalation

In IPA Phase 2, the *DCF*s’ values were assumed to be without bias and of the highest precision. Since it was assumed that a “reference man” in a “reference biosphere” was exposed over the

## 7. Dose Assessment

10,000-year period when radionuclides were released from the geologic repository, the same *DCF*s were used for calculations of dose during each of the 70-year human lifetimes considered in *DITTY*. The *DCF*s for the radioactive daughters that are produced *in vivo* were generally also described with the same metabolic parameters as those for the parent radionuclide.

The *DCF*s for inhalation and ingestion, used in IPA Phase 2, which were prepared by Dr. Paul Rittman of Westinghouse Hanford Company, from the revised computer code *INTDF* (Version 1.483) (see Napier *et al.*, 1988a; pp. 3-13-3-16), are the "worst-case" values. These parameters, which pertain to each radionuclide used in *DITTY*, maximize either the inhalation dose by an intentional selection of the chemical form with the worst-case solubility in the lung, or the ingestion dose, by selection of the chemical form that results in the largest uptake in the small intestine ( $f_1$  value) for each radionuclide, or both. When normalized to an annual basis, the *DCF*s generated by *INTDF*, a *DITTY* sub-routine, are essentially the same as those reported in EPA's Federal Guidance Report No. 11 (i.e., to within two significant figures, but with a few differences for very short-lived nuclides) (EPA, 1988).

The dose-commitment period for all *DCF*s used in this study is 50 years. This is consistent with 10 CFR Part 20 and also with the recommendations of both national and international committees on radiation protection. A 50-year dose-commitment period was also suggested by EPA for Appendix B of 40 CFR Part 191 (see EPA, 1993; 58 *FR* 7936). Since *DITTY* assumes that an individual will experience an annual intake of radionuclides during each year of his 70-year lifetime, the use of this 50-year dose commitment period will overestimate his lifetime dose for those radionuclides with a long biological half-life (but in no case by more than a factor of 2).

### 7.5.2 *DCF*s for External Exposure

The *DCF*s for air submersion and for direct radiation exposure to radionuclides deposited on land surfaces (ground shine) were used in this study are unchanged from those as found in the databases of the *DITTY* code. These values will be reviewed when EPA publishes Federal Guidance No. 12 (in preparation), a tabulation of dose

coefficients for external exposure to photons and electrons emitted by radionuclides distributed in environmental media.

## 7.6 Selection of Parameters for the Ingestion Pathways

The bases for selection of data used in the terrestrial-ingestion pathway models of *DITTY* are discussed below.

### 7.6.1 Drinking-Water Parameters

The original version of the database *BIO-ACI.DAT* contained factors to simulate the treatment of drinking water by a municipal water-treatment plant. For IPA Phase 2, drinking water was assumed to be taken from a surface well without any treatments to remove radionuclides (all treatment factors were set to a value of 1). This is equivalent to the assumption that the concentration of a radionuclide in drinking water has the same concentration as it had in the ground water that feeds the well. The IPA Phase 2 analysis did not consider mitigating measures available in present-day technology. These measures may include devices to monitor waterborne radiation or procedures, such as water treatment or condemnation of the well.

### 7.6.2 Food-Transfer Parameters

The documentation in *DITTY* does not identify the sources of the soil-to-food transfer parameters stored in the *DITTY* file *FTRANS.DAT*. The *User's Manual* for *DITTY* indicates that the "... sources of these parameters are to be published in a separate document" (see Napier *et al.*, 1988b; pp. 2.28-2.29). Since literature citations were not available during IPA Phase 2, *FTRANS.DAT* parameters were replaced by "generic" parameters taken from the well-known study by Baes *et al.* (1984).

The "Baes" parameters used in this study ( $B_v$ ,  $B_r$ ,  $F_f$ , and  $F_m$ ) are based on clearly-defined protocols that were used to select them from the multiplicity of experimental values reported in the literature. For example, for the soil-to-crop values, the Baes *et al.* study attempted to select concentration ratios that were based on detailed literature studies in which the soil and plant concentrations were **both** measured at "edible maturity" of the plant. These literature citations show that

large variations (orders of magnitude) of these parameters in various environmental settings are not uncommon, and therefore most studies use site-specific values to increase the reliability of dose estimates.

The *DITTY* parameters for each chemical element that was stored in the file *FTRANS.DAT* were replaced by the following types of Baes parameters (dry-weight to dry-weight basis):

- A  $B_r$  value (Baes *et al.*, 1984; Figure 2.1) replaced each soil-to-leafy-vegetable concentration ratio;
- The same  $B_r$  value (*op cit.*, Figure 2.2) replaced each of the four soil-to-edible-crop concentration ratios (these crops are vegetable, root, grain, and fruit);
- A  $F_f$  value (*op cit.*, Figure 2.25) replaced the feed-to-meat transfer coefficient; and
- A  $F_m$  value (*op cit.*, Figure 2.24) replaced the feed-to-milk transfer coefficient. The poultry and egg pathways were not used in the IPA Phase 2 studies, and therefore these food-transfer coefficients were not modified.

These new values, which are stored in a new file *FTRANS.CFB*, were used for all calculations of dose in IPA Phase 2.

The leaching factors for soil in *FTRANS.CFB* are unchanged from the values in *FTRANS.DAT*. The magnitudes of the leaching factors in *DITTY* are directly proportional to the percolation rate of water through the rooting zone and into deeper soil layers (an over-watering term of 15 centimeters/year was assumed in *DITTY*). In IPA Phase 2, small variations in the leaching factors for very mobile radionuclides (e.g. technetium and iodine), were shown to have a significant impact on the cumulative magnitude of dose. For models like *DITTY*, that involve long-term deposition of radionuclides in soil, the leaching factors should be obtained from site-specific investigations, to properly characterize the retention of radionuclides in soil and their biological availability to crops (International Atomic Energy Agency (IAEA), 1982).

### 7.6.3 Growing-Season Parameters

The site-specific agricultural parameters for Yucca Mountain that were entered as input data to *DITTY* included: the length of the growing season, the irrigation rate for crops during the growing season, and the yields of the various types of crops. The lengths of the growing season depend on the crop type. One of the most important crops in Nevada is alfalfa, which can grow up to 250 days each year and produce up to eight 30-day harvests each year. For most vegetables, the first growing season begins in February and ends in early-March; the second season begins in mid-August and ends in mid-October. Very little appears to grow during the hot, dry summer months between late-May and late-August (Mills, 1993).

The lengths of the growing period selected for this study were: For leafy vegetables, 45 days; for "other" vegetables, 90 days. For alfalfa, and for those pasture grasses that are consumed as by animals as forage, the growing season was taken as 30 days (Kennedy and Strenge, 1992; Table 6.12).

### 7.6.4 Irrigation Rate for Crops

The State of Nevada issues water-use permits that limit the maximum pumping rate from wells in the vicinity of Yucca Mountain to 127 liters/month/square meter (~152 centimeters/year) of irrigated land (Personal comm., Nevada State Engineer's Office). For areas within 100 kilometers of the geologic repository, the irrigation period was assumed to coincide with the average length of the growing season (i.e. 60 days). Irrigation was assumed to proceed at the maximum pumping rate allowed by the water permit (see "Rate of Irrigation" in Section 7.8.2).

### 7.6.5 Crop Yields (Human Consumption)

The yields of the irrigated crops (in kilograms per square meter), and the quantities consumed by humans (in kilograms per year, in parenthesis) are taken from Tables 6.14 and 6.15, respectively, in Kennedy and Strenge (1992, Vol. 1). The values used in *DITTY* are: leafy vegetables, 2.0 (11); "other" vegetables, including grains, fruits and root vegetables, 4.0 (172); the pasture grasses and alfalfa that fatten beef cattle and leads to milk production, 1.5 (milk, 100 kilograms/year and beef, 59 kilograms/year). These values are not

## 7. Dose Assessment

inconsistent with those found to grow in Nevada lowlands (Nevada Agricultural Statistics Service, 1988).

Milk cows are assumed to consume vegetation at the rate of 55 kilograms/day and beef cattle at 68 kilograms/day. Milk cows are assumed to drink water at the rate of 60 liters/day and beef cattle at 50 liters/day. These parameters are default values in *DITTY* (found in data statements).

### 7.7 Selection of Parameters for the Inhalation Pathways

#### 7.7.1 Meteorological Data

The meteorological data selected for *DITTY* was a composite of the annual averaged STAR (Stability Array) data measured by the National Oceanographic and Atmospheric Administration between 1986 and 1990, at Station Number 03160, Desert Rock, Nevada, which is 935 meters above sea level (U.S. Department of Commerce (USDC), 1992). Data were available for seven stability classes, six wind speeds and for 16 compass directions. Data from this particular location were selected because of their availability. These data was used to calculate the concentrations of airborne radionuclides in the region surrounding the geologic repository.

All releases of radioactivity from the geologic repository were assumed to occur at ground level and to disperse radially out to a distance of 100 kilometers. (The distance between radial segments illustrated in Figure 7-2 is 20 kilometers.) A Gaussian plume model was used to convert releases of radioactivity to long-term, sector-averaged  $X/Q$  values (expressed in units of seconds per cubic meter released). In this study,  $X/Q$  values were estimated by *DITTY* at the following distances: 2.5, 7.5, 15, 30, 50, 70, and 90 kilometers. These distances are measured radially from the release point in the GROA to the midpoints of the wedge-shaped sectors shown in Figure 7-2 (e.g., a mid-point distance of 30 kilometers (North) is midway between the 20-kilometer (North) and 40-kilometer (North) distance intervals).

#### 7.7.2 Regional Population Distribution at Yucca Mountain

The size of the regional population exposed to airborne releases of radioactivity was assumed to

be stable throughout the entire 10,000-year period. Members of this population were located at the mid-points of the wedge-shaped sectors shown in Figure 7-2 (i.e., those distances identified in Item (1), above).

The dispersion studies were extended to 100 kilometers, to include the 5500 persons who were residents of the city of Pahrump in 1988. This regional population distribution in Figure 7-2 was taken from Logan *et al.* (1982) and was updated with information obtained from DOE's 1988 Site Characterization Plan (see DOE, 1988; Table 3-21).

### 7.8 Application of the Dose-Assessment Methodology to Yucca Mountain: Biosphere Scenarios

#### 7.8.1 Application of the "Critical-Group" Concept

Whenever a radiological assessment is undertaken before the operation of a new nuclear facility, the specific individuals who may receive the highest exposures and greatest risks in future time cannot be identified. In these circumstances, it is appropriate to **define** a hypothetical critical group (i.e., those persons who receive the highest exposures) because this approach avoids the need to forecast future lifestyles, attitudes to risk, and developments in the diagnosis and treatment of disease. In principle, the critical group should be defined by age, sex, and ethnic origins since intakes, metabolism, and dosimetry of radionuclides are all strongly conditioned by these factors (IAEA, 1982). As noted in Section 7.4, a rough estimate of the variation of lifetime dose with the age of initial exposure may be inferred from the Statement of Considerations for the final 10 CFR Part 20 rule.

#### 7.8.2 Hypothetical Biosphere Scenario: Waterborne Release

Section 191.15 of 40 CFR Part 191 requires that "... all potential pathways ... from the disposal system to people shall be considered ... including the assumption that individuals consume 2 liters/day of drinking water from a significant source of

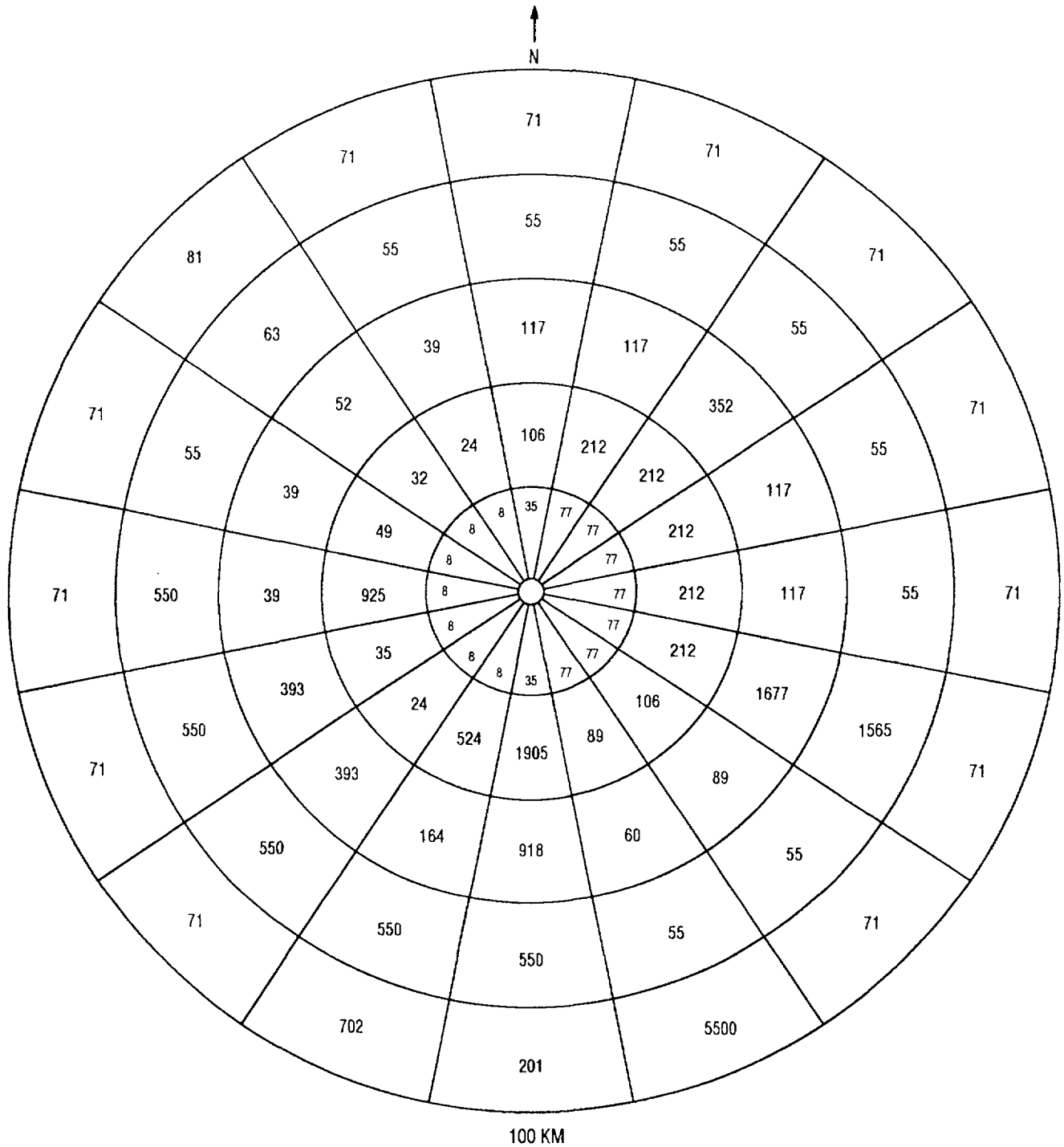


**Figure 7-2** Estimated population distribution in the vicinity of Yucca Mountain, Nevada (The population distribution, as of December 1988, is 22,200. Adopted from Logal *et al.* (1982) and DOE (1988).)

## 7. Dose Assessment

ground water outside of the controlled area." A contemporary farm family of three persons was selected as the hypothetical critical group, to illustrate the capability for dose assessment that was incorporated into the TPA computer code in IPA Phase 2.

**Location:** The hypothetical family is assumed to maintain a year-round residence on an average-sized farm (approximately 1093 hectares) located at the boundary of the controlled area (10 CFR 60.2) that surrounds the geologic repository at Yucca Mountain. Contaminated water pumped from a local well irrigates two areas on this farm: a 88-hectare tract, an area which is set aside as irrigated pasture land for calves (yearlings) and other cattle (agricultural statistics for Nevada for the 1987-88 period estimates that approximately 100 farms, with a irrigated land area of 12,146 hectares, are irrigated in Nye County); and a fenced-in tract of 1.2 hectares, which is used to grow a large portion of the family vegetables (leafy and other), fruits and grains for home consumption (the growing periods and yields of crops, and the human consumption of meats and crops were adopted from Kennedy and Strenge (1992, Tables 6.12-6.15)). The remaining 1004 hectares of un-irrigated and un-contaminated land are used to graze mature beef cattle.

**Drinking Water:** Each member of this contemporary family is assumed to obtain all of his/her drinking water (2 liters/day of drinking water for 365 days/year) from a contaminated well at the boundary of the controlled area. The composition of this well water is assumed to be similar to that found in U.S. Geological Survey Well J-13. Well J-13 is located approximately 13 kilometers southeast from the controlled area boundary of the repository. The current capacity of the pump at Well J-13 is 2385 liters/minute (maximum) which is approximately 4 million liters/day (see Czarnecki, 1992; Table 1).

**Rate of Irrigation:** Fluxes of radionuclides to the well used by the farm family emanate from the seven subareas in the model of the repository for the Yucca Mountain site, as depicted in Figure 4.6, and are calculated by the TPA computer code that invokes the models for source term releases, flow, and transport. The seven geologic repository sub-areas have different physical and chemical properties that govern the times of release of the

radionuclides from the waste form and the travel time through the geosphere. Thus, the concentration of the radionuclides in the well at the point of use by the farm family is a complicated function of time.

To obtain the concentrations of radionuclides in the contaminated well water after a waterborne release, the fluxes of radionuclides in the aquifer (calculated at the location of the well) were diluted to a volume of 4 million liters/day. Approximately 4 million liters/day would be required to irrigate the garden plot and the pasture area (88 hectares irrigated at a rate of 127 liters/square meter-month). This dilution flow was considered consistent with the water usage by the farm family and for stock watering. These concentrations were calculated at selected times during the 10,000-year period of study and were used as input to *DITTY*.

**Consumption of Foods:** Reports by the USDC indicate that no farms in Nye County sell dairy products for profit (USDC, 1989; p. 138). The farm family is therefore assumed to own cows only to provide dairy products for their own consumption. Of the 136 farms identified in Nye County in 1987, only eight farms raised poultry, and only nine farms raised hogs and pigs (*op cit.*). The family is assumed to purchase pork, poultry, eggs, and small quantities of fruits, vegetables, and grains at a local supermarket supplied with un-contaminated foodstuffs by a distributor from another geographical area. The family is assumed to consume 100 percent of their beef and milk from farm animals that feed on vegetation irrigated by contaminated well water.

**Inside/Outside Activities:** Annually, the hypothetical person is assumed to spend 6424 hours (73 percent) inside his home (TV, sleep, etc.), and to spend 2336 hours outside the home (farming, herding cattle, and recreation). If the hours spent inside the home are weighted by a shielding factor of 0.5 (NRC, 1977; p. 43) and added to the hours spent outside, the effective time that this person would be exposed to external ionizing radiation (ground shine and submersion in airborne radioactivity) would be 5548 hours/year.

**Exported Beef Cattle:** Beef cattle (60 percent mature and 40 percent calves) sold for profit are assumed to obtain 100 percent of their feed from the contaminated vegetation raised on the 88 hectares of irrigated pasture land on the family

farm. Half of these animals (43 calves and 32 cattle), that are exported off the farm and sold for profit each year, are estimated to produce 10,377 pounds/year of edible beef. This quantity of beef will feed 177 persons/year, if it is assumed that one person consumes 129 pounds (59 kilograms) of beef each year (approximately 1 hamburgers/day every day of the year).

### 7.8.3 More Realistic Biosphere Scenario: Waterborne Release

A more realistic biosphere scenario would involve exploitation of ground waters near Yucca Mountain, to supplement the municipal water supply for regional populations. Water consumers in the region would then form the critical group whose doses would be limited by an individual protection standard (Federline, 1993). This scenario may be explored further in future IPA analyses.

### 7.8.4 Hypothetical Biosphere Scenarios: Airborne Releases

**Mechanisms of Release to the Atmosphere:** In IPA Phase 2, contaminated soil (or gaseous  $^{14}\text{C}$ ) was assumed to be transported to the ground surface above the repository as a result of disruptions of the geologic repository either by human intrusion (e.g., by exploratory drilling) or by an extrusive volcano (only for cone magma events). As many as 20 radionuclides might contribute to the radioactivity in this contaminated soil. During the 10,000-year period in this study, the times that the releases to the atmosphere from the contaminated ground surface could occur are governed by model parameters. The time of release is therefore a variable, because it depends on the particular vector set used to generate the dose for any given scenario (these times and the vector sets are determined by LHS sampling of appropriate model parameters).

Only a fraction of this released radioactivity was assumed to become available for transport by the air pathway to members of the public beyond the controlled area of the repository. The fractions of the radioactivity that were assumed to become airborne were: 0.04 for the human intrusion scenarios; 0.30 for the magmatic eruption scenarios; and 1.0 for the  $^{14}\text{C}$  scenarios. (These values were stored in the *AIRCOM* module of the TPA computer code (see Section 2.1.3).) All the airborne

radioactivity was assumed to be respirable (whether in the solid, liquid, or gaseous states). Any radioactivity that did not become airborne was considered to remain undisturbed at the point of release to the above-ground surface.

The NRC staff made preliminary estimates of the fractions of radioactivity, released from the human intrusion and volcano scenarios, that became airborne. For the human intrusion scenario, a company that manufactures drill bits advised the staff that for a large hole, which was drilled into a hard formation such as granite, approximately 25 percent of the drilling would pass through a 200-mesh screen. (This means that 25 percent of the cuttings would be smaller than 62 microns). The staff assumed that the grain sizes of cuttings below 62 microns followed a uniform distribution. From a typical plot of grain size versus cumulative percentage of cuttings retained in the various-sized sieves (e.g., see Freeze and Cherry, 1979; p. 351), the staff estimated that one-sixth of this material would be smaller than 10 microns. It follows that roughly 4 percent of the total mass of the drill cuttings would be smaller than 10 microns ( $25/6 = 4$  percent). For the volcano scenario, the NRC staff obtained the respirable airborne fractions from Fisher and Schmincke (1984). For "explosive" volcanic eruptions, they claim that between 10 to 30 percent of the material that becomes airborne is smaller than 10 microns.

**Calculation of Dose for Airborne Releases:** The sequence of calculations by the TPA computer code that results in an estimate of the doses to the regional population (or the farm family) after exposure to an airborne release of radioactivity from the geologic repository is as follows. First, the consequence modules *DRILLO2*, *VOLCANO*, and *C14* calculate the quantities of radionuclides in contaminated soil (or gaseous  $^{14}\text{C}$ ) that are released to the ground surface in any given year. These quantities of surface radioactivity are then multiplied by the corresponding fractions stored in the *AIRCOM* module to generate the quantities of radioactivity that becomes airborne and respirable during that year. These latter values are in a format that is compatible with the *DITTY* module (curies per year released to air at various times).

*DITTY* calculates the concentrations of radionuclide in the various media (refer to Figure 7-1) that result from an airborne release and converts

## 7. Dose Assessment

these to dose. The semi-infinite plume model was used to calculate doses caused by submersion in contaminated air. For this exercise, wind speeds measured at the Desert Rock Station were not corrected to ground-level.

**Airborne Releases of  $^{14}\text{C}$ :** The models for  $^{14}\text{C}$  (gaseous release), human intrusion, and magmatic eruption were used to estimate the releases of gaseous  $^{14}\text{C}$  to the atmosphere. Eventually, all of the  $^{14}\text{C}$  that escapes from degraded waste package canisters emplaced in the repository is assumed to travel through the geosphere and to be gradually released to the atmosphere as carbon dioxide gas. In *DITTY*, this  $^{14}\text{C}$  is further assumed to be incorporated into vegetation by the photosynthesis process, with a resulting specific activity in the plant that is identical to that in the contaminated atmosphere. *DITTY* also assumes that 10 percent of the specific activity in soil is transferred to the edible plant, to augment the photosynthesis process.

In Section 4.3, the releases of  $^{14}\text{C}$  were estimated to occur over an area of several square kilometers. But, in this study, all  $^{14}\text{C}$  releases to the atmosphere were assumed to emanate from a point source located at the approximate center of the GROA. The exposure values reported in IPA Phase 2 for  $^{14}\text{C}$  are therefore expected to overestimate collective dose, since the concentrations of gaseous  $^{14}\text{C}$  from the area source would be more diffused, and therefore smaller, than those from a point source.

### 7.9 Conclusions and Possible Considerations for Future Dose Assessments

#### 7.9.1 Conclusions

Although dose-related parameters were not sampled in this total-system performance assessment, the uncertainty inherent in the dose assessment calculation can be significant, and adds to the uncertainty being propagated in the release model. Much of the uncertainty in dose is associated with inherent uncertainties in the parameters used for the human physiology and environmental pathway models in the *DITTY* computer code. The *DCF* may not always reflect the individual differences (e.g., age, metabolism, sex, etc.)

in human response to ionizing radiation. The parameters used in this study for the environmental pathway analyses are not always site-specific, and furthermore, are considered to be invariant in space and time. Nevertheless, the results of the dose assessment provide valuable insights regarding the performance of the geologic repository, and are summarized below:

- A gaseous release of  $^{14}\text{C}$  makes a significant contribution to the *Normalized Release*,<sup>3</sup> but its corresponding impact on the cumulative population dose is insignificant.
- The radionuclides that made the largest contributions to the population doses (accumulated over 10,000 years) were:  $^{94}\text{Nb}$ ,  $^{210}\text{Pb}$ ,  $^{243}\text{Am}$ , and  $^{237}\text{Np}$ . (Refer to Section 8.3.2. for additional discussion.)
- The scenario classes most likely to impact dose were those composed of some combination of the following independent events: drilling into a waste package canister, plus a change in climate, plus a seismic event. (Refer to Figure 9-7b in Section 9.3 and the discussion of climate in Section 9.2.3 for additional discussion.)
- The average annual inhalation dose to an individual in the Yucca Mountain region was negligible compared to the average annual dose caused by the ingestion of contaminated drinking water and locally-grown contaminated food (both averaged over a 10,000-year period as discussed in Section 9.6).
- Further data development and site characterization are desirable, if not necessary, to help reduce the uncertainty in many important parameters in the biosphere model (such as the leaching rates in soil).

#### 7.9.2 Considerations for Future Dose Assessments

The following recommendations should be considered for adoption in future dose assessments that might be conducted by the staff as part of its IPA work.

<sup>3</sup>Defined as cumulative total releases of radionuclides at the accessible environment. See Section 8.1.

**1—Improve the DITTY dose-assessment model**

- Display the results of dose assessments with multi-dimensional plots (cumulative and organ doses should be functions of both the type of radionuclide and the exposure pathway).
- Re-calculate the *DCF*s used in IPA Phase 2, to obtain a more accurate estimate of population doses for long-lived radionuclides (as discussed in Section 7.6).
- Verify that the model parameters currently used in *DITTY* are applicable to the Yucca Mountain site; identify the ranges of these parameters.

**2—Evaluate other dose-assessment computer codes**

- Evaluate other computer codes that could be used to estimate long-term individual and collective exposures and that should be explored if dose becomes a performance requirement. One code that has these capabilities to be explored is *GENI-S* (see Leigh *et al.*, 1993). Many of the databases in this code are common to the *DITTY* code used in this study.
- Evaluate atmospheric dispersion (or diffusion) models that can calculate

atmospheric concentrations caused by releases of radionuclides from area sources. These models could be used to obtain better dose estimates for releases of gaseous  $^{14}\text{C}$ .

- Evaluate atmospheric dispersion models that consider aerosols of a variety of particle sizes, shapes, and densities.
- Evaluate demographic models that can project the growth of a population. This feature would be useful for calculation of collective dose.
- Evaluate methods employed by international organizations for calculation of dose into the far future (e.g., BIOMOVS and the Nuclear Energy Agency).
- Incorporate the “1990 Recommendations of the International Commission on Radiological Protection” (ICRP, 1990), into the codes used for dose calculations, when adopted by the Agency.

**3—Conduct sensitivity/uncertainty analyses**

- Apply the statistical sensitivity and uncertainty methodology developed in IPA Phase 2 for the geosphere models to the dose-assessment models.

## 8 SENSITIVITY AND UNCERTAINTY ANALYSIS<sup>1</sup>

### 8.1 Introduction

The purpose of sensitivity and uncertainty analyses is to gain an understanding of the relationships between the repository performance measures and the input parameters used to formulate the models. The overall performance measures for the geologic repository used in the Iterative Performance Assessment (IPA) Phase 2 analysis are cumulative total releases of radionuclides at the accessible environment (*Normalized Release*) and doses to the exposed population (*Effective Dose Equivalent*). Because of the complexity of the systems comprising a geologic repository, it is not usually possible to develop exact analytical expressions for the functional relationship between repository performance and the input parameters used to formulate the models. Empirical relationships may be inferred by inspecting the model performance measures and input parameters in a variety of ways. This section will illustrate a number of techniques used for determining the relationships among parameters and their importance to the model performance.

Performance assessments for the geologic repository are based on conceptual models, embodied as computer programs, and measured field and laboratory data. Because of the inherent variabilities and sparsity of the measured data and the underlying uncertainty concerning the processes included in the models, the results of any performance assessment have significant uncertainty. An important aspect of conducting a performance assessment for a geologic repository is quantifying the sensitivity of the results to, and the uncertainty associated with, the values of the input parameters. An analysis of model sensitivity will provide information concerning which input parameters are most important to the results. A better understanding of those parameters that have the most influence on the results can hopefully lead to improvement in the models. Likewise, from a review standpoint, identification of the most sensitive parameters provides a means of comparing and evaluating different performance assessment models and indicates where reviews of

data should be concentrated. This section discusses how variation in model output reflects variation in the input parameters.

### 8.2 Overview of Techniques and Methods

#### 8.2.1 Background

A variety of techniques have been used to quantify the uncertainty and sensitivity in complex models for assessing radiological impact on man and the environment. These include: the Monte Carlo method (Helton 1961); fractional factorial design (Cochran, 1963); differential analysis (Baybutt *et al.*, 1981); response surface methodology; Fourier amplitude sensitivity (Helton *et al.*, 1991); and the Limit-State Approach (Wu *et al.*, 1992). No one technique is definitive and several can be used together to evaluate total-system performance assessments. Because comparisons of the methods employed in each approach may be found in several works (Zimmerman *et al.*, 1991; Helton *et al.*, 1991; and Wu *et al.*, 1992), only a limited evaluation is provided here. The Monte Carlo approach was used in the present performance assessment. Regression analysis and differential analysis as means of determining sensitivity to individual parameters are compared in Section 8.4.4.

#### 8.2.2 IPA Phase 1 Sensitivity and Uncertainty Analyses

IPA Phase 1 examined sensitivity and uncertainty for radionuclide releases at the accessible environment for a geologic repository in unsaturated tuff (see Section 9.5, "Sensitivities and Uncertainties for Liquid-Pathway Analysis," in Codell *et al.*, 1992). The consequence models were significantly simpler than those in the present study, and there was a narrower range of scenarios considered.

##### 8.2.2.1 Sensitivity Analyses

Four sensitivity analyses were performed for IPA Phase 1: (a) sensitivity analyses demonstrating the effect of individual parameters on the resultant Complementary Cumulative Distribution Function (CCDF) for cumulative release to the accessible environment (10 CFR 60.112); (b) regression analyses using stepwise linear regression

<sup>1</sup>The figures shown in this chapter present the results from a demonstration of staff capability to review a performance assessment. These figures, like the demonstration, are limited by the use of many simplifying assumptions and sparse data.

## 8. Sensitivity and Uncertainty

to estimate the sensitivity to key parameters in the consequence models; (c) determination of relative importance of radionuclides in the waste; and (d) sensitivity of CCDFs to performance of the natural and engineered barriers. The sensitivity analyses considered only liquid releases, not those from drilling. Gas release was not part of the IPA Phase 1 total-system performance assessment results, but was included as an auxiliary analysis (see Appendix D, "Gaseous Release of C14," in Codell *et al.*, 1992).

### 8.2.2.2 Uncertainty Analyses

The Phase 1 IPA included only two events and processes different from the base-case conditions: pluvial conditions and drilling. These were combined into four scenarios (i.e., base case, base case plus drilling, pluvial conditions without drilling, and pluvial conditions with drilling). Uncertainty analyses were restricted to presentation of CCDF plots of cumulative release at the accessible environment (*Normalized Release*) for each of the scenarios, separately, and a combined CCDF for all scenarios factored by the scenario probability. The CCDFs were the result of the uncertainty in the sampled parameters propagated through the analysis. *Effective Dose Equivalent* was not calculated as a performance measure for the IPA Phase 1 study. Construction of CCDFs is described in Section 9.2 of this report.

### 8.2.3 Techniques

The techniques used in the evaluation of the performance assessment model include studying the distributions of the input and output variables, evaluating correlations between individual input parameters and the performance measures, and overall model sensitivity to independent variables. The techniques used in this analysis have been described by a number of authors (Draper and Smith, 1966; Mendenhall and Schaeffer, 1973; Bowen and Bennett, 1988; and Sen and Srivastava, 1990) and several have been applied previously to total-system performance assessments (Iman and Conover, 1979; Helton *et al.*, 1991; and McKay, 1992).

The use of regression analysis in this work was an extension of the regression analyses done in IPA Phase 1 (see Codell *et al.*, 1992; p. 62). Previously, the regression analysis was used to determine the

most important variables and estimate sensitivities of the total-system performance assessment model output to individual independent variables. In IPA Phase 2, the following techniques for development of a regression equation to emulate the total-system performance assessment model were investigated: transformation of data (Iman and Conover, 1979; and Seitz *et al.*, 1991); test for heteroscedasticity (residual variation—see Draper and Smith, 1966; Bowen and Bennett, 1988; and Sen and Srivastava, 1990); and Mallows'  $C_p$  statistic (Sen and Srivastava, 1990). In addition to several techniques used in previous performance assessment work (e.g., the stepwise linear regression), the following techniques were evaluated for determining parameter importance and sensitivity (Kolmogorov-Smirnov and Sign tests (Bowen and Bennett, 1988)); and differential analysis (Helton *et al.*, 1991).

The sensitivity and uncertainty analyses were done with the commercially-available statistical package, *S-plus* (Version 3.1) (Statistical Sciences, Inc., 1991). Programs written in *S-plus* were used in this work to do the compartmental-component analysis, stepwise linear regression analysis, multilinear regression analysis, and statistical tests such as the Kolmogorov-Smirnov test and Mallows'  $C_p$  statistic.

## 8.3 Selection of Most Influential Independent Parameters

### 8.3.1 Subset Selection by Stepwise Regression Analysis

Stepwise regression analysis has been used in previous total-system performance assessment work (Codell *et al.*, 1992; and Helton *et al.*, 1991) to determine the independent variables that have the most influence on the model output. Stepwise regression analysis selects variables to be in a linear equation based on the correlation coefficient between a single independent variable and the dependent variable (Draper and Smith, 1966; and Iman *et al.*, 1980).

Selection of variables for the linear model by stepwise regression analysis may be based on a variety of criteria, such as the  $F$ -statistic, the Mean Square Error, the correlation coefficient, or the  $C_p$  statistic. As variables are added to the regression equation, the coefficient of determination,  $R^2$ , is calculated (Seitz *et al.*, 1991). The coefficient

of determination is the square of the multiple correlation coefficient (Walpole and Myers, 1978) and is proportional to the total variance of the dependent parameter that is explained by the regression model; it increases as more variables are added to the model (Intriligator, 1978). In this analysis, the  $F$ -statistic was used for variable selection; the subset giving the largest  $R^2$  was chosen.

In stepwise regression, parameters are ranked in order of importance to the total-system performance assessment model by their effect on the coefficient of determination,  $R^2$  (Seitz *et al.*, 1991). The variable associated with the largest change in  $R^2$  is ranked as the most important.

Subset selection by the stepwise regression technique may be performed at varying levels of significance,  $\alpha$ . The level of significance  $\alpha$  is the probability that a parameter will be rejected from the regression equation when it should be included. Helton *et al.* (1991) performed stepwise regression analyses at the 0.01 level of significance. In this analysis, the stepwise regression analyses were done for 0.01 and 0.05 level of significance. For the base case (0000) scenario, fifteen parameters were selected by the stepwise regression from a suite of 195 parameters at the 0.01 level of significance, whereas 24 parameters were selected at the 0.05 level of significance. Six parameters were selected at the 0.01 level of significance, from a suite of 29 independent parameters by Helton *et al.*, for the Waste Isolation Pilot Project performance assessment. Helton *et al.* noted that as the number of independent parameters increases, there is more chance for selection of a spurious parameter. An analysis of the relationship between the number of independent parameters used as input to the total-system performance assessment model, the level of significance, and the number of the stepwise-selected parameters was not done in IPA Phase 2. However, such an analysis is needed in order to establish the most appropriate number of variables for the selected subset. A discussion of Mallows'  $C_p$  statistic for determining the number of parameters for the "best" fit of a model by a regression equation is given in Section 8.6.2.2.

A small set of parameters that were important in all IPA Phase 2 scenarios were the corrosion

potential parameters, *ecorr6*, *ecorr7*, and *ecorr8* that were used in the *SOTEC* module (see Chapter 5 and Appendix A). Infiltration was the most important parameter for the scenarios (see Table 8-1) in which climatic (pluvial) consequences were not considered (*0000*, *oodo*, *osoo*, *oovv*). The gas retardation coefficient (*betaf*) and fracture permeability (*permf*) for the Topopah Springs member (*CI4* gas module) were also included in the list of the most important parameters. The  $UO_2$  alteration rate for sub-area 2 of the repository, *forwar2* (*SOTEC*), was among the important parameters for the scenarios with climatic consequences, *cooo* and *csdv*. Tables 8-2 to 8-5 list the parameters selected by stepwise regression for the base case (*0000*) and fully disturbed case (*csdv*) for the 0.01 level of significance.

It should be noted that the same subsets were selected for all scenarios without climatic disturbances, *0000*, *oodo*, *osoo*, *oovv*. Similarly, the scenarios with climatic effects, *cooo* and *csdv*, had the same subsets of important parameters.

Table 8-1 Scenario Classes Modeled in the IPA Phase 2 Analysis

Scenario Class	Scenario Class Identifier
Base Case	0000
Climate Change Only (Pluvial)	cooo
Seismicity Only	osoo
Drilling Only	oodo
Magmatic Activity Only	oovv
Drilling + Seismicity	osdo
Drilling + Seismicity + Magmatic Activity	osdv
Drilling + Seismicity + Climate Change	csdo
Drilling + Seismicity + Magmatic Activity + Climate Change <sup>a</sup>	csdv

<sup>a</sup>Fully disturbed

8. Sensitivity and Uncertainty

Table 8-2 Results of Stepwise and Multilinear Regression: *Normalized Release for Base Case (0000) Scenario<sup>a</sup>*

<i>Parameter Name</i>	<i>Regression Coefficient</i>	<i>Confidence Interval<sup>b</sup></i>	<i>Standardized Regression Coefficient</i>	<i>Rank Regression Coefficient</i>	<i>Elasticity Coefficient</i>	<i>Uncertainty Coefficient</i>
INFIL(UN)	4.86E + 02	1.12E + 02	0.400	0.417	0.390	0.160
ECORR6	-3.35E-03	1.06E-06	-0.312	-0.348	-2.69	0.0976
ECORR7	-2.68E-03	1.06E-03	-0.248	-0.282	-2.14	0.0619
RETARD3	-1.44E-03	5.57E-03	-0.242	-0.216	-0.510	0.0587
ECORR8	1.28E + 03	5.72E + 02	0.205	0.243	0.176	0.042
AKR3	9.34E + 14	4.03E + 14	0.213	0.274	0.255	0.046
Kd39Th	-7.18E-01	4.78E-01	-0.148	-0.092	-0.119	0.019
ECORR5	-2.79E + 01	2.25E + 01	-0.114	-0.082	-0.213	0.0130
RETARD1	-6.20E-03	5.56E-03	-0.104	-0.110	-0.219	0.0108
KdCm1	1.43E-01	1.27E-01	0.104	0.066	0.089	0.0107
AKR2	9.79E + 13	8.24E + 13	0.110	0.106	0.132	0.0121
AKR4	1.60E + 14	1.34E + 14	0.120	0.126	0.131	0.0121
Kd26Am	4.12E-02	4.21E-02	0.090	0.074	0.077	0.008
SOL4Am	2.03E + 03	2.00E + 03	0.094	— <sup>c</sup>	0.068	0.009
FORWAR2	5.69E + 02	5.71E + 02	0.092	— <sup>c</sup>	0.068	0.008

<sup>a</sup>See Appendix A for a description of the parameter names. Coefficients are described in Section 8.4.

<sup>b</sup>Values expressed can be added to or subtracted from the *Regression Coefficient*.

<sup>c</sup>Parameter not selected.

**Table 8-3 Results of Stepwise and Multilinear Regression: Effective Dose Equivalent for Base Case (oooo) Scenario<sup>a</sup>**

<i>Parameter Name</i>	<i>Regression Coefficient</i>	<i>Confidence Interval<sup>b</sup></i>	<i>Standardized Regression Coefficient</i>	<i>Rank Regression Coefficient</i>	<i>Elasticity Coefficient</i>	<i>Uncertainty Coefficient</i>
INFIL(UN)	2.91E + 07	4.20E + 06	0.657	0.870	1.03	0.432
FUNNEL2	8.27E + 04	4.63E + 04	0.169	0.091	0.469	0.0286
ECORR6	-6.45E + 01	3.708E + 01	-0.165	-0.138	-2.29	0.0272
FORWAR2	3.57E + 07	2.15E + 07	0.158	0.101	0.217	0.0249
SOL4AM	1.04E + 08	7.46E + 07	0.132	0.042	0.154	0.0175
RDIFF13	4.38E + 07	3.77E + 07	0.110	0.072	0.151	0.0121
KD39Th	-1.87E + 04	1.79E + 04	-0.099	-0.038	-0.136	0.0098
ECORR5	-8.18E + 05	8.43E + 05	-0.092	-0.053	-0.278	0.0085
RPOR21	1.51E + 05	1.54E + 05	0.093	0.043	0.061	0.0087
ECORR7	-3.62E + 01	3.71E + 01	-0.093	-0.140	-1.28	0.0086

<sup>a</sup>See Appendix A for a definition of the parameter names. Coefficients are described in Section 8.4.

<sup>b</sup>Values expressed can be added to or subtracted from the *Regression Coefficient*.

**Table 8-4 Results of Stepwise and Multilinear Regression: Normalized Release for Fully Disturbed (csdv) Scenario<sup>a</sup>**

<i>Parameter Name</i>	<i>Regression Coefficient</i>	<i>Confidence Interval<sup>b</sup></i>	<i>Standardized Regression Coefficient</i>	<i>Rank Regression Coefficient</i>	<i>Elasticity Coefficient</i>	<i>Uncertainty Coefficient</i>
ECORR6	-6.71E-03	1.37E-03	-0.36	-0.385	-2.22	0.133
ECORR7	-4.55E-03	1.37E-03	-0.25	-0.333	-1.50	0.061
FORWAR2	2.09E + 03	8.41E + 02	0.20	0.158	0.12	0.038
ECORR8	1.93E + 03	8.44E + 02	0.18	0.179	0.11	0.033
FORWAR3	1.46E + 03	8.45E + 02	0.14	0.121	0.08	0.019
KD39TH	-1.25E + 00	7.04E-01	-0.14	-0.124	-0.09	0.020
RETARD3	-1.33E-02	8.04E-03	-0.13	-0.148	-0.19	0.017
FUNNEL2	2.87E + 00	1.82E + 00	0.13	0.120	0.15	0.016
VOLMAX2	-8.64E + 01	6.08E-01	0.11	0.032	0.14	0.013
HIT19	1.02E + 00	7.29E-01	0.11	0.118	0.13	0.012

<sup>a</sup>See Appendix A for a definition of the parameter names. Coefficients are described in Section 8.4.

<sup>b</sup>Values expressed can be added to or subtracted from the *Regression Coefficient*.

## 8. Sensitivity and Uncertainty

**Table 8-5 Results of Stepwise and Multilinear Regression: Effective Dose Equivalent for Fully Disturbed (csdy) Scenario<sup>a</sup>**

<i>Parameter Name</i>	<i>Regression Coefficient</i>	<i>Confidence Interval<sup>b</sup></i>	<i>Standardized Regression Coefficient</i>	<i>Rank Regression Coefficient</i>	<i>Elasticity Coefficient</i>	<i>Uncertainty Coefficient</i>
FORWAR2	2.13E + 08	8.48E + 07	0.219	0.378	0.407	0.048
FORWAR3	1.63E + 08	1.54E + 07	0.167	0.126	0.310	0.028
ECORR6	-2.60E + 02	1.47E + 02	-0.154	0.346	-2.88	0.024
ECORR8	1.39E + 08	8.54E + 07	0.143	0.087	0.215	0.020
Kd114Se	3.75E + 06	2.84E + 06	0.115	— <sup>c</sup>	0.215	0.013
DRILL21	9.85E + 00	7.48E + 00	0.114	0.099	0.437	0.013
VOLMAX4	-8.07E + 04	6.13E + 04	-0.115	-0.046	-0.430	0.013
Kd104Ni	1.14E + 06	8.51E + 05	0.116	— <sup>c</sup>	0.217	0.014
ZONE7	-8.65E + 04	7.35E + 04	-0.102	— <sup>c</sup>	-0.383	0.010
Kd44Ra	6.65E + 03	5.70E + 04	0.102	— <sup>c</sup>	0.191	0.010
WAREA4	8.97E + 04	7.35E + 04	0.106	— <sup>c</sup>	0.398	0.011
FUNNEL2	2.14E + 05	1.89E + 05	0.101	0.237	0.380	0.010
PERMF1	1.82E + 21	1.65E + 21	0.096	0.119	2.34	0.009
HIT19	8.37E + 04	7.35E + 04	0.099	0.086	0.037	0.010
Kd50Pb	1.36E + 04	1.26E + 04	0.095	— <sup>c</sup>	0.177	0.009
BETAF3	-3.94E + 04	3.48E + 04	-0.098	— <sup>c</sup>	-1.49	0.010
PORM1	5.08E + 05	7.33E + 05	0.060	— <sup>c</sup>	0.050	0.004
BETAM	3.54E + 04	3.48E + 04	-0.088	-0.058	-0.709	0.008
VOLMAX6	-6.04E + 04	6.13E + 04	-0.086	— <sup>c</sup>	-0.321	0.007

<sup>a</sup>See Appendix A for a definition of the parameter names. Coefficients are described in Section 8.4.

<sup>b</sup>Values expressed can be added to or subtracted from the *Regression Coefficient*.

<sup>c</sup>Parameter not selected.

A means of confirming the selection of the most important parameters for the model is through the use of scatter plots (Helton *et al.*, 1991). By plotting the performance measure (*Normalized Release* or *Effective Dose Equivalent*) against the input variable (e.g., undisturbed infiltration) linear or discontinuous relationships among the parameters may be seen. However, because the performance measures are a function of many independent parameters, distinct relationships may be difficult to detect from scatter plots alone.

### 8.3.2 Compartmental Component Analysis

Compartmental component analysis was used to illustrate the relative importance of individual

radionuclides or release pathways to the *Normalized Release* or *Effective Dose Equivalent*. The compartmental component analysis was done primarily with the use of boxplots. The boxplot (Tukey, 1977; and Helton *et al.*, 1991) is a means of assessing the effect of the full range and distribution of a given component (radionuclide or geosphere pathway) on the output. The boxplot (Figure 8-1) consists of a "box," the ends of which represent the lower and upper quartiles of the distribution (25<sup>th</sup> percentile ( $x_{.25}$ ) and 75<sup>th</sup> percentile ( $x_{.75}$ ), respectively). The "I" symbol (whisker) represents the values in the distribution that are  $x_{.25} - 1.5(x_{.75} - x_{.25})$  and  $x_{.75} + 1.5(x_{.75} - x_{.25})$  (Helton *et al.*, 1991). Values outside the whiskers ("outliers") are represented with lines.

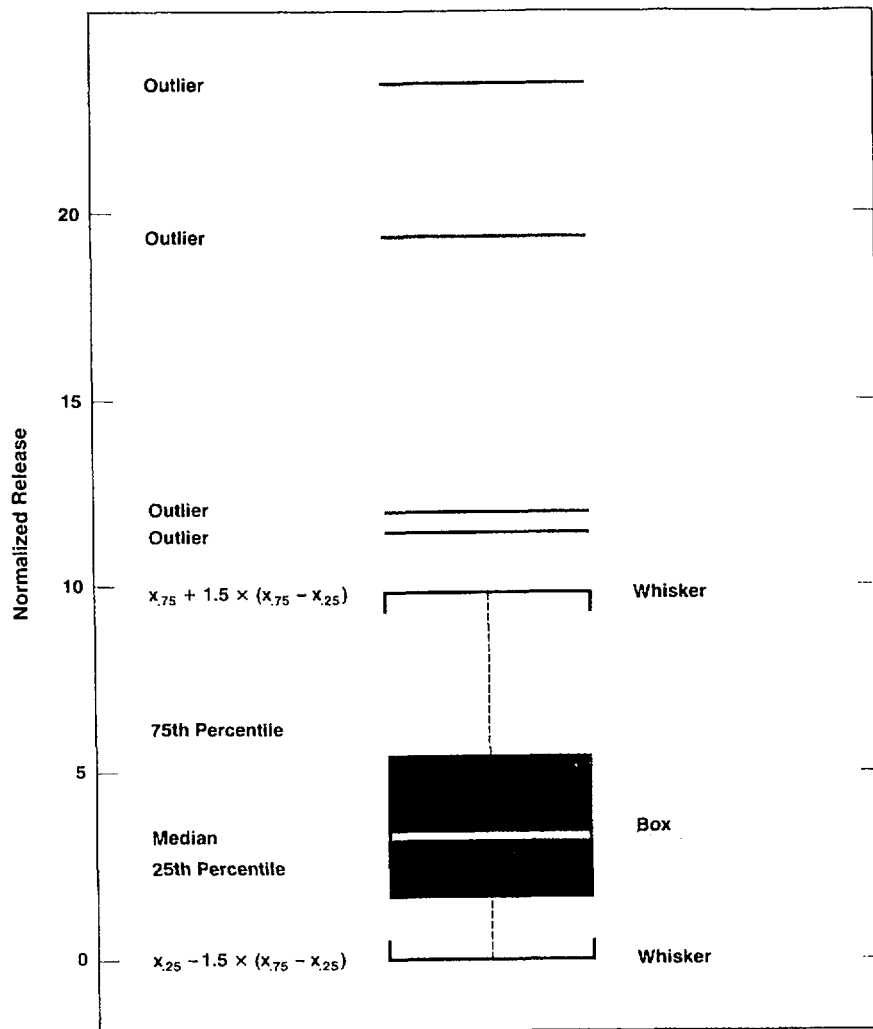


Figure 8-1 Example boxplot showing interquartile region, the whiskers at  $1.5 \times$  (interquartile) and outliers in the distribution

## 8. Sensitivity and Uncertainty

### 8.3.2.1 Contribution of Individual Nuclides to the Normalized Release and Effective Dose Equivalent

The contribution of individual nuclides to the *Normalized Release* was evaluated in terms of the absolute contribution, the fraction of the total contribution, and the contribution of different transport pathways to the collective release to the accessible environment. The contributions by seven representative radionuclides to the *Normalized Release* and to the *Effective Dose Equivalent* for the base case (0000) are shown in Figures 8-2 and 8-3, respectively. Corresponding results for the fully disturbed case (csdv) are illustrated in Figures 8-4 and 8-5.

The dominant radionuclide contributor to the *Normalized Release* is  $^{14}\text{C}$ , primarily in the gaseous pathway (Figures 8-2 and 8-4). Fifty percent of the vectors in the base case (0000) have  $^{14}\text{C}$  releases greater than 0.8 times the U.S. Environmental Protection Agency (EPA) limit. Although gaseous  $^{14}\text{C}$  is important to the *Normalized Release*, it is a very small contributor to the *Effective Dose Equivalent* (Figures 8-3 and 8-5).  $^{243}\text{Am}$  is an important contributor to the *Normalized Release* and *Effective Dose Equivalent*, whereas  $^{240}\text{Pu}$  and  $^{99}\text{Tc}$  are important contributors to the fully disturbed (csdv) scenario *Normalized Release*. In some cases, these nuclides exhibit releases greater than the EPA limit.

Federal Regulation 40 CFR Part 191<sup>2</sup> provides that 10 percent of the total releases to the accessible environment may have a *Normalized Release* between 1 and 10. In the IPA Phase 2 total-system performance assessment, more than fifty percent of the vectors gave a *Normalized Release* greater than 1, in large part because of the

gaseous  $^{14}\text{C}$  release. More than 25 percent of the liquid pathway releases yield a *Normalized Release* greater than 1.

The nuclides making the largest contribution to the *Effective Dose Equivalent* are  $^{94}\text{Nb}$ ,  $^{210}\text{Pb}$ ,  $^{237}\text{Np}$ , and  $^{243}\text{Am}$ .  $^{94}\text{Nb}$ ,  $^{237}\text{Np}$ , and  $^{243}\text{Am}$  are important because of their long half-lives, whereas  $^{210}\text{Pb}$  continues to build up over time with decay of nuclides in the  $^{238}\text{U}$  series, particularly  $^{234}\text{U}$ .

### 8.3.2.2 Releases by Pathway

The relative release by pathway differs between the base (0000) and the fully disturbed (csdv) cases. In the base case (0000) scenario, the contribution to the *Normalized Release* is roughly divided between the liquid and the gaseous pathways. The mean contribution to the *Normalized Release* is higher in the liquid pathway for *Normalized Release* less than 1, whereas the mean contribution to the *Normalized Release* is higher in the gaseous pathways for *Normalized Release* between 1 and 10. This is anticipated because much of the exceedence of the EPA limit of 1 is because of gaseous  $^{14}\text{C}$  release. The releases for the fully disturbed (csdv) scenario are divided much differently among liquid, gaseous, and direct pathways (Figure 8-6). The mean fractional contribution to the *Normalized Release* for the liquid pathway is 0.8, whereas the mean fractional contribution to the *Normalized Release* for the gaseous pathway is 0.2. The direct pathway (via drilling or volcanism), while a much smaller contributor to the *Normalized Release*, exhibits *Normalized Release* values as high as 15.

### 8.3.3 Significance of Independent Parameters – Kolmogorov-Smirnov Test and Sign Test

The stepwise regression analysis used the change in the coefficient of determination,  $R^2$ , to determine which parameters were the most important in the total-system performance assessment model. The Kolmogorov-Smirnov (K-S) test and the Sign test were also used to determine the importance of the input parameters (Bowen and Bennett, 1988). These tests, unlike stepwise regression analysis, test the relationship between the parameters and results, without assuming a specific functional form.

<sup>2</sup>Currently, a revised set of standards specific to the Yucca Mountain site is being developed in accordance with the provisions of the Energy Policy Act of 1992. The Energy Policy Act of 1992 (Public Law 102-486), approved October 24, 1992, directs NRC to promulgate a rule, modifying 10 CFR Part 60 of its regulations, so that these regulations are consistent with EPA's public health and safety standards for protection of the public from releases to the accessible environment from radioactive materials stored or disposed of at Yucca Mountain, Nevada, consistent with the findings and recommendations made by the National Academy of Sciences, to EPA, on issues relating to the environmental standards governing the Yucca Mountain repository. It is assumed that the revised EPA standards for the Yucca Mountain site will not be substantially different from those currently contained in 40 CFR Part 191, particularly as they pertain to the need to conduct a quantitative performance assessment as the means to estimate postclosure performance of the repository system.

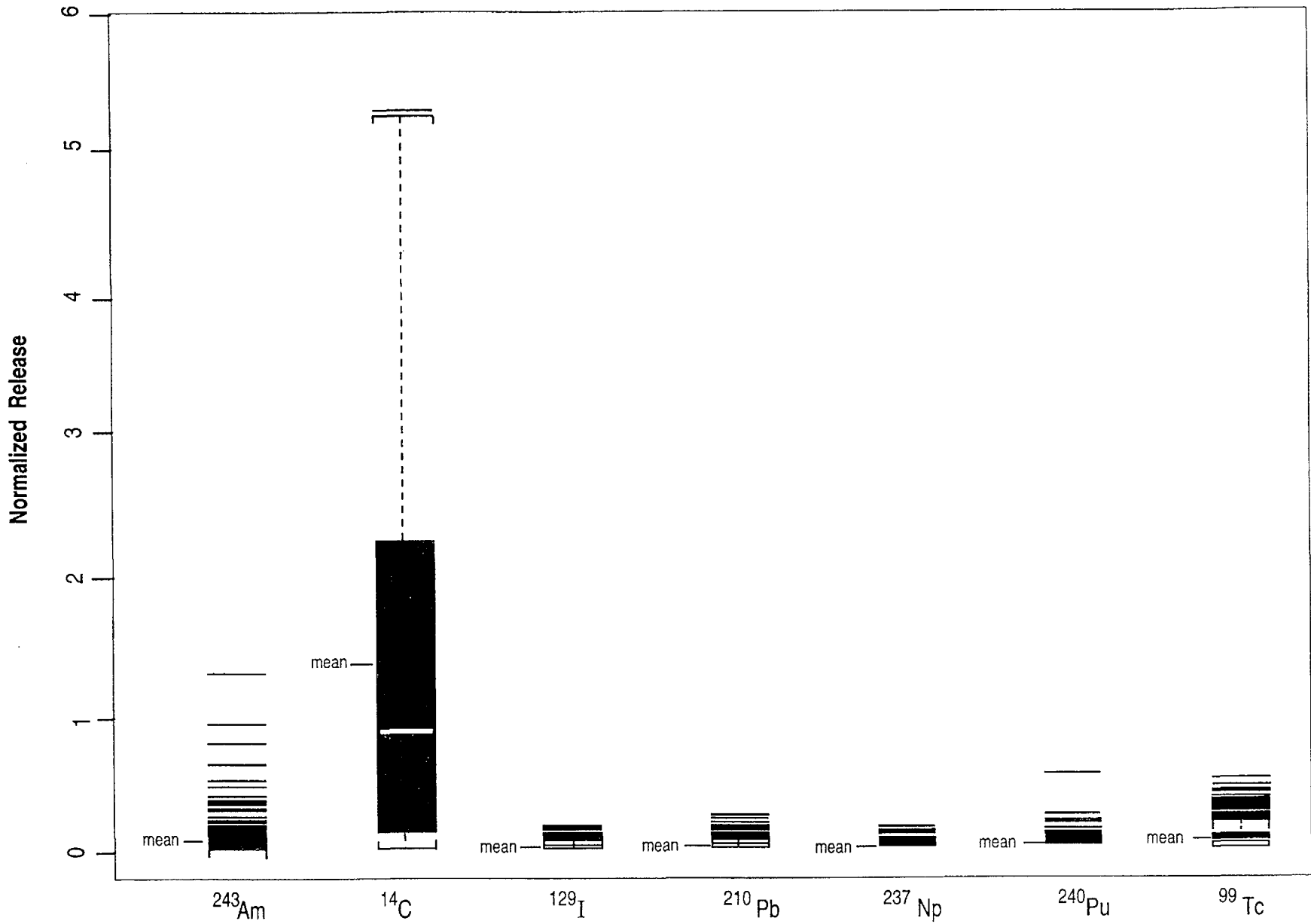


Figure 8-2 Absolute contributions to *Normalized Release* by selected radionuclides, base case (0000) scenario

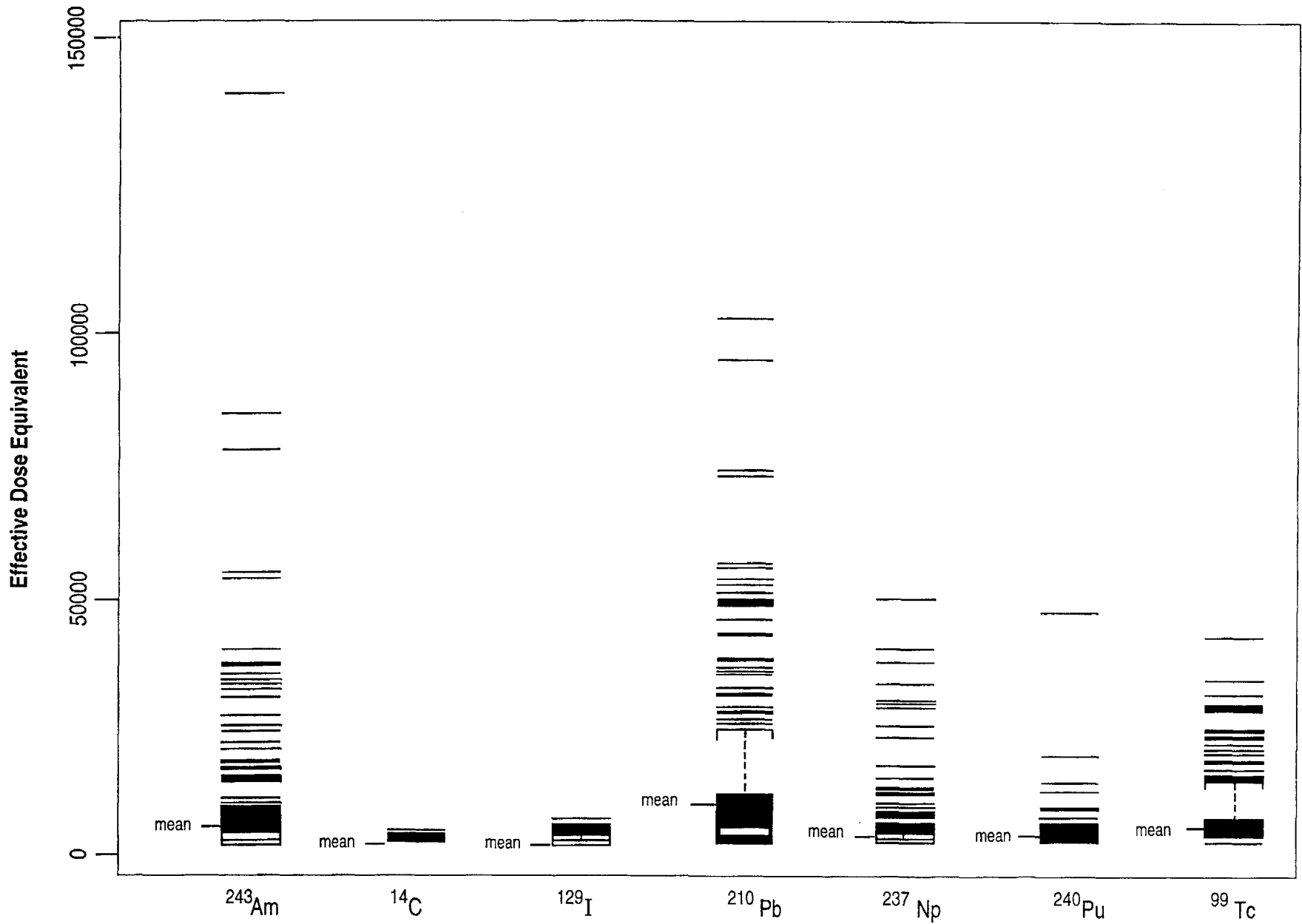


Figure 8-3 Absolute contributions to *Effective Dose Equivalent* by selected radionuclides, base case (oooo) scenario

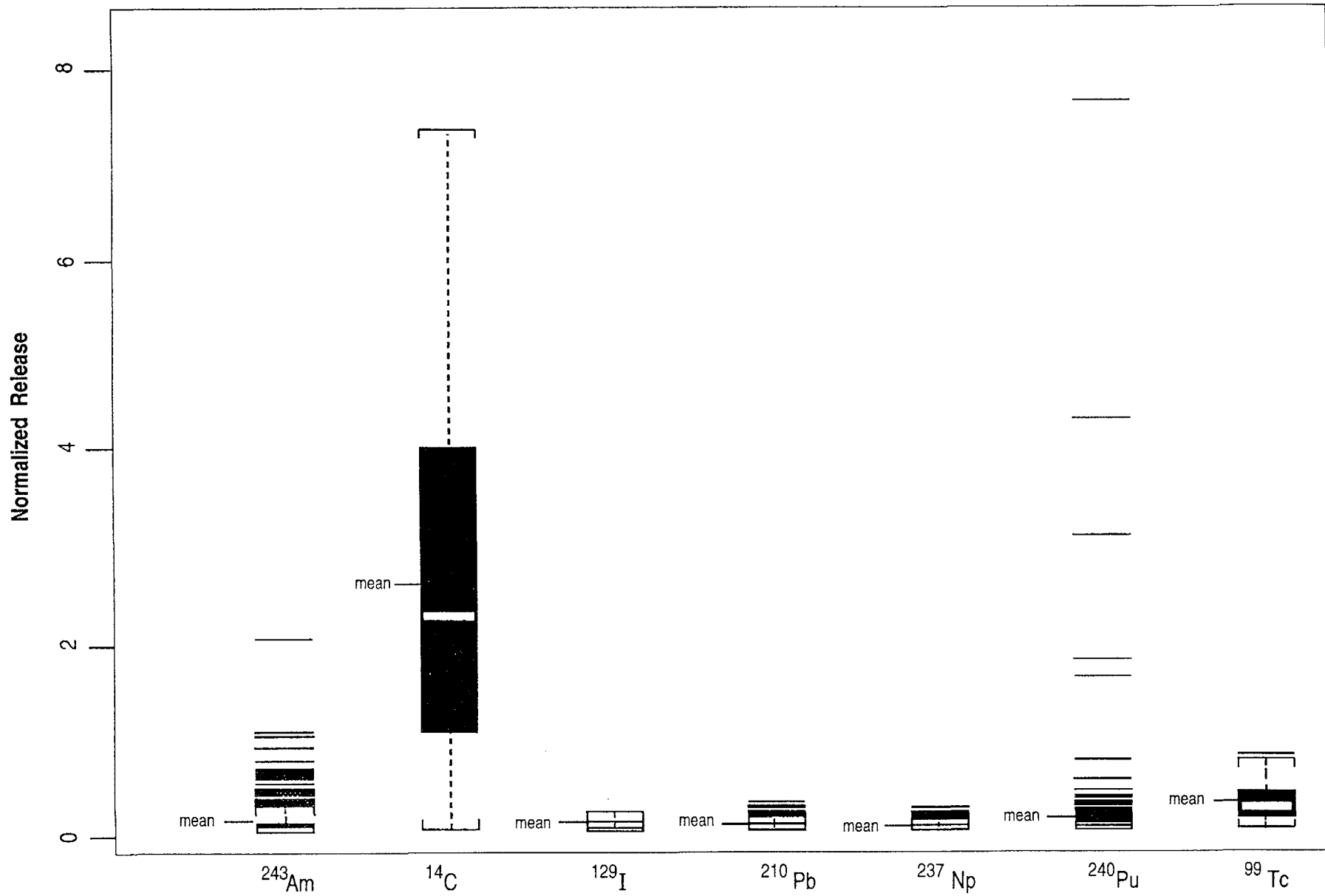


Figure 8-4 Absolute contributions to *Normalized Release* by selected radionuclides, fully disturbed (*csdv*) scenario

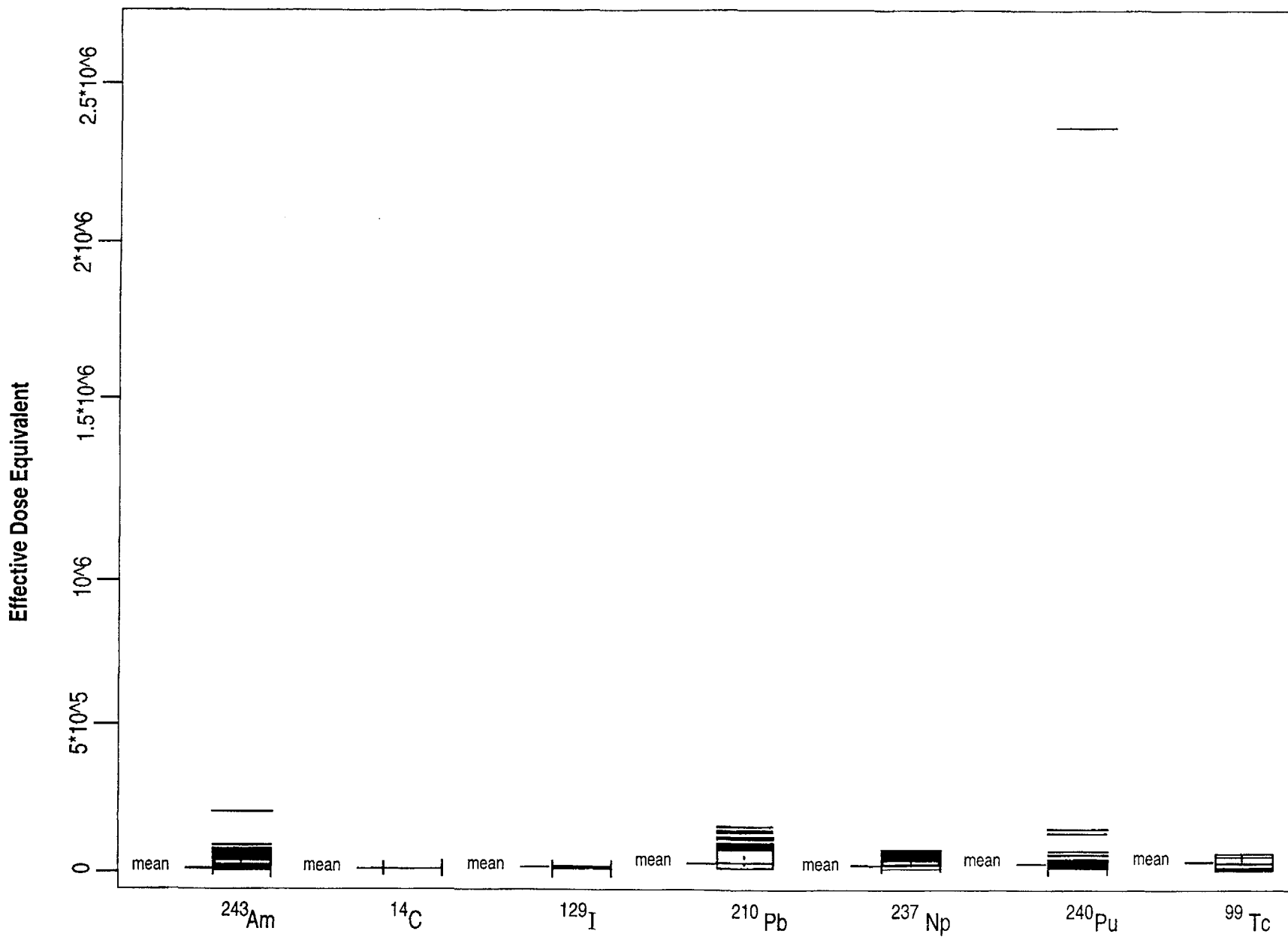


Figure 8-5 Absolute contributions to *Effective Dose Equivalent* by selected radionuclides, fully disturbed (csd) scenario

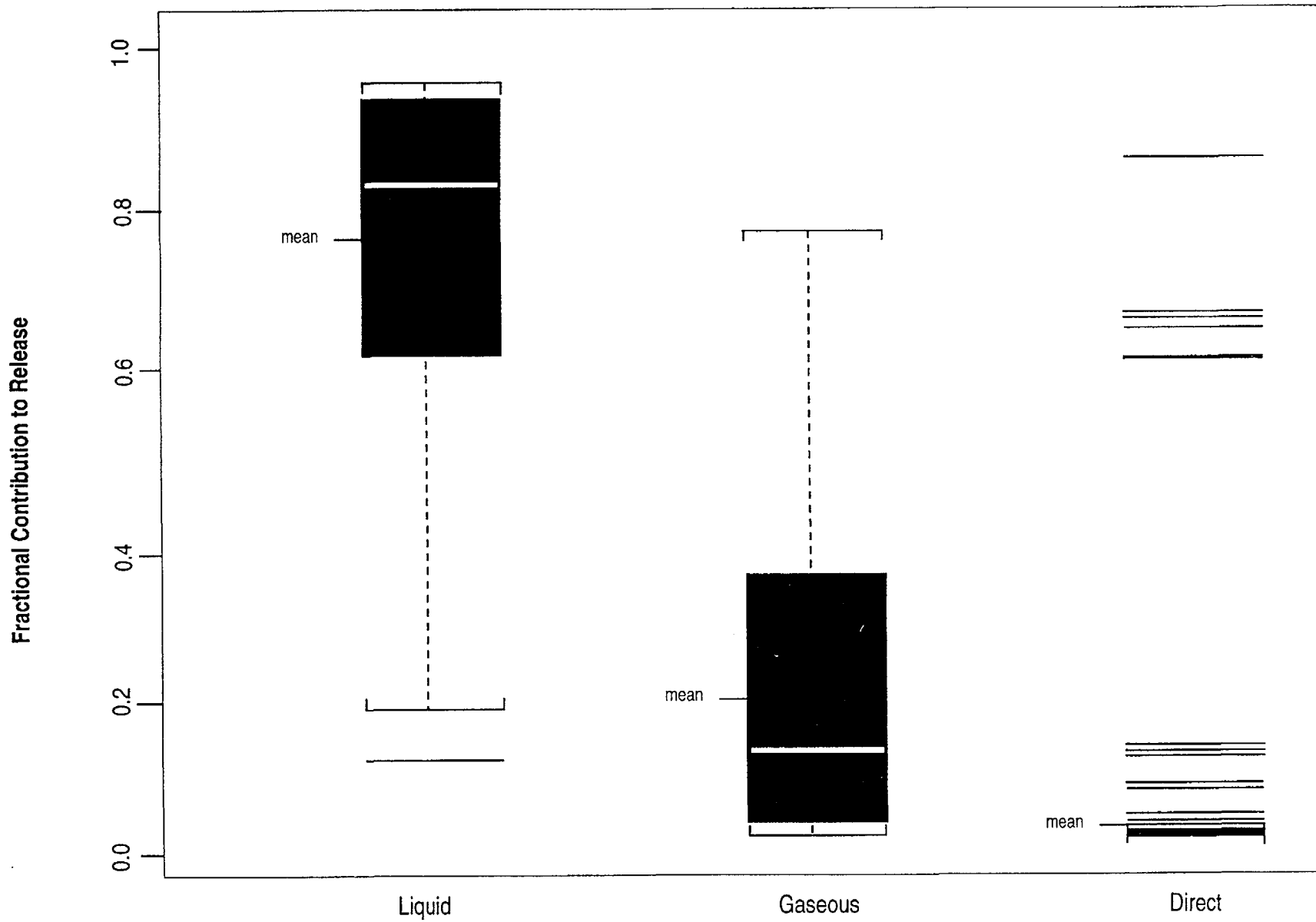


Figure 8-6 Fractional contributions to *Normalized Release* by geosphere pathway

## 8. Sensitivity and Uncertainty

### 8.3.3.1 The Kolmogorov-Smirnov Test

The K-S test (Bowen and Bennett, 1988) is generally used to test whether two distributions are the same. It was used in the present context as a test of whether a subset of the LHS-determined values for a given input parameter conforms to the distribution defined for the variable. The subsets of input values used in the K-S analysis correspond to the vectors in which the 40 largest values for *Normalized Release* or *Effective Dose Equivalent* were generated in a given scenario. For each input parameter, the defined or theoretical distribution was compared to the distribution of the values in the subsets (Figure 8-7). If the theoretical and subset distributions are similar, the interpretation is that the input parameter will have little or no effect on the results. Conversely, a significant difference between the theoretical distribution and subset distribution would indicate that the parameter is important to the performance measure. Figure 8-7a is a plot of the theoretical distribution (solid line) and the distribution of the sampled values (dots) for the fracture *beta* parameter. The two distributions are very similar, whereas the distributions for undisturbed infiltration (Figure 8-7b) are very different. Fifty percent of the values (cumulative density = 0.5 to 1.0) from the theoretical distribution (solid line) for infiltration rate are greater than 0.00075, whereas 80 percent (cumulative density = 0.2 to 1) of the sampled values (dots) are greater than 0.00075. These large values for the *infiltration rate* are thus significant in affecting the total-system performance assessment (TPA) computer model output as *Normalized Release*.

### 8.3.3.2 The Sign Test

The Sign test (Bowen and Bennett, 1988) is another test for comparing whether two distributions are the same. Each observation in the subset sample is represented by a plus (+) sign or a minus (-) sign, depending whether it is smaller or larger than the median of the known distribution. The test statistic is the total number of plus (+) signs, and is compared to the number of plus signs expected for a given theoretical distribution and number of samples. If the distributions are significantly different, the independent variable is considered to have an important effect on the total-system performance assessment model output.

Table 8-6 presents the results of applying the K-S and Sign tests to the base case (0000) scenario results for the 0.05 level of significance. The parameters are listed in order of their values for the K-S test. In general, when the K-S test and Sign test were performed on a set of independent parameters one-at-a-time, the resulting subset of important independent parameters agreed with the set of independent parameters selected by the stepwise regression. However, this agreement is conditional on the fact that the samples tested were made up of only the largest values of the *Normalized Release* or *Effective Dose Equivalent*.

The advantage of the K-S and Sign tests over the stepwise regression analysis is that the correlation with the performance measure is strictly related to the distribution of the independent parameter. Different ranges of the performance measure can also be explored to determine the most significant parameters in other parts of the parameter space.

## 8.4 Sensitivity Analysis

### 8.4.1 Introduction

The objective of sensitivity analysis is to establish the relative importance of parameters to the conceptual model. One measure of model sensitivity is the amount of variation in model output affected by variation in the model input. The model output, *Y*, cumulative release of radionuclides at the accessible environment (*Normalized Release* or *Effective Dose Equivalent*) can be expressed in terms of the independent parameters:

$$Y = f(x_1, x_2, \dots, x_n) \quad (8-1)$$

Model sensitivity can be defined as the first partial derivative of the model output response *Y* with respect to the input parameters  $x_i$ :

$$s_i = \frac{\partial Y}{\partial x_i} \quad (8-2)$$

The sensitivity, as defined in the above relationship, has dimensions. To compare sensitivity among parameters in the model, the sensitivities can be normalized and made dimensionless. This may be done in a variety of ways. One method of making the sensitivities dimensionless is to multiply the sensitivity by a ratio of *Y* and  $x_i$ :

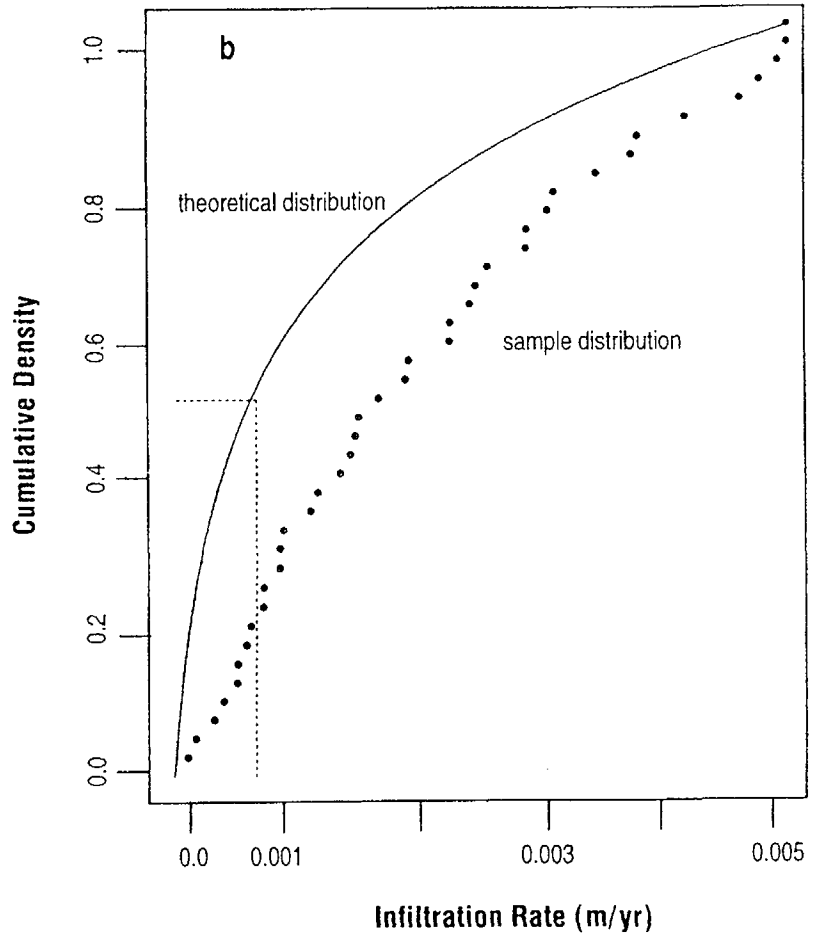
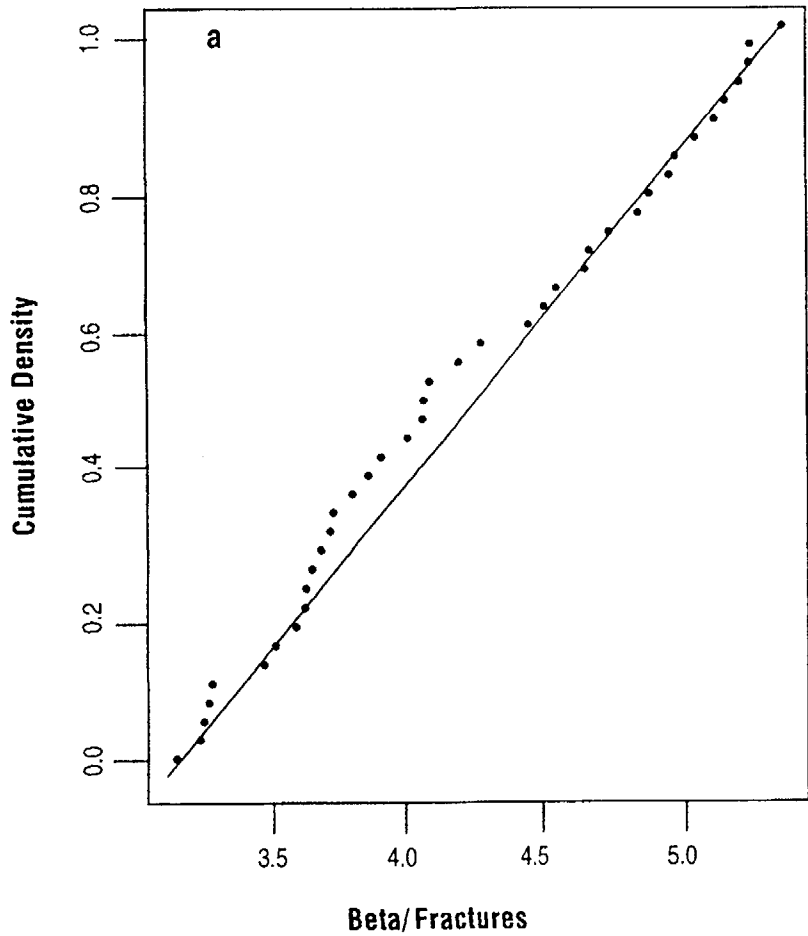


Figure 8-7 Distributions used in the Kolmogorov-Smirnov test ((a) Beta coefficient for fractures; (b) Undisturbed infiltration rate.)

## 8. Sensitivity and Uncertainty

$$s' = \frac{\partial Y}{\partial x_i} \cdot \frac{x_i}{Y} \quad (8-3)$$

If the values for  $x_i$  and  $Y$  used in the ratio  $x_i/Y$  are the estimated means of  $x_i$  and  $Y$ , the sensitivity is known as the "elasticity" (Intriligator, 1978).

Another way to remove the dimensions and the differences in scale is to standardize each value for the input and response parameters by subtracting the estimated mean  $\bar{x}$  and dividing by the standard deviation  $\sigma_x$  (Seitz *et al.*, 1991):

$$x_i^* = \frac{x_i - \bar{x}}{\sigma_x} \quad (8-4)$$

**Table 8-6 Important Parameters Selected by the Kolmogorov-Smirnov and Sign Tests for the Base Case (ooo) Scenario at the 0.05 Level of Significance<sup>a</sup>**

<i>Normalized Release</i>	<i>TPA Module</i>	<i>Collective Effective Dose Equivalent</i>	<i>TPA Module</i>
INFIL(UN)	FLOWMOD	INFIL(UN)	FLOWMOD
ECORR8	SOTEC	FUNNEL2	SOTEC
AKR3	C14	RPOR(1,2)	SOTEC
RETARD2	C14	ECORR6	SOTEC
SOL4Am	SOTEC	FORWAR2	SOTEC

<sup>a</sup>See Appendix A for a definition of the variable names.

The sensitivities  $\partial Y^*/\partial x_i^*$  will have values between 0 and  $\pm 1$ , which facilitates comparison between disparate parameters.

A number of methods may be used to estimate the sensitivity of the model output to a given independent parameter. Differential analysis (Helton *et al.*, 1991), involves determining the local sensitivity of the response to an individual parameter. Regression analysis may be used to estimate the sensitivity of the model in relation to an individual parameter, or to a group of parameters. Estimations of model performance and overall model sensitivity may be generated with a regression equation.

Generally, a linear regression equation is represented as a linear combination of the independent parameters:

$$Y = a_0 + \sum_{i=1}^N \beta_i x_i + \epsilon_i \quad (8-5)$$

where  $a_0$  is the intercept,  $\beta_i$  are the regression coefficients and  $\epsilon_i$  is the error (Sen and Srivastava, 1990).

Many submodels in a typical performance assessment behave non-linearly with respect to the values of the input parameters. Regression can include polynomials and cross products of the  $N$  independent parameters. For example:

$$Y = a_0 + \sum_{i=1}^N \beta_i x_i + \sum_{i=1}^N \sum_{j=1}^N \beta_{ji} x_j x_i + \epsilon_i \quad (8-6)$$

The regression analyses for IPA Phase 2 considered only linear forms and combinations of the

parameters, such as that expressed in Equation (8-5).

### 8.4.2 Estimation of Sensitivities by Regression Analysis

Multilinear regression was used to estimate the sensitivities of the model with respect to the most important parameters selected by stepwise regression analysis. The estimated regression coefficients for the untransformed data have dimensions. To compare sensitivities for the individual parameters, two different transformations of the data were executed before doing the regression analysis: standardization (Seitz *et al.*, 1991) and rank transformation (Iman and Conover, 1979).

#### 8.4.2.1 Standardization

Data can be standardized to eliminate the dimensions and any scale effects, as illustrated in Equation (8-4) above. The result of this transformation is that all transformed parameter values have a mean of zero and a standard deviation of one. The regression coefficients estimated, using standardized data, are also a measure of the fraction of the standard deviation change in the response,  $Y$ , as affected by a fraction of the standard deviation  $\sigma_x$  change in the independent parameter (Helton *et al.*, 1991). Thus, the coefficients estimated from regression of the standardized data will be indicative of the importance to the model.

#### 8.4.2.2 Rank Transformation

Rank transformation of the data also eliminates the dimensions and scale associated with the parameters (Iman and Conover, 1979). The rank transformation involves replacing the data used in the model with their corresponding ranks, as determined by ordering the 400 observations from the minimum (1) to maximum (400). The same transformation is done to values of the model output.

The estimated regression coefficients for regressions done with untransformed data, the standardized, and rank-transformed data for the base (0000), and the fully-disturbed (csdv) cases are given in Tables 8-2 to 8-5. Because the regression coefficients are estimates, the 95 percent confidence interval was determined for each of the raw

regression coefficients. It should be noted that while the regression coefficients are a measure of sensitivity of the model output to the input variables, they are particular to specific models and are not generically applicable.

### 8.4.3 Estimation of Sensitivities by Differential Analysis

Another method used primarily for sensitivity analyses is differential analysis. This approach consists of approximating the response surface by its Taylor series expansion about a reference point ( $x^0$ ) such as the mean:

$$Y = Y(x^0) + \sum_{i=1}^N \frac{\partial Y(x^0)}{\partial x_i} (x_i - x_i^0) + (\text{higher order terms}) + \epsilon_i \quad (8-7)$$

By truncating the Taylor series at the first term, the partial derivative of the response with respect to variable  $x_i$  for a small perturbation from the reference point is defined:

$$\frac{\partial Y(x^0)}{\partial x_i} = \frac{Y - Y(x^0)}{x_i - x_i^0} \quad (8-8)$$

The partial derivatives can be evaluated analytically in some cases, but it is often too difficult to do this directly. A number of techniques, such as the adjoint method and Green's function method, have also been developed (Zimmerman *et al.*, 1990) to increase the efficiency of the evaluation of derivatives analytically within complex computer codes. The partial derivatives can also be evaluated numerically by calculating the performance at the reference point and at points nearby, by perturbing one independent variable at a time.

There are important drawbacks to differential analysis. The Taylor series approximation of the partial derivatives is inherently local, and may not reflect accurately the sensitivity at points far from the evaluation point. Another drawback to differential analysis is that the evaluation of the derivatives is often difficult and expensive. Numerical evaluation of the derivatives, as in Equation (8-8), requires one or more evaluations of the performance assessment model for each derivative, and is often too costly to consider for a large number of input parameters.

## 8. Sensitivity and Uncertainty

Differential analysis provides no information on the possible existence of thresholds or discontinuities in either the independent parameters or the response of the model to the distribution (Helton *et al.*, 1991) (e.g., the change from matrix to fracture flow in unsaturated media). It is possible, however, to evaluate the partial derivatives at any point in the parameter space. Efficient techniques for finding points in the parameter space that are highly significant (e.g., sensitive or high-consequence) have been developed, and demonstrated on a simple representations of a geologic repository (Wu *et al.*, 1992).

### 8.4.4 Comparison of Sensitivity Coefficients Estimated from Regression and Differential Analyses

Multilinear regression was used to estimate the first derivatives of *Normalized Release* ( $Y$ ) with respect to the input variables  $x_i$  (i.e.,  $\partial Y/\partial x_i$ ). These first derivatives are estimates of the coefficients of the multilinear regression equation. In differential analysis, the first derivatives are estimated at a "reference" point; in this analysis, the mean of each input variable. Each input variable is perturbed a small amount from the mean value, one variable at a time, and the first derivatives calculated as described in Equation (8-8).

Differential analysis should not give the same results as regression analysis for the first derivatives (Wu *et al.*, 1992) because multilinear regression analysis uses information from all regions of the parameter space, whereas differential analysis estimates the derivatives at only one point in parameter space.

The analysis for the present comparison was performed for the base case (0000) scenario and the 14 most significant input variables in the following manner:

- (1) The mean value of each parameter in the 400-vector Latin Hypercube Sampler (LHS) input file was calculated;
- (2) A new input file containing 15 vectors was generated. The first vector contained the average values for each parameter. The next 14 vectors contained the average values for

each parameter except for one of the most significant parameters, which differed from its average by a small amount (e.g., 10 percent);

- (3) The TPA computer code was run using the new input file for the base case, to generate 15 output vectors of *Normalized Release*; and
- (4) The partial derivatives for *Normalized Release* with respect to the 14 independent parameters were estimated using Equation (8-8); the difference between the *Normalized Release* from vector 1 and vectors 2 through 15, divided by the difference in the independent parameter.

The sensitivity coefficients from the differential analysis and multilinear regression for the 14 most significant parameters are compared in Table 8-7. The results agree reasonably well in some cases (e.g., *INFIL(UN)*, *undisturbed infiltration*) and generally have the same sense. The most striking difference is the large number of cases in which differential analysis gave a zero sensitivity. This could be a reflection of the insensitivity to those parameters in the region of the reference point. Additionally, many of the TPA modules switch from one behavior to another rather abruptly, depending on the input parameters. For example, the transition from matrix flow to fracture flow in the module *FLOWMOD* is non-linear over the range of infiltration rates. The insensitivity of the model to several parameters at the reference point indicates the need to apply differential analysis at several points on the response surface.

### 8.4.5 Model Sensitivity Analysis

#### 8.4.5.1 CCDF Sensitivity

In this work, the CCDF, that is ( $1 - CDF$  (*Cumulative Distribution Function*)), which, in a single figure, plots the magnitude and uncertainty of the *Normalized Release* at the accessible environment, is the main vehicle for conveying uncertainty results. However, the CCDF gives no explicit information on the contribution to total uncertainty by each of the input parameters.

Plots illustrating the sensitivity of the CCDF to a single parameter or condition were generated by screening the output vectors according to a criterion, and using only the remaining vectors to produce the CCDFs. The CCDFs of screened

Table 8-7 Comparison of First Derivatives of *Normalized Release* by Regression and Differential Analysis<sup>a</sup>

<i>Parameter Name</i>	$\frac{\partial Y}{\partial x_i}$ <i>Regression</i>	$\frac{\partial Y}{\partial x_i}$ <i>Differential</i>	<i>Elasticity Regression</i>	<i>Elasticity Differential</i>
INFIL(UN)	502	377.4	0.403	0.495
ECORR6	-0.0033	0	-2.66	0
ECORR7	-0.0027	0	-2.14	0
RETARD3	-0.015	-0.00194	-0.518	-0.112
ECORR8	1317	0	0.182	0
AKR3	9.6E + 14	3.65E + 13	0.264	0.016
KD39Th	-0.713	0	-0.118	0
ECORR5	-27.3	0	-0.213	0
RETARD1	-0.0062	-0.0021	-0.219	-0.036
KD1Cm	0.014	0	0.049	0
AKR2	9.79E + 13	5.66E + 13	0.132	0.012
AKR4	1.6E + 14	-1.7E + 13	0.131	-0.0022
Kd26Am	0.041	0	0.077	0
SOL4Am	2030	597	0.068	0.0033

<sup>a</sup>See Appendix A for a definition of the parameter names.

data illustrating the sensitivity to performance measures of individual natural and engineered barriers are presented in Section 9.5.

#### 8.4.5.2 Sensitivity of Results to Number of Vectors

The sensitivity of the results to the number of LHS vectors in each scenario is illustrated by comparing spurious correlations among the input parameters and by the sensitivity of the CCDF to the number of vectors.

##### 8.4.5.2.1 Spurious Correlations

Although it is possible to specify correlations among parameters when generating input vectors

with the LHS method, this feature was not evoked in IPA Phase 2 (i.e., there was no deliberate attempt to produce correlations among input parameters). Spurious correlations are apparent correlations of the input parameters among themselves, when no correlations were intended. Although computer programs for generating LHS (Iman *et al.*, 1980) generally contain algorithms for minimizing these effects, correlation of the model output variables to the independent parameters is confounded by spurious correlations, if too few vectors are available for the statistical tests.

To demonstrate the problem with spurious correlations, three computations of *Normalized Release* were done with inputs of 100, 200, and 400 vectors generated by the LHS technique. Each vector had

## 8. Sensitivity and Uncertainty

445 parameters, 195 of which were sampled for the base case (0000). The correlation coefficient between each input parameter  $x_i$  and the *Normalized Release*,  $Y$ , calculated from the performance assessment model was calculated and plotted against the largest correlation between  $x_i$  and any other independent parameter. These plots illustrate a limitation of the sensitivity analyses; if the spurious correlations among independent parameters are as large or larger than the correlation between the dependent-independent parameters, then one cannot determine the validity of the latter correlations. Figure 8-8 for 100 vectors clearly shows that the correlations among independent parameters are as large or larger than the correlations between the independent parameters and model output for a significant fraction of the vectors, thereby confounding interpretation of the results for sensitivity. The results are similar for 200 vectors, but are not shown here. Figure 8-9 illustrates that for 400 vectors, the largest correlations between the independent parameters and model output are distinctly larger than the correlations among the independent parameters.

### 8.4.5.2.2 Sensitivity of the CCDF to Number of Vectors

CCDFs of *Normalized Release* were generated from runs of 50, 100, 150, 200, and 400 vectors, and presented in Figure 8-10. Visually, the CCDFs were quite similar, suggesting a relative lack of sensitivity to the number of vectors.

The conclusions that can be drawn from this analysis are that the usefulness of the sensitivity analysis was limited for fewer than 400 vectors per scenario, as shown by comparing the magnitude of the largest spurious correlations to the model output-independent parameter correlations. However CCDFs were much less sensitive to the number of vectors per scenario.

## 8.5 Uncertainty Analysis

Different types of uncertainty associated with the modeling of physicochemical processes can be distinguished—in particular:

- The statistical uncertainty because of the inherent random nature of the processes, and
- The state-of-knowledge uncertainty.

The latter uncertainty may be subdivided further into parameter and model uncertainty. Parameter uncertainty is caused by insufficient knowledge about the input information, and can manifest itself in several forms. For example, if a single parameter characterizes a facet of the model (e.g., hydraulic conductivity of a rock unit), then uncertainty about its value would lead to selecting a distribution for the probabilistic sampling of that parameter with wider limits than if the parameter were well characterized. Because it usually is not possible to characterize a spatially varying property of the rock, such as permeability by a single parameter, using a single parameter value over the entire field of calculation to represent a spatially varying parameter also introduces uncertainty.

For IPA Phase 2, the repository was represented by a highly simplified conceptual model, which in many cases, ignored the large spatial variability of the geosphere (e.g., the hydraulic properties of each layer were considered spatially homogeneous for each vector, ignoring the considerable heterogeneity). These parameters could be made to vary in time and space; however, this would make the modeling much more complicated. Models within the system representing the performance assessment do in fact include spatial and temporal variability, but these are only indirectly a result of the values of the input parameters. For example, gas flow is represented in two dimensions and is transient in time. Additionally, some of the parameters such as hydraulic conductivity implicitly take into consideration the spatial scales of correlation to account for the length of flow paths.

Modeling uncertainty is caused by simplifying assumptions and the fact that the models used may not accurately simulate the true physical process. This study, as was the case in the IPA Phase 1 study (Codell *et al.*, 1992), deals primarily with the effects of parameter uncertainty.

Iman and Helton (1985, p. 1-1) give an apt definition of uncertainty, which has been adopted for the present study:

“Uncertainty analysis is defined here to be the determination of the variation or model imprecision in  $Y$  that results from the collective variation in the model variables  $x_1, \dots, x_k, \dots$ . A convenient tool for providing such information is the estimated cumulative

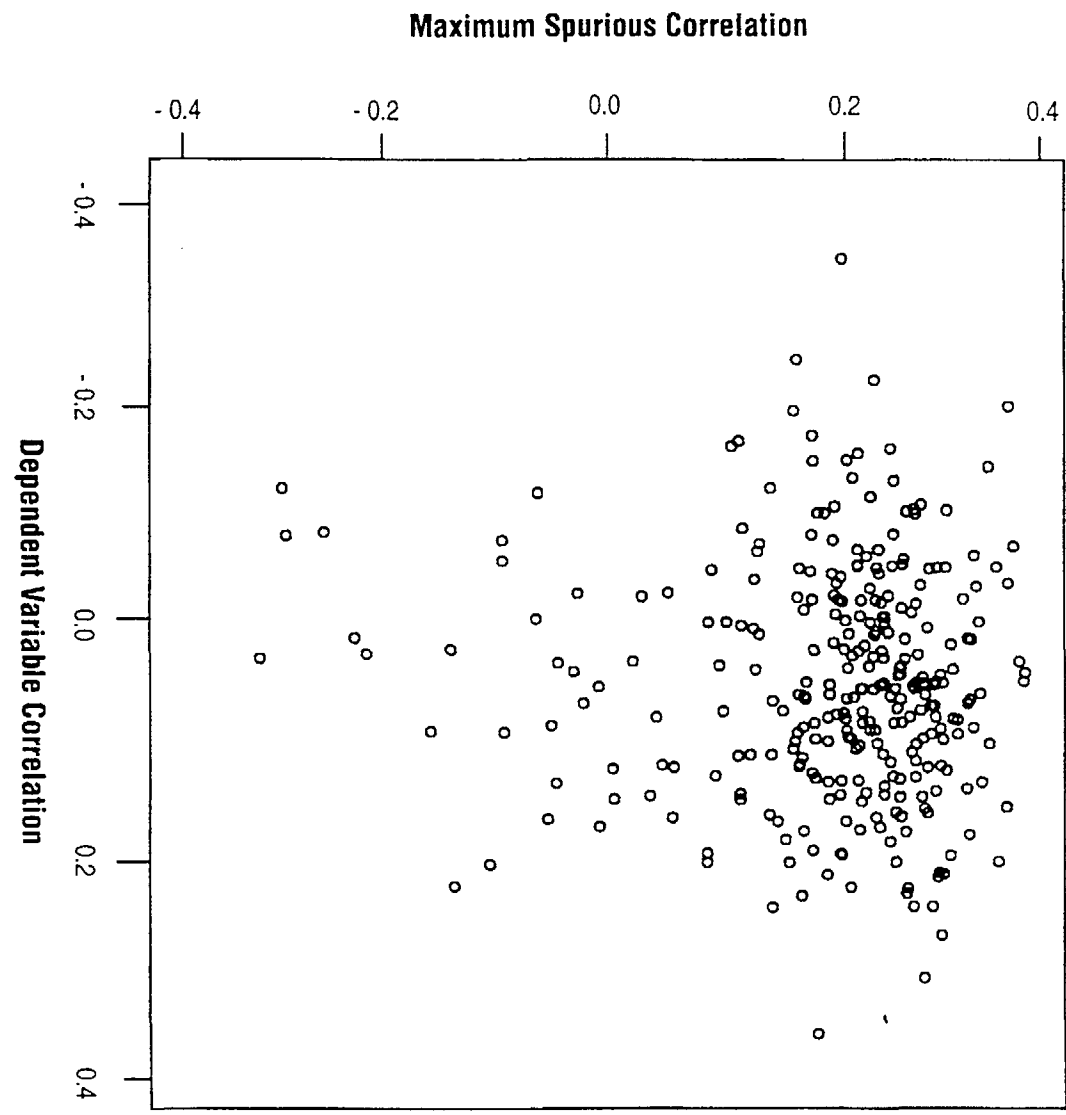


Figure 8-8 Maximum spurious correlations among independent parameters versus correlations between model output and independent parameters for 100 vectors

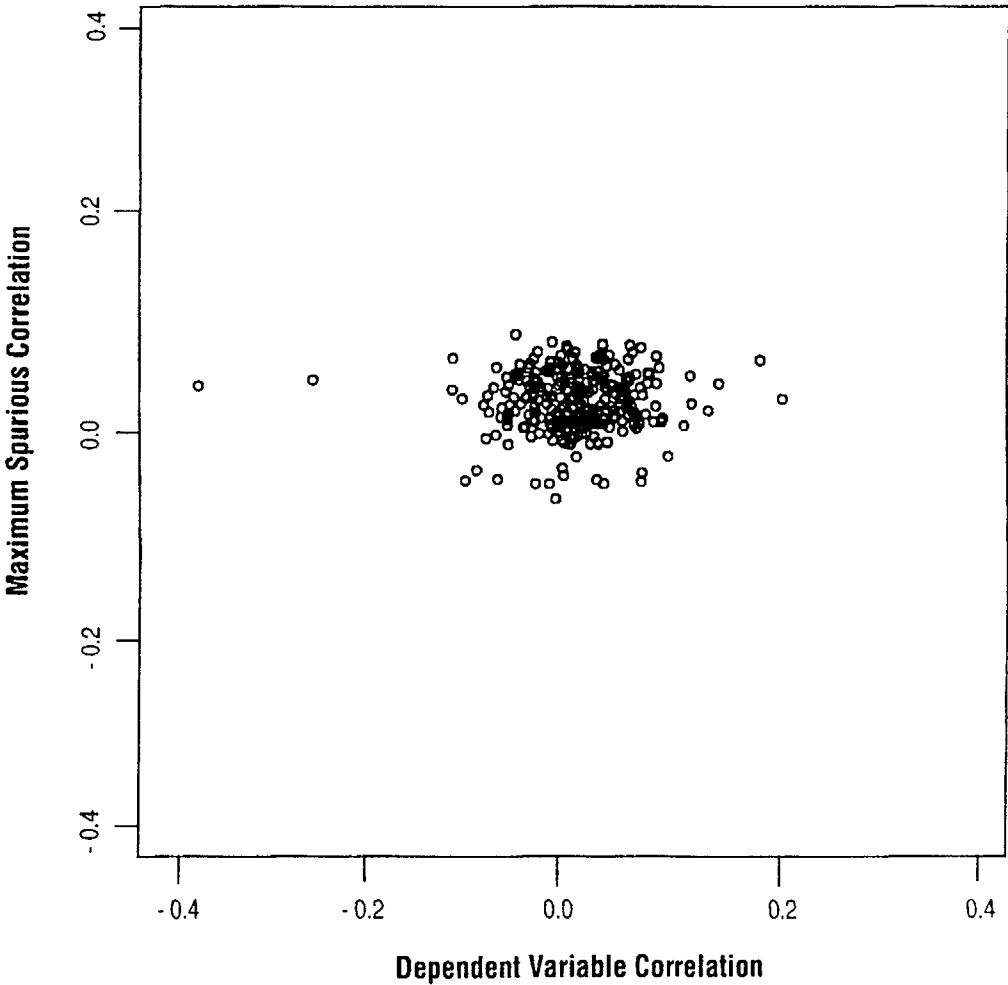


Figure 8-9 Maximum spurious correlations among independent parameters versus correlations between model output and independent parameters for 400 vectors

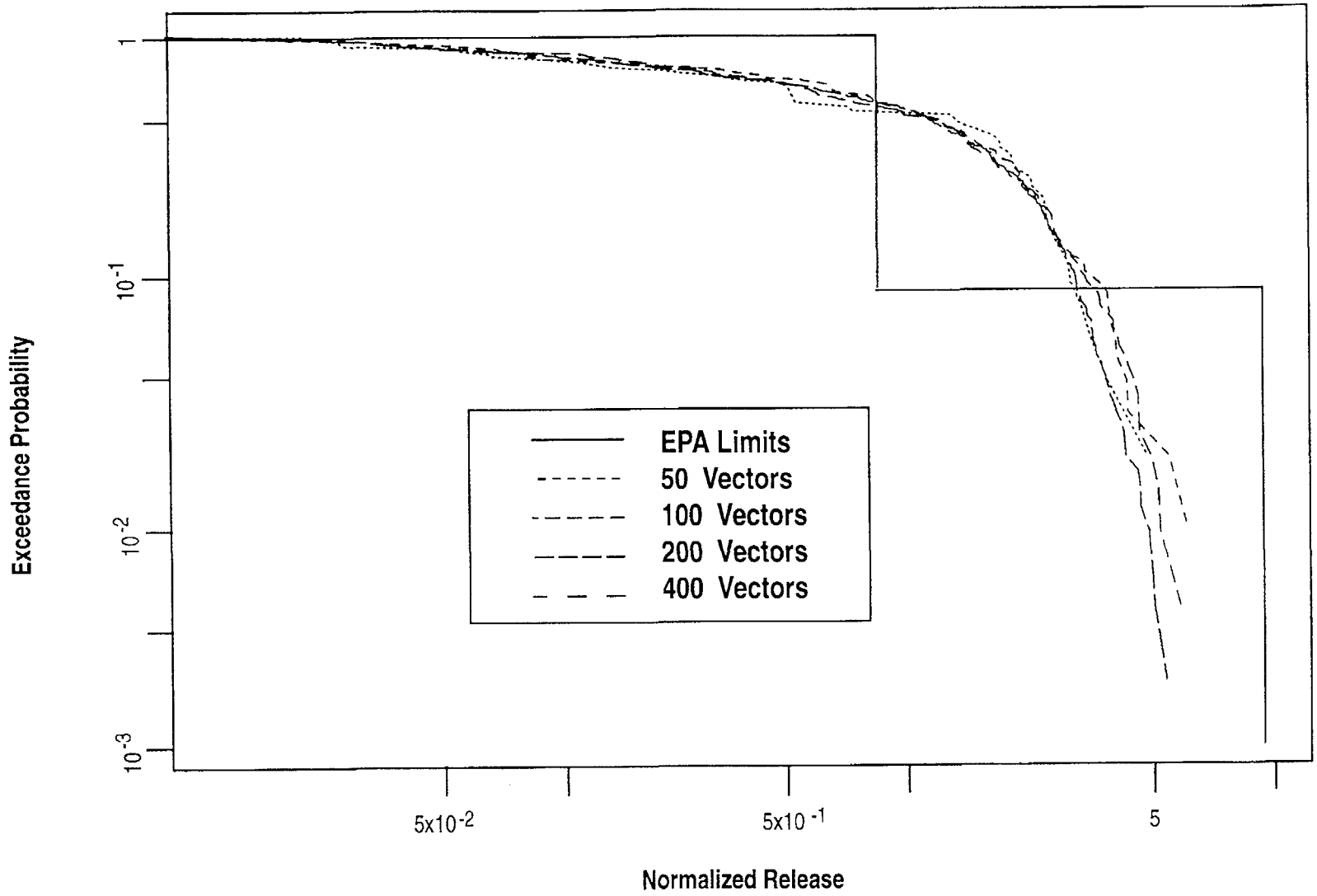


Figure 8-10 Sensitivity of base case (0000) scenario CCDF to the number of vectors

## 8. Sensitivity and Uncertainty

distribution function (CDF) for  $Y$  since it summarizes the variability in computer model output which results from the input assumptions."

Although the main presentation of uncertainty in IPA Phase 2 will rest on the CCDF, an additional means of describing uncertainty, the "uncertainty coefficient," has also been developed.

### *Uncertainty Coefficient*

It would be useful to define an "uncertainty coefficient" to represent the contribution of uncertainty from each of the input parameters, but there does not appear to be any standard definition of such a term. Leading toward a definition that can be used in the present work, Zimmerman *et al.* (1990) present an expression for the uncertainty, using the response surface in which the actual model is represented by the multilinear regression of the model results:

$$\begin{aligned} \text{Var}(Y) = E[(Y - \bar{Y})^2] = \sum_i \beta_i^2 \text{Var}(x_i) \\ + \sum_i \sum_j \beta_i \beta_j \text{Cov}(x_i, x_j) \end{aligned} \quad (8-9)$$

where  $Y$  is the value of the response,  $\beta_i$  is the regression coefficient  $\partial Y / \partial x_i$ ,  $E[\ ]$  is the expected value,  $\bar{Y}$  is the estimated mean of  $Y$ ,  $\text{Var}$  is the variance, and  $\text{Cov}$  is the covariance. For the IPA Phase 2 calculations, the independent parameters are not deliberately correlated, so it is assumed that the covariance term is zero. In this analysis, the quantity  $\text{Var}(Y)$  is estimated by estimating  $\beta_i$  and  $\text{Var}(x_i)$ .

Assuming that there is no covariance among the independent parameters, Equation (8-9) presents a way in which the variance of the response can be tied to variance and sensitivity of each of the independent parameters. Based on this assumption, it is possible to define an "uncertainty" coefficient  $U_i$ :

$$U_i = \frac{\beta_i^2 \text{Var}(x_i)}{\text{Var}(Y)} \quad (8-10)$$

This term is numerically equivalent to the square of the "standardized regression coefficient" described in Section 8.4.2. Ideally, if all the independent parameters were included in the model,

the sum of  $U_i$  for all independent parameters would be unity. Non-zero covariance of the independent parameters will cause  $\sum U_i$  to deviate from unity. The sums of the uncertainty coefficients presented in Tables 8-2 to 8-5 are equal to the coefficient of determination,  $R^2$ , for each regression analysis.

## 8.6 Emulation of the Total-System Performance Assessment Model Using Multilinear Regression

One aspect of doing multilinear regression that has not been explored previously by the NRC staff is the application to emulating the total-system performance assessment model. The regression equation can be used with the suite of values for the input parameter to estimate the response,  $\hat{Y}$ . The estimated response may then be compared with the full model output (*Normalized Release* or *Effective Dose Equivalent*) to determine how good the regression equation approximation of the model is. The following discussion outlines some of the procedures used to better fit the regression equation to the model and illustrates how the regression equation can be used to estimate model performance.

### 8.6.1 Estimation of the Response

Values of the response for the simplest form of the multilinear regression equation were calculated using the raw data for the input parameters ( $x_i$ ) and the estimated regression coefficients,  $b_i$  (Tables 8-2 to 8-5).

$$\hat{Y} = a_0 + b_1 x_1 + \dots + b_n x_n \quad (8-11)$$

It should be noted that although the form of the regression described here is linear, several parameters used in IPA Phase 2 do not exhibit a linear relationship with the performance measure.

A non-linear relationship between the response and the independent parameters can often be determined by plotting the residuals for the regression against the values for a given independent parameter (Figure 8-11). If the residuals  $e_i = (Y_i - \hat{Y}_i)$  are a function of an independent parameter, there will be a grouping or trend in residuals as a function of the independent parameter (Figure 8-11a). In Figure 8-11a, there is a

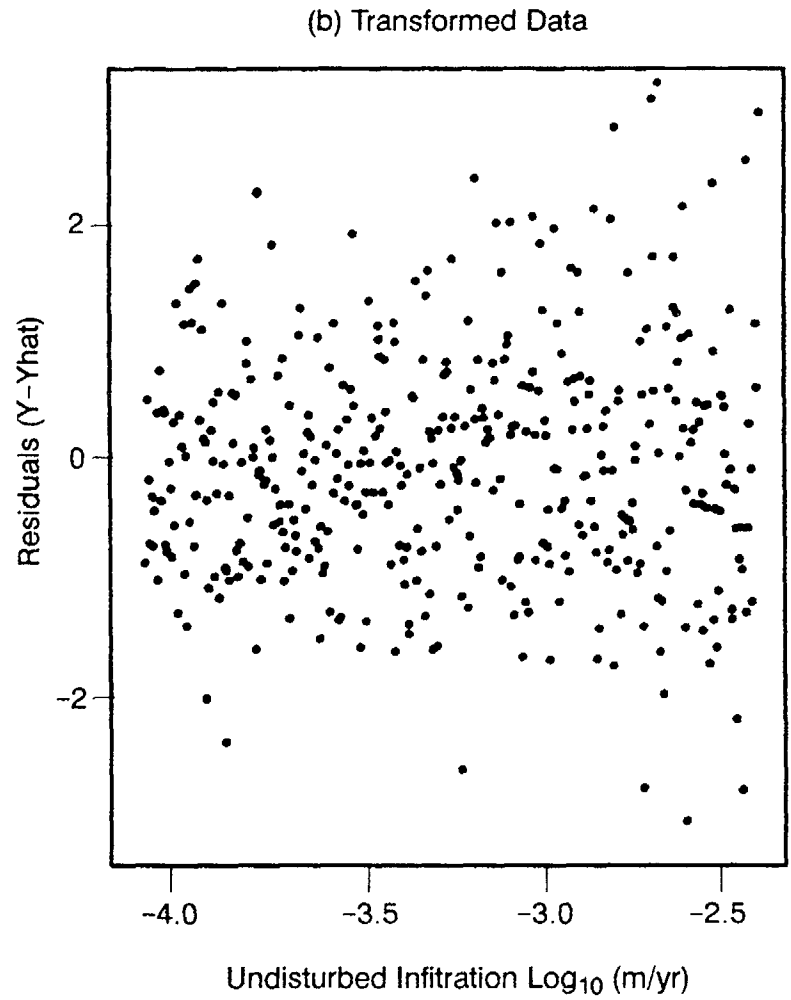
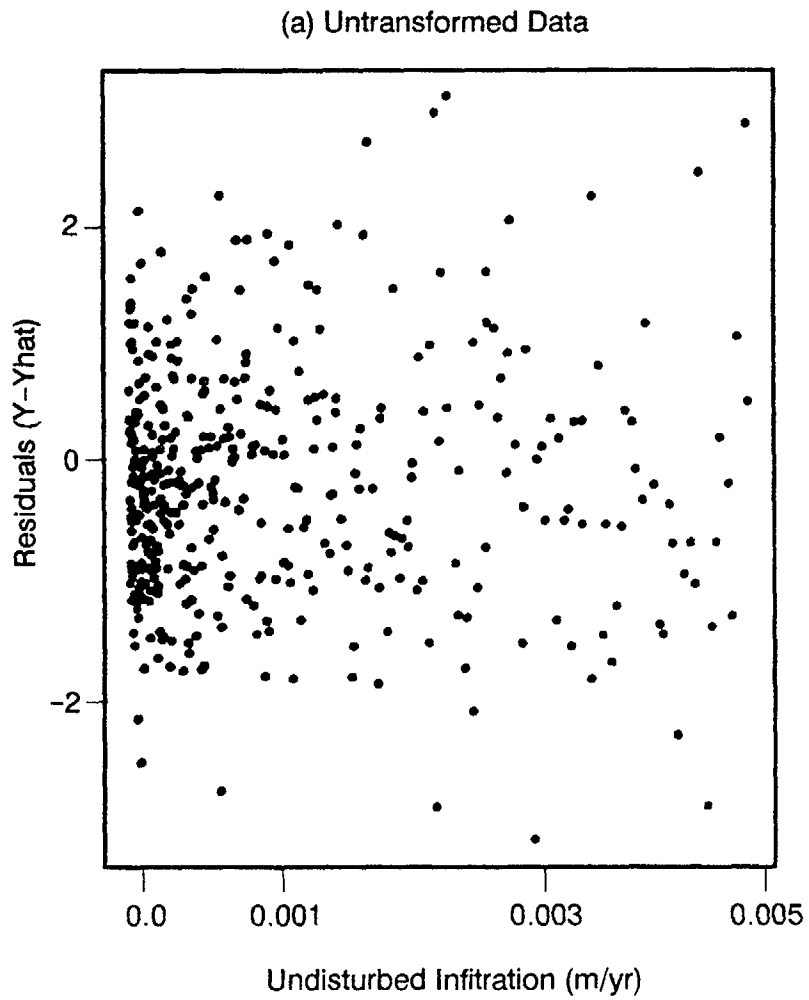


Figure 8-11 Plot of residuals from multilinear regression as a test for heteroscedasticity

## 8. Sensitivity and Uncertainty

skewed distribution of the points toward low infiltration values. Transformation of the independent parameter to a non-linear form (e.g.,  $1/x$ ,  $\log(x)$ ,  $x^2$ ) may be appropriate (Sen and Srivastava, 1990). By transforming the independent parameter (e.g., *infiltration* to  $\log(\textit{infiltration})$ ), the residuals plot (Figure 8-11b) is changed to indicate no functional relationship between the residuals and the independent parameter. This indicates that the new form of the parameter may help provide a better fit of the model.

The process of transforming parameters, doing subset selection and regression analysis, is an iterative process. Several iterations may be required to get the best fit of the model by the regression equation. Non-linear regression techniques are also available, but beyond the scope of the present project.

A regression equation was constructed for the purpose of emulating the total-system performance assessment model. Twenty parameters selected by stepwise regression analysis were used; some parameters were transformed as discussed above.

Figure 8-12 is a plot of the estimated values for *Normalized Release*,  $\hat{Y}$ , from the regression equation versus the *Normalized Release* for the base case (0000) computed by the TPA computer code. It should be noted that the estimated response parameter  $\hat{Y}$  is a function of specific  $b_i$  and specific values of  $x_i$ . Other regression equations will give different results. The purpose of the plot is to illustrate the degree of fit between the response variable determined by the regression equation and the performance measure computed by the TPA computer code. The correlation coefficient between the estimated response  $\hat{Y}$  and the *Normalized Release* is 0.78, which corresponds to a coefficient of determination of 0.61. The 95 percent confidence interval is noted on the plot and indicates the region in which there is high confidence of finding the least-squares fit line. Figure 8-13 illustrates the CCDFs for the estimated responses  $\hat{Y}$  and the *Normalized Release* from the total-system performance assessment model.

## 8.6.2 Evaluation of the Goodness of Fit

### 8.6.2.1 Correlation Coefficient

The correlation coefficient is often used to estimate the linear relationship between two variables (Walpole and Myers, 1978). The more linear the relationship, the closer the correlation coefficient is to unity. Ideally, the better the regression equation estimates the full total-system performance assessment model, the closer the correlation coefficient is to 1 (or -1). The square of the correlation coefficient, the coefficient of determination ( $R^2$ ) indicates the percent of the full model that is explained by the regression model. The coefficient of determination for the regression equation with twenty parameters is 0.61. Because the coefficient of determination and the absolute value of the correlation coefficient increase as more parameters are added to the model, they are not necessarily good indicators of the optimal number of parameters to be included in the regression model. Proper selection of the form of the independent parameters is essential to constructing a regression equation that will emulate the total-system performance assessment model well.

### 8.6.2.2 Mallows' $C_p$ Statistic

Helton *et al.* (1991) stated that as the number of independent parameters increases, there is a greater chance for spurious correlations that result in the inclusion of a variable in the regression model. Mallows'  $C_p$  statistic (Mallows, 1973; and Sen and Srivastava, 1990) was used in this analysis, in an attempt to evaluate the optimal number of parameters that should be included in the regression model.

Mallows'  $C_p$  statistic compares the error of the restricted model (the regression equation for the subset of parameters) to the error of the full (total-system performance assessment) model (all of the independent parameters):

$$C_p = \frac{\sum_{i=1}^p (Y - \hat{Y})^2}{s^2} - (n - 2p) \quad (8-12)$$

where  $Y$  is the response for the full model with all parameters,  $\hat{Y}$  is the response for the restricted model,  $s^2$  is the unbiased estimate of the variance (mean square error) for the full model,  $n$  is the number of observations, and  $p$  is the number of

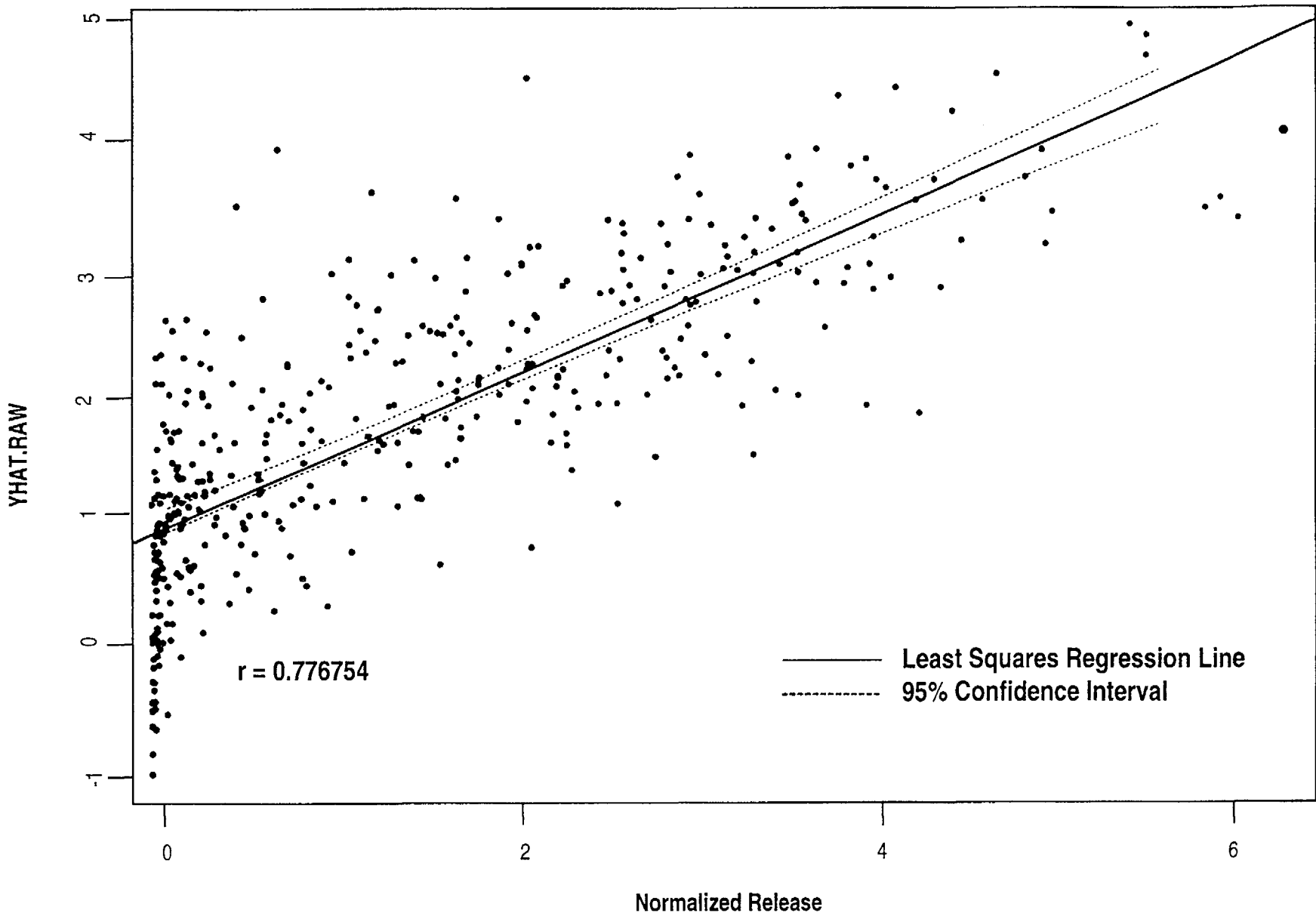


Figure 8-12 Plot of predicted response (YHAT.RAW) from multilinear regression analysis versus *Normalized Release* calculated by the TPA computer code, base case (0000) scenario

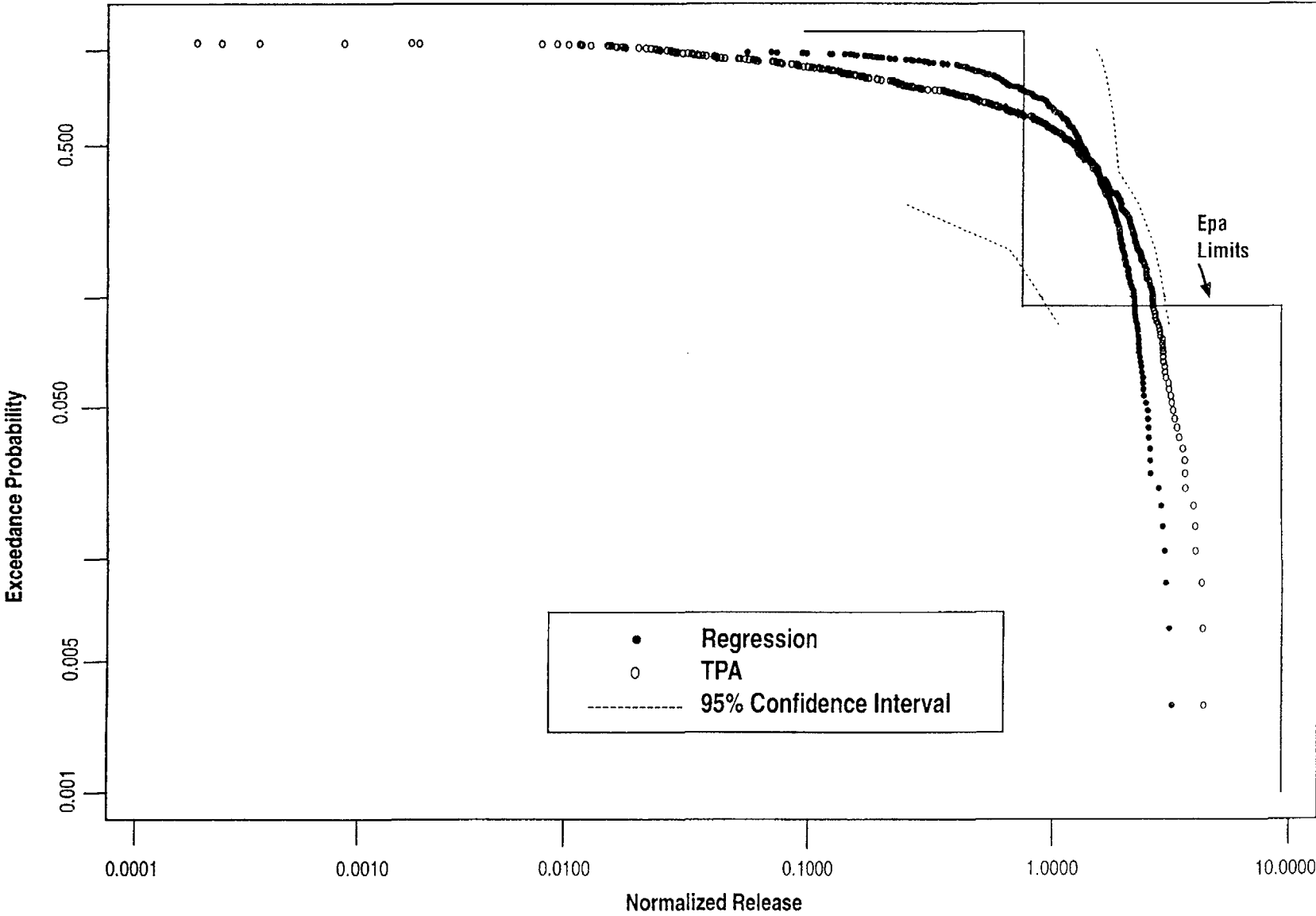


Figure 8-13 Comparison of CCDFs for predicted response (YHAT.RAW) and Normalized Release from the TPA computer code, base case (0000) scenario

independent parameters in restricted model, plus one (Walpole and Meyers, 1978).

When  $C_p \simeq p$ , the optimal number of parameters for the regression equation has been chosen. In this analysis, the use of the  $C_p$  statistic for selecting the optimal number of parameters did not give results that were easily interpretable. The  $C_p$  statistic is very sensitive to small changes in the fit if  $(n - 2p)$  is large (Gunst and Mason, 1980). Attempts were made to reduce the number of independent parameters to consider, by first performing stepwise linear regression, with the  $F$ -test criterion using  $\alpha = 0.1$ , and then doing a subsequent subset selection, with  $\alpha = 0.05$ . The comparison of the  $\alpha_{.05}$  model with the  $\alpha_{0.1}$  model still did not provide easily interpretable results. More work is needed to establish the optimal number of parameters for subset selection and multilinear regression. One aspect that should be considered is the predictive capability of the individual independent parameters. Another aspect to consider is how effectively this statistic might be applied to highly non-linear models.

## 8.7 Sensitivity and Uncertainty Auxiliary Analyses

The IPA Phase 2 staff took part in a computational exercise to evaluate several methods of sensitivity and uncertainty analyses. The purpose of these analyses was to demonstrate, on relatively simple flow and transport problems, several methods for sensitivity and uncertainty analysis useful for evaluation of total-system performance assessments.

The work was presented in two reports. The first report (Gureghian *et al.*, 1992) covers the derivation and verification of the closed-form analytical solutions for one-dimensional saturated transport of a radionuclide in a fractured, layered system with diffusion into the rock matrix. The material properties of individual fractures and rock matrix layers were assumed to be homogeneous and isotropic. The sorption phenomenon in fractures and matrix was described by a retardation coefficients. The solutions of the model are based on analytical inversions of the Laplace transforms, verified with inversions performed numerically. The first module of the computer program calculates the space-time dependent concentration of a decaying species migrating in the fractures and the sur-

rounding matrix. The second module predicts the local sensitivities of releases to the independent parameters.

The second report (Wu *et al.*, 1992) evaluates and demonstrates the use of several sensitivity and uncertainty analysis methods using the analytical model developed by Gureghian *et al.* The Limit-State Approach, which was developed initially for structural reliability analyses, was investigated for its usefulness in IPA. This approach is based on partitioning the performance results into two parts, one in which the performance measure is smaller than a chosen value called the Limit-State, and the other in which the performance measure is larger. The optimal expansion point in parameter space, known as the Most Probable Point (MPP), has the property that its location on the Limit-State surface is closest to the origin. Additionally, the projections onto the parameter axes of the vector from the origin to the MPP are the sensitivity coefficients. Once the MPP is determined and the Limit-State surface approximated, the probability of the performance measure being less than the Limit-State can be evaluated. By choosing a succession of Limit-States, the entire cumulative distribution of the performance measure can be determined. Determining the location of the MPP is the crux of the methodology. Methods for determining the MPP and improving the estimate of probability are discussed in the report.

The Limit-State Approach is significantly more complex than the more commonly used Monte Carlo or Latin Hypercube sampling methods. To aid understanding of the Limit-State Approach, all steps of the method were explained by applying it to two simple examples. The first involved calculation of the cumulative probability distribution of the Darcy velocity  $V$ , given by  $V = -KI$ , where  $K$  and  $I$  are the hydraulic conductivity and hydraulic gradient, respectively. Although simple, this example turned out to be difficult for the application of the Limit-State Approach, because of the possibility of change of sign of  $I$  and hence  $V$ .

The second example applied the Limit-State Approach to a one-dimensional transport problem developed in Gureghian *et al.*, and compared the results among the more conventional methods such as Monte Carlo, LHS, and differential analysis for computing both the CCDF and the sensitivity coefficients. This problem included 25

## 8. Sensitivity and Uncertainty

independent parameters. The uncertainty analysis used the CCDF for cumulative release as the basis for comparison between the methods. Results indicated that the Limit-State Approach had the potential of being much more efficient in terms of computational resources than Latin Hypercube or Monte Carlo Sampling. In one case, the Limit-State Approach was able to duplicate the CCDF produced by a 5000-vector Monte Carlo run with only about 600 vectors, and in other cases far fewer.

In general, computational efficiency is proportional to the desired accuracy and the choice of an approach will depend on the nature of the problem. However, the reports demonstrate that the Limit-State Approach permits the analyst to concentrate on the critical performance region, with the potential for optimizing the use of the consequence model where it can contribute the most information. By contrast, sampling methods such as Monte Carlo or LHS must cover the entire parameter space, regardless of its importance. In addition, the Limit-State Approach leads to probabilistic sensitivity analyses, with essentially no additional work. In particular, the efficiency of the Limit-State Approach is independent of the probability level. Therefore, it is more suitable for evaluating the tails of the distribution than LHS or Monte Carlo sampling. However, the Limit-State Approach is relatively difficult to implement.

The computational efficiency of the Limit-State Approach in general depends on the number of independent parameters and the efficiency of evaluating local sensitivities. When the number of independent parameters is large, the Limit-State Approach may no longer be efficient unless the sensitivities can be determined efficiently, but at the expense of simplicity. The efficiency of the standard Monte Carlo method depends only on the probability level and desired accuracy. It is not clear that the Limit-State Approach will be the best approach for problems involving large numbers of independent parameters.

### 8.8 Conclusions and Suggestions for Further Work

The sensitivity and uncertainty analyses in IPA Phase 2 involved evaluation of a number of techniques that have potential use in the evaluation of

the performance assessment models in a potential license application. Many of the techniques used have been used in previous performance assessment work: stepwise regression analysis, CCDFs, differential analysis, and boxplots. In addition, the Kolmogorov-Smirnov and Sign tests were used to determine parameters important to the total-system performance assessment model. Techniques for developing regression equation to emulate the total-system performance assessment model were examined for potential use in determining CCDF sensitivity to changes in parameter distribution type, for example.

Selection of the significant parameters by stepwise regression analysis, the  $K-S$  test, and the Sign test gave similar results. Regression analysis can only be applied over the entire parameter space. The  $K-S$  test can also be applied to different parts of the parameter space, in order to test for locally important parameters.

The use of standardized data for stepwise regression gave the same results as the untransformed/raw data and had the advantage of giving dimensionless coefficients that could then be compared. The estimated multilinear regression coefficients for the standardized data were used to determine the "uncertainty coefficient" that defined the percentage of the variance of the model response, attributable to variance in the independent parameter.

The results of differential analysis for 14 parameters about the mean for all parameters agreed fairly well with the multilinear regression coefficients. Several parameters exhibited zero sensitivity about the mean, which points to the importance of determining local sensitivities at several points in the parameter space.

The question of how many vectors (observations) will give valid results needs to be explored. The Latin Hypercube sampling strategy reduces the number of vectors needed to do a Monte Carlo simulation. The covariance of the independent variables for 400 vectors was small but non-zero. Difficulties associated with application of the  $C_p$  statistic indicates that perhaps more vectors are needed. The sampling of more vectors will have the disadvantage of requiring longer run times. Yet, it should significantly reduce the number of spurious correlations that can result in picking the wrong variables by stepwise regression.

The assumption that covariance was zero was made in the sensitivity and uncertainty analyses. Future work to consider grouping of parameters or covariance among the input parameters is important to developing a better understanding of model sensitivities.

The development of a regression equation for the purpose of verifying important parameter selection by emulating the total-system performance assessment model has potential use in the license application review process. It should be emphasized that regression equations can never replace the total-system performance assessment model, but are a tool by which to study the sensitivities

associated with performance assessment models. The linear estimation used in this analysis is the simplest technique; a number of others can be explored in future phases of this work.

In general, the techniques used in the IPA Phase 2 sensitivity and uncertainty analysis were easy to implement. No single technique is valid for the sensitivity and uncertainty analyses. The use of a combination of techniques is essential to bringing out various aspects of the total-system performance assessment model. Future evaluation of other techniques such as the "hat" function (Sen and Srivastava, 1990) or the Limit-State Approach will help to establish which techniques will be most useful to the license application review process.

## 9 ANALYTICAL RESULTS<sup>1</sup>

### 9.1 Introduction and Caveats Concerning the Results of IPA Phase 2

This chapter presents the results of the simulation runs of the total-system performance assessment (TPA) computer code using the parameter distributions presented in Appendix A of this report. The results of the simulations are presented as complimentary cumulative distribution functions (CCDFs) of *Normalized Release* and *Effective Dose Equivalent* (defined in Chapter 8), distribution bar graphs, and scatter plots.

The results are presented for demonstration purposes and are not intended to indicate the potential for repository compliance or non-compliance with any of the 10 CFR Part 60 performance requirements.

The following caveats should be taken into consideration when reviewing the results of the Iterative Performance Assessment (IPA) Phase 2 effort:

1. **The models used here are based on limited site data and have had limited review.**  
*Preliminary results from some models such as the gas transport and <sup>14</sup>C retardation model have been presented at U.S. Nuclear Regulatory Commission/U.S. Department of Energy (DOE) Technical Exchanges and before the U.S. Environmental Protection Agency's (EPA's) Scientific Advisory Board. Although the overall modeling was more sophisticated than that of IPA Phase 1, it was recognized that input data were still very limited. In addition, scientists do not yet agree on how adequately the various models represent repository processes.*
2. **The results presented here cannot be confirmed as accurately representing the behavior of the repository.**  
*The staff has examined the results of runs for individual vectors to ensure that for these*

*limited cases, the TPA model appears to be performing as designed. However, other than software quality assurance (QA) and the above mentioned checks, there is no comprehensive validation procedure for the TPA model available at present, to ensure that the computed CCDFs are accurate representations of the behavior of the repository system.*

3. **There are numerous unverified simplifying assumptions in many of the models.**  
*The models for flow and transport considered only a steady rate of infiltration and a constant environment, and did not take into account the significant variations in the driving forces likely to occur over the performance assessment period. Also, the models considered that the geosphere was spatially uniform in the lateral direction, and did not take into account the large variations in material properties that exist at the site. In addition, the behavior of many thousands of waste packages was represented by ensemble averages, using seven representative waste packages.*
4. **There are large uncertainties in the input data.**  
*Although the TPA model is intended to deal with some data uncertainty through the Latin Hypercube Sampling (LHS) process, many of the most important parameters have variations over several orders of magnitude. For many parameter distributions, the means and distribution shapes are based on only a few measurements. Also, the analysis did not recognize correlations among the independent variables in the Monte Carlo analyses, and treated all variables as independent. These situations are likely to lead to extremes in consequences. However, spatial correlations were considered, somewhat, in choosing hydrogeologic variables.*
5. **Coupled effects between processes and events in the scenarios have not been fully modeled nor evaluated.**  
*In IPA Phase 2, an attempt was made to couple some events and processes such as corrosion and repository cooling. However, complex coupled interactions such as moisture movement (including infiltration) and gas*

<sup>1</sup>The figures shown in this chapter present the results from a demonstration of staff capability to review a performance assessment. These figures, like the demonstration, are limited by the use of many simplifying assumptions and sparse data.

## 9. Analytical Results

transport have not been modeled in IPA Phase 2.

### 6. The dose calculation is for illustrative purposes.

The dose calculation is based on assumptions regarding a postulated biosphere consisting of a farm irrigated by well water, a family living on the farm, and a distant population consuming cattle raised on the farm. There has been relatively little research, as a part of IPA Phase 2, on the likelihood of these or other assumptions regarding future biospheres. In addition, many of the coefficients in the dose model are generic and not specific to the repository region.

## 9.2 Conditional CCDFs and Exceedance Probability Curves

### 9.2.1 Construction of the CCDFs

The CCDFs, which express the uncertainty in the model results for population doses and EPA limits for cumulative release over 10,000 years, are presented in different forms, including:

- Conditional CCDFs for each scenario;
- Conditional CCDFs showing performance of individual and engineered barriers; and
- Total CCDFs combining all scenarios for both release and dose.

*Normalized Release*, which is the primary measure of consequences displayed by the CCDF is computed by dividing each radionuclide that enters the accessible environment by its limit specified in Appendix A, Table 1 of 40 CFR Part 191 (*Code of Federal Regulations*, Title 40, "Protection of Environment"), and summing the resulting ratios. *Effective Dose Equivalent*, the other measure of consequences displayed by the CCDF, is described in Section 7.3.3.

Both conventional mean CCDFs and "hair" diagrams have been constructed. The following discussion presents salient points of CCDF construction for IPA Phase 2.

#### 9.2.1.1 Conditional CCDFs

A conditional CCDF is a CCDF constructed for a single scenario class with the assumption that the scenario class has a probability of occurrence of 1.0. For each scenario class evaluated under IPA Phase 2, a conditional CCDF was constructed in the following manner:

- A vector represents a single sampling for all of the sampled variables. The total number of vectors to be selected has to be known before sampling so that each selection for each variable is made from equally probable distributions;
- Each vector is assigned an equal probability within the scenario (i.e., for 400 vectors, each vector has a probability  $p_i = 1/400$ );
- The set of vectors is sorted from lowest to highest consequences  $R$  (cumulative release or dose);
- The exceedance probability  $E$  of the sorted consequences is calculated by the following formula:

$$E_i = 1 - \sum_{i=1}^{N'} p_i' , \quad (9-1)$$

where  $p_i'$  is the probability of the  $i^{\text{th}}$  vector of the sorted set, and  $N'$  is the number of vectors in the set; and

- The CCDF is the graph of  $E_i$  versus its sorted consequences  $R$ .

#### 9.2.1.2 Screened Conditional CCDFs

This CCDF uses a set of vectors derived from the 400-vector base case scenario by screening for compliance with regulations or ranges of model input parameters. It is constructed identically to the conditional CCDF described above, but for  $N' =$  the number of remaining vectors, and still assuming equal probability for each remaining vector,  $p_i = 1/N'$ . Examples of possible screening criteria are waste package lifetimes greater than 300 years (or 1000 years) and infiltration rates less than 0.3 millimeters/year.

#### 9.2.1.3 Total CCDF

The total CCDF is constructed by combining vectors from all scenarios. The probability of each

vector  $p_k$ , however, is taken to be the scenario probability  $p_j$  divided by the number of vectors  $N_j$  in the scenario:

$$p_k' = \frac{p_j}{N_j} \quad (9-2)$$

The consequences are then sorted, as before, from lowest to highest. The exceedance probability is then defined:

$$E_k = \sum_{k=1}^{N'} p_k' \quad (9-3)$$

where  $N'$  is the total number of vectors, and  $p_k'$  are the probabilities for the sorted consequences.

#### 9.2.1.4 "Hair" Diagrams

Helton *et al.* (1991, Section VI) develops an alternative method of displaying uncertainty about scenarios and parameters for probabilistic models. In this technique, "hair diagrams," there is one CCDF or "hair" per vector, which displays the cumulative probability for each vector (for which there is a new set of sampled parameters) displayed over the range of scenarios. Among the advantage of hair diagrams, Helton *et al.* states the following:

"... they maintain the distinction between scenarios, probabilities for scenarios,

consequences and fixed but imprecisely known quantities.... Further, these representations lead naturally to CCDFs and distributions of CCDFs. The distributions of CCDFs are important because they display the variability that is averaged over to obtain the mean CCDFs that are typically used for comparison with the EPA release limits."

Because one line is plotted for each vector, hair diagrams are complicated and difficult to interpret. To simplify them visually, yet preserve the statistical information they contain, the boundaries of the hair diagram are summarized by finding the density function of the exceedance probability at a range of values of cumulative release, and plotting only the 5<sup>th</sup>, 50<sup>th</sup>, and 95<sup>th</sup> percentiles of this density function; (i.e., for a given value of cumulative release  $R_i$ , the exceedance probabilities are interpreted from all hairs, their values sorted, and the 20<sup>th</sup>, 200<sup>th</sup>, and 380<sup>th</sup> values saved to be plotted as the 5<sup>th</sup>, 50<sup>th</sup>, and 95<sup>th</sup> percentile of the hairs.

#### 9.2.2 Conditional CCDFs for Various Scenario Classes

Four-hundred (400) vector runs were made for nine scenario classes. These classes are identified in the following table (Table 9-1) along with their estimated probabilities of occurrence over the next 10,000 years.

Table 9-1 Estimated Probabilities for the Scenario Classes Modeled in the IPA Phase 2 Analysis

Scenario Class	Scenario Class Identifier <sup>a</sup>	Estimated Probability
Base Case	0000	≈ 0.0
Climate Change Only (Pluvial)	co00	≈ 0.0
Seismicity Only	os00	$7.9 \times 10^{-8}$
Drilling Only	oodo	≈ 0.0
Magmatic Activity Only	ooov	≈ 0.0
Drilling + Seismicity	osdo	0.35
Drilling + Seismicity + Magmatic Activity	osdv	$1.0 \times 10^{-2}$
Drilling + Seismicity + Climate Change	csdo	0.62
Drilling + Seismicity + Magmatic Activity + Climate Change <sup>b</sup>	csdv	$2.0 \times 10^{-2}$

<sup>a</sup>See Section 9.2.3 for explanations of the identifiers.

<sup>b</sup>Fully disturbed.

## 9. Analytical Results

Scenario classes *csdv*, *csdo*, *osdv*, and *osdo* were chosen from the 16 possible scenarios (see Chapter 3) to calculate the exceedance probabilities of the releases and doses from their conditional exceedance probability curves (CCDFs). These are the only scenario classes with occurrence probabilities large enough to make a significant contribution to total performance. The other cases were chosen to evaluate the effect on exceedance probabilities by disruptive events acting alone. It is assumed that any significant interaction between disruptive events (within the capabilities of the models to predict) will be picked up in the fully disturbed (*csdv*) case.

### 9.2.3 Basic Scenarios

The basic scenarios computed for the purpose of comparison are: the base (or undisturbed) (*oooo*) scenario; the fully disturbed (*csdv*) scenario; the base case disturbed by climate-only (*cooo*) scenario; the base case disturbed by drilling-only (*oodo*) scenario; the base case disturbed by seismic-only (*osoo*) scenario; and the base case disturbed by magmatism-only (*oovv*) scenario. The conditional exceedance probabilities (or CCDFs) for the *Normalized Release* for each scenario are presented in Figure 9-1. The dotted lines represent compliance with the EPA release standard.<sup>2</sup> The conditional exceedance probabilities for dose estimates<sup>3</sup> are presented in Figure 9-2.

**Scenario plots** as defined in this report are scatter plots of the results for one scenario plotted against the results of another LHS scenario. For the IPA Phase 2 analysis, the LHS sets contained 400 vectors for all production runs. Since all scenario

runs used the same LHS set and most of the same independent variables, these plots allow the visual inspection of the effects of the scenario on the model outputs. Scenario plots were used to compare the single-event scenarios against the base case; that is, scenario *cooo* (pluvial infiltration and higher water table); *osoo* (seismicity); *oodo* (human intrusion by exploratory drilling); and *oovv* (magmatism); against *oooo* (undisturbed or base case).

The base case (*oooo*) scenario represents the calculated releases and doses from the repository over a 10,000-year performance period, under conditions as they are presently perceived to exist (allowing for parameter uncertainty) and without disturbing events such as drilling, earthquakes, magmatism, or change to a pluvial climate. The thresholds defined for two of these disturbing events, earthquakes and drilling, give them probabilities of occurrence of almost 1.0 during the period of performance. Hence, the probability of occurrence of scenarios not containing these events is almost 0.0. The probability of having a pluvial climate within the performance assessment period is estimated to be 0.64. Therefore, the probability of the base case is very low, and is computed primarily for comparison rather than as a major contributor to the total exceedance probability curve. The fully disturbed (*csdv*) scenario represents the opposite extreme from the base case. In the fully disturbed case, all disruptive events being considered (seismicity, drilling, magmatism, and pluvial) are allowed to act on the repository. This scenario is expected to show the effects of interactions among events, as well as the effects of the events, themselves. An example of an expected interaction is pluvial climate (high water level and increased infiltration) and seismically induced waste package failures.

As can be seen by comparing the climate-only (*cooo*) scenario with the fully disturbed case (*csdv*) in Figure 9-1, almost all the increase in *Normalized Release* in the high probability part of the fully disturbed CCDF over the base case CCDF is due to the influence of the pluvial climate (described in Section 6.2). Figure 9-3 is a scenario plot comparing the releases from the pluvial scenario with the releases from the base case for the same vectors. The influence of climate on the total releases is very significant for most vectors, even

<sup>2</sup>Currently, a revised set of standards specific to the Yucca Mountain site is being developed in accordance with the provisions of the Energy Policy Act of 1992. The Energy Policy Act of 1992 (Public Law 102-486), approved October 24, 1992, directs NRC to promulgate a rule, modifying 10 CFR Part 60 of its regulations, so that these regulations are consistent with EPA's public health and safety standards for protection of the public from releases to the accessible environment from radioactive materials stored or disposed of at Yucca Mountain, Nevada, consistent with the findings and recommendations made by the National Academy of Sciences, to EPA, on issues relating to the environmental standards governing the Yucca Mountain repository. It is assumed that the revised EPA standards for the Yucca Mountain site will not be substantially different from those currently contained in 40 CFR Part 191, particularly as they pertain to the need to conduct a quantitative performance assessment as the means to estimate postclosure performance of the repository system.

<sup>3</sup>Those persons who were assumed to be exposed in the CCDFs for the dose include: the members of the farm family (three persons); and members of the regional population (177 of them are assumed to consume contaminated beef).

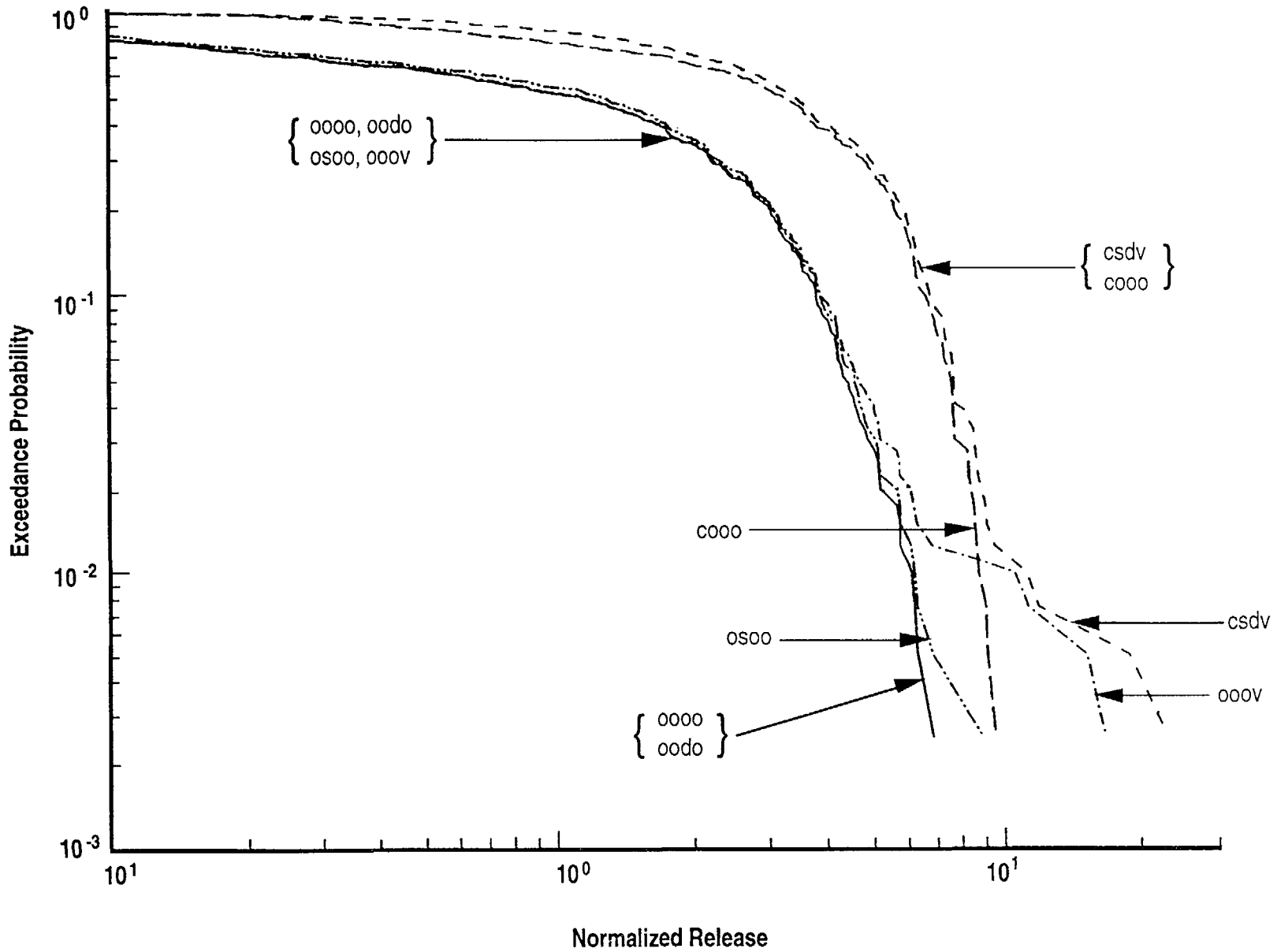


Figure 9-1 Conditional CCDFs for Normalized Release for basic scenarios (Scenario class identifiers are described in Table 9-1.)

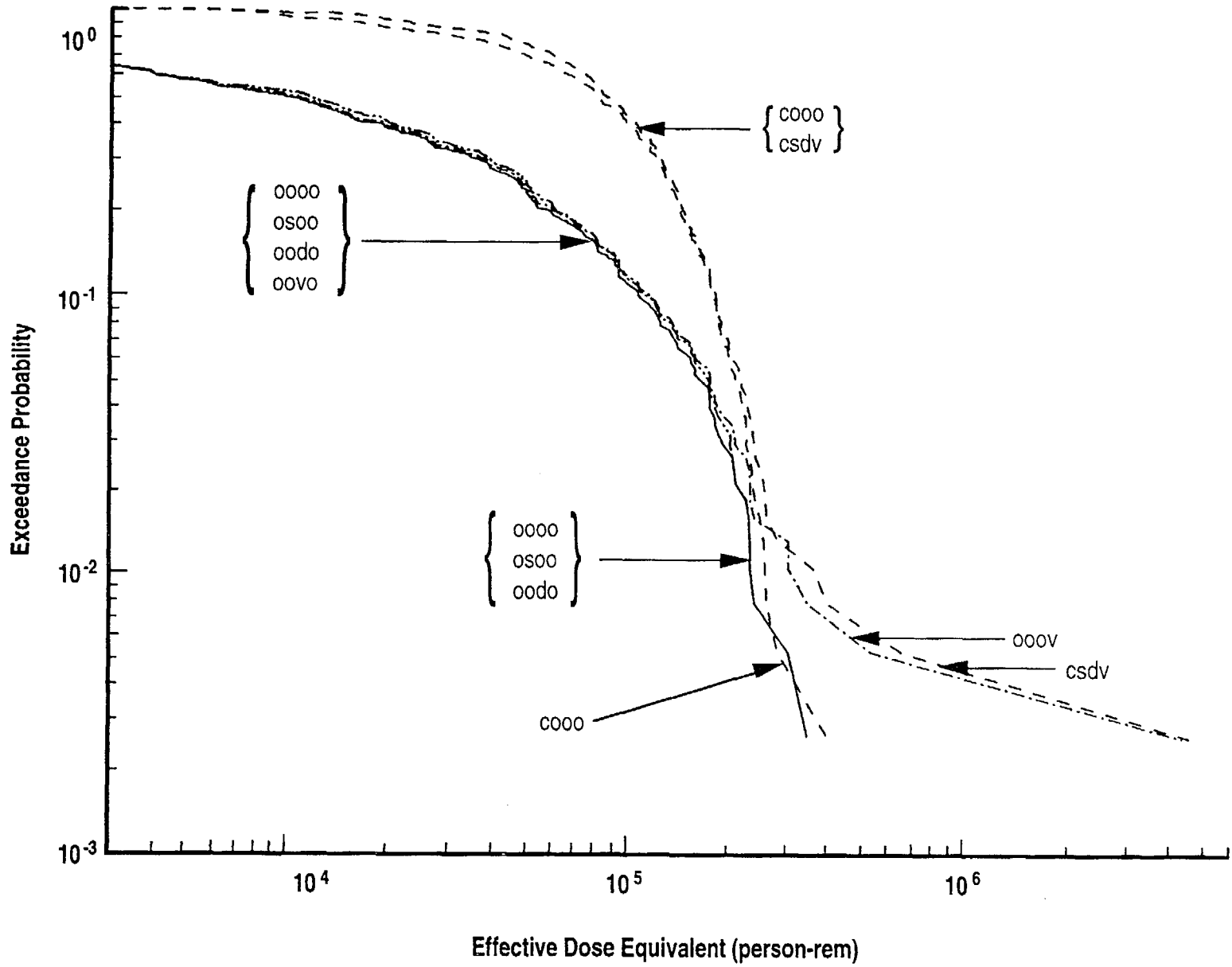


Figure 9-2 Conditional CCDFs for *Effective Dose Equivalent*  
 (Scenario class identifiers are described in Table 9-1.)

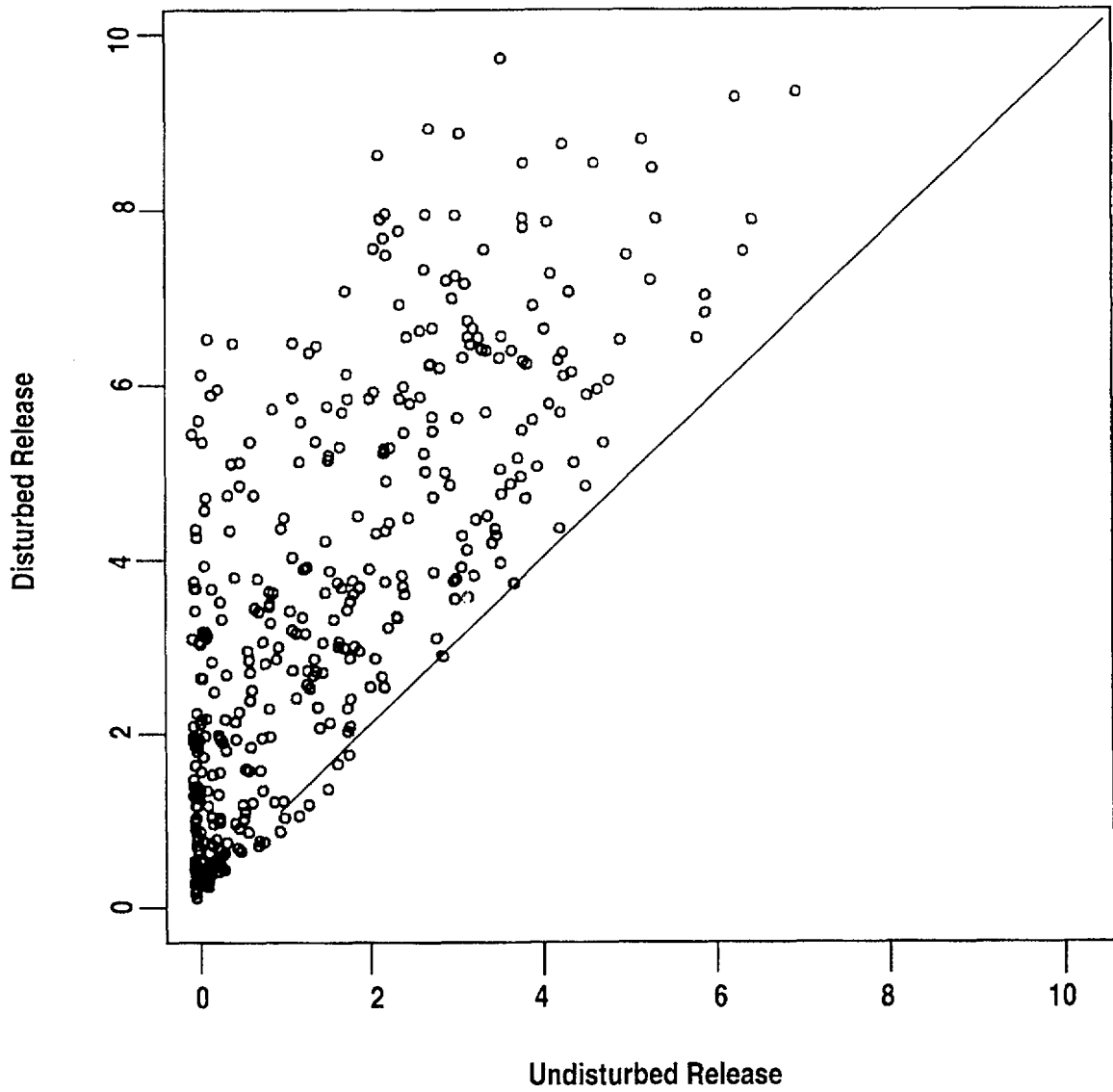


Figure 9-3 Scenario plot of pluvial scenario versus base case scenario

## 9. Analytical Results

though the gas pathway is insensitive to infiltration (the IPA Phase 2 models did not explicitly consider the effects of infiltrating water on either the release of gaseous radionuclides, nor their transport in the geosphere). Although the effect of the pluvial conditions is large, there are some vectors that are nearly the same or even smaller for the pluvial case. This observation is probably caused by the following conditions:

- Contributions to cumulative release from the gas pathway are relatively large, compared with the liquid pathway; and
- The higher water table during the pluvial scenario causes radionuclides to be released from the vadose zone into a less permeable and slower moving saturated zone than would be the case for the non-pluvial conditions. This results in a smaller release to the accessible environment for the same release to the saturated zone.

Human intrusion, as presented in the base case disturbed by drilling-only scenario (*oodo*) (see Section 6.3), in Figure 9-1, does not appear to have a discernable effect on the exceedance probabilities. There appears to be a low likelihood of a direct hit and relatively minor consequences when a hit is actually made. The scenario plot, Figure 9-4, shows the releases from the liquid, gas, and direct pathways for the drilling-only scenario compared with the base case. There are only minor differences in the releases from drilling, virtually all caused by the direct releases of contaminated rock. Without the releases of contaminated rock, the comparison would plot almost perfectly as a straight line. There are only minor differences in liquid and gas releases caused by a few prematurely failed waste packages, but the results are too small to be visible on a plot. It should be noted that a more in-depth analysis, for example, one accounting for the effects of drilling fluid, could show an increase in consequences and the significance of the scenario.

The seismic-failure mechanism described in Section 6.4 is considered to be very conservative. However seismic failure appears to have only a small effect on the CCDF, as shown by the comparison in Figure 9-1. Seismic loading usually shortens waste package lifetime by a small

amount, resulting in little increase in the *Normalized Release*.

The effect of seismicity is more apparent on the scenario plot, Figure 9-5a. This figure shows the total releases for the seismic-only (*osoo*) scenario compared with the base case scenario. There are a significant number of vectors with higher releases. The way in which the seismic model is employed must permit all containers in any zone to fail simultaneously when the seismic criteria are exceeded. The vectors having the largest relative release for the seismic scenario had seismic parameters allowing relatively early seismic failure, which contributed mostly to large gaseous releases from the temperature-dependent  $^{14}\text{C}$  source term and transport models. Liquid-only releases, presented in scenario plot, Figure 9-5b, showed a more modest effect of early seismic failures.

Like pluvial climate (*cooo*), magmatism (*ooov*) appears to be the only other event to have a significant, discernable effect on the shape of the exceedance probability plot, as shown in Figure 9-1. Unlike climate, however, magmatism appears to affect only the low probability part of the curve. The likely explanation is that, as with drilling into a waste package canister, the probability of a dike intersection with the repository is very low even under the conditional assumption that the scenario exists. With the magmatism model (see Section 6.5) the probability of an intersection when coupled with the scenario probability and its consequences is high enough and the consequences high enough, that the event of magmatism was able to make a discernable modification to the base case exceedance probabilities at the tail of the distribution function.

The scenario plot in Figure 9-6 shows the total releases from liquid, gas, and direct pathways for the magmatic scenarios. There are a relatively few vectors with large releases. Most of the releases are identical with the base case because there were no magmatic events that happened within the repository area and affected releases. The largest releases were caused by magmatic cones that were assumed to bring radioactive contaminants directly to the surface. In a few cases, magmatic dikes caused premature container failure, but did not bring any contaminant directly to the surface. Subtracting out the direct releases, premature failure caused only minor excess

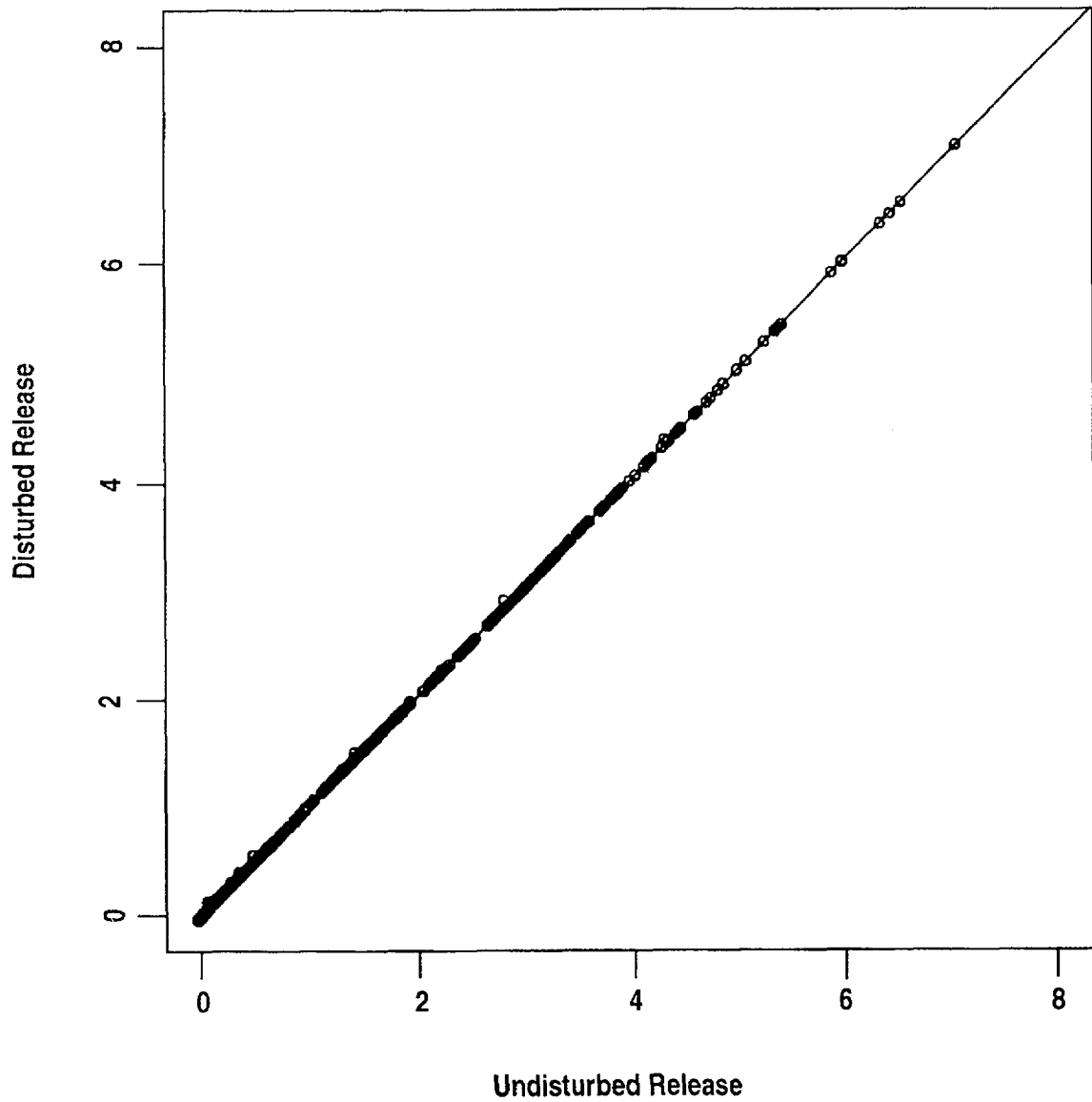


Figure 9-4 Scenario plot of drilling scenario versus base case scenario

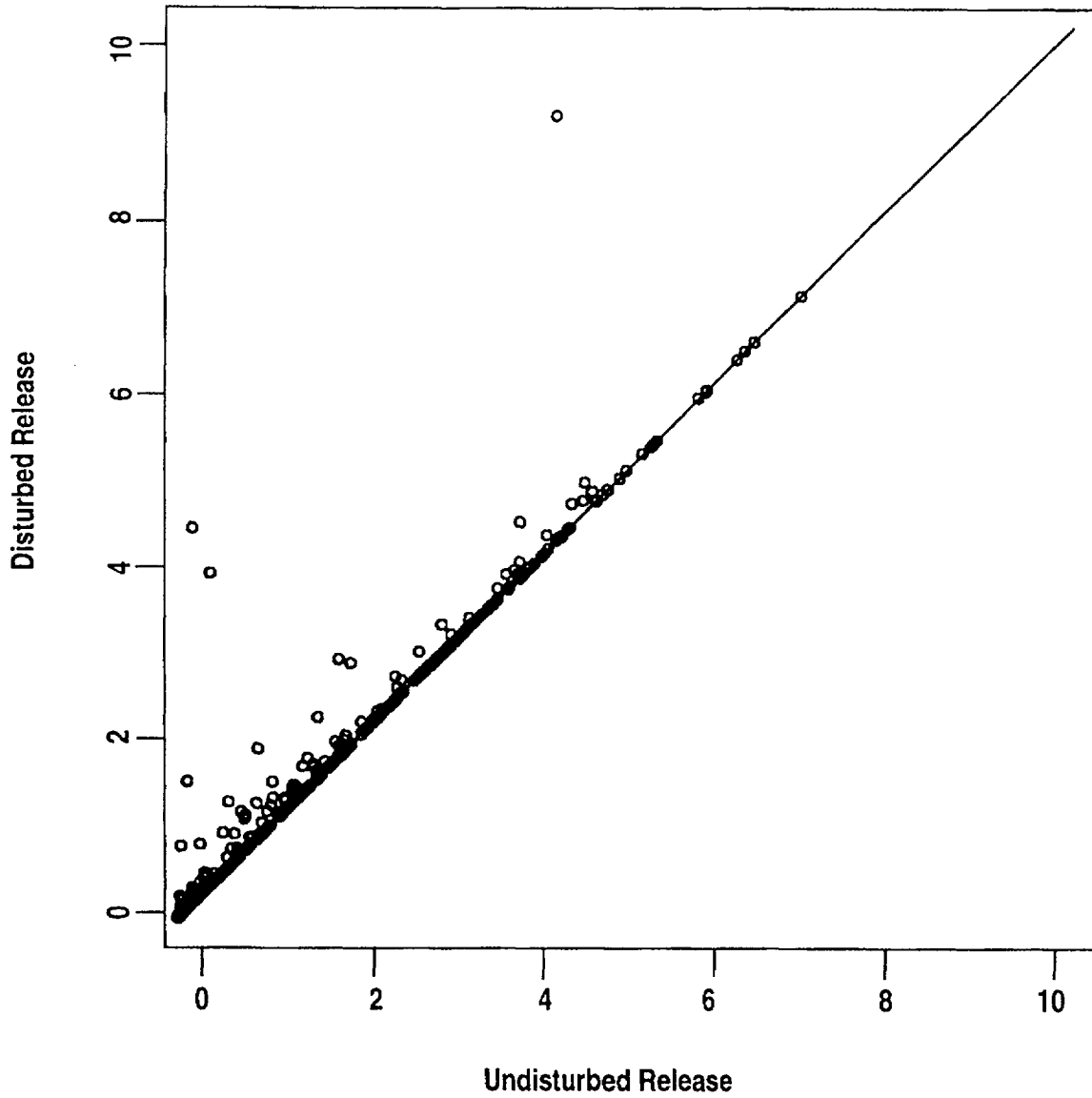


Figure 9-5a Scenario plot of seismic scenario versus base case scenario

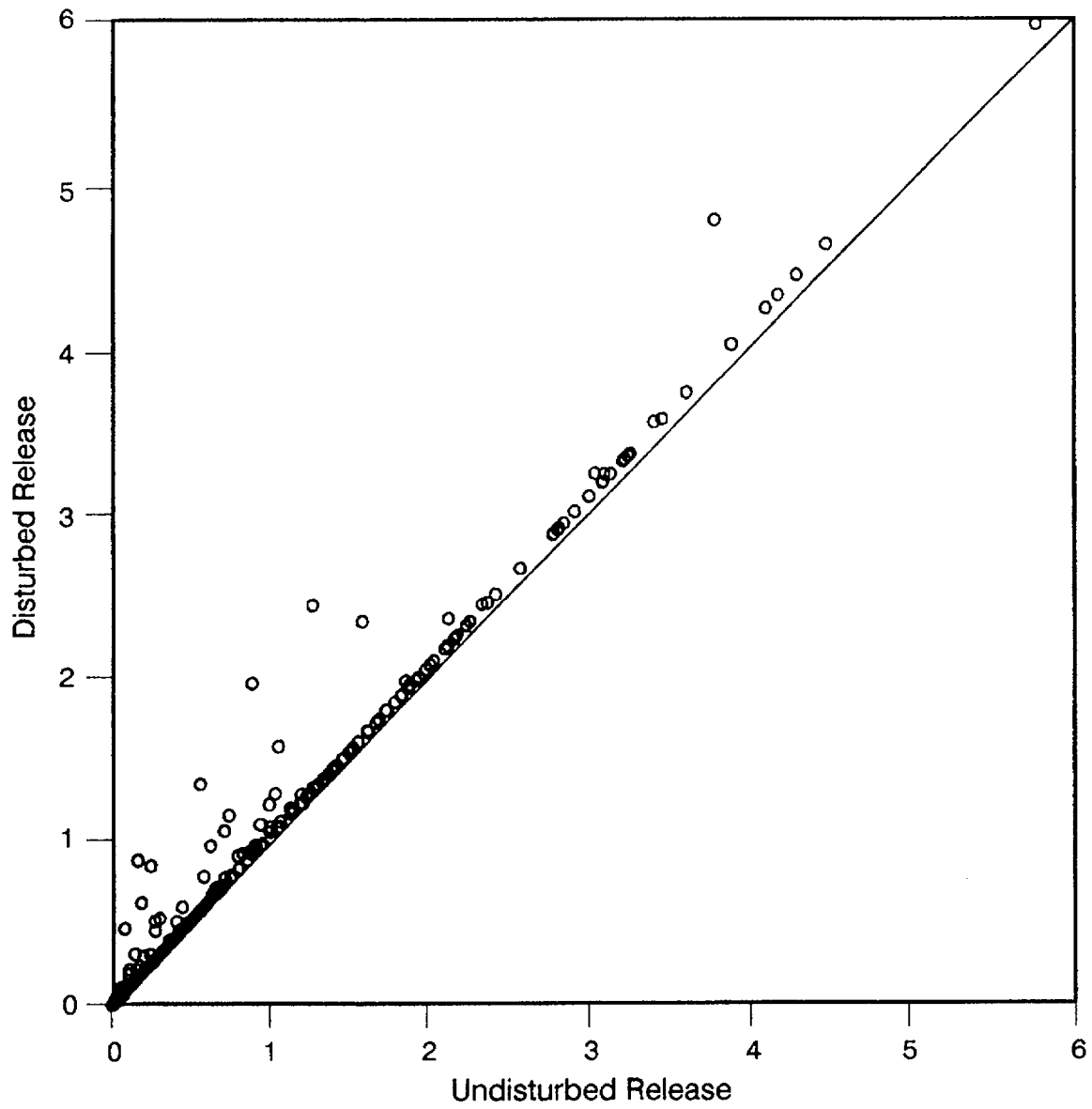


Figure 9-5b Scenario plot of seismic scenario versus base case scenario (liquid releases only)

9. Analytical Results

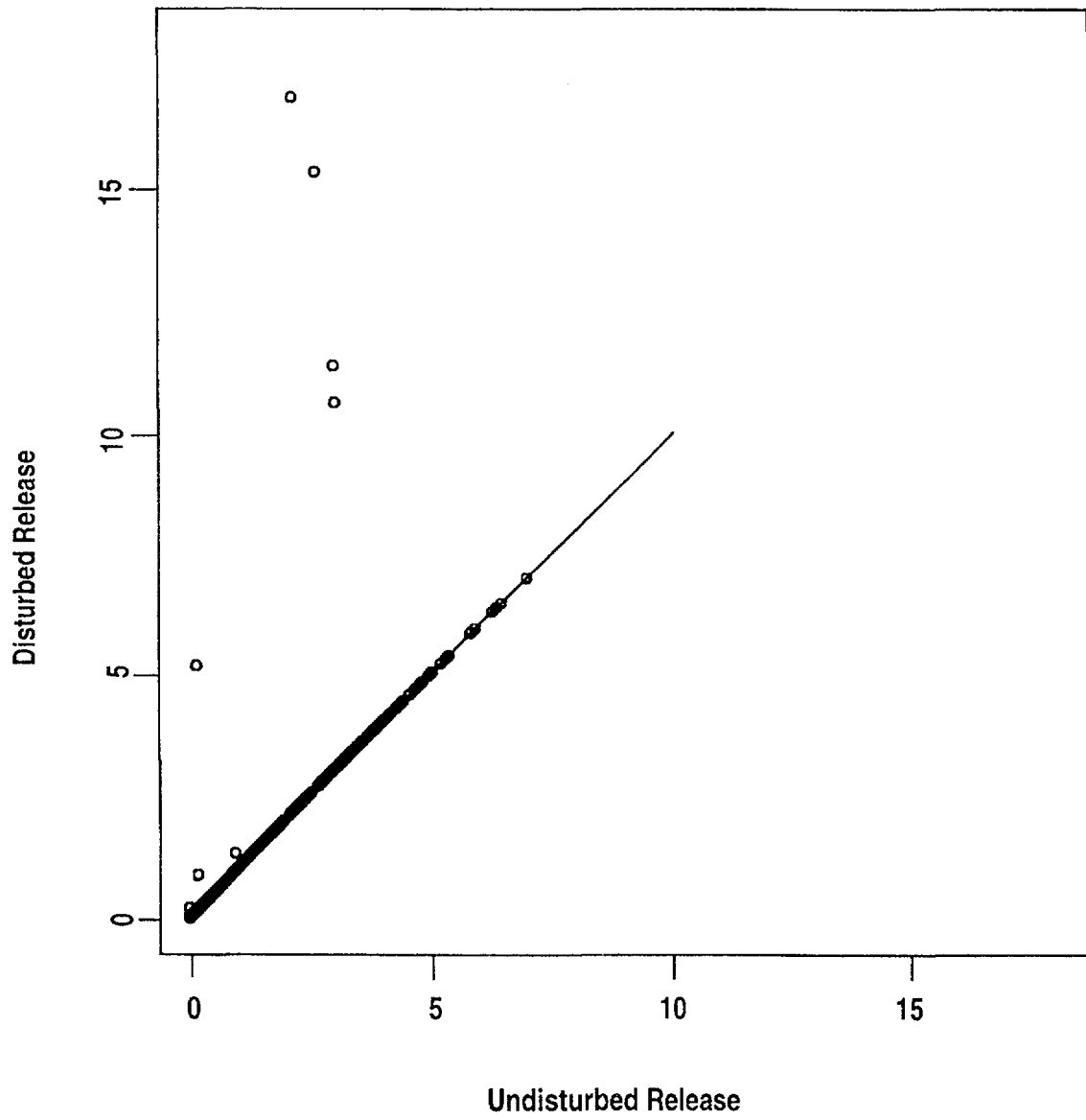


Figure 9-6 Scenario plot of magmatic scenario

releases of liquid and gas, too small to be visible on a plot.

### 9.3 Total System CCDF

The total CCDF for cumulative release for the significant scenarios, *csdo*, *osdo*, *csdv* and *osdv*, was constructed by the procedure described in Section 9.2.1 and is shown in Figure 9-7a. The corresponding CCDF for dose is shown in Figure 9-7b. It should be noted that although the effects of a high-probability event such as pluvial-climate can still be recognized in the total CCDF, the effects of low-probability events such as magmatism are obscured. To better preserve the effects of both low- and high-probability events, Figure 9-8a shows the same information used to construct the total CCDF, but plotted as a "hair" diagram, as described in Section 9.2.1. Figure 9-8b shows the 5<sup>th</sup>, 50<sup>th</sup>, and 95<sup>th</sup> percentiles of the hairs, as boundaries from the hair diagram. The significance of the "hair diagram" is to present the entire range of credible releases from the repository as a function of scenario probability and parameter uncertainty. The curve shown in Figure 9-7a incorporates scenario probability and parameter uncertainty into a single curve, without providing a means of separately evaluating the effects of either.

### 9.4 Differences Between IPA Phases 1 and 2, and Comparison of Results

A complete discussion of results from this total-system performance assessment and future total-system performance assessments must include an evaluation of why the results differ among various analyses. If a baseline CCDF is established, the effects of changing assumptions and parameter values can be quantitatively examined. At the present time, the only baseline developed by the staff for comparison is the CCDF from the IPA Phase 1 study. IPA Phases 1 and 2 were significantly different in terms of scope and approach, in many areas. A description of the major improvements in IPA Phase 2 over Phase 1 provides an indication of the amount and relative significance of factors that may be influencing the difference.

#### 9.4.1 Improvements in IPA Phase 2 Likely to Affect Results

##### 9.4.1.1 Scenarios

Only a limited set of scenario classes was considered in IPA Phase 1, drilling and pluvial conditions, resulting in four scenarios. However, for the IPA Phase 2 analysis, the staff applied the Sandia National Laboratories (SNL) scenario-selection methodology for use in the consequence analysis of a potential high-level (HLW) waste disposal site (see Cranwell *et al.*, 1990). Based on the staff evaluation and modification of the SNL methodology, four scenario classes were considered (climate change, seismicity, magmatism, and human intrusion) from which 16 scenarios resulted. In IPA Phase 1, the occurrence probability of pluvial climate was assumed to be 0.10. In IPA Phase 2, the occurrence probability of pluvial climate was determined to be 0.64 (Chapter 3). The probability of the drilling scenario class at the site was determined to be approximately equal to 1.0 in both IPA Phase 1 and Phase 2.

##### 9.4.1.2 Pathways

The IPA Phase 1 effort identified and accounted for a number of important attributes of the Yucca Mountain site (e.g., stratigraphic changes below the repository in the unsaturated zone and differences between matrix and fracture flow). As discussed in Chapter 4, the IPA Phase 2 effort not only has maintained the important attributes identified in the Phase 1, study but has added further modeling complexity such as:

- Saturated zone pathways to the accessible environment;
- Calculation of radionuclide concentration for dose assessment; and
- Both fracture and matrix pathways allowed within a vector.

The additional complexity provided additional insights into: the performance of fractured rock as geologic barrier; data requirements; and the capabilities of the utilized computational methods.

Also, three transport pathways were considered in IPA Phase 2 (i.e., gaseous, aqueous, and direct) compared with one transport pathway (i.e., aqueous) in Phase 1. In the gas-phase transport

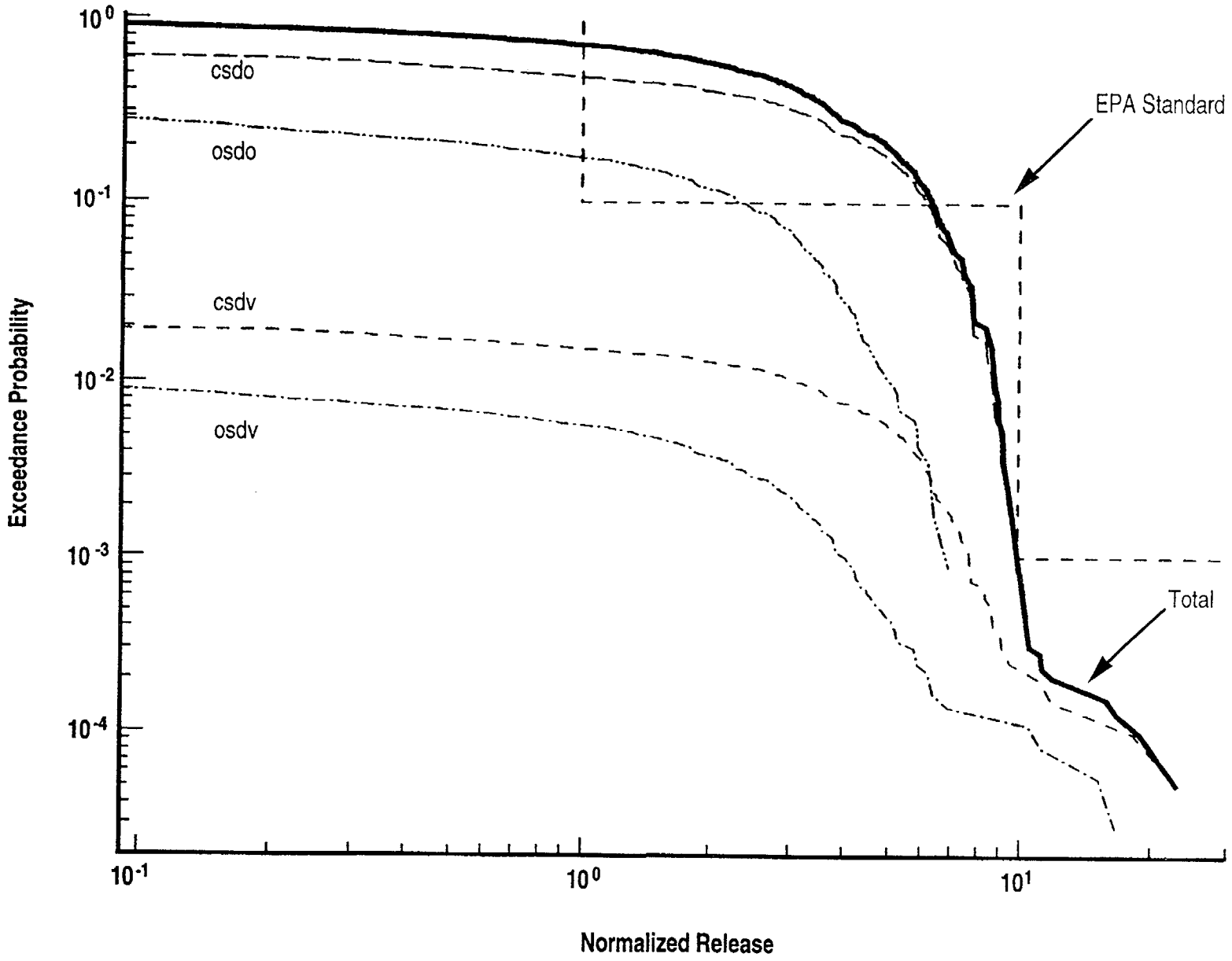


Figure 9-7a Total CCDF for Normalized Release from significant scenarios (Scenario class identifiers are described in Table 9-1.)

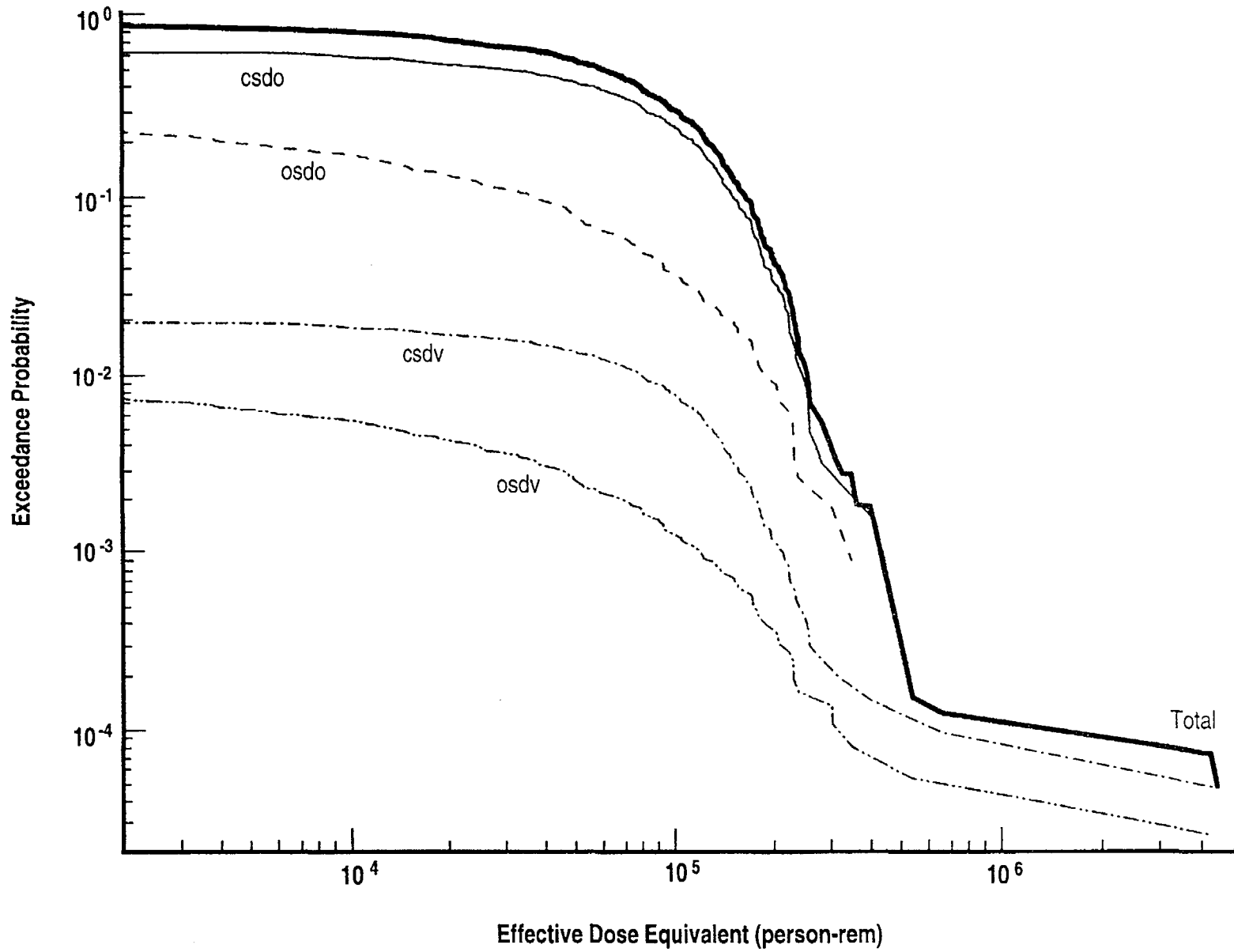


Figure 9-7b Total CCDF for *Effective Dose Equivalent* from significant scenarios (Scenario class identifiers are described in Table 9-1.)

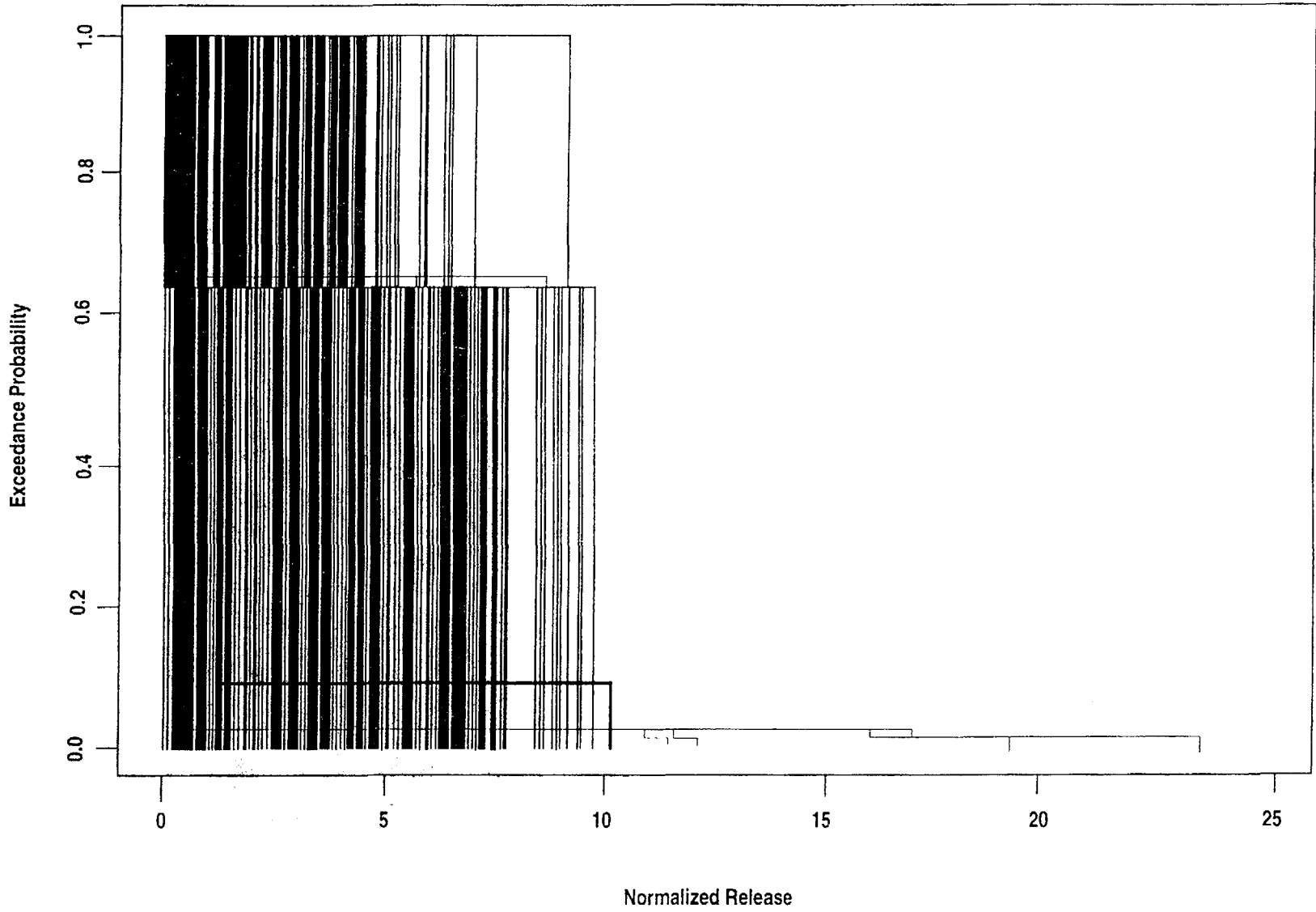


Figure 9-8a "Hair diagram" showing all *Normalized Release* vectors (for scenarios *osdo*, *osdv*, *csdo*, and *csdv*)

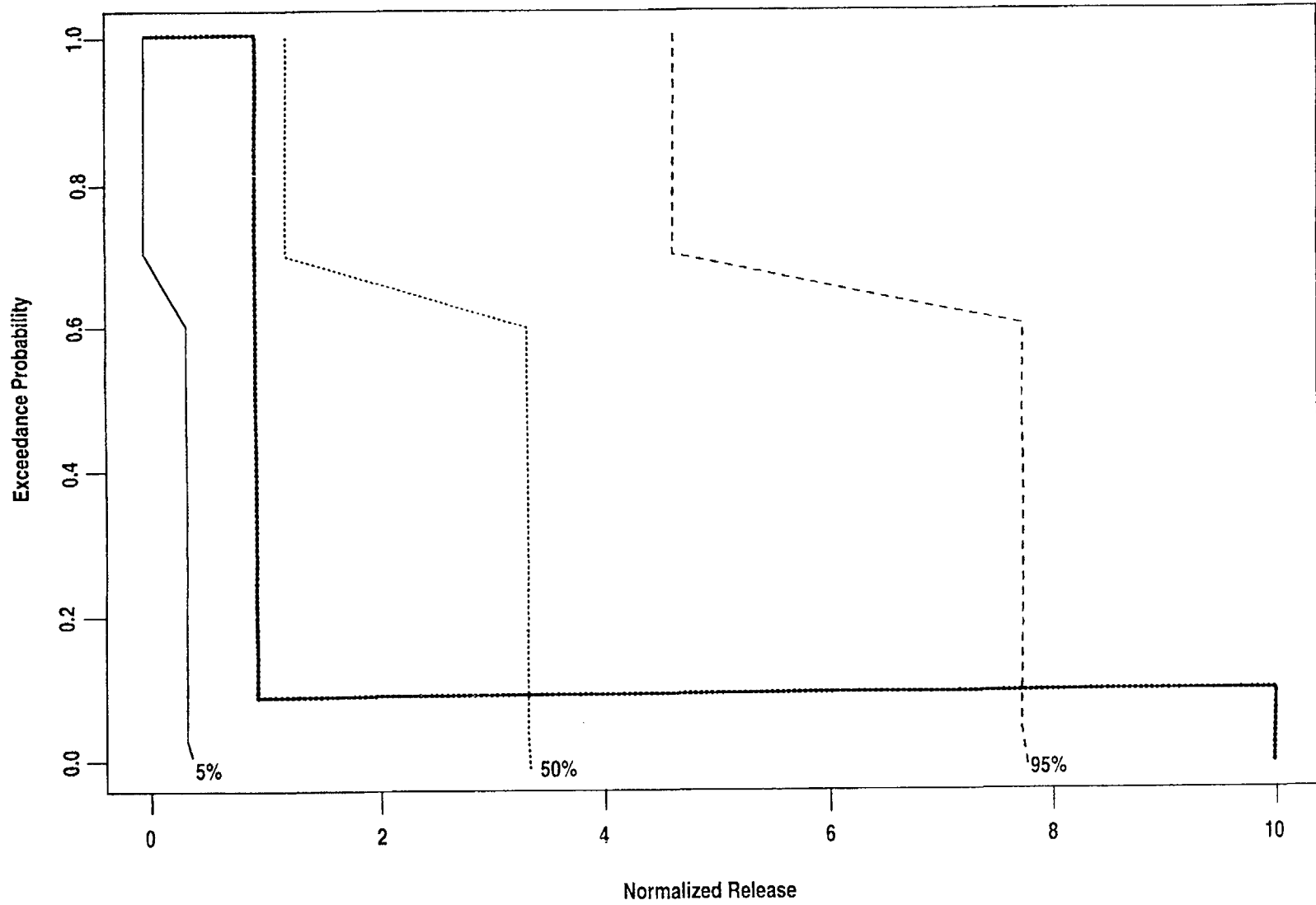


Figure 9-8b Percentile values of release vectors from "hair diagrams"

## 9. Analytical Results

calculations, advection, radioactive decay, and temperature effects were considered. The retardation coefficients used for the gas-phase calculation also accounted for equilibrium speciation.

### 9.4.1.3 Source Term

The modeling of waste-package failure was non-mechanistic in IPA Phase 1. The model used by the staff to calculate the source term in IPA Phase 1 was that incorporated in the *NEFTRAN* computer code obtained from SNL (see Longsine *et al.*, 1987). In this model, radionuclide releases would occur only after failure of the waste package, characterized as a single failure time for the entire repository.

As discussed in Chapter 5, the staff developed its own computer code to calculate the source term in IPA Phase 2. The *SOTEC* module (see Sagar *et al.* (1992)) deals with the calculation of aqueous and gaseous radionuclide time- and space-dependent source terms for the geologic repository. It does so by considering the variations in those physical processes expected to be important for the release of radionuclides from the engineered barrier system (EBS).

Three primary calculations are done in *SOTEC*: (a) failure of waste packages because of a combination of corrosion processes and mechanical stresses; (b) the leaching of spent nuclear fuel; and (c) the release of  $^{14}\text{CO}_2$  gas from the oxidation of  $\text{UO}_2$  and other components in spent nuclear fuel and hardware. Other principal features of the IPA Phase 2 source term model include representation of the repository by seven separate regions (or sub-areas) and the consideration of 20 radionuclides, based on a screening analysis. The IPA Phase 1 analysis considered 28 radionuclides. The screening analysis for radionuclides is described in Section 5.2.4 of this report.

### 9.4.2 Possible Reasons for Differences in Results

Figure 9-9 shows the total system CCDFs for the IPA Phase 1 and Phase 2 analyses. The Phase 1 CCDF has relatively higher releases in the high-risk portion of the curve (i.e., the left side), but lower releases in the low-risk portion. As dis-

cussed in Section 9.4.1, the Phase 1 and Phase 2 models were quite different in a number of important aspects, so it is difficult to pinpoint the exact causes of the differences in results. Some of the differences in the total system CCDFs may have been caused by the following specific factors:

1. **Waste package failure model.** The IPA Phase 1 study had a non-mechanistic model of waste package canister failure, which assumed a probability distribution of failure times. Furthermore, all canisters in the four modeled repository sub-areas were assumed to fail at the same time. The IPA Phase 2 model employs a mechanistic model of canister failure that calculates the failure time based on assumptions about canister wetting, corrosion, and seismic forces. Furthermore, the failure times of the canisters in the seven modeled sub-areas were independent of each other.
2. **Release rate from failed canisters.** The IPA Phase 1 model for source term based release rate of dissolved radionuclides from the waste form on the solubility of either the uranium matrix or the individual radionuclides for a given flow rate through the canister, and carried away only in the advective flow. Carbon-14 gaseous releases were not included explicitly in the IPA Phase 1 model. The IPA Phase 2 model includes several important improvements:
  - Solubility limited by collection of isotopes of each element;
  - A temperature-dependent model for  $^{14}\text{C}$  release from several compartments of the fuel; and
  - Diffusive as well as advective transport from the canister.
3. **Several of the parameters common to both IPA Phases 1 and 2 had different values.** Rate of water influx—This value was an assumed fraction of the infiltration rate in IPA Phase 1, but was calculated explicitly from the fracture-flow modeling in Phase 2. Only fracture flow at the repository horizon contributed to advective transport through the canister.

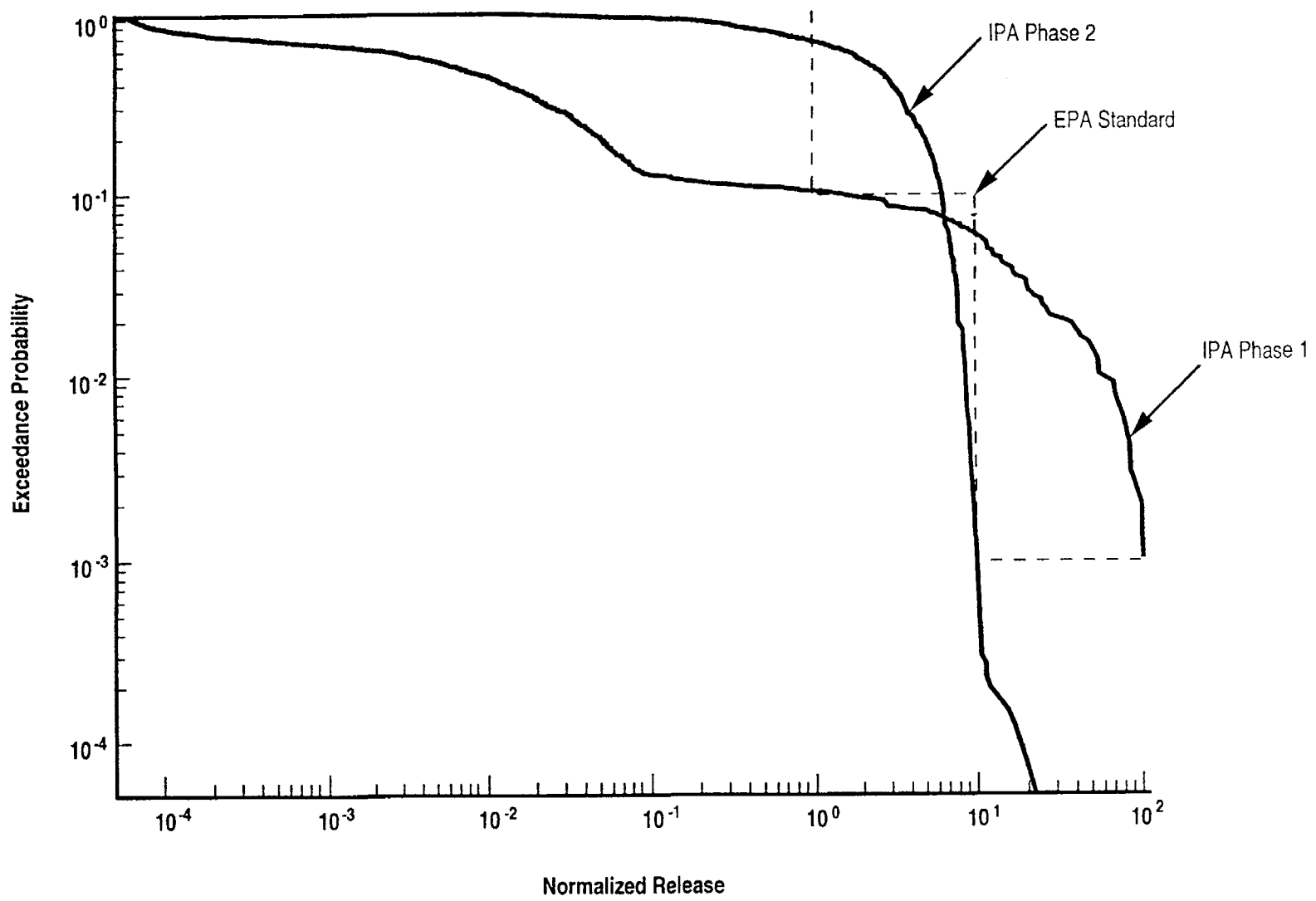


Figure 9-9 Comparison of CCDFs for IPA Phase 1 and Phase 2 results

## 9. Analytical Results

*Contact fraction with waste*—The fraction of infiltrating water contacting the waste was chosen from a uniform distribution in both the IPA Phase 1 and 2 models from a range related to the cross-sectional area of the boreholes. The contact fraction was chosen to be 0.002 to 0.01 in Phase 1. The equivalent range for IPA Phase 2 was about 0 to 0.002, which is considerably lower. Furthermore, only the fracture flow portion of the total infiltration could reach the waste package in Phase 2, whereas both the fracture and matrix flow parts of the flow could be involved in Phase 1.

*Infiltration Rate*—The range of infiltration rates for the base case (oooo) and the pluvial-climate case (cooo) was the same in both IPA Phase 1 and Phase 2. The type of distribution chosen was different, however. A uniform distribution was chosen in Phase 1 for both the base case and the pluvial case. For IPA Phase 2, a log-uniform distribution was assumed for both cases.

4. **Radionuclide contributions.** The largest contributors to cumulative release at the accessible environment for the IPA Phase 1 study were the isotopes of plutonium, but they were relatively unimportant in Phase 2. The solubility range of plutonium for IPA Phase 1 was  $5.0 \times 10^{-5}$  to  $3.0 \times 10^{-3}$  kilograms/cubic meter sampled from a log-uniform distribution. In IPA Phase 2, thermodynamic calculations and the consideration of both oxidizing and reducing environments resulted in a range of  $2.0 \times 10^{-7}$  to  $5.0 \times 10^{-4}$  kilograms/cubic meter, which is considerably smaller. Furthermore, solubility in Phase 1 was based on single radionuclides, whereas the IPA Phase 2 model considered all isotopes of an element in this determination.
5. **Carbon-14 gaseous releases.** The IPA Phase 1 model did not include the releases of  $^{14}\text{C}$  gas to the accessible environment. The release of  $^{14}\text{C}$  gas was a major contributor to the cumulative release to the accessible environment in the IPA Phase 2 model. Furthermore, the IPA Phase 2 model predicted this release to occur at high conditional probabilities and independent of the release of the dissolved radionuclides.

6. **Scenario probabilities.** Except as noted under Item 3, above, the application of the pluvial-climate scenario has been reasonably similar in both IPA Phases 1 and 2. However, the probability of the pluvial climate was arbitrarily assumed to be 0.10 in IPA Phase 1 and determined by analysis of paleo-hydrologic data to be 0.64 in IPA Phase 2. In both IPA phases, pluvial-climate conditions result in a significant increase in releases at high conditional probabilities.

### 9.4.3 Conclusions

The modeling improvements from IPA Phase 1 to Phase 2 were numerous and in some cases cannot be easily separated, such as in the case of waste canister-failure mechanisms resulting in the release of  $^{14}\text{C}$  and other radionuclides and the incorporation of a gas-transport pathway. Hence, the calculation of a quantitative measure of the effect of each individual change or improvement is not considered feasible. A visual inspection of the curves indicates that the difference in occurrence probabilities assigned to the pluvial-climate scenario, and the incorporation of the gas pathway in Phase 2 may be the primary factors. In future IPA phases it will be feasible to analyze the effect on the CCDF for every significant change in the analysis, including modifications to models, parameter distributions, and scenario classes.

### 9.5 Effects of Modeled Performance of Natural and Engineered Barriers on Total System Performance

This section presents repository performance in terms of factors related to the behavior of the engineered and natural barriers. In IPA Phase 2, the factors investigated were the integrity of the waste packages, the rate of release of radionuclides from the engineered barriers, and the travel time of water through the geosphere. One of the primary goals of the IPA effort is to give insight to the effectiveness and ability to implement NRC's regulation applicable to the geologic repository. The regulatory requirements in 10 CFR 60.113 address "three subsystem performance objectives," namely substantially complete containment (SCC) of waste in the waste packages (10 CFR 60.113(a)(1)(ii)(A)), controlled fractional release rate from the EBS (10 CFR 60.113(a)(1)(ii)(B)), and pre-waste-emplacement ground-water

travel time (GWTT) (10 CFR 60.113(a)(2)). The results presented in this section portray the overall (total) system performance in terms of the staff's understanding of the primary factors contributing to waste containment. The calculations are not for the purpose of directly drawing a comparison between overall system performance in terms of release or dose and the subsystem performance measures. There are primarily two reasons for this distinction: (1) the subsystem performance measures are supposed to be independent requirements ensuring a minimal performance of each of the multiple barriers in a geologic repository, unrelated to the total system performance; and (2) the characterizations of SCC, EBS release rate, and GWTT used in IPA Phase 2 are crude and incomplete, and do not exactly conform to the definitions of those quantities in 10 CFR Part 60. For example, the "liquid" travel time, as used in this report, does not include the 10 CFR Part 60 concept of the "disturbed zone" (10 CFR 60.2) and is for post-emplacment rather than pre-emplacment conditions. Furthermore, the "liquid" travel time calculated in the TPA computer code program (described in Chapter 4) is an abstraction based on the fastest combination of possible fracture and matrix pathways, and does not correspond to a realistic flow path. Nevertheless, the following comparisons shed light on the importance of the engineered and natural barriers to the total system performance.

Screened Conditional CCDFs are used for these comparisons. As explained in Section 9.2.1, these plots are generated by "screening out" vectors according to a criterion, and using only the remaining vectors to produce the CCDFs. The criteria used in the present study were:

- Infiltration less than 1 or 2 millimeters/year (discussed in Section 10.3).
- Travel time of water in geosphere less than 1200, 1100, and 1000 years (discussed in Section 9.5.1).
- Release rates of radionuclides from the EBS less than  $10^{-5}$ /year of the 1000 year inventory (discussed in Section 9.5.2).
- Waste package lifetimes of 300 or 1000 years (discussed in Section 9.5.3).

### 9.5.1 Effect of Travel Time of Water through the Geosphere

The NRC regulations in 10 CFR 60.113(a)(2) prescribe that the site for a geologic repository possesses the property of pre-waste emplacement GWTT along the fastest pathway from the disturbed zone to the accessible environment of less than 1000 years (or other criteria chosen by the Commission (10 CFR 60.113(b))). Since there is not yet an unambiguous definition of GWTT, four distinct "liquid" travel times have been defined for each vector for the present study:

- *Fastest*—the minimum time for the transport of a non-diffusing particle along the fastest combination of possible matrix and fracture pathways in any of the seven flow columns representing the repository.
- *Most flux*—the travel time through the pathway associated with the greatest flux from the repository to the accessible environment.
- *Flux averaged*—the average travel time for all paths, weighted by the flux in each path.
- *Averaged*—the average travel time for all paths, irrespective of the flux in each path.

For the purpose of IPA Phase 2, only liquid releases were included in this analysis; releases of gaseous  $^{14}\text{C}$  were completely insensitive to liquid travel time. Carbon-14 was the major contributor to the normalized releases; therefore the inclusion of gaseous releases would have further masked the sensitivity of *Normalized Release* to travel time. Figure 9-10a shows the scatter plot of liquid travel time versus normalized liquid release for each of the four definitions of travel time listed above. Fastest travel time and most flux travel time are similarly distributed with travel times controlled by fracture flow clustered at the short time end and travel times controlled by matrix flow at the long time end. Also, similarly distributed are average travel time and flux averaged travel time. The fact that the fastest travel times and most flux travel times are clustered around 1000 years for cases controlled by fracture flow is an aspect of the site and the models chosen. Correlation coefficients were also calculated for the relationship between normalized liquid release and travel time for the four definitions. The flux normalized travel time had the highest coefficient

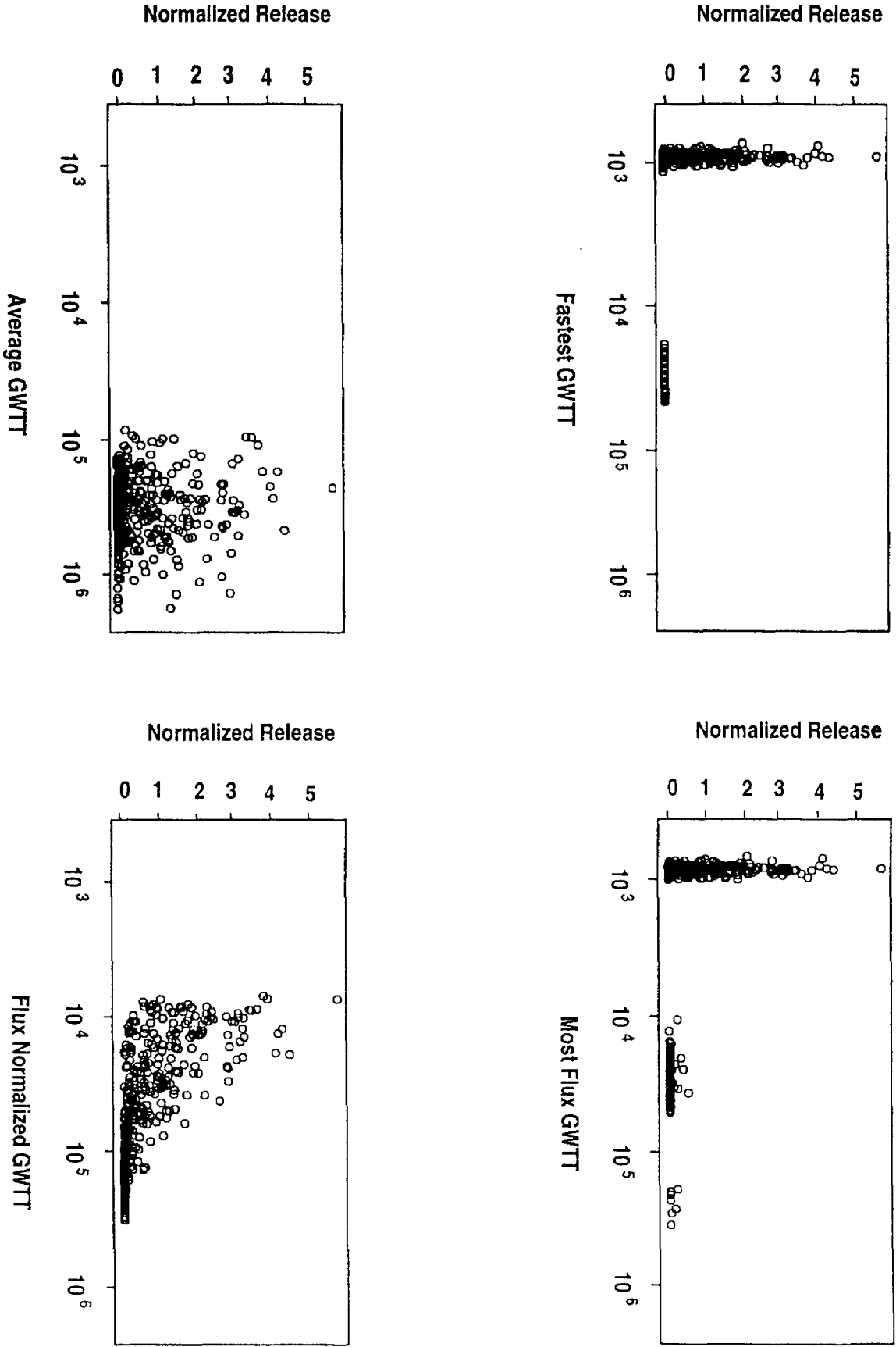


Figure 9-10a Scatter plot of liquid travel times

correlation (-.52), followed by most flux (-.23), fastest (-.17), and average (-.05).

Figure 9-10b shows the sensitivity of the CCDF of liquid release in the base case (0000) scenario to excluding all or portions of cases with some fracture flow. As expected, excluding all cases involving a fast path to the accessible environment reduces liquid releases to very small amounts. Excluding some of the fast path cases by using a criterion of 1000 or 1100 years does not have a significant effect on the CCDF even though a large portion of the fast path cases is being removed.

### 9.5.2 Effect of Release Rate from the EBS

The NRC regulations set forth in 10 CFR 60.113 (a)(1)(ii)(B) specify that the release rate of any radionuclides from the EBS should be  $10^{-5}$ /year or less of the 1000 year inventory. Figure 9-11 shows that the CCDF for the base case (0000) scenario responds mildly to screening out the vectors that had release rates greater than  $10^{-5}$ /year of the 1000-year inventory and greater than 0.1 percent of the calculated total release rate limit.

### 9.5.3 Effect of Waste Package Lifetime

Figure 9-12a shows the distribution of waste package failure time for the base case scenario. Figure 9-12b shows the CCDF sensitivity to screening for waste package lifetimes (other than initial failures) that are less than 300 or 1000 years, as specified in 10 CFR 60.113(a)(1)(ii)(A). Long waste package lifetimes substantially decrease the release. Much of this benefit is derived from the suppression of releases of  $^{14}\text{C}$  from early failures of waste containers, during the time when the containers are hot and gaseous travel times are shortest. Figure 9-12c shows the CCDF sensitivity plot for the same case, but for gaseous releases only. Figure 9-12d shows a scatterplot for all vectors of gaseous  $^{14}\text{C}$  release to the accessible environment as a function of minimum failure time. There is a clear trend of high gaseous releases for short waste package lifetimes.

The effect of waste package failure time on compliance with the NRC release rate criterion was also investigated. Figure 9-12e is a scatter plot of fraction of the 1000-year inventory being released

through the EBS, for dissolved radionuclides (including  $^{14}\text{C}$ ) versus the time of the maximum release for four selected radionuclides. The bimodal nature of the plots for three of the radionuclides is caused by the large differences in cooling time (and therefore time-of-container failure) for different parts of the geologic repository. There does not appear to be any significant relationship between time of release and EBS release rate of dissolved radionuclides. Americium-241 has a relatively short half-life and is not a daughter of any of the other radionuclides in the list, and therefore does not display a bi-modal distribution. Although not plotted, one would expect that short failure times would also be related to higher releases of gaseous  $^{14}\text{C}$  because of the dependence of the release model on temperature.

### 9.5.4 Effects of the Performance of All Natural and Engineered Barriers

Figure 9-13 shows the CCDFs for total liquid and gas cumulative releases in the base case scenario, with the effects of all natural and engineered barriers separately and in unison. Screening the vectors on the basis of barrier performance leads to a CCDF considerably better (in terms of compliance) than the unscreened vectors. Note that only 18 of the 400 vectors "passed" the screening tests, so the CCDF might not be statistically convergent.

## 9.6 Illustration of Individual Annual Dose Calculation

In IPA Phase 2, two types of average annual individual ingestion doses (rems/year) were derived from the 10,000-year cumulative population doses calculated by *DITTY*: (1) a crude estimate of dose for an individual member of the farm family who obtains his/her only source of drinking water from the contaminated well discussed in Chapter 7; and (2) a crude estimate of dose for the 177 individuals who reside within 100 kilometers of Yucca Mountain and who eat contaminated beef (whose only source of food was vegetation irrigated with the contaminated well water). Estimates of these individual doses are presented as histograms in Figure 9-14.

The doses in Figure 9-14 should not be construed as accurate estimates of individual annual doses

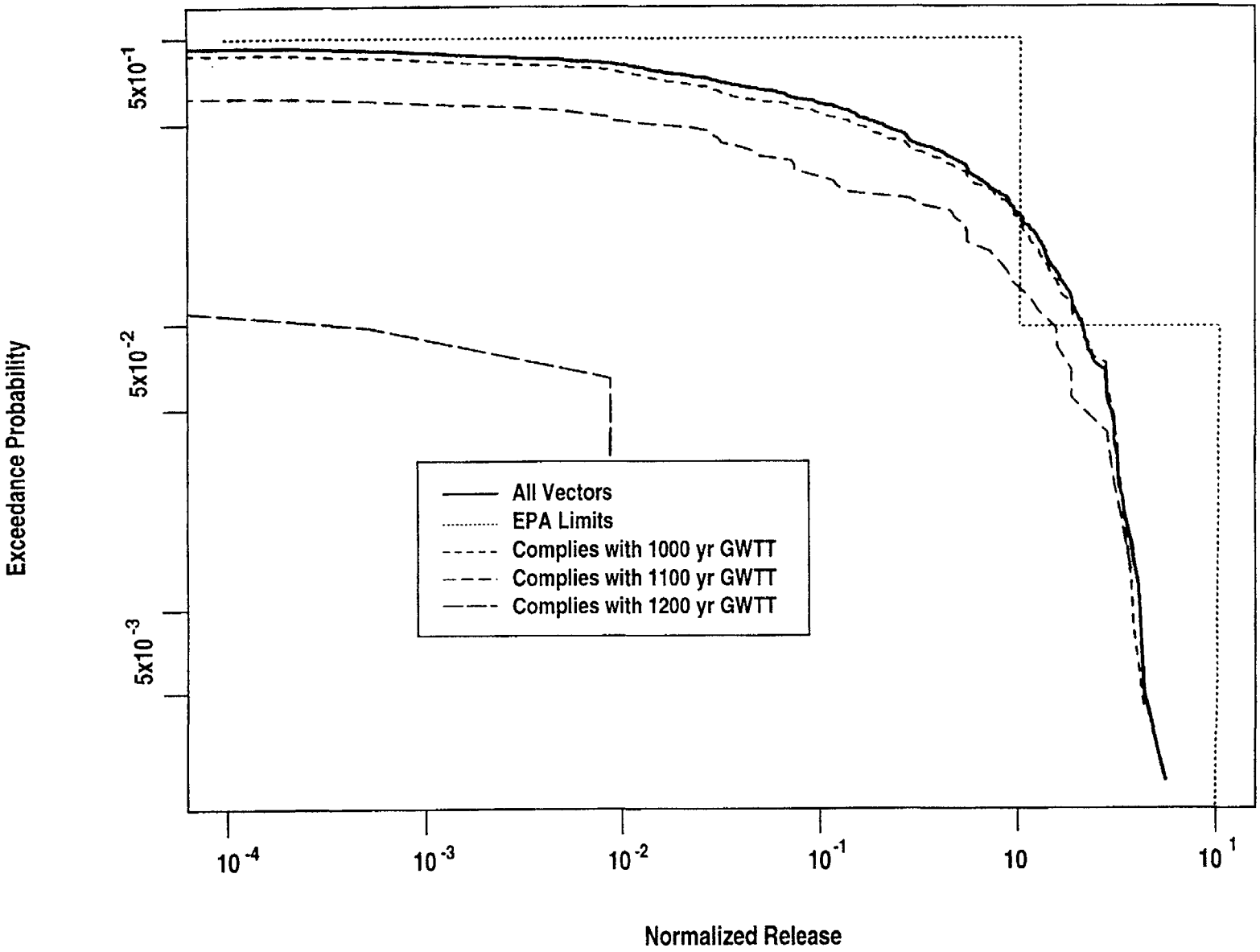


Figure 9-10b CCDF sensitivity plot 'fastest' liquid travel time

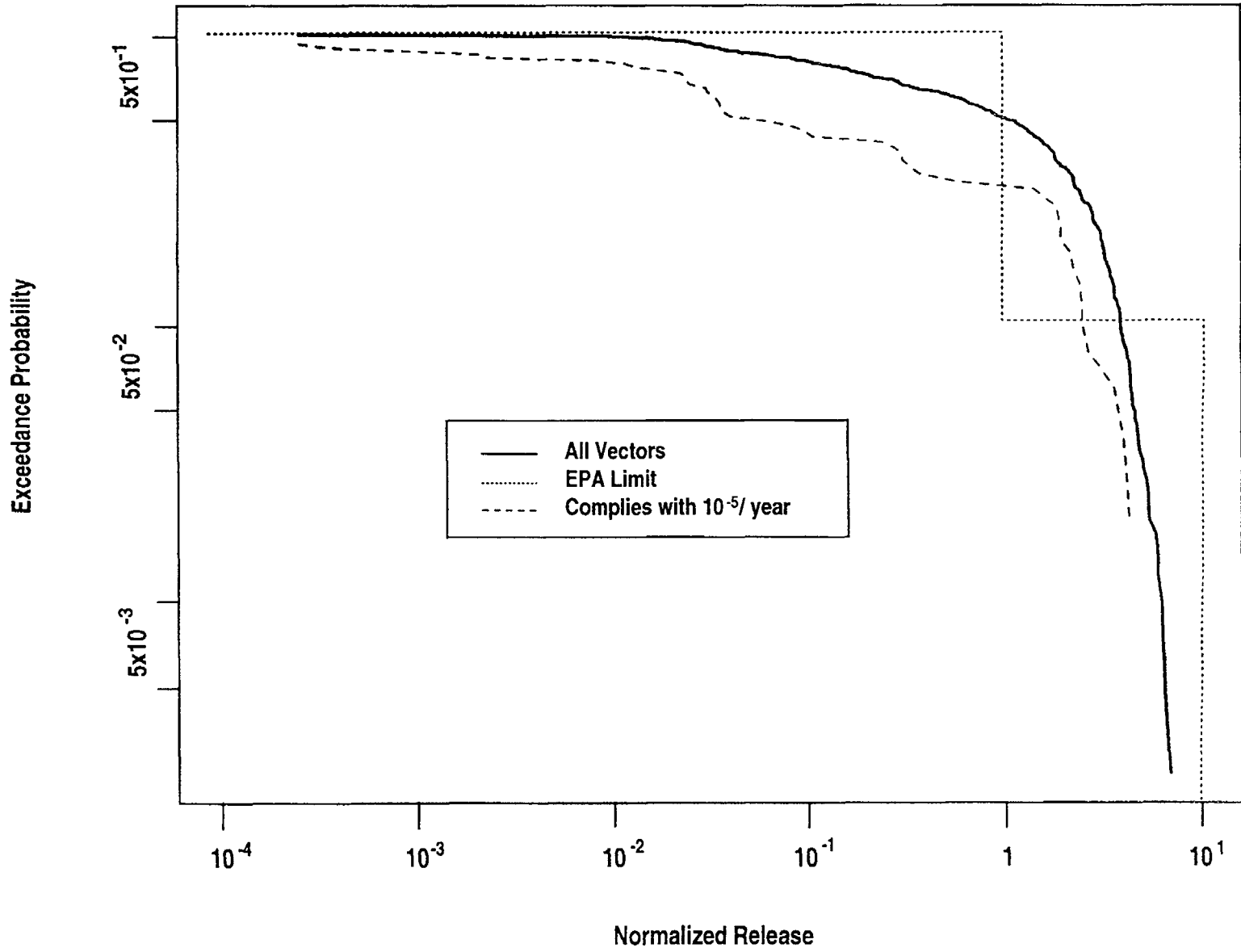


Figure 9-11 CCDF sensitivity plot for release rate from EBS (base case scenario)

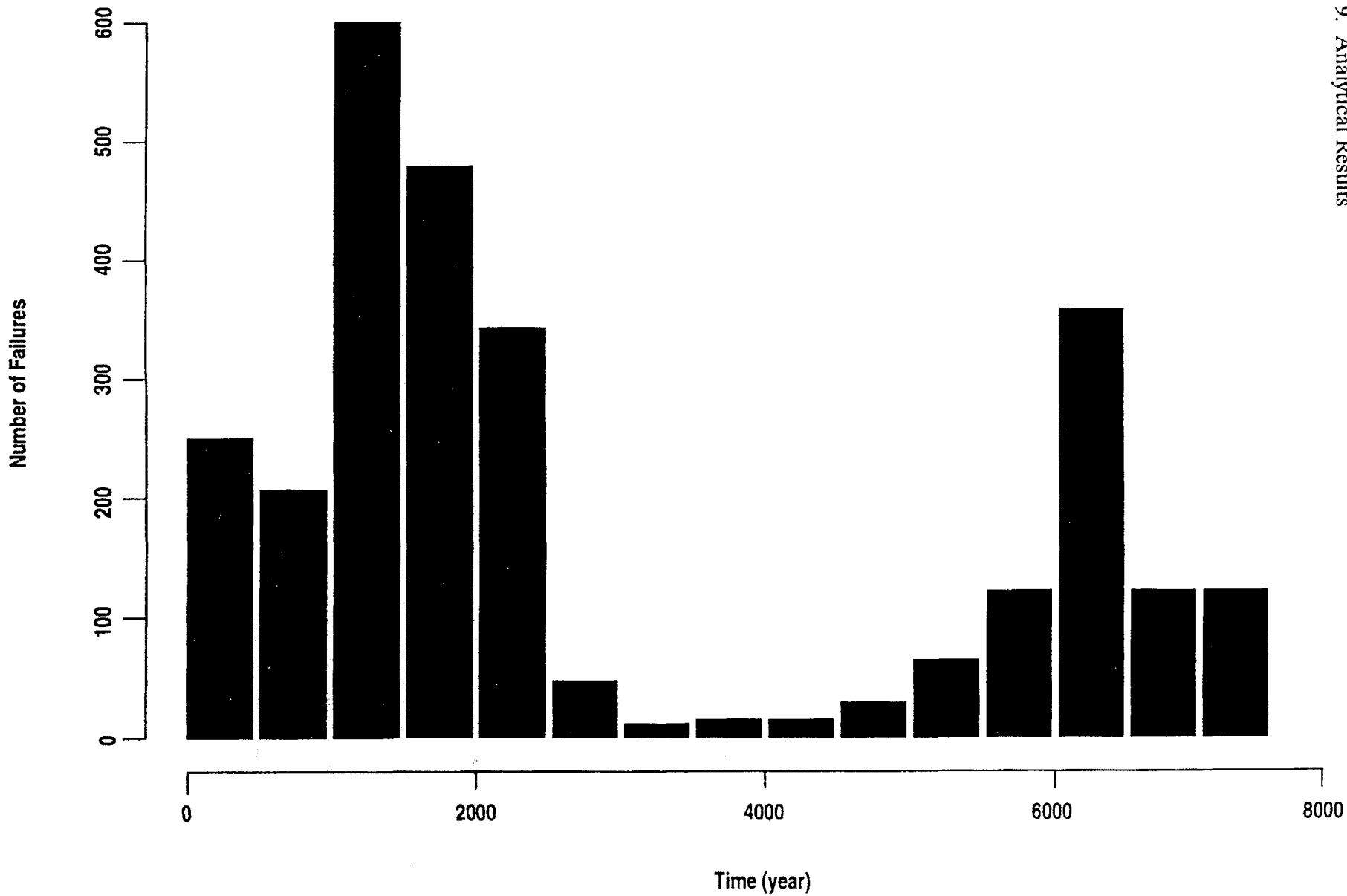


Figure 9-12a Distribution of waste package failure times for base case scenario

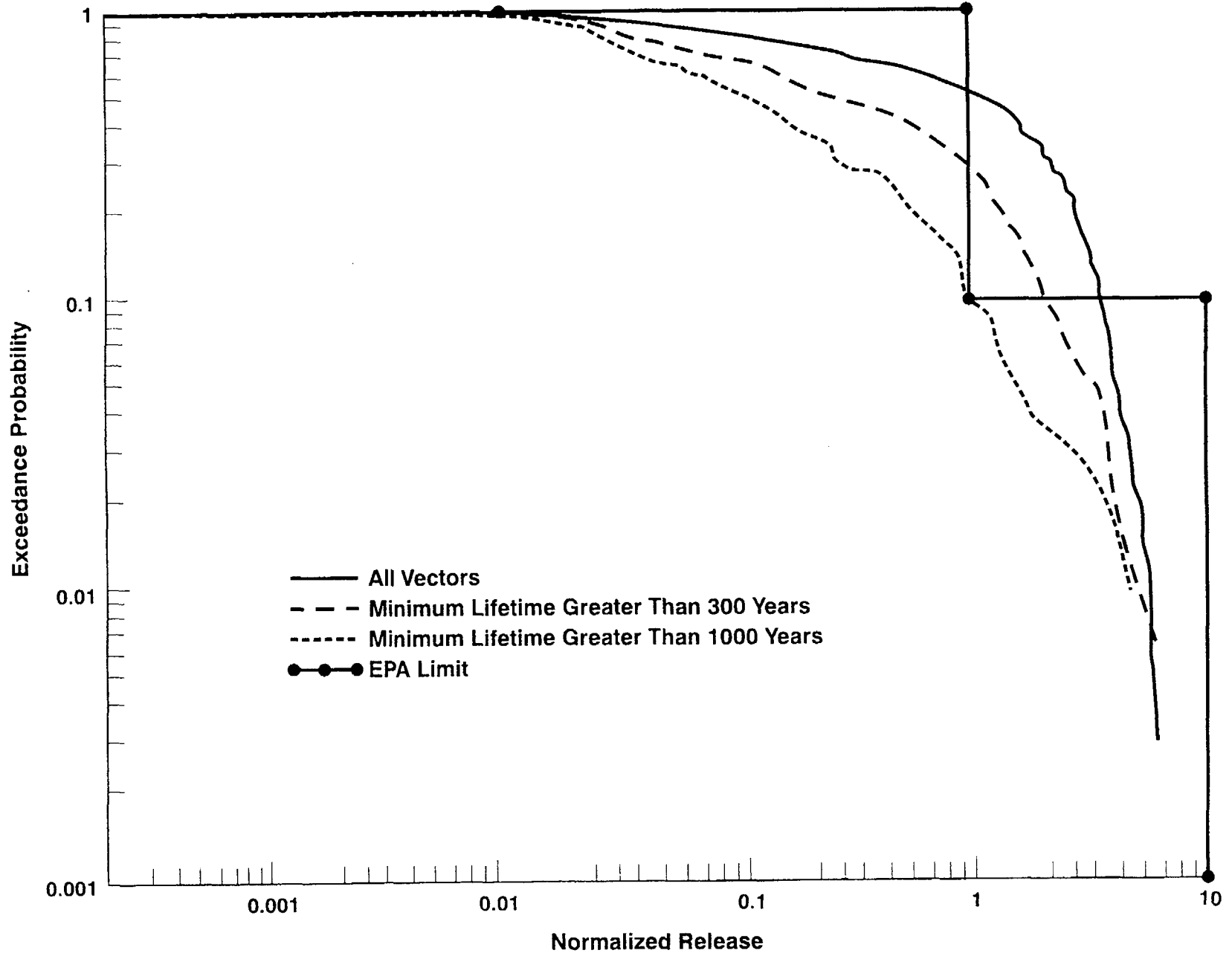


Figure 9-12b CCDF sensitivity plot for waste package failure times for base case scenario

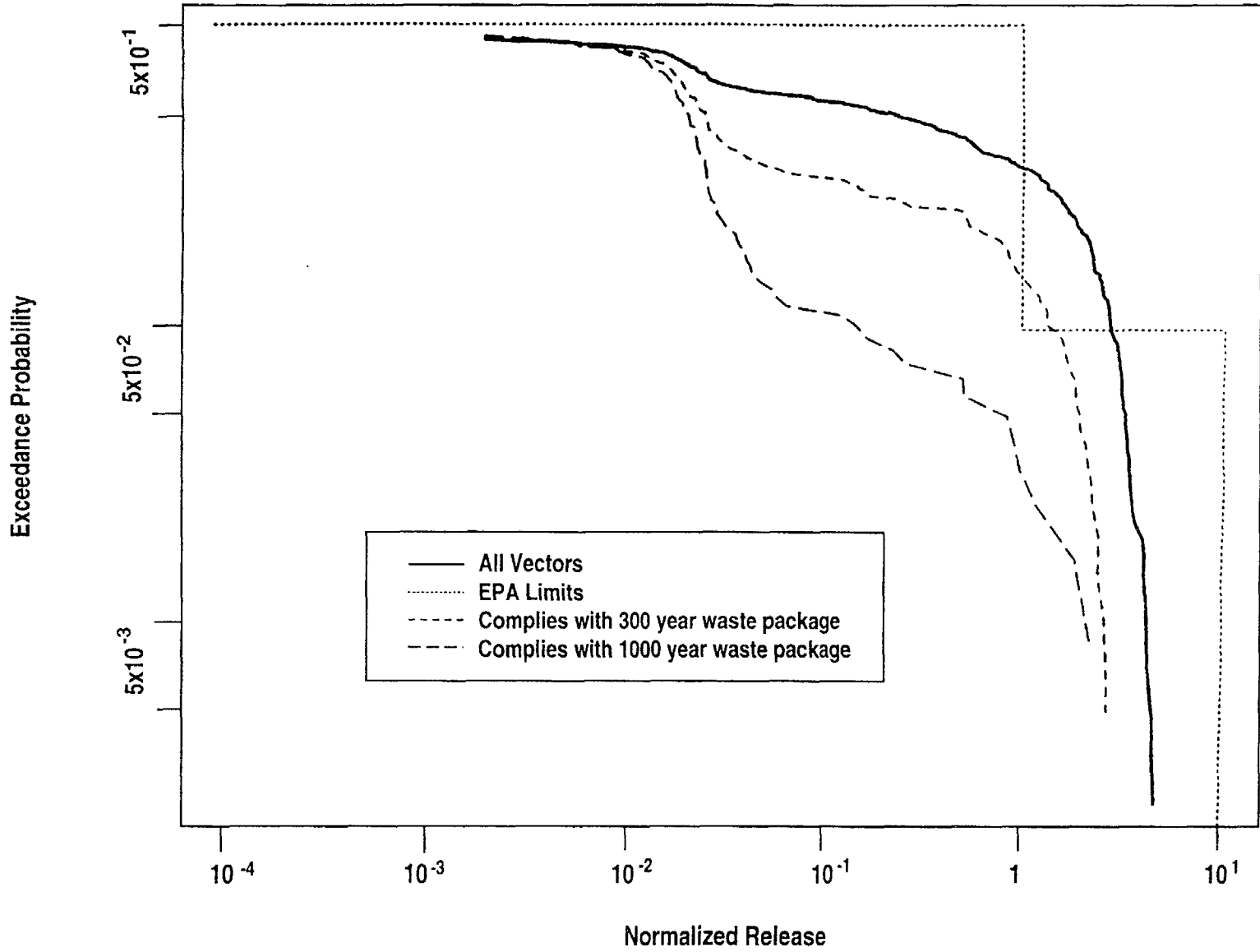


Figure 9-12c CCDF sensitivity plot for waste package failure times for base case scenario (gaseous release only)

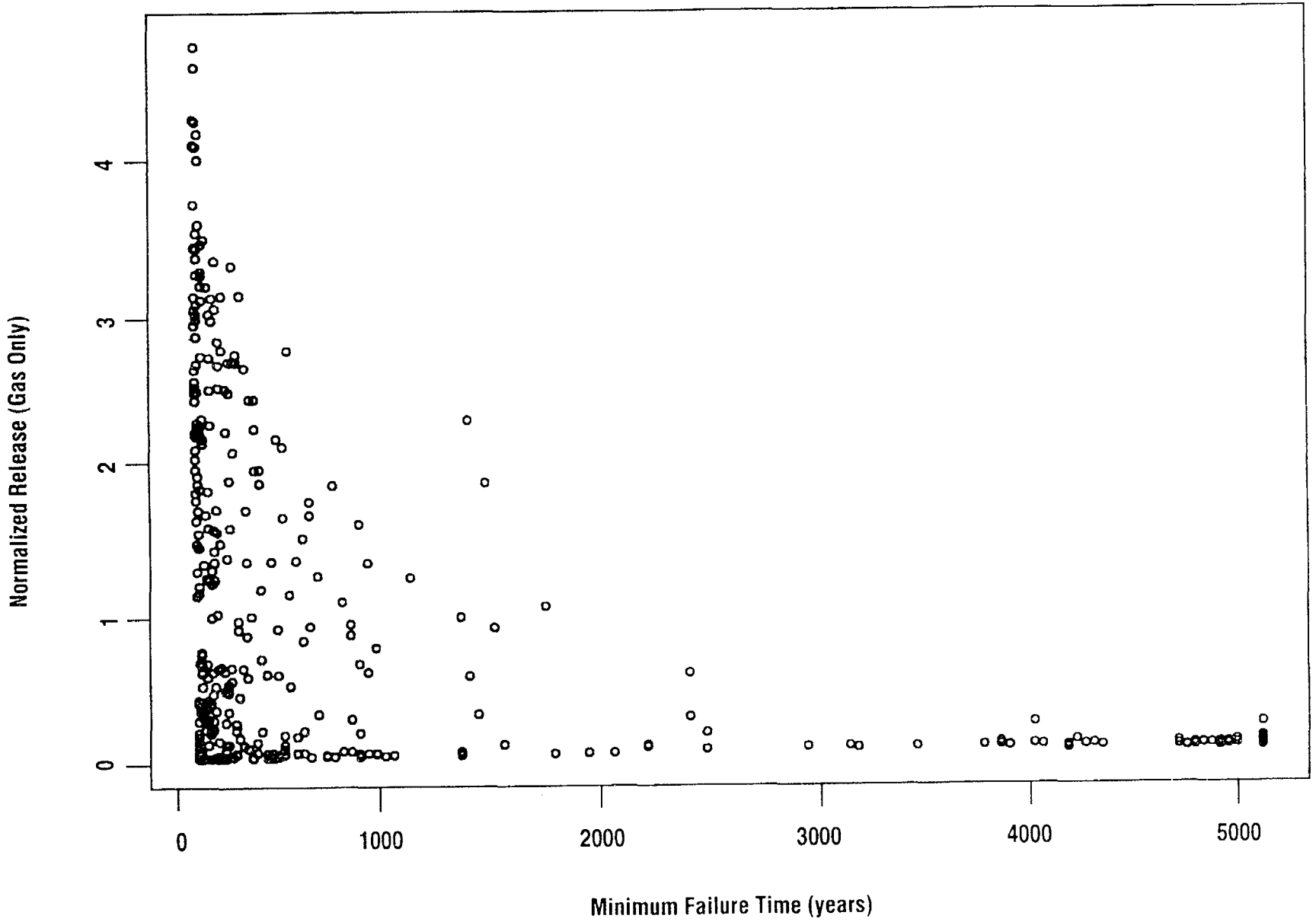


Figure 9-12d Scatter plots of releases to environment versus waste package failure times for base case scenario

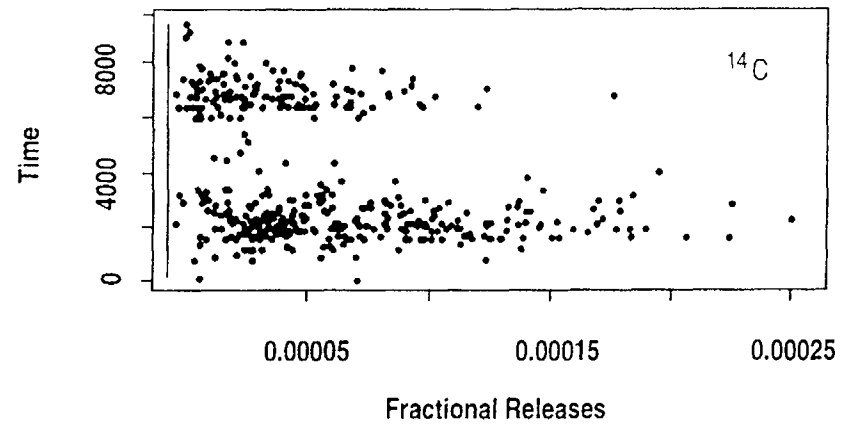
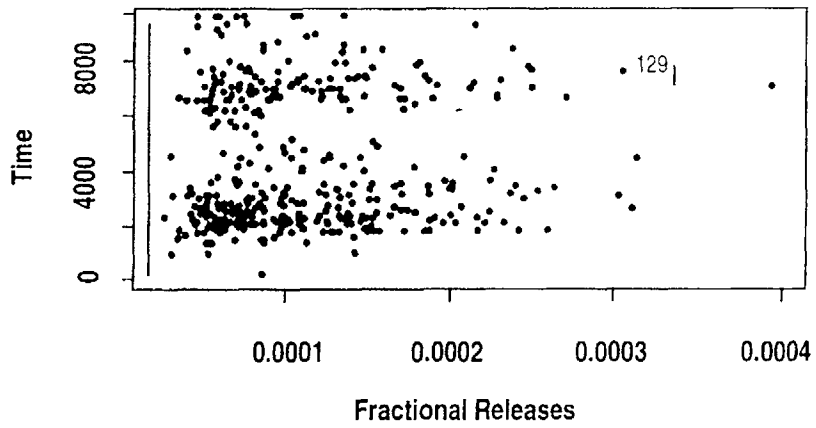
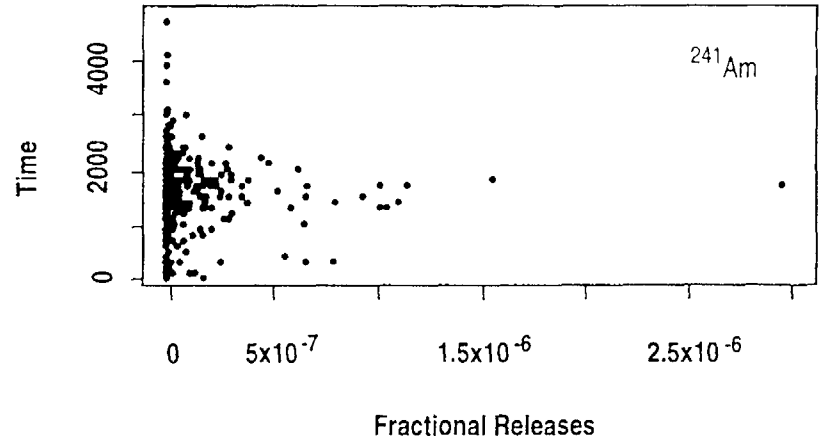
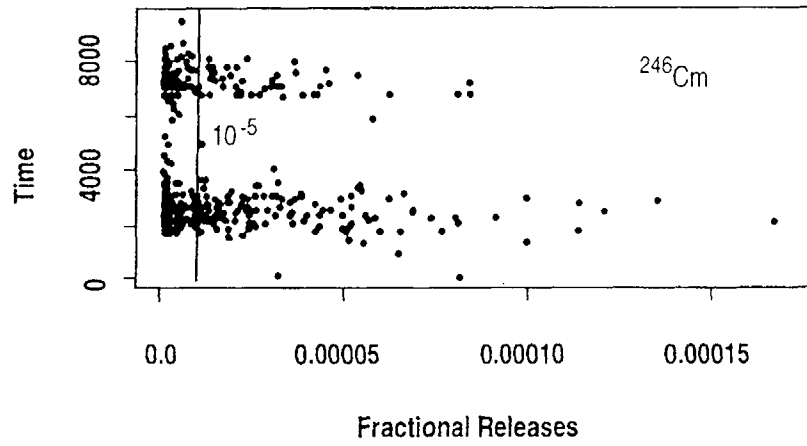


Figure 9-12e Scatter plots of EBS release rates versus time of release for base case scenario

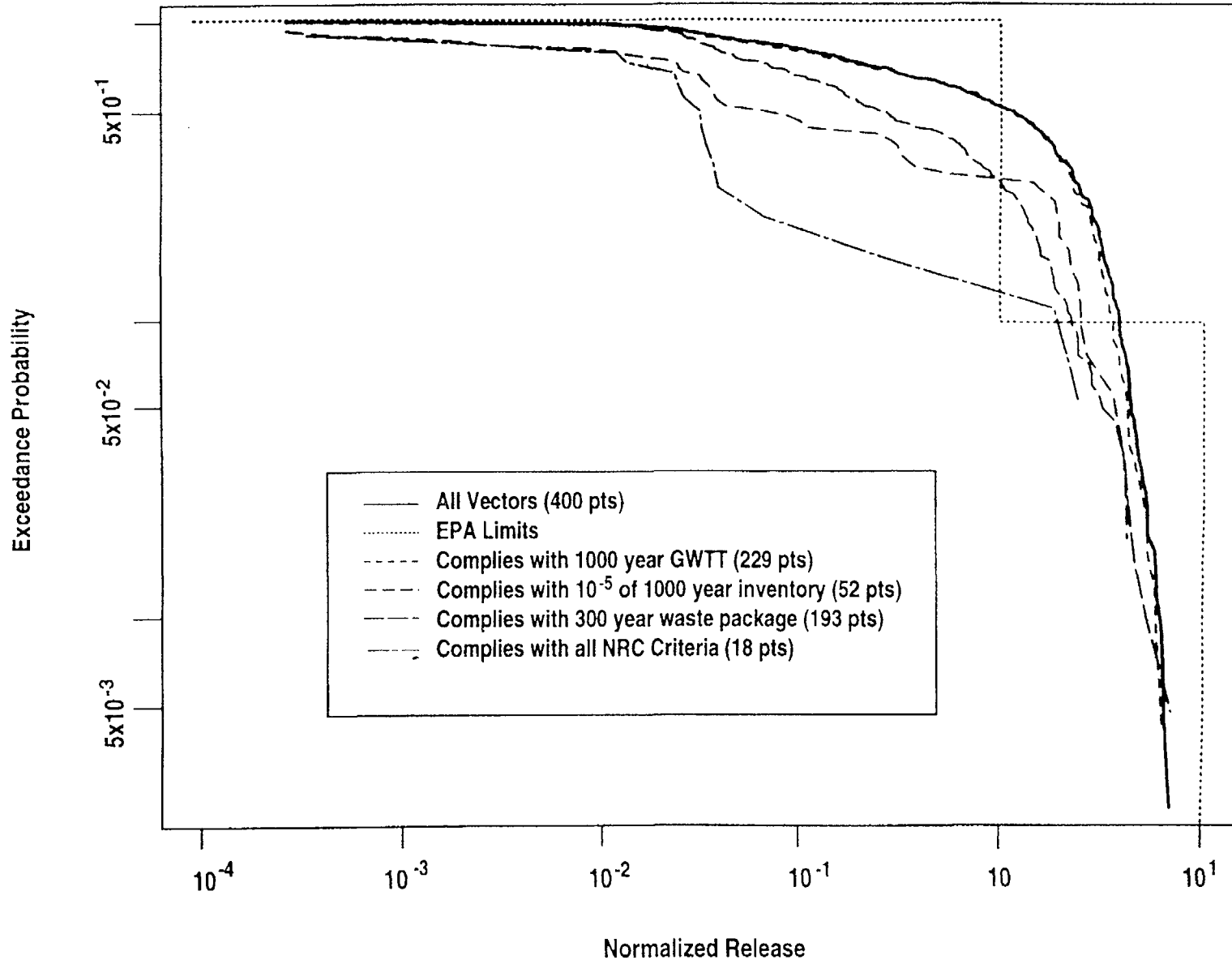


Figure 9-13 CCDF sensitivity plot for all 10 CFR Part 60 subsystem requirements

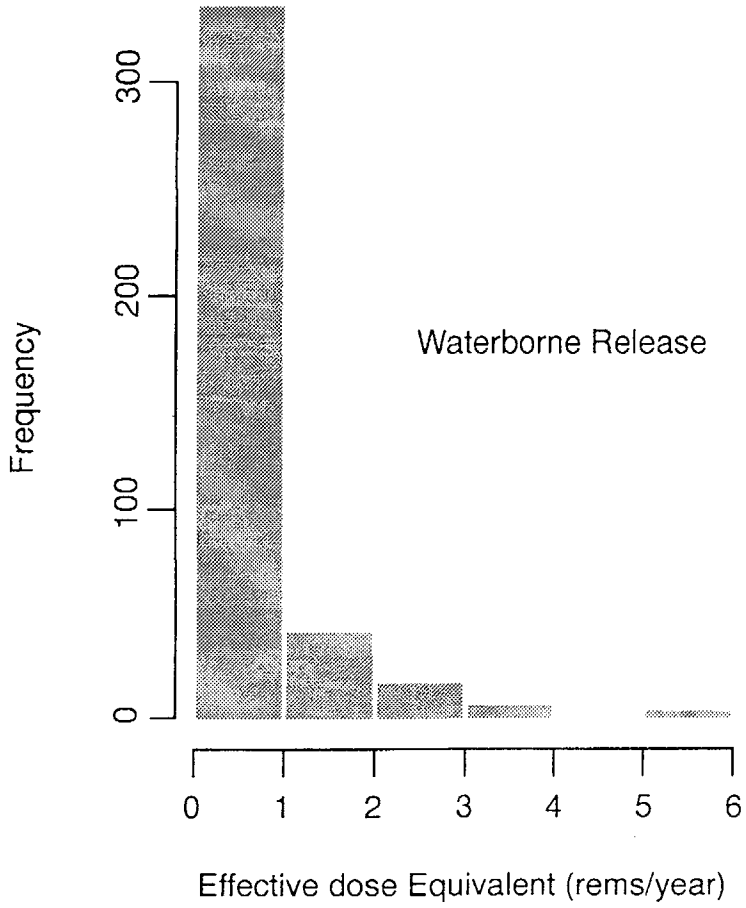
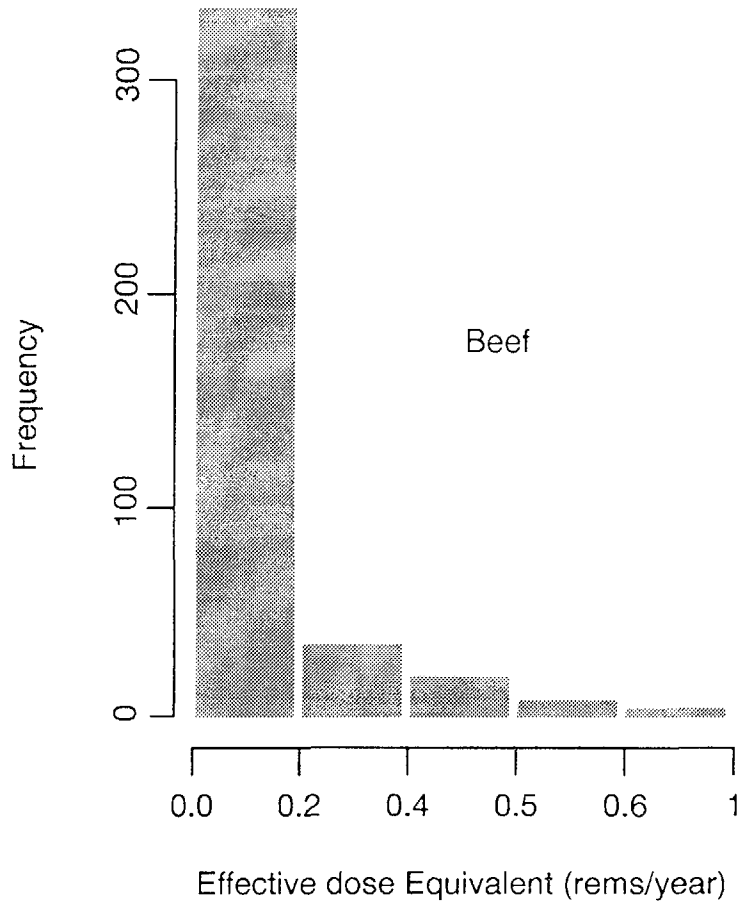


Figure 9-14 Illustration of annual individual dose calculation (base case scenario)

at Yucca Mountain, Nevada. They were included in this report only to illustrate some of the statistical techniques available to the NRC staff for use in future performance assessments. The method used to calculate individual doses in Figure 9-14 is based on the incorrect assumption that the release rate of any single radionuclide into water or beef remains approximately constant throughout the entire 10,000-year period of exposure. Since the times of release of radionuclides from the repository were random (as determined by LHS sampling), and the concentrations in the accessible environment because of these releases are generally pulses or step functions, this assumption is not appropriate. The crude individual dose values in Figure 9-14 therefore underestimate the "peak" individual dose values by an unknown amount.

The doses in Figure 9-14 were derived as follows. For any scenario class, each of the 400 vectors obtained from parameter distributions by LHS sampling was used to generate a corresponding 10,000-year population dose. The 400 dose values plotted in Figure 9-14 correspond to the set of 400 vectors associated with a scenario class in IPA Phase 2. For each vector, the fraction of 10,000-year dose calculated by *DITTY*, which was caused either by ingestion of contaminated beef or contaminated drinking water, was divided by 10,000 years (the exposure period) and either by 3 or 177 (the number of members in the family or the number of beef eaters) to obtain the very crude estimates of the individual doses in rems/year. The doses caused by the inhalation of airborne radioactivity by the 22,200 individuals (those who reside within 100 kilometers of the repository) were of the order of millirems over the 10,000-year exposure period. Since the individual doses caused by inhalation were negligible compared with the individual doses caused by ingestion of water and beef, they were not included in the histograms of Figure 9-14.

In future phases of IPA, more appropriate computer codes (e.g., *GENII* (see Napier *et al.*, 1988)) may be required to obtain significantly better estimates of these individual annual doses. In addition, the transport modules will have to supply time-varying concentration data to the dose modules. In future performance assessments, the NRC staff may also need to devise a strategy to relate distributions of individual doses obtained in a

probabilistic performance assessment (such as those illustrated in Figure 9-14) to a deterministic individual dose standard such as that proposed in 40 CFR 191.15 (EPA, 1993; 58 *FR* 7935).

## 9.7 Summary and Conclusions

In this chapter, the results of the total-system performance assessment analyses were presented in terms of CCDFs, conditional CCDFs, single-vector CCDFs, scatter plots, and screened conditional CCDFs. Although the graphs were presented for demonstration purposes only, many of the representations were found to be especially useful for examining some specific aspects of the analyses. The scenario plots, for example, have proven to be a useful tool for evaluating the effect of disruptive event scenarios on individual vectors. Also, scenario-conditional CCDFs and single-vector CCDF plots ("hair diagrams") proved to be useful for displaying the results of variable uncertainty and scenario probability assumptions.

The difference between CCDFs of releases in the IPA Phase 1 and Phase 2 analyses was primarily caused by the greatly increased probability of the pluvial-climate scenario class in Phase 2, and the addition of the gas pathway for  $^{14}\text{C}$  migration in Phase 2.

The relationship between the performance of the natural barrier as measured by liquid travel time and the EPA release criterion depends on what definition of liquid travel time is used. When liquid travel time is defined along the "fastest" pathway or the "most flux pathway," there is a bi-modal distribution because of the sharp distinction between matrix and fracture controlled flow. When travel time is "averaged" or "flux-normalized" this bi-modal distribution does not occur. Correlation analysis showed a significant relationship between flux-normalized travel time and *Normalized Release*. For an averaged liquid travel time there was almost no correlation. Certainly, the type of flow (fracture or matrix) that is strongly influenced by the sampled infiltration rate appears to be the primary factor in reducing waterborne radionuclide movement to the accessible environment.

Little correlation was shown between the fractional release rate performance measure and the *Normalized Release*. Meeting the NRC EBS

## 9. Analytical Results

release-rate criterion, alone, did not guarantee a *Normalized Release* less than 1. The staff concludes that more work is necessary to evaluate the relationship of the NRC EBS release-rate criterion to total system performance, as well as the feasibility of repository designs to meet the criterion.

Waste package lifetime appeared to have a significant effect on the *Normalized Release* for the liquid and gaseous components. Early waste canister failures were generally found to result in large  $^{14}\text{C}$  releases to the accessible environment, primarily because of enhanced transport from large thermal gradients, and increased rates of  $^{14}\text{CO}_2$  generation at higher temperatures. Significant sensitivity of releases to waste package failure times was observed in the 300- to 1000-year range. The effect of release time (a function of waste package lifetime)

on compliance with the NRC EBS release-rate criterion, however, did not appear to be significant.

The effect of compliance with all of the NRC subsystem performance requirements, on meeting the EPA release limit, must be considered inconclusive, because of the small number of realizations that met all three criteria. Future analyses, using selected ranges of sampled values and more realistic (less conservative) models, may provide more definitive insights.

The individual dose calculation, although illustrative for the sake of comparison, is neither conservative nor accurate. Significant improvement in all phases of the performance assessment will be required if individual dose is to be calculated for regulatory purposes.

## 10 CONCLUSIONS AND RECOMMENDATIONS

### 10.1 Introduction

As noted in Chapter 1, a major goal of the Iterative Performance Assessment (IPA) effort is to develop the necessary knowledge, tools, and methodologies to provide a basis for the U.S. Nuclear Regulatory Commission staff to evaluate the adequacy of the U.S. Department of Energy's (DOE's) site characterization program (in the context of integrated repository performance) as well as for reviewing the performance assessment submitted as part of a potential license application. Further development of these tools and procedures is planned in future IPA iterations. In reviewing the results of IPA Phase 2, the staff evaluated the adequacy of the methodology and the adequacy of the scientific bases used for these analyses. This evaluation is discussed in Section 10.2.

The staff gained insights from developing and evaluating the system code computational modules, performing the auxiliary analyses, and performing the sensitivity and uncertainty analyses on the results of IPA Phase 2. These insights include the relative importance of various site characteristics, design features, and repository processes to repository performance. Insights gained from performance assessment results (and limited by the accuracy of the models used) include evaluation of the relationships between the performance of natural and engineered barriers and performance of the repository, and evaluation of dose and release estimates and their relationship to scenario class and pathway. Insights and conclusions are discussed in Section 10.3.

Section 10.4 discusses additional research, modeling improvements and supporting analyses that will be needed to improve the methodology and scientific basis of future performance assessments. In Section 10.4.1, necessary research falling under the responsibility of DOE or its contractors has also been included. In some cases it will be necessary for NRC, as well as DOE, to pursue a more thorough understanding of the scientific bases of the subsystem models, as well as improvements to the codes that incorporate the models, so that NRC can evaluate critical DOE assumptions, conceptual descriptions, and

mathematical representations of repository performance.

### 10.2 Evaluation of IPA Phase 2 Methodology and Scientific Bases for Analyses

#### 10.2.1 Adequacy of Methodology

The methodology evaluated, which is described in previous chapters, includes the simulation structure and treatment of uncertainty, scenario analysis, consequence analysis, the calculation of complementary cumulative distribution functions (CCDFs) for the normalized release and dose, and the use of auxiliary analyses to support model assumptions. An objective of IPA Phase 2 was to evaluate particular aspects of the performance assessment methodology, developed and transferred to NRC by the Sandia National Laboratories (SNL), including the models and codes for flow and transport in partially saturated fractured rock (i.e., *DCM3D*—flow; *NEFTRAN II*—radio-nuclide chain transport) and the scenario analysis methodology. The purpose of this section is to discuss the adequacy of various aspects of the IPA Phase 2 performance assessment methodology, including that developed by SNL.

The Monte Carlo simulation of multiple vectors or realizations, used in IPA Phase 2, is a common approach to uncertainty analysis, and was used in the IPA Phase 1 study (Codell *et al.*, 1992) and other recent studies, such as the SNL performance assessments for the Waste Isolation Pilot Plant (WIPP) (Helton *et al.*, 1991), the SNL performance assessments for Yucca Mountain (Barnard *et al.*, 1992; and Wilson *et al.*, 1994), and the Pacific Northwest Laboratory (PNL) performance assessment for Yucca Mountain (Eslinger *et al.*, 1993). This procedure allows the propagation of parameter uncertainty through a series of linked models. Model uncertainty and uncertainty resulting from the spatial variability of the parameters, however, are not reflected directly in the results (although some of these uncertainties have been represented by input parameter variability).

The SNL scenario selection methodology (Cranwell *et al.*, 1990), whose modification and implementation were described in Chapter 3, provided

## 10. Conclusions and Recommendations

an adequate basis for the staff's scenario analysis in IPA Phase 2. Sixteen mutually exclusive scenario classes, with associated estimated probabilities, were generated from an initial list of 17 potentially disruptive events and processes, of which four events and processes remained after screening for combination into scenario classes. These 16 scenario classes were provided for incorporation in the consequence analysis. Definition of repository system boundaries for the analysis kept the number of scenarios requiring evaluation to a tractable number.

The consequence models, described in Chapters 4 to 6, represent a limited attempt to estimate, for the most part using mechanistic models, the performance of the repository under selected scenario classes for each sampled realization. The increasingly mechanistic nature of the consequence models is considered to be a positive improvement over IPA Phase 1, because it has and will allow in future developments, more representative and realistic coupling between processes, and because the use of mechanistic models allows a more direct and transparent identification of needed information and data. The IPA Phase 2 models have not been run for time-varying boundary conditions (e.g., time-varying percolation flux through the repository for source term and dissolved transport models). However, some of the models allow for transient conditions caused by repository heat (e.g., gas flux for  $^{14}\text{C}$  transport), which is a function of time. Changing near-field temperatures caused by repository heat also influence the start of waste package corrosion and fuel alteration rates. Changing far-field temperatures influence gas transport. An alternative to this limited dynamic approach may be to employ stochastic time series generation of environmental processes, such as that employed in a performance assessment in the United Kingdom (see HMIP/DOE, 1993). Also, in the IPA Phase 2 consequence models (described in Chapter 6), limitations in site characterization data and excessively long computer code run times required the use of one- (1-D) and two-dimensional (2-D) transport models, where a full three-dimensional (3-D), transient approach may have been more appropriate. Although 3-D models may remain impractical to include directly in the IPA evaluations, they can be used to develop abstracted codes.

The calculation of CCDFs, described in Chapt. 9, was based on the assumption of equal probability for each realization determined for a scenario class. There were three presentations of CCDFs in IPA Phase 2: (1) conditional CCDF curves for each scenario class representing the parameter uncertainty; (2) composite or total CCDF curves representing all scenario classes; and (3) "hair diagrams," which are CCDF curves for multiple parameter vectors, each representing all scenario classes. The conditional CCDFs present repository behavior for each scenario class. They are combined to form the composite or total CCDF by weighting each by its scenario probability. The "hair diagram" presents the same information in a different way, keeping separate the scenario and parametric probabilities. For that reason, the extremes of system behavior may be better demonstrated with the hair CCDFs. For example the effects of extreme parametric values can be displayed for both high probability events (climate change) and low probability events (magmatism). The mean of all of the hair CCDFs gives the same composite or total CCDF that would be calculated by combining the scenario CCDFs.

A comparison between the CCDF of cumulative radionuclide release resulting from the IPA Phase 2 analysis and the CCDF computed by the earlier Phase 1 analysis demonstrated several significant differences. Much of the difference could be explained by the incorporation of the gas transport pathway in Phase 2 and the assignment of a higher probability of occurrence for the pluvial (climate) event. Similar comparisons in future climate phases of IPA should be easier and more informative because comparisons are expected to be made after each incremental change rather than only at the completion of major revisions in the total-system performance assessment.

Auxiliary analyses are an important part of NRC's IPA methodology. Auxiliary analyses were used for development of the abstracted models described in Chapters 4 and 5 from more sophisticated models, to synthesize parameter values and distributions from more fundamental data, and to place the results of the analyses in perspective. The auxiliary analyses were used to set some constant parameters such as water level during the pluvial climate event, geochemical parameters for various strata and radionuclides, and to determine the 1-D flow path characteristics for the liquid flow and transport computations. The

auxiliary analyses proved to be an indispensable and integral element of the staff IPA effort.

The use of the *DCM3D* and *NEFTRAN II* computer programs proved to be useful for implementing the conceptual models for liquid flow and transport of radionuclides, respectively. *DCM3D* was not used directly in the total-system performance assessment (TPA) computer code, but was used principally to partition the groundwater flow between the fracture and matrix systems for input to *NEFTRAN II*. The transport of radionuclides was simulated using *NEFTRAN II*, which accounted for element-specific retardation, radioactive decay, and generation of radioactive progeny. This simple representation kept the fracture and matrix flow systems separate. More complex representations may require features of the computer programs not used in the current analysis (e.g., transient flow fields, matrix diffusion, and 3-D models) or computer programs that represent additional processes (e.g., multi-phase flow).

Overall, the methodology provides a structured, analytical approach for estimating performance of a potential geologic repository. Various aspects of the methodology require improvement, such as consequence models, and the estimation of scenario probabilities, as discussed in Section 10.4.

### 10.2.2 Adequacy of Scientific Basis for the IPA Phase 2 Analyses

For the purposes of this discussion, the scientific basis for analysis was considered to be published information about the site and the proposed repository design, published research conducted by DOE and its contractors, and NRC-sponsored research. Broader scientific and technical literature, including published performance assessments such as that performed for the WIPP project (Helton *et al.*, 1991), was used to supplement this information.

The scientific basis for analysis is improving through site characterization activities and research. However, the existing scientific basis is far from adequate to allow an accurate assessment of compliance with any of the applicable performance objectives with reasonable assurance. The paucity of data about the site is probably the greatest inadequacy. For example, the state of site

characterization at the time these analyses were performed did not support a consensus among hydrologists about conceptual models of water movement through Yucca Mountain nor the appropriate paradigm for modeling transport of radionuclides. Far-field geochemistry, especially in its application to transport by fracture flow, is another area where conservative approximations have been used in the IPA Phase 2 analysis to account for uncertainty. In this analysis, there was assumed conservatively to be no retardation in the fractures. Credible models of retardation processes, especially in fractures, would reduce the level of conservatism for this process.

The NRC staff has modeled the 1988 Site Characterization Plan (SCP) repository design (DOE, 1988) to the extent practical, although the staff is aware of proposed design changes. Because of the preliminary nature of the design, many of the calculations have been performed as conservative or bounding analyses. Examples of such analyses are the seismic failure model for the waste packages, the waste package corrosion model, and the waste dissolution model. To the extent practicable, the SCP design has been used as a basis for modeling. Many aspects of the repository design are expected to change and the waste package design is likely to change significantly. Changes in placement configuration, such as from vertical to horizontal, will affect the waste dissolution and release models. Changes to thermal loading will affect the near-field hydrology of the waste packages and the circulation of rock gas.

### 10.2.3 Conclusions Regarding IPA Phase 2 Methodology and Analyses

The methodology can and must be improved as more data become available and the understanding of the site matures. However, the staff considers the present methodology suitable to gain insight into the significance of many of the germane parameters and processes and to gain insights regarding model development, repository performance, and research and technical assistance needs. However, the data and scientific understanding of the site are not sufficient at the current time to predict potential repository performance with certainty. Furthermore, several areas of modeling need improvement in order to have confidence in the estimates of performance. The computed CCDFs presented in this report

## 10. Conclusions and Recommendations

should not be taken to be indicative of actual repository system performance.

### 10.3 Insights and Conclusions From IPA Phase 2

#### 10.3.1 Significant Insights and Conclusions from Model Development and from the Sensitivity and Uncertainty Analyses

The purpose of this section is to discuss insights identified through model development and the sensitivity and uncertainty analysis that have a significant effect on the results of the performance assessment. Most of these insights at this stage of the IPA process deal with site aspects, repository design, and repository processes.

As noted in Chapter 4, two features of the site that appear to strongly influence the results of the performance assessment are: (1) the rock media are unsaturated and therefore have the potential for advective transport of gas upward to the atmosphere; and (2) the rock media are fractured and have the potential for fast liquid pathways for radionuclide transport to the water table and beyond. The quantitative effects of both these features have been relatively difficult to model in a consistent manner. For example, permeability and porosity for flow through fractures in the dual porosity model for the repository cross-section stratigraphy were estimated from fracture aperture widths and the number of fractures per unit area, whereas permeability and porosity for the matrix were based on core analysis. Both of these data types are based on local (small-scale) observations and need to be supplemented by data collected at a larger scale.

From the regression analyses for the base case scenario and other scenario classes not involving pluvial climate, infiltration rate was found to be the most important sampled parameter. There is strong correlation at low to moderate infiltration rates (base case) and weaker correlation at the high infiltration rates (pluvial case). In the former case, there was both matrix flow and fracture flow, but in the latter case, the flow was predominantly in fractures. Under conditions of significant fracture flow, radionuclide travel times tended to be low, with relatively little decay. The accompanying figure (Figure 10-1) shows a significant

decrease of liquid radionuclide releases for the base case CCDF when vectors with infiltration rates greater than 1 or 2 millimeters/year were eliminated from the CCDF.

Although the flux of liquid water through the repository depends on the parameters infiltration, hydraulic conductivity, and porosity, performance correlates most strongly to infiltration. The saturated hydraulic conductivity and porosity vary from layer to layer for each vector, and are assumed to be uncorrelated. There is only one value of infiltration per vector for all layers, however. Since, in the 1-D representation of unsaturated flow, infiltrating water must pass through all layers, the sensitivity to the value of hydraulic conductivity or porosity of any single layer is reduced.

A number of model simplifications (e.g., 1-D flow paths, permeability ranges, and seven sub-areas for the total repository area) were used to abstract the 3-D problem and allow analysis of the uncertainties with reasonable computer execution times for the Phase 2 analysis. However, the proposed repository is a transient, 3-D, partially saturated system with significant air and water vapor movement in a fractured, porous medium, complicated by potentially significant heat transfer and the associated flows of gas and liquid. How these phenomena can be approximated by simplifying assumptions and still provide an adequate representation for the calculation of system performance is poorly understood at this time and needs further investigation.

The Phase 2 analysis conservatively assumed that there was no retardation in the fractures and did not consider the process of matrix diffusion in the modeling. Future iterations need to evaluate the nature and magnitude of the conservatism of these assumptions and the relationship of fracture coatings to geochemical processes.

The design of the waste package container and its emplacement configuration is expected to have a strong influence on repository performance. As discussed in Section 10.2.2, the design of the waste package will greatly affect waste package failure times and release mechanisms. IPA Phase 2 analyses had varying degrees of ability to treat design details; e.g., *SOTEC* was based on vertically

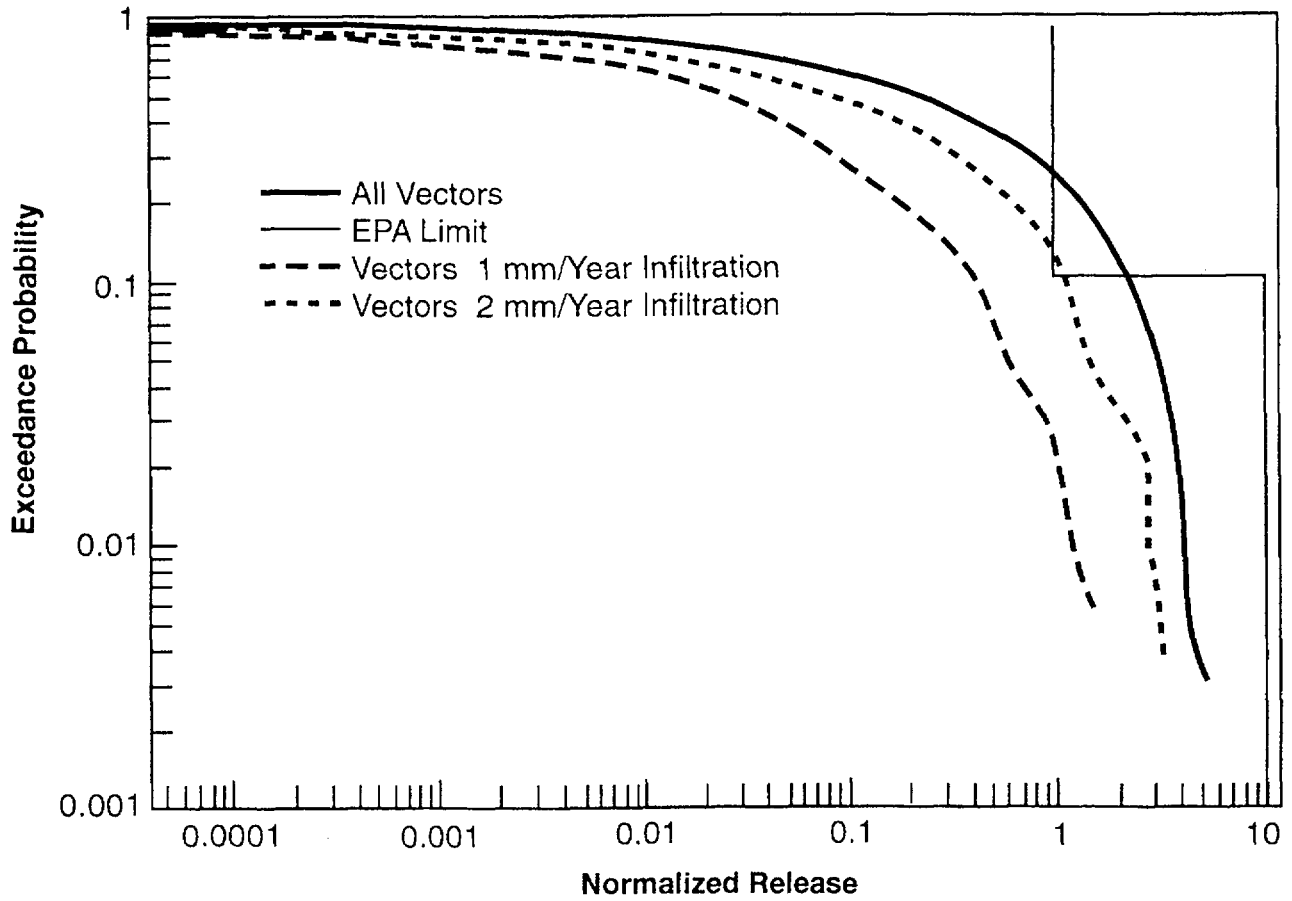


Figure 10-1 CCDF for dissolved radionuclides, base case scenario (Vectors screened for less than 1 or 2 mm/yr infiltration.)

## 10. Conclusions and Recommendations

emplaced waste packages, with no option for horizontal emplacement. *DRILLO* had the option for horizontal emplacement, but it was not used. Various options for treating the configuration of the waste package will probably need to be incorporated in some of the modules of the system code.

The corrosion-related parameters that showed strong correlation with performance were the (electrochemical) potentials for pitting and crevice corrosion, and the active corrosion rate. Corrosion affects the time of waste package failure under static and seismic conditions. Dissolution-related parameters include the fuel alteration rate and solubilities of radionuclides. Other factors found to be important control the interaction of water with the waste package and influence whether and how water contacts the waste.

Failure of the waste packages by corrosion and transport of dissolved radionuclides from the waste package are expected to depend on contact with liquid water. In IPA Phase 2, waste packages were assumed to remain dry until their surface temperature dropped below the boiling point, and came into contact with liquid water from dripping fractures and wet rock. Future models need the ability to consider plausible rewetting mechanisms for dry rock, the possible influx of liquid water such as dripping fractures, condensation of water vapor on waste package surfaces because of capillary and solution effects, rise in the water table, and water reflux driven by repository or geothermal heat.

Repository heat load is a design parameter that has the potential to significantly affect performance. The present analysis is based on the assumption of a hot repository with a design power loading of 57 kilowatts/acre. This loading results in a strong thermally induced gas flow when typical hydrologic properties are assumed for the rock strata, as shown in Section 4.3. This loading is assumed to cause a period of dryness for the waste packages; that is, there is a period for which the temperature of the rock surrounding any particular waste package will be above the boiling point of water, assumed to protect it from corrosion. Temperature also affects corrosion rates and the rate of oxidation of spent nuclear fuel. Hence, the overall sensitivity of the total-system performance assessment to any particular loading is not clear at this point, because only one

loading was assumed for all simulations. A parametric study of repository thermal loading may provide additional insights in future phases.

Gas transport parameters were also identified to be important. Parameters identified are the gas permeability and retardation coefficient for  $^{14}\text{C}$  in the Topopah Spring Unit. The gas transport of  $^{14}\text{C}$  will be complicated by variations in moisture in the transport medium and gas flow, because of the heat of the decaying nuclear waste as well as chemical processes leading to retardation of carbon. Geochemical modeling of  $^{14}\text{C}$  transport demonstrated a retardation factor of approximately 30 to 40, primarily because of the transfer of carbon between the  $\text{CO}_2$  in the gas phase and dissolved carbonate and bicarbonate in the liquid phase. Some  $^{14}\text{C}$  might be trapped temporarily in precipitating calcite during the period when temperatures are rising, and released from the calcite as it redissolves as temperatures fall. Although not modeled in IPA Phase 2, percolation of moisture and its effect on the upward movement of vapor may tend to reduce  $^{14}\text{C}$  releases during pluvial periods, possibly reducing the sensitivity total normalized release to percolation rate.

Seismicity and volcanism caused large releases compared with the undisturbed (base) case, but did not appear to have a significant effect on the total CCDF. However, more realistic modeling of infiltration, corrosion, seismicity and magmatism could significantly change the importance of disruptive effects relative to one another, as well as their influence on the total CCDF. For example, a more detailed study of magmatism may include changing groundwater chemistry and accelerating the corrosion of nearby waste packages.

Several potentially volatile compounds of  $^{99}\text{Tc}$ ,  $^{79}\text{Se}$ , and  $^{129}\text{I}$  will be present in spent nuclear fuel. Conservative estimates of gaseous releases of these radionuclides during volcanism and normal operations demonstrated relatively insignificant impacts, so this potential phenomenon was given a low priority for the IPA Phase 2 study.

### 10.3.2 Insights and Conclusions Regarding System and Subsystem Performance

This section presents some insights and conclusions regarding system and subsystem performance in terms of factors related to the behavior of the engineered and natural barriers. As noted

earlier, the factors that were investigated in IPA Phase 2 were the integrity of the waste package canisters, the rate of release of radionuclides from engineered barriers, and the travel time of water through the geosphere. The regulatory requirements in 10 CFR 60.113 address "three subsystem performance objectives," namely substantially complete containment (SCC) of waste in the waste packages (10 CFR 60.113(a)(1)(ii)(A)), controlled fractional release rate from the engineered barrier system (EBS) (10 CFR 60.113(a)(1)(ii)(B)), and pre-waste-emplacement ground-water travel time (GWTT) (10 CFR 60.113(a)(2)). The conclusions are not for the purpose of directly drawing a comparison between overall system performance in terms of release or dose and the subsystem performance measures. There are primarily two reasons for this distinction: (1) the subsystem performance measures are supposed to be independent requirements ensuring a minimal performance of each of the multiple barriers in a geologic repository, unrelated to the total system performance; and (2) the characterizations of SCC, EBS release rate, and GWTT used in IPA Phase 2 are crude and incomplete, and do not exactly conform to the definitions of those quantities in 10 CFR Part 60. For example, travel time as used here does not include the concept of the disturbed zone and is for post-emplacement rather than pre-emplacement conditions. Furthermore, travel time calculated in *FLOWMOD* is an abstraction based on the fastest combination of possible fracture and matrix pathways, and does not correspond to a realistic flow path. Nevertheless, the following comparisons shed light on the importance of the engineered and natural barriers to the total system performance.

CCDFs have been drawn by "screening out" vectors that did not meet a given criterion. The screened CCDFs used with the barriers' performance showed waste package lifetime to have a significant effect on the normalized release for liquid and gaseous source term components in the 300-year to 1000-year range. Early waste package failures were generally found to result in large  $^{14}\text{C}$  releases to the accessible environment, primarily because of enhanced transport from large thermal gradients, and increased rates of  $^{14}\text{CO}_2$  generation at higher temperatures. The relationship between "liquid" travel time and the U.S. Environmental Protection Agency (EPA) release

criterion<sup>1</sup> was strong, for flux weighted "liquid" travel time. However, travel times calculated as a result of averaging or flux weighting sub-area travel times were generally in excess of 10,000 years. The relationship between "fastest" travel times from among the seven repository sub-areas and the *Normalized Release* was most significant when used as a factor to determine the presence or absence of fracture controlled flow.

Release of  $^{14}\text{C}$  through the gaseous pathway contributed significantly to the *Normalized Release* while not affecting significantly the *Effective Dose Equivalent* estimate. This is probably because the normalized release limit for  $^{14}\text{C}$  is related to the world-wide circulation of  $^{14}\text{C}$  and the resulting dose, whereas the dose calculation in this study is limited to the assumed population in a circular area of 50-kilometer radius.

The 10,000-year median collective dose for the fully disturbed case was approximately an order of magnitude greater than the corresponding dose for the base case scenario. For the *Normalized Release*, the median (i.e., 50 percent probability) of the fully disturbed case was about 5 times the median of the base case. For both dose and *Normalized Release* at the median probability, the most important disturbing event is pluvial climate and the resulting increase in percolation rate. The contributions by the ingestion pathway dominated the collective doses from both scenarios. The average annual dose to an individual in the region from inhalation was negligible compared with that from ingestion of contaminated drinking water and locally-grown contaminated food. In scenario classes involving magmatism, order of magnitude increases over the base case dose resulted from direct releases to the surface during an extrusive magmatic event. The same type of event increased the *Normalized Release* by about a factor of 4. The radionuclides that made the largest contributions

<sup>1</sup>Currently, a revised set of standards specific to the Yucca Mountain site is being developed in accordance with the provisions of the Energy Policy Act of 1992. The Energy Policy Act of 1992 (Public Law 102-486), approved October 24, 1992, directs NRC to promulgate a rule, modifying 10 CFR Part 60 of its regulations, so that these regulations are consistent with EPA's public health and safety standards for protection of the public from releases to the accessible environment from radioactive materials stored or disposed of at Yucca Mountain, Nevada, consistent with the findings and recommendations made by the National Academy of Sciences, to EPA, on issues relating to the environmental standards governing the Yucca Mountain repository. It is assumed that the revised EPA standards for the Yucca Mountain site will not be substantially different from those currently contained in 40 CFR Part 191, particularly as they pertain to the need to conduct a quantitative performance assessment as the means to estimate postclosure performance of the repository system.

## 10. Conclusions and Recommendations

to population dose (cumulated over 10,000 years) were  $^{94}\text{Nb}$ ,  $^{210}\text{Pb}$ ,  $^{243}\text{Am}$ , and  $^{237}\text{Np}$ .

### 10.4 Recommendations

#### 10.4.1 Recommendations for Additional Scientific Input

Based on the insights and conclusions described above as well as recommendations identified in the Phase 1 report, there is a need for continuing research by both NRC and DOE in the general areas of hydrology and geochemistry, waste form and waste package container materials, repository hydrothermal effects, and probabilities and effects of disruptive events. The ability to identify research needs from the work performed in IPA Phase 2 is limited by the lack of sophistication of the models and paucity of data. When site characterization results are adequate to allow detailed modeling of hydrologic characteristics for different scales, ongoing research in scale effects will prove useful. The same is expected to be true of advanced corrosion and waste dissolution topics, shaft and borehole sealing, natural analogs, and seismic research. Hence, there is a significant amount of research being pursued that will eventually support performance assessment, but cannot be directly justified by insights and conclusions from the present analysis.

**Fracture-Matrix Interactions.** Considerable research in hydrology will need to be directed at achieving a better understanding of fracture-matrix interactions. Flow in fractured or fractured-porous media can be represented in several ways: (1) *discrete fracture models* that send flow explicitly in discrete channels and in the porous matrix; (2) *equivalent continuum models* that represent the averaging of the matrix and fracture system into an equivalent porous medium; and (3) *dual-continuum models* that treat the matrix and fracture as separate but interacting continua. Experimental information for fracture-matrix interactions is scarce and is needed to provide insights on the applicability of these approaches. DOE will need to provide detailed characterization of the fracture properties in the repository horizon as a minimum, for examination of near-field hydrothermal effects; and to a degree sufficient to determine percolation, liquid transport, and/or vapor transport properties through the rest of the Yucca Mountain area.

Field measurement of gas flow rates and determination of Yucca Mountain pneumatic properties by DOE will need to be continued for adequate modeling of gas transport.

**Regional Hydrology.** Further research will also be required in the area of regional hydrology to determine maximum water levels and boundary conditions for site hydrologic modeling especially for disruptive consequences. DOE should consider investigating the steep gradient near the site because of the possible influence on future site groundwater elevations.

**Percolation.** DOE will need to continue the field measurement of deep percolation and its correlation with precipitation. NRC should explore the possible use of such correlations with expert elicitation information in climatology to determine ranges of percolation rates as a function of climatological assumptions. The development of a more sophisticated climate model should also be pursued.

**Geochemical Models.** NRC and DOE research in geochemistry, including laboratory studies, field studies, and natural analogs must continue to provide adequate verification of present geochemical models or, if required, the bases for alternative models. Research in this area should emphasize flow through fractures because of the importance demonstrated for fracture flow. Further research in gas transport geochemistry should also be undertaken to determine if there are significant barriers to  $^{14}\text{CO}_2$  release in the geosphere.

**Corrosion Models.** DOE should continue to collect data on the corrosion of waste container materials. Both NRC and DOE research in corrosion should be directed at obtaining a better understanding of the corrosion mechanism and how corrosion is likely to progress under conditions of high humidity or in contact with water of high ionic strength. In addition, models to determine accurately the contact of the waste form with liquid water will be highly design-specific to the repository concept finally adopted. Much of this work is expected to stem from confirmatory laboratory-scale and field heater tests used to validate mathematical models of two-phase heat and mass transfer. Since the experimental data must be necessarily of short duration and small-scale relative to those of the repository, reliable

mathematical models may be the only way to extrapolate results to greater times and distances. In this regard, the basis for the development of these models will rely on a mechanistic understanding of the processes and events related to the waste package's interaction with its environment. NRC needs to pursue an independent understanding of these processes to evaluate DOE's assumptions. DOE will need to continue characterization of the spent fuel waste form (inventories and dissolution rates) as these control the source term.

**Magmatism.** Additional geologic information is needed regarding volcanic processes to improve the probability estimates of the magmatic scenario. This information includes determining the role of volatiles in driving magma ascent, the importance of multiple dike intrusions, and the role of pre-existing geologic structure. The effects of uncertainty in geochronological data should also be evaluated. Additional improvements may also have to be made regarding magma interaction with water. NRC should develop an independent understanding in this area.

#### 10.4.2 Recommendations Regarding Modeling Improvements and Supporting Analyses in NRC's IPA Activities

The following recommendations are listed by chapter and include recommendations for modeling improvements and additional analyses based on conclusions in the chapters and include recommendations from the IPA Phase 1 Report (see Chapter 10, "Preliminary Suggestions for Future Work," in Codell *et al.*, 1992) that have not yet been implemented (see Section 1.2.5 of this report). Some of these recommendations parallel those of Section 10.4.1, but emphasize analysis rather than research.

##### 10.4.2.1 TPA Computer Code

1. **Software Quality Assurance requirements need more prominence in module development.** There were a number of difficulties encountered during the development of the Phase 2 modules and their integration into the TPA system code. Many of the problems could probably be traced to a lack of documented module designs, lack of module integration designs, and lack of documented module testing. The TPA computer code and its modules need to be developed under a more

consistent environment, incorporating aspects of modern code development such as object-oriented design and principles of software quality assurance. The computational platform should be standardized to employ UNIX tools for software development and debugging. Requirements for individual code modules should be specified in advance of integrating them into the system code. There should be careful attention to interfaces among the TPA computer code and its modules.

2. **Future IPA developments will require more model abstraction and efficient computing techniques.** The computational requirements of the TPA computational modules can be prohibitive, and significant simplifications were required in order to achieve acceptably low execution costs. It is recommended that more attention be given to abstracting the complicated phenomena to achieve efficient computational modules, and examination of the feasibility of applying high-performance computing procedures including massive parallel computers and advanced computational methods (e.g., adaptive grids, domain decomposition, and efficient matrix solvers).
3. **The TPA computer code must be easily ungraded.** It is recommended that the TPA system code be considered a dynamic entity, to be upgraded in future IPA iterations. Possible upgrades include: addition of new modules, changed scope of current modules, centralized use of databases, uniform interfaces between modules, and uniform coding practices among modules.

##### 10.4.2.2 Scenario Analysis Module

1. **Staff judgments in screening the initial set of events and processes (EPs) should be reassessed using appropriate mathematical models and numerical codes, as recommended by Cranwell *et al.* (1990).** This could lead to the assignment of different probabilities to the EPs and result in a different outcome to the screening.
2. **Future work should investigate methods for generating individual scenarios "representative" of the scenario classes to which they belong.** The approach taken in the IPA Phase 2 scenario analysis generated scenario classes (i.e.,

## 10. Conclusions and Recommendations

unique combinations of events or processes without regard to the order in which they occur). Generating representative events would likely involve the need to "partition" the individual scenario classes into appropriate subevents or subprocesses and then examining various combinations.

3. **Obtain geoscience input for modeling faulting, uplift, and subsidence at Yucca Mountain.** In the IPA Phase 2 scenario analysis, the vibratory ground motion from local faulting was combined with regional seismicity. Regional uplift and subsidence were considered to have negligible consequences in the screening analysis, and no attempt was made to model these events. In future IPA iterations, all of these events will be modeled, probably in auxiliary analyses, to make a determination about whether they should be included.

### 10.4.2.3 Flow and Transport Module

1. **Examine modeling issues affecting percolation.** Conceptual model assumptions with respect to percolation should have a major effect on water flux through a repository located in the unsaturated zone. Issues that can be investigated with auxiliary analyses include the relationship between highly transient rainfall and percolation estimates, the effect of topographic lows and fault zones as sources of increased recharge, how spatial variability in hydrologic parameters affect percolation, and the effect of fracture imbibition on percolation.
2. **Examine modeling assumptions affecting fracture-matrix interaction.** Modeling assumptions regarding the interaction between matrix and fractures are very important due to differences in fluid velocities and retardation of the two flow systems. Auxiliary analyses could improve the understanding of conceptual modeling assumptions regarding small-scale interactions at the fracture-matrix interface (e.g., detailed simulations to examine the equilibration of pressure between the fracture and matrix considering transient conditions and the effects of mineral coatings on fracture surfaces) and large-scale effects concerning the flow field within a hydrogeologic unit (e.g., examine how the small-scale effects propagate through a geologic unit). These further analyses can be used to modify current IPA models and revise parametric ranges.
3. **Examine hydrogeologic features and heterogeneity that could allow a "short circuit" through the unsaturated zone.** The IPA Phase 2 flow and transport analyses assumed that fluid flow and radionuclide transport could be represented as 1-D stream tubes for each of the hydrogeologic units. Two- and 3-D analyses could investigate the impact of fault zones and perched water on pathways through the unsaturated zone. If the impact is of sufficient magnitude, then additional pathways could be added to the flow and transport analysis in future iterations.
4. **Examine the coupling of water in the gaseous and liquid phases.** The model of the repository is highly idealized. The prototype is transient, 3-D, partially saturated flow with significant air and water vapor movement in a fractured, porous medium complicated by potentially significant heat transfer and the associated flows of gas and liquid affecting the redistribution of moisture. Abstracted models need to be tested through simulation, comparing the results with those of the more complete model developed in the auxiliary analyses, which includes the coupling of water movement in the liquid and gaseous phases under non-isothermal conditions. Simulation efforts could examine the variation in moisture contents and fluid flux through the repository caused by vapor movement and condensation (this effect would be especially pronounced during the thermal phase of the repository).
5. **Examine refinements in the saturated zone modeling to improve concentration estimates for dose calculations.** The calculation of dose requires a determination of the radionuclide concentration. The concentration determination requires consideration of flow and dispersion, in the saturated zone, that is not normally required for the calculation of time-integrated discharge (*Normalized Release*) for comparison with the EPA standard.
6. **Assess the usefulness of additional intermediate calculations for understanding the flow and transport results.** The IPA Phase 2 analyses

performance measures were integrated discharge and radionuclide dose. These results are often difficult to explain in the absence of other information on modeling results for individual modules (e.g., fluid flux or water velocity for the groundwater pathway, and release rates for the source term module). It would be beneficial to further examine the modeling approaches and identify intermediate calculations that could be performed to provide further insights on model and system performance.

7. **Evaluate the importance of thermally- and barometrically-driven air flow on performance.** In IPA Phase 2, thermal gradient-driven gas transport was incorporated in the calculation of the CCDF. Other pneumatic effects such as barometric pumping should be considered in future iterations of IPA.

#### 10.4.2.4 Source Term Module

1. **The models in SOTEC will have to be modified in response to the current waste disposal concepts that differ from the SCP design assumed for the IPA Phase 2.** IPA Phase 2 was based on the waste package concept described in DOE's 1988 SCP of single-walled packages placed vertically in boreholes, with an air gap between the container and the surrounding rock. The current models will have to be modified as DOE progresses in site characterization and makes decisions about its thermal loading strategy, waste package design, waste package materials, and additional engineered barriers.
2. **Develop more mechanistic models for waste package corrosion.** The present version of SOTEC used in IPA Phase 2 considered simplified models for corrosion. Needed improvements to SOTEC include codes abstracted from complex physics-based models, including a mechanistic model for initiation and propagation of localized corrosion, taking into account the geochemical environment and mechanical stresses.
3. **Improve models for the effects of heat.** The present temperature model uses a semi-analytical approach for conduction-only. More realistic models could take heat and mass transfer in two-phase flow into account to better estimate the temperature in the near field and the transfer of liquid water and water vapor inputs needed to predict the onset of corrosion and the interaction of liquid water with the waste.
4. **Take spatial and temporal variability into account in source term models.** IPA Phase 2 began to explore ensemble averages of the temporally and spatially varying environmental parameters that should be used to represent a large number of waste packages with relatively few calculations. Improved source term models should also take the variability of the properties of the fuel into account either explicitly or by defining effective input parameters that capture the variability without making the models too complex for total-system performance assessments.
5. **Improve models for the release of gaseous  $^{14}\text{C}$ .** The IPA Phase 2 model considers the release of gaseous  $^{14}\text{CO}_2$  emanating from the waste, based on steady-state diffusion of oxygen and  $^{14}\text{CO}_2$ . Failure to include the transient diffusion of oxygen evident from the data could lead to inaccurate predictions of conversion rates at low temperatures. The model could be improved by considering transient diffusion. Also, the present implementation of the model for the release of gaseous  $^{14}\text{C}$  mixes the contribution from the seven repository sub-areas for use in the 2-D gas flow model. The model should be revised to take into account variations in release rate for each sub-area.
6. **Consider modes of waste package failure other than corrosion.** Waste packages might also fail from mechanisms other than corrosion, such as seismic shaking, volcanism, and inadvertent human intrusion. Although IPA Phase 2 considered failure by drilling, volcanism and seismicity, the models were highly simplified. Models for failure by volcanism might take into account mechanisms of interaction between magma and the waste packages (e.g., corrosive gases and viscous forces). Improved models for human intrusion might consider the site-specific likelihood for drilling, shear forces from drilling fluids, or other mechanisms that could bring radioactive material to the surface. These disruptive events could

## 10. Conclusions and Recommendations

also have a significant effect on the other aspects of the repository performance. Analytical expressions for buckling are only available for simplified geometries and loading conditions with static loads. A buckling model for a complex geometry and multiple and transient loads would require a complicated and computationally intensive simulation unsuited for IPA. Once the engineering design has been finalized, the structural failure of the waste packages from dynamic and other forces could be analyzed deterministically by numerical and experimental techniques and abstracted for IPA. These analyses would include the possible impact of mechanical fatigue of the waste packages from recurrent, low-intensity seismic activity. Improved models of seismic failure might take into account the range of frequencies of earth motion, and realistic dynamic modes of the waste packages.

7. **Improve model for the dissolution of radionuclides from the waste form.** The chemistry within the waste package was treated in a highly simplified manner in IPA Phase 2. The model could be improved by taking into account the formation and subsequent transport of colloids, speciation of the elements released to the water, the contribution of minerals from the ground water and structural materials in the waste package, the changing temperature, and other factors such as ionizing radiation.
8. **Improve model for transport of radionuclides from the waste package.** Mass transfer out of the waste package by flowing water and diffusion was included in IPA Phase 2, based on DOE's 1988 SCP conceptual waste package design. The transport model, in conjunction with the waste form dissolution model, should consider the rates that water contacts and enters the waste package canister, interacts with the waste form, and transports radionuclides from the waste package by both advection and diffusion. The model should recognize that the suite of waste packages will represent a broad range of varying stages of degradation, with some completely intact and others significantly degraded from both anticipated and unanticipated processes and events. These conditions are progressive

over the 10,000-year period of regulatory interest. Although conservatively neglected in *SOTEC*, the model could include recognition that degraded waste packages, including failed fuel (e.g., defective cladding), can still contribute to the isolation or controlled release of radionuclides.

9. **Include models for other waste forms.** The staff's first two IPAs focused on evaluating the performance of waste packages for spent nuclear fuel. In future IPAs, the staff should develop a source term model for the expected inventory of glass waste packages with special consideration to the kinetics of glass dissolution, formation of secondary silicate mineral, colloid formation, and mass transport of radionuclides. Further, waste forms other than light-water reactor spent nuclear fuel and defense-related vitrified wastes (glass) may ultimately need to be considered if they are determined to be potentially significant sources. These may include any transuranic or greater-than-Class-C wastes.

### 10.4.2.5 Disruptive Consequence Analysis

1. **Consolidate calculations of radionuclide inventory in the drilling model.** The drilling code calculates inventory using the Bateman equations and determines the inventory from the time of the earliest drilling event. Greater efficiency may have been attainable by calculating the evolution of the inventory one time only. The inventory could then be moved from one bin to another as needed, rather than having this calculation repeated in several different modules. Having a unified list of inventories would provide more information on the migration of the nuclides through the geosphere and make accounting simpler for radionuclides that migrate through both liquid and gaseous pathways.
2. **Allow multiple waste package failure times in the drilling model.** The effects of the number of drilling events are predicted to be small relative to the other releases calculated in Phase 2, in part because drilling affects only a small number of waste packages. However, for cases where there is both drilling combined with volcanism or seismicity, the source term model predicts all failures occur at the earliest time for any event. This simplifying

modeling assumption could lead incorrectly to predictions of large total releases, when a later disruption (volcanic or seismic event) causes widespread failure of waste packages. The drilling code (*DRILLO*—described in Section 6.3) and the source term code (*SOTEC*—described in Chapter 5) should be modified to allow multiple waste package at different times within the same run.

3. **Reduce the number of variables and tie the sampled parameters to the extent of drilling activity in the drilling model.** The drilling model required 92 sampled parameters to determine whether, where, and when there was a strike on a waste package. The model should be simplified to require fewer sampled parameters that would be more meaningful in the sensitivity and uncertainty analysis.
4. **Surface releases should be based on site-specific mechanisms.** Although IPA Phase 2 considered failure by drilling, volcanism, and seismicity, the models were highly simplified. Future models might consider the site-specific likelihood for drilling, shear forces from drilling fluids, and mechanisms that could bring radioactive material to the surface.

#### 10.4.2.6 Dose Assessment Module

1. **Improve the *DITTY* dose assessment model.** The results of dose assessments should be evaluated as functions of radionuclide type and exposure pathway. In addition, the dose conversion factors used in IPA Phase 2 should be re-calculated to obtain a more accurate estimate of population doses for long-lived radionuclides (as discussed in Section 7.6). Also, the model parameters currently used in *DITTY* must be verified as being applicable to the Yucca Mountain site.
2. **Evaluate other dose assessment computer codes.** Codes that should be evaluated include codes for estimating long-term individual and collective exposures, atmospheric dispersion models, and demographic models. Methods employed by international organizations (e.g., the Biospheric Model Validation Study and the Nuclear Energy Agency) for calculation of doses into the far future should be evaluated. The recommendations of the International

Commission on Radiological Protection (ICRP, 1990) should be incorporated into the codes, if adopted by NRC.

3. **Apply the statistical sensitivity and uncertainty methodology developed in IPA Phase 2 for the geosphere models to the dose assessment models.** Sensitivity and uncertainty analyses can be used to identify the most important dose assessment parameters and the sensitivity of the dose estimate to these parameters.

#### 10.4.2.7 Sensitivity and Uncertainty Analysis

1. **Sensitivity and uncertainty analysis should explore the use of dimensional analysis to form factors based on combinations of other parameters.** Dimensional analysis is a useful technique for determining the functional relationships among variables. Principles of dimensional analysis might be applied for the purpose of simplifying the repository system, with its hundreds of independent parameters, into an equivalent system with fewer parameters. These dimensionless factors would make the task of analyzing the system and determining important parameters simpler.
2. **Importance sampling techniques such as the Limit-State Approach should be evaluated.** The Limit-State Approach (Wu *et al.*, 1992), discussed in Section 8.4, has the potential for easing the computational burden experienced in the IPA Phase 2 study by reducing the number of vectors needed to construct the CCDFs and perform the sensitivity analyses. This approach should be evaluated further on the full repository system model. However, as presently implemented, the Limit-State Approach cannot deal with hundreds of independent parameters. The number of independent variables analyzed by the Limit-State Approach must be reduced, either by selecting the most important parameters by stepwise regression analysis, or combining parameters into groups.
3. **A method of directly obtaining CCDF sensitivity to individual parameters should be developed.** Sensitivity analyses have been developed to determine the effect of changes in the input parameters of the models on scalar measures of repository performance such as cumulative release and effective dose equivalents. Some

## 10. Conclusions and Recommendations

effort should be directed at developing a robust method for evaluating system sensi-

tivity for a probabilistic performance measure (e.g., the CCDF).

## 11 REFERENCES

### Chapter 1. Introduction

Barnard, R.W., *et al.*, "TSPA: 1991 An Initial Total-System Performance Assessment for Yucca Mountain", Albuquerque, New Mexico, Sandia National Laboratories, SAND91-2795, September 1992. [Prepared for the U.S. Department of Energy.]

Bath, G.D. and C.E. Jahren, "Interpretations of Magnetic Anomalies at a Potential Repository Site Located in the Yucca Mountain Area, Nevada Test Site," U.S. Geological Survey, Open File Report 84-120, 1984.

Center for Nuclear Waste Regulatory Analyses, "Development and Control of Scientific and Engineering Software," San Antonio, Texas, Technical Operating Procedure [TOP]-018, Revision 1 (Change 0), September 30, 1991.

Codell, R.B., *et al.*, "Initial Demonstration of the NRC's Capability to Conduct a Performance Assessment for a High-Level Waste Repository," U.S. Nuclear Regulatory Commission, NUREG-1327, May 1992.

Cranwell, R.M., *et al.*, "Risk Methodology for Geologic Disposal of Radioactive Waste: Scenario Selection Procedure," U.S. Nuclear Regulatory Commission, NUREG/CR-1667, April 1990. [Prepared by the Sandia National Laboratories.]

Crowe, B.M., *et al.*, "Status of Volcanic Hazard Studies for the Nevada Nuclear Waste Storage Investigations," Los Alamos, New Mexico, Los Alamos National Laboratory, LA-9325-MS, March 1983.

dePolo, C.M., "The Maximum Background Earthquake for the Basin and Range Province, Western North America," Nevada Bureau of Mines and Geology, in press [January 1993 preprint].

Longsine, D.E., E.J. Bonano, and C.P. Harlan, "User's Manual for the NEFTRAN Computer Code," U.S. Nuclear Regulatory Commission, NUREG/CR-4766, September 1987. [Prepared by the Sandia National Laboratories.]

Napier, B.A., *et al.*, "GENII: The Hanford Environmental Radiation Dosimetry Software System," Richland, Washington, Pacific Northwest Laboratory, PNL-6584, 3 vols., December 1988. [Prepared for the U.S. Department of Energy.]

O'Neill, J.M., J.W. Whitney, and M.R. Hudson, "Photogeologic and Kinematic Analysis of Lineaments at Yucca Mountain, Nevada: Implications for Strike-Slip Faulting and Oroclinal Bending," U.S. Geological Survey, Open File Report 91-623, 1992.

Sagar, B., *et al.*, "SOTEC: A Source Term Code for High-Level Geologic Repositories—User's Manual (Version 1.0)," San Antonio, Texas, Center for Nuclear Waste Regulatory Analyses, CNWRA 92-009, July 1992. [Prepared for the U.S. Nuclear Regulatory Commission.]

Silling, S.A., "Final Technical Position on Documentation of Computer Codes for High-Level Waste Management," U.S. Nuclear Regulatory Commission, NUREG-0856, June 1983.

U.S. Department of Energy, "Site Characterization Plan Overview, Yucca Mountain Site, Nevada Research and Development Area, Nevada," Nevada Operations Office/Yucca Mountain Project Office, Nevada, DOE/RW-0198, December 1988.

U.S. Environmental Protection Agency, "Environmental Standards for the Management of Spent Nuclear Fuel, High-Level and Transuranic Wastes [Final Rule]," *Federal Register*, vol. 50, no. 182, September 19, 1985, pp. 38066-38089.

U.S. Nuclear Regulatory Commission, "Disposal of High-Level Radioactive Wastes in Geologic Repositories [Proposed Rule]," *Federal Register*, vol. 46, no. 130, July 8, 1981, pp. 35280-35296.

U.S. Nuclear Regulatory Commission, "Disposal of High-Level Radioactive Wastes in Geologic Repositories [Final Rule]," *Federal Register*, vol. 48, no. 120, June 21, 1983, pp. 28194-28229.

U.S. Nuclear Regulatory Commission, "License Application Review Plan for a License Application for a Geologic Repository for Spent Nuclear

## 11. References

Fuel and High-Level Radioactive Waste, Yucca Mountain Site, Nevada—Draft Review Plan,” Office of Nuclear Material Safety and Safeguards/Division of Waste Management, NUREG-1323, September 1994.

### Chapter 2. Total-System Performance Assessment Computer Code

Ababou, R. and A.C. Bagtzoglou, “BIGFLOW: A Numerical Code for Simulating Flow in Variably Saturated, Heterogeneous Geologic Media (Theory and Users’ Manual—Version 1.1),” U.S. Nuclear Regulatory Commission, NUREG/CR-6028, June 1993. [Prepared by the Center for Nuclear Waste Regulatory Analyses.]

Amtec Engineering, Inc., *TECPLOT User’s Manual: Interactive Plotting for Scientists and Engineers (Version 4.0)*, Bellevue, Washington, 1984.

Apted, M.J., A.M. Liebetrau, and D.W. Engel, “The Analytical Repository Source-Term (AREST) Model: Analysis of Spent Fuel as a Nuclear Waste Form,” Richland, Washington, Pacific Northwest Laboratory/Battelle Memorial Institute, PNL-6347, February 1989. [Prepared for the U.S. Department of Energy.]

Center for Nuclear Waste Regulatory Analyses, “Development and Control of Scientific and engineering Software,” San Antonio, Texas, Technical Operating Procedure [TOP]-018, Revision 1 (Change 0), September 30, 1991.

Codell, R.B., *et al.*, “Initial Demonstration of the NRC’s Capability to Conduct a Performance Assessment for a High-Level Waste Repository,” U.S. Nuclear Regulatory Commission, NUREG-1327, May 1992.

Dudley, A.L., *et al.*, “Total System Performance Assessment Code (TOSPAC), Volume 1: Physical and Mathematical Bases,” Albuquerque, New Mexico, Sandia National Laboratories, SAND85-0002, December 1988. [Prepared for the U.S. Department of Energy.]

Frietas, C.J., N.A. Eisenberg, and R.G. Baca, “DRILLO Code: A Modules for Simulation of Human Intrusion Scenarios, Model Disruption, and User Guide,” San Antonio, Texas, Center for

Nuclear Waste Regulatory Analyses, CNWRA 94-005, February 1994. [Prepared for the U.S. Nuclear Regulatory Commission.]

Iman, R.L. and M.J. Shortencarier, “A FORTRAN 77 Program and User’s Guide for the Generation of Latin Hypercube and Random Samples for Use in Computer Models,” U.S. Nuclear Regulatory Commission, NUREG/CR-3624, March 1984. [Prepared by the Sandia National Laboratories.]

Janetzke, R.W. and B. Sagar, “preFOR: A Pre-Processor for FORTRAN Files: User’s Manual,” San Antonio, Texas, Center for Nuclear Waste Regulatory Analyses, CNWRA 91-003, April 1991a. [Prepared for the U.S. Nuclear Regulatory Commission.]

Janetzke, R.W. and B. Sagar, “RDFREE: A FORTRAN Utility for Format Free Input: User’s Guide,” San Antonio, Texas, Center for Nuclear Waste Regulatory Analyses, CNWRA 91-005, June 1991b. [Prepared for the U.S. Nuclear Regulatory Commission.]

Lin, C.S., R.G. Baca, and R. Drake, “VOLCANO Code—A Module for Simulation of Magmatic Scenario Model Description and User Guide,” San Antonio, Texas, Center for Nuclear Waste Regulatory Analyses, CNWRA 93-010, October 1993. [Prepared for the U.S. Nuclear Regulatory Commission.]

Longsine, D.E., E.J. Bonano, and C.P. Harlan, “User’s Manual for the NEFRAN Computer Code,” U.S. Nuclear Regulatory Commission, NUREG/CR-4766, September 1987. [Prepared by the Sandia National Laboratories.]

Lung, H-C., P.L. Chambré, T.H. Pigford, and W.W-L. Lee, “Transport of Radioactive Decay Chains in Finite and Semi-Finite Porous Media,” Lawrence Berkeley Laboratory/University of California, LBL-23987, September 1987. [Prepared for the U.S. Department of Energy.]

Margulies, T., *et al.*, “Probability Analysis of Magma Scenarios for Assessing Geologic Waste Repository Performance,” American Society of Mechanical Engineers, New York, Paper 92-WA/SAF-11, 7 p., 1992. [Presented at the ASME Winter Meeting, November 8-13, 1992, Anaheim, California.]

- Napier, B.A., *et al.*, "GENII: The Hanford Environmental Radiation Dosimetry Software System," Richland, Washington, Pacific Northwest Laboratory, PNL-6584, 3 vols., December 1988. [Prepared for the U.S. Department of Energy.]
- Nienhuis, P. and T. Appelo, "Adaptation of PHREEQE for Use in a Mixing-Cell Flowtube: PHREEQM—User Guide (October 1990)," U.S. Geological Survey, *Training Course on Geochemistry for Groundwater Systems*, Denver, Colorado, April 22 - May 3, 1991.
- Olague, N.E., *et al.*, "User's Manual for the NEFRAN II Computer Code," U.S. Nuclear Regulatory Commission, NUREG/CR-5618, February 1991. [Prepared by the Sandia National Laboratories.]
- Parkhurst, D.L., D.C. Thorstenson, and L.N. Plummer, "PHREEQE—A Computer Program for Calculating Mass Transfer for Geochemical Reactions in Gound Water," U.S. Geological Survey, WaterResources Investigations Report, WRI-80-96, 1980. [Revised 1990]
- Pruess, K., "TOUGH User's Guide," U.S. Nuclear Regulatory Commission, NUREG/CR-4645, August 1987. [Prepared by the Lawrence Berkeley Laboratory and the Sandia National Laboratories.]
- Sagar, B., *et al.*, "SOTEC: A Source Term Code for High-Level Geologic Repositories—User's Manual (Version 1.0)," San Antonio, Texas, Center for Nuclear Waste Regulatory Analyses, CNWRA 92-009, July 1992. [Prepared for the U.S. Nuclear Regulatory Commission.]
- Sagar, B. and R.W. Janetzke, "Total-System Performance Assessment Computer Code: Description of Executive Module," San Antonio, Texas, Center for Nuclear Waste Regulatory Analyses, CNWRA 91-009, July 1991. [Prepared for the U.S. Nuclear Regulatory Commission.]
- Sagar, B. and R.W. Janetzke, "Total-System Performance Assessment Computer Code: Description of Executive Module (Version 2.0)," San Antonio, Texas, Center for Nuclear Waste Regulatory Analyses, CNWRA 93-107, August 1993. [Prepared for the U.S. Nuclear Regulatory Commission.]
- Shidhar, N., *et al.*, "Engineered Barrier System Performance Assessment Codes (EBSPAC) October 1, 1992, through September 25, 1993," San Antonio, Texas, Center for Nuclear Waste Regulatory Analyses, CNWRA 93-021. October 1993. [Prepared for the U.S. Nuclear Regulatory Commission.]
- Torak, L.J., "A Modular Finite-Element Model (MODFE) for Areal and Axisymmetric Ground-Water Flow-Problems, Part 1: Model Description and User's Manual," U.S. Geological Survey, Open-File Report 90-194, 1992.
- Updegraff, C.D., C.E. Lee, and D.P. Gallegos, "DCM3D: A Dual-Continuum, Three-Dimensional, Ground-Water Flow Code for Unsaturated, Fractured, Porous Media," U.S. Nuclear Regulatory Commission, NUREG/CR-5536, February 1991. [Prepared by the Sandia National Laboratories.]
- Chapter 3. Scenario Analyses Module**
- Algermissen, S.T., *et al.*, "Probabilistic Estimates of Maximum Acceleration and Velocity in Rock in the Contiguous United States," U.S. Geological Survey, Open File Report 82-1033, 1982.
- Andersson, J., *et al.*, "The Joint SKI/SKB Scenario Development Project," Stockholm, Sweden, Statens Kärnkraftinspektion (SKI) [Swedish Nuclear Power Inspectorate], SKI Technical Report 89:14, December 1989.
- Apostolakis, G., *et al.*, "Techniques for Determining Probabilities of Events and Processes Affecting the Performance of Geologic Repositories: Suggested Approaches," U.S. Nuclear Regulatory Commission, NUREG/CR-3964, vol. 2, June 1991. [Prepared by the Sandia National Laboratories.]
- Benson, L.V. and P.W. McKinley, "Chemical Composition of Groundwater in the Yucca Mountain Area, Nevada, 1971-1984," U.S. Geological Survey, Open File Report 85-484, 1985.
- Bernreuter, D.L., *et al.*, "Seismic Hazard Characterization of 69 Nuclear Power Plant Sites East of the Rocky Mountains: Methodology, Input Data and Comparison of Previous Results for Ten Sites," U.S. Nuclear Regulatory Commission, NUREG/CR-5250, vols. 1-8, January 1989. [Prepared by the Lawrence Livermore National Laboratory.]

## 11. References

- Bonano, E.J., *et al.*, "Demonstration of a Performance Assessment Methodology for High-Level Radioactive Waste Disposal in Basalt Formations," U.S. Nuclear Regulatory Commission, NUREG/CR-4759, June 1989. [Prepared by the Sandia National Laboratories.]
- Bonano, E.J., *et al.*, "Elicitation and Use of Expert Judgment in Performance Assessment for High-Level Radioactive Waste Repositories," U.S. Nuclear Regulatory Commission, NUREG/CR-5411, May 1990. [Prepared by the Sandia National Laboratories.]
- Campbell, K.W., *et al.*, "A Preliminary Methodology for the Regional Zonation of Peak Ground Acceleration," National Science Foundation, *Proceedings of the Third International Earthquake Microzonation Conference*, June 28–July 1, 1982, Seattle, Washington, 1:365–376 [1982].
- Carrigan, C.R., *et al.*, "Potential for Water-Table Excursions Induced by Seismic Events at Yucca Mountain, Nevada," *Geology*, 19:1157–1160 [1991].
- Codell, R.B., *et al.*, "Initial Demonstration of the NRC's Capability to Conduct a Performance Assessment for a High-Level Waste Repository," U.S. Nuclear Regulatory Commission, NUREG-1327, May 1992.
- Connor, C.B. and B.E. Hill, "Volcanism Research (Chapter 10)" in Sagar, B. (ed.), "NRC High-Level Radioactive Waste Research at CNWRA, January–June, 1993," San Antonio, Texas, Center for Nuclear Waste Regulatory Analyses, CNWRA 93-01S, August 1993.
- Cornell, C.A., "Engineering Seismic Risk Analysis," *Bulletin of the Seismological Society of America*, 58:1583–1606 [1968].
- Cornell, C.A., "Probabilistic Analysis of Damage to Structure under Seismic Loads," in Howells, D.A., I.P. Haigh, and C. Taylor (eds.), "Dynamic Waves in Civil Engineering," *Society for Earthquake and Civil Engineering Proceedings*, July 7–9, 1970, University College of Swansea, pp. 471–493 [1971]. [Published by Wiley-Interscience, New York.]
- Cranwell, R.M., *et al.*, "Risk Methodology for Geologic Disposal of Radioactive Waste: Scenario Selection Procedure," U.S. Nuclear Regulatory Commission, NUREG/CR-1667, April 1990. [Prepared by the Sandia National Laboratories.]
- Crowe, B.M., *et al.*, "Calculation of the Probability of Volcanic Disruption of a High-Level Radioactive Waste Repository within Southern Nevada, USA," *Radioactive Waste Management and the Nuclear Fuel Cycle*, 3(2):167–190 [December 1982].
- Crowe, B.M. and F.V. Perry, "Volcanic Probability Calculation for the Yucca Mountain Site: Estimation of Volcanic Rates," American Nuclear Society, *Proceedings of the Topical Meeting on Nuclear Waste Isolation in the Unsaturated Zone (FOCUS '89)*, September 17–21, 1989, Las Vegas, Nevada, pp. 326–334 [1989].
- Crowe, B.M., *et al.*, "Recurrence Models of Volcanic Events: Applications to Volcanic Risk Assessment," in American Nuclear Society/American Society of Civil Engineers, *High-Level Radioactive Waste Management: Proceedings of the Third International Conference, April 12–16, 1992*, Las Vegas, Nevada, 2:2344–2355 [1992].
- Crowe, B., *et al.*, "Status of Volcanism Studies the Yucca Mountain Site Characterization Projects," Los Alamos, New Mexico, Los Alamos National Laboratory, LA-12908-MS, February 1995 [Updated March 1995]. [Prepared for the U.S. Department of Energy.]
- DeWispelare, A.R., *et al.*, "Expert Elicitation of Future Climate in the Yucca Mountain Vicinity: Iterative Performance Assessment Phase 2.5," Center for Nuclear Waste Regulatory Analyses, CNWRA 93-016, August 1993. [Prepared for the U.S. Nuclear Regulatory Commission.]
- Electric Power Research Institute, "Seismic Hazard Methodology for the Central and Eastern United States (vols. 1 and 2)," Palo Alto, California, Research Project Number P-101, 1986.
- Garside, L.J. and J.H. Schilling, "Thermal Waters of Nevada," Nevada Bureau of Mines, *Geologic Bulletin*, No. 91, 1979.
- Garside, L.J., *et al.*, "Oil and Gas Developments in Nevada," Nevada Bureau of Mines, *Geologic Bulletin*, No. 104, 1988.
- Ho, C-H., "The Mathematical Model of Volcanism at Yucca Mountain," Carson City,

- State of Nevada Agency for Nuclear Projects/  
Nuclear Waste Project Office, 1990. [Prepared by  
the University of Nevada, Las Vegas.]
- Ho, C-H., *et al.*, "Eruptive Probability Calculation  
for the Yucca Mountain Site, USA: Statistical  
Estimation of Recurrence Rates," *Bulletin of  
Volcanology*, 54:50-56 [1991].
- Ho, C-H., "Risk Assessment for the Yucca  
Mountain High-Level Nuclear Waste Repository  
Site: Estimation of Volcanic Disruption,"  
*Mathematical Geology*, 24(4):347-364 [1992].
- Hodgkinson, D.P. and T.J. Sumerling, "A Review  
of Approaches to Scenario Analysis for Reposi-  
tory Safety Assessment," OECD Nuclear Energy  
Agency/International Atomic Energy Agency/  
Commission of the European Communities,  
*Proceedings of the Symposium on the Safety  
Assessments for Radioactive Waste Repositories*,  
October 9-13, 1989, Paris, France, pp. 333-352  
[1990].
- Hunter, R.L. and Mann, C.J., "Chapter 3:  
Climatology" in "Techniques for Determining  
Probabilities of Events and Processes Affecting  
the Performance of Geologic Repositories:  
Literature Review," U.S. Nuclear Regulatory  
Commission, NUREG/CR-3964, vol. 1, June 1989.  
[Prepared by the Sandia National Laboratories.]
- International Atomic Energy Agency, "Safety  
Assessment for the Underground Disposal of  
Radioactive Wastes," International Atomic Energy  
Agency, Vienna, Austria, Safety Series No. 56,  
1981.
- Margulies, T., *et al.*, "Probability Analysis of  
Magma Scenarios for Assessing Geologic Waste  
Repository Performance," American Society of  
Mechanical Engineers, New York, Paper  
92-WA/SAF-11, 7 p., 1992. [Presented at the  
ASME Winter Meeting, November 8-13, 1992,  
Anaheim, California.]
- Maldonado F., and S.L. Koether, "Stratigraphy,  
Structure, and Some Petrographic Features of  
Tertiary Volcanic Rocks at the USW G-2 Drill  
Hole, Yucca Mountain, Nye County, Nevada,"  
U.S. Geological Survey, Open-File Report 83-732,  
1983.
- McBirney, A.R., "Volcanology," in Hunter, R.L.  
and C.J. Mann (eds.), *Techniques for Determining  
Probabilities of Geologic Events and Processes  
(Studies in Mathematical Geology No. 4)*, New  
York, Oxford University Press, pp. 167-184, 1992.
- McGuire, R.K., "FORTRAN Computer Program  
for Seismic Risk Analysis," U.S. Geological  
Survey, Open File Report 76-67, 1976.
- Meremonte, M.E. and A.M. Rogers, "Historical  
Catalog of Southern Great Basin Earthquakes  
1868-1978," U.S. Geological Survey, Open File  
Report 87-80, 1987.
- Raney, R. G., "Possible Effects of Surface and  
Underground Mining Proximal to a Closed High-  
Level Radioactive Waste Repository at Yucca  
Mountain, Nye County, Nevada," U.S. Bureau of  
Mines, 1990a. [Report to the U.S. Nuclear  
Regulatory Commission.]
- Raney, R.G., "Active Mines and Prospects Within  
a Thirty-Mile Radius of the Proposed High-Level  
Repository Site at Yucca Mountain, Nye County,  
Nevada, Subsequent to January 1988 (As of July  
1990)," U.S. Bureau of Mines, 1990b.
- Ross, B., "A First Survey of Disruption Scenarios  
for a High-Level Waste Repository at Yucca  
Mountain, Nevada," Albuquerque, New Mexico,  
Sandia National Laboratories, SAND85-7117,  
December 1987. [Prepared by Disposal Safety,  
Incorporated (Washington, D.C.) for the U.S.  
Department of Energy.]
- Science Applications International Corporation,  
"Report of Early Site Suitability Evaluation of the  
Potential Repository Site at Yucca Mountain,  
Nevada," SAIC-91/8000, January 1992. [Prepared  
for the U.S. Department of Energy.]
- Schweickert, R.A., "Evidence for a Concealed  
Dextral Strike-Slip Fault Beneath Crater Flat,  
Nevada [Abstract]," Geological Society of  
America, *1989 Annual Meeting: Abstracts with  
Program*, November 6-9, 1989, St. Louis, Missouri,  
21(6):A90 [1989].
- Scott, R.B. and J.G. Rosenbaum, "Evidence of  
Rotation about a Vertical Axis during Extension  
at Yucca Mountain, Southern Nevada [Abstract],"  
*EOS Transactions*, American Geophysical Union,  
67(16):358 [April 22, 1986].

## 11. References

- Shaw, H.R., "Uniqueness of Volcanic Systems," U.S. Geological Survey Professional Paper 1350, 1987.
- Sheridan, M.F., "A Monte Carlo Technique to Estimate the Probability of Volcanic Dikes," in High-Level Radioactive Waste Management," American Nuclear Society/American Society of Civil Engineers, *Proceedings of the Third International Conference: High-Level Radioactive Waste Management*, April 12-16, 1992, Las Vegas, Nevada, 2:2033-2038 [1992].
- Smith, E.I., *et al.*, "The Area of Most Recent Volcanism Near Yucca Mountain, Nevada: Implications for Volcanic Risk Assessment," American Nuclear Society/American Society of Civil Engineers, *Proceedings of the International Topical Meeting: High-Level Radioactive Waste Management*, April 8-12, 1990, Las Vegas, Nevada, 1:81-90 [1990].
- Spaulding, W.G., "Vegetation and Climates of the Last 45,000 years in the Vicinity of the Nevada Test Site, South-Central, Nevada," U.S. Geological Survey Professional Paper 1329, 1985.
- Stephens, M.E. and B. Goodwin, "Systematic Scenario Analysis for the Post-Closure Assessment of the Canadian Concept for U.S. Nuclear Waste Disposal," OECD Nuclear Energy Agency/International Atomic Energy Agency/Commission of the European Communities, *Proceedings of the Symposium on the Safety Assessments for Radioactive Waste Repositories*, October 9-13, 1989, Paris, France, pp. 405-416 [1990].
- TERA Corporation, *Bayesian Seismic Hazard Analysis: A Methodology*, Berkeley, California, 1978.
- Thornbury, W.D., *Regional Geomorphology of the United States*, New York, John Wiley & Sons, 1967.
- URS/John A. Blume & Associates, "Technical Basis and Parametric Study of Ground Motion and Surface Rupture Hazard Evaluations at Yucca Mountain, Nevada," Albuquerque, New Mexico, Sandia National Laboratories, SAND86-7013, September 1987. [Prepared for the U.S. Department of Energy.]
- U.S. Department of Energy, "Site Characterization Plan Overview, Yucca Mountain Site, Nevada Research and Development Area, Nevada," Nevada Operations Office/Yucca Mountain Project Office, Nevada, DOE/RW-0198, December 1988a.
- U.S. Department of Energy, "Site Characterization Plan, Yucca Mountain Site, Nevada Research and Development Area, Nevada," Nevada Operations Office/Yucca Mountain Project Office, Nevada, DOE/RW-0199, 9 vols., December 1988b.
- U.S. Environmental Protection Agency, "Environmental Standards for the Management of Spent Nuclear Fuel, High-Level and Transuranic Wastes [Final Rule]," *Federal Register*, vol. 50, no. 182, September 19, 1985, pp. 38066-38089.
- U.S. Environmental Protection Agency, "Environmental Radiation Protection Standards for the Management and Disposal of Spent Nuclear Fuel, High-Level and Transuranic Wastes [Proposed Rule]," *Federal Register*, vol. 58, no. 242, December 20, 1993, pp. 66398-66416.
- U.S. Nuclear Regulatory Commission, "10 CFR Part 60, Disposal of High-Level Radioactive Wastes in Geologic Repositories: Conforming Amendments," *Federal Register*, vol. 51, no. 118, June 19, 1986, pp. 22288-22301.
- Vaniman, D., *et al.*, "Variations in Authigenic Mineralogy and Sorptive Zeolite Abundance at Yucca Mountain, Nevada, Based on Studies of Drill Cores USW GU-3 and G-3," Los Alamos, New Mexico, Los Alamos National Laboratory, LA-9707-MS, June 1984. [Prepared for the U.S. Department of Energy.]
- Winograd, I.J. and B.J. Szabo, "Water-Table Decline in the South-Central Great Basin during the Quaternary: Implications for Toxic Waste Disposal," in Carr, M.D. and J.C. Yount (eds.), "Geologic and Hydrologic Investigations of a Potential Nuclear Waste Disposal Site at Yucca Mountain, Southern Nevada," U.S. Geological Survey Bulletin 1790, 1988.
- Yount, J.C., *et al.*, "Neotectonics of the Walker Lane, Pyramid Lake to Tonopah, Nevada—Part I," in Lahren, M.M., J.H. Trexler, Jr., and C. Spinoso (eds.), "Crustal Evolution of the Great Basin and Sierra Nevada: Cordilleran/Rocky Mountain Section," Department of Geological Sciences, University of Nevada at Reno, Geological Society of America Guidebook, pp. 383-408, 1993.

#### Chapter 4. Flow and Transport Module

Ababou R., "Approaches to Large Scale Unsaturated Flow on Heterogeneous, Stratified, and Fractured Geologic Media," U.S. Nuclear Regulatory Commission, NUREG/CR-5743, August 1991. [Prepared by the Center for Nuclear Waste Regulatory Analyses.]

Ababou, R. and A.C. Bagtzoglou, "BIGFLOW: A Numerical Code for Simulating Flow in Variably Saturated, Heterogeneous Geologic Media (Theory and Users' Manual—Version 1.1)," U.S. Nuclear Regulatory Commission, NUREG/CR-6028, June 1993. [Prepared by the Center for Nuclear Waste Regulatory Analyses.]

Ahola, M. and Sagar, B., "Regional Groundwater Modeling of the Saturated Zone in the Vicinity of Yucca Mountain, Nevada," San Antonio, Texas, Center for U.S. Nuclear Waste Regulatory Analyses, CNWRA 92-001, January 1992. [Prepared for the Nuclear Regulatory Commission.]

Amter, S. and B. Ross, "Simulation of Gas Flow Beneath Yucca Mountain, Nevada, with a Model Based on Fresh Water Head," in Post, R.G. (ed.), *Waste Management '90: Proceedings of the Symposium*, February 25-March 1, 1990, Tucson, Arizona, 2:915-925 [1990].

Bagtzoglou, A.C., R. Ababou, and B. Sagar, "Effects of Layering, Dipping Angle, and Faulting on Two-Dimensional Variably Saturated Flow (IPA Phase II)," San Antonio, Texas, Center for Nuclear Waste Regulatory Analyses, CNWRA 92-004, February 1992. [Prepared for the Nuclear Regulatory Commission.]

Bagtzoglou, A.C., *et al.*, "Effect of Some Common Geological Features on Two-Dimensional Variably Saturated Flow," in Interrante, C.G., and R.T. Pabalan (eds.), *Scientific Basis for Nuclear Waste Management XVI: Materials Research Society Symposium Proceedings*, 294:929-936 [1993].

Barnard, R.W., *et al.*, "TSPA: 1991 An Initial Total-System Performance Assessment for Yucca Mountain", Albuquerque, New Mexico, Sandia National Laboratories, SAND91-2795, September 1992. [Prepared for the U.S. Department of Energy.]

Barton, C., W. Page, and T. Morgan, "Fractures in Outcrops in the Vicinity of Drill Hole USW G-4, Yucca Mountain, Nevada—Data Analysis and Compilation," U.S. Geological Survey, Open File Report 89-92, 1989.

Benson, L.V., *et al.*, "Chemical Composition of Ground Water and the Locations of Permeable Zones in the Yucca Mountain Area, Nevada," U.S. Geological Survey, Open File Report 83-854, 1983.

Bentley, C.B., *et al.*, 1983, "Geohydrologic Data for Test Well USW H-5, Yucca Mountain Area, Nye County, Nevada," U.S. Geological Survey, Open File Report 83-853, 1983.

Blankennagel, R.K., "Hydraulic Testing Techniques of Deep Drill Holes at Pahute Mesa Nevada Test Site," U.S. Geological Survey, Open File Report 67-18, 1967.

Bowyer A., "Computing Dirichlet Tessellations," *The Computer Journal*, 24(2):162-166 [1981].

Broxton, D.E., *et al.*, "Chemistry of Diagenetically Altered Tuffs at a Potential Nuclear Waste Repository, Yucca Mountain, Nye County, Nevada," Los Alamos, New Mexico, Los Alamos National Laboratory, LA-10802-MS, October 1986.

Classen, H.C., "Water Quality and Physical Characteristics of Nevada Test Site Water-Supply Wells," U.S. Geological Survey, Open File Report 74-158, 1973.

Codell, R.B., U.S. Nuclear Regulatory Commission/Office of Nuclear Material Safety and Safeguards [NRC/NMSS], Memorandum to M.R. Knapp, NRC/NMSS [Subject: "Analytical Model for Repository Temperature"], May 4, 1984.

Codell, R.B., *et al.*, "Initial Demonstration of the NRC's Capability to Conduct a Performance Assessment for a High-Level Waste Repository," U.S. Nuclear Regulatory Commission, NUREG-1327, May 1992.

Cooley, R.L., "A Method of Estimating Parameters and Assessing Reliability for Models of Steady State Groundwater Flow, 1—Theory and Numerical Properties," *Water Resources Research*, 13:318-324 [1977].

## 11. References

- Cooley, R.L., "A Method of Estimating Parameters and Assessing Reliability for Models of Steady State Groundwater Flow, 2—Application of Statistical Analysis," *Water Resources Research*, 15:603-617 [1979].
- Cooley, R.L., "Incorporation of Prior Information on Parameters into Nonlinear Regression Groundwater Flow Models, 1—Theory," *Water Resources Research*, 18:965-976 [1982].
- Craig, R.W., *et al.*, "Geohydrologic Data for Test Well USW H-6, Yucca Mountain Area, Nye County, Nevada," U.S. Geological Survey, Open File Report 83-856, 1983.
- Craig, R.W. and J.H. Robison, "Geohydrology of Rocks Penetrated by Test Well UE-25p#1, Yucca Mountain Area, Nye County, Nevada," U.S. Geological Survey, Water Resources Investigations Report, WRI-34-4248, 1984.
- Craig, R.W. and K.A. Johnson, "Geohydrologic Data for Test Well UE-25p#1, Yucca Mountain Area, Nye County, Nevada," U.S. Geological Survey, Water Resources Investigations Report, WRI-84-450, 1984.
- Craig, R.W., "Geohydrology of Rocks Penetrated by Test Well USW H-6, Yucca Mountain, Nye County, Nevada," U.S. Geological Survey, Water Resources Investigations Report, WRI-89-4025, 1991.
- Czarnecki, J.B., "Simulated Effects of Increased Recharge on the Ground-Water Flow System of Yucca Mountain and Vicinity, Nevada-California," U.S. Geological Survey, Water Resources Investigations Report, WRI-84-4344, 1984.
- Czarnecki, J.B., "Simulated Effects of Increased Recharge on the Ground-Water Flow System of Yucca Mountain and Vicinity, Nevada-California," U.S. Geological Survey, Water-Resources Investigations Report, WRI-84-4344, 1985.
- Czarnecki, J.B., "Characterization of the Sub-regional Ground-Water Flow system at Yucca Mountain and Vicinity, Nevada-California," *Radioactive Waste Management and the Nuclear Fuel Cycle*, 13:51-61 [1989].
- Czarnecki, J.B., "Preliminary Simulations Related to a Large Horizontal Hydraulic Gradient at the North End of Yucca Mountain, Nevada [Abstract]," American Institute of Hydrology, 1990 Spring Meeting: Abstracts with Program [Topic: Minimizing Risk to the Hydrologic Environment], March 12-16, 1990, Las Vegas, Nevada, p. 18, 1990a.
- Czarnecki, J.B., "Geohydrology and Evapotranspiration at Franklin Lake Playa, Inyo County, California," U.S. Geological Survey, Open-File Report 90-356, 1990b.
- Czarnecki, J.B., "Simulated Water-Level Declines Caused by Withdrawals from Wells J-13 and J-12 Near Yucca Mountain, Nevada," U.S. Geological Survey, Open-File Report 91-478, 1992.
- Czarnecki, J.B. and R.K. Waddell, "Finite-Element Simulation of Ground-Water Flow in the Vicinity of Yucca Mountain, Nevada-California," U.S. Geological Survey, Water-Resources Investigations Report, WRI-84-4349, 1984.
- Czarnecki, J.B. and W.E. Wilson, "Site Characterization and Conceptual Models of the Regional Groundwater Flow System, Yucca Mountain and Vicinity, Nevada-California [Abstract]," in Post, R.G. (ed.), *Waste Management '89: Proceedings of the Symposium on Waste Management*, February 26-March 2, 1989, Tucson, Arizona, 1:473 [1989].
- Drever, J.I., *The Geochemistry of Natural Waters*, Englewood Cliffs, New Jersey, Prentice Hall, Inc., 1988.
- Dudley, A.L., *et al.*, "Total-System Performance Assessment Code (TOSPAC), Volume 1: Physical and Mathematical Bases," Albuquerque, New Mexico, Sandia National Laboratories, SAND85-0002, December 1988.
- Dykhuisen, R.C., "A New Coupling Term for Dual-Porosity Models," *Water Resources Research*, 26:351-356 [1990].
- Freeze, R. A. and J.A. Cherry, *Groundwater*, Englewood Cliffs, New Jersey, Prentice Hall, Inc., 1979.
- Healey, D.L., F.G. Clutson, and D.A. Glover, "Borehole Gravity Meter Surveys in Drill Holes USW G-3, UE-25p#1, and UE-25c#1, Yucca

- Mountain Area, Nevada," U.S. Geological Survey, Open File Report 84-672, 1984.
- Keynan, J.H. and F.G. Keyes, *Thermodynamic Properties of Steam Including Data for the Liquid and Solid Phases*, New York, John Wiley and Sons, 1936.
- Klaveter, E.A. and R.R. Peters, "Fluid Flow in a Fractured Rock Mass," Albuquerque, New Mexico, Sandia National Laboratories, SAND85-0855, March 1986.
- Lahoud, R.G., *et al.*, "Geohydrology of Volcanic Tuff Penetrated by Test Well UE-25b#1, Yucca Mountain, Nye County, Nevada," U.S. Geological Survey, Water Resources Investigations Report, WRI-84-4253, 1984.
- Lobmeyer, D.H., *et al.*, "Geohydrologic Data for Test Well UE-25b#1, Nevada Test Site, Nye County, Nevada," U.S. Geological Survey, Open File Report 83-855, 1983.
- Lobmeyer, D.H., "Geohydrology of Rocks Penetrated by Test Well USW G-4, Yucca Mountain, Nye County, Nevada," U.S. Geological Survey, Water Resources Investigations Report, WRI-86-4015, 1986.
- Longsine, D.E., E.J. Bonano, and C.P. Harlan, "User's Manual for the NEFTRAN Computer Code," U.S. Nuclear Regulatory Commission, NUREG/CR-4766, September 1987. [Prepared by the Sandia National Laboratories.]
- Lung, H-C., P.L. Chambré, T.H. Pigford, and W.W.-L. Lee, "Transport of Radioactive Decay Chains in Finite and Semi-Finite Porous Media," Lawrence Berkeley Laboratory/University of California, LBL-23987, September 1987. [Prepared for the U.S. Department of Energy.]
- Mualem, Y., "A Catalogue of the Hydraulic Properties of Unsaturated Soils," Haifa, Israel, Hydrodynamics and Hydraulic Laboratory, Technion Institute of Technology, Research Project No. 442, 1976.
- Meijer, A., "Yucca Mountain Project Far-Field Sorption Studies and Data Needs," Los Alamos, New Mexico, Los Alamos National Laboratory, LA-11671-MS, September 1990.
- Montazer, P. and W.E. Wilson, "Conceptual Hydrologic Model of Flow in the Unsaturated Zone, Yucca Mountain, Nevada," U.S. Geological Survey, Water-Resources Investigations Report, WRI-84-4345, 1984.
- Nienhuis, P. and T. Appelo, "Adaptation of PHREEQE for Use in a Mixing-Cell Flowtube: PHREEQM—User Guide (October 1990), U.S. Geological Survey, *Training Course on Geochemistry for Groundwater Systems*, Denver, Colorado, April 22-May 3, 1991.
- Nitao, J.J. and T.A. Buscheck, "Infiltration of a Liquid Front in an Unsaturated, Fractured Porous Media [sic][Medium]," *Water Resources Research*, 27:2099-2112 [1991].
- Olague, N.E., *et al.*, "User's Manual for the NEFTRAN II Computer Code," U.S. Nuclear Regulatory Commission, NUREG/CR-5618, February 1991. [Prepared by the Sandia National Laboratories.]
- Ortiz, T.S., *et al.*, "A Three-Dimensional Model of Reference Thermal/Mechanical and Hydrological Stratigraphy at Yucca Mountain, Southern Nevada, Albuquerque, New Mexico, Sandia National Laboratories, SAND84-1076, October 1985. [Prepared for the U.S. Department of Energy.]
- Pabalan, R.T., "Nonideality Effects on the Ion Exchange Behavior of the Zeolite Mineral Clinoptilolite," in Abrajano, T., Jr. and L.H. Johnson (eds.), *Scientific Basis for Nuclear Waste Management XIV: Materials Research Society Symposium Proceedings*, 212:559-567 [1991].
- Parsons, A.M., N.E. Olague, and D.P. Gallegos, "Conceptualization of a Hypothetical High-Level Nuclear Waste Repository Site in Unsaturated, Fractured Tuff," U.S. Nuclear Regulatory Commission, NUREG/CR-5495, January 1991. [Prepared by the Sandia National Laboratories.]
- Peters, R.R., *et al.*, "Fracture and Matrix Hydrologic Characteristics of Tuffaceous Materials from Yucca Mountain, Nye County, Nevada," Albuquerque, New Mexico, Sandia National Laboratories, SAND84-1471, December 1984.
- Peters, R.R., J.H. Gauthier, and A.L. Dudley, "The Effect of Percolation Rate on Water-Travel

## 11. References

- Time in Deep, Partially Saturated Zones," Albuquerque, New Mexico, Sandia National Laboratories, SAND85-0854, February 1986.
- Peters, C.A., *et al.*, "A Preliminary Study of the Chemistry of Pore Water Extracted from Tuff by One-Dimensional Compression," in Kharaka Y.K., and A.S. Maest (eds.), *International Water-Rock Interaction Symposium Proceedings*, July 13-23, 1992, Park City, Utah, pp. 741-745 [1992]. [Published by A.A. Balkema, Rotterdam, Holland.]
- Prickett, T.A. and C.C. Lonquist, "Selected Digital Computer Techniques for Groundwater Resource Evaluation," Illinois State Water Survey Bulletin No. 55, 1971.
- Prindle, R.W. and P.L. Hopkins, "On Conditions and Parameters Important to Model Sensitivity for Unsaturated Flow Through Layered, Fractured Tuff: Results of Analyses for HYDROCOIN Level 3 Case 2," Albuquerque, New Mexico, Sandia National Laboratories, SAND89-0652, October 1990.
- Reardon, E.J., "K<sub>d</sub>'s—Can They Be Used to Describe Reversible Ion Sorption Reactions in Contaminant Migration?," *Groundwater*, 19:279-286 [1981].
- Ross, B., S. Amter, and N. Lu, "Numerical Studies of Rock Gas Flow in Yucca Mountain," Albuquerque, New Mexico, Sandia National Laboratories, SAND91-7034, February 1992.
- Runchal, A.K. and B. Sagar, "PORFLOW: A Mathematical Model for Fluid Flow, Heat, and Mass Transport in Variably Saturated Geologic Media—Users Manual (Version 1.0), Richland, Washington, Westinghouse Hanford Company, WHC-EP-0041, July 1989.
- Rush, F.E., *et al.*, "Geohydrologic and Drill-Hole Data for Test Well USW H-1, Adjacent to Nevada Test Site, Nye County, Nevada," U.S. Geological Survey, Open File Report 83-141, 1983.
- Rush, F.E., "Geohydrology of Test Well USW H-1, Yucca Mountain, Nye County, Nevada," U.S. Geological Survey, Water-Resources Investigations Report, WRI-83-4032, 1984.
- Sagar, B. and A.K. Runchal, "PORFLOW: A Mathematical Model for Fluid Flow, Heat, and Mass Transport in Variably Saturated Geologic Media—Theory and Numerical Methods (Version 1.0)," Richland, Washington, Westinghouse Hanford Company, WHC-EP-0042, March 1990.
- Scott, R.B., *et al.*, "Geologic Character of Tuffs in the Unsaturated Zone at Yucca Mountain, Southern Nevada," in Mercer, J.W., P.S.C. Rao, and I.W. Marine (eds.), "Role of the Unsaturated Zone in Radioactive and Hazardous Waste Disposal," Ann Arbor, Michigan, Ann Arbor Science Publishers, pp. 289-335, 1983.
- Scott, R.B., "Stratigraphic and Structural Relations of Volcanic Rocks in Drill Holes USW GU-3 and USW G-3, Yucca Mountain, Nye County, Nevada," U.S. Geological Survey, Open File Report 84-491, 1984.
- Scott, R.B. and J. Bonk, "Preliminary Geologic Map of Yucca Mountain, Nye County, Nevada, with Geologic Sections," U.S. Geological Survey, Open File Report 84-494, 1984.
- Spengler, R.W., *et al.*, "Stratigraphy and Structure of Volcanic Rocks in Drill Hole USW-G1, Yucca Mountain, Nye County, Nevada," U.S. Geological Survey, Open File Report 81-1349, 1981.
- Thomas, K., "Summary of Sorption Measurements Performed with Yucca Mountain, Nevada, Tuff Samples and Water from Well J-13," Los Alamos, New Mexico, Los Alamos National Laboratory, LA-10960-MS, 1987.
- Thordarson, W., "Geohydrologic Data and Test Results from Well J-13, Nevada Test Site, Nye County, Nevada," U.S. Geological Survey, Water-Resources Investigations Report, WRI-83-4171, 1983.
- Thordarson, W., *et al.*, "Geohydrology of Test Well USW H-3, Yucca Mountain, Nye County, Nevada," U.S. Geological Survey, Water-Resources Investigations Report, WRI-84-4272, 1985.
- Tsang, Y.W. and K. Pruess, "A Study of Thermally Induced Convection Near a High-Level Nuclear Waste Repository in Partially Saturated Fractured Tuff," *Water Resources Research*, 23:1958-1966 [1987].

Updegraff, C.D., C.E. Lee, and D.P. Gallegos, "DCM3D: A Dual-Continuum, Three-Dimensional, Ground-Water Flow Code for Unsaturated, Fractured, Porous Media," U.S. Nuclear Regulatory Commission, NUREG/CR-5536, February 1991.

U.S. Department of Energy, "Site Characterization Plan, Yucca Mountain Site, Nevada Research and Development Area, Nevada," Nevada Operations Office/Yucca Mountain Project Office, Nevada, DOE/RW-0199, 9 vols., December 1988a.

U.S. Department of Energy, "Site Characterization Plan Overview, Yucca Mountain Site, Nevada Research and Development Area, Nevada," Nevada Operations Office/Yucca Mountain Project Office, Nevada, DOE/RW-0198, December 1988b.

van Genuchten, M.T., "A Closed-Form Equation for Predicting the Hydraulic Conductivity of Unsaturated Soils," *Soil Science Society of America Journal*, 44:892-898 [1980].

Waddell, R.K., "Two-Dimensional, Steady-State Model of Ground-Water Flow, Nevada Test Site and Vicinity, Nevada-California," U.S. Geological Survey, Water Resources Investigations Report, WRI-82-4085, 1982.

Weast, R.C. (ed.), *CRC Handbook of Chemistry and Physics (65th Edition)*, Boca Raton, Florida, CRC Press, Inc., 1984.

Weeks, E.P., "Effect of Topography on Gas Flow in Unsaturated Fractured Rock: Concepts and Observations," in Evans, D.D. and T.J. Nicholson (eds.), "Flow and Transport Through Unsaturated Fractured Rock," American Geophysical Union, Geophysical Monograph 42, pp. 165-170, 1987.

Whitfield, M.S., *et al.*, "Geohydrologic and Drill-Hole Data for Test Well USW H-4, Yucca Mountain, Nye County, Nevada," U.S. Geological Survey, Open File Report 84-449, 1984.

Whitfield, M.S., *et al.*, "Geohydrology of Rocks Penetrated by Test Well USW H-4, Yucca Mountain, Nye County, Nevada," U.S. Geological Survey, Water-Resources Investigations Report, WRI-85-4030, 1985.

WoldeGabriel, G., *et al.*, "Preliminary Assessment of Clinoptilolite K/Ar Results from Yucca Mountain, Nevada, USA: A Potential High-Level Radioactive Waste Repository Site," in Kharaka, Y.K. and A.S. Maest (eds.), *International Water-Rock Interaction Symposium Proceedings*, July 13-23, 1992, Park City, Utah, pp. 457-461 [1992]. [Published by A.A. Balkema, Rotterdam, Holland.]

## Chapter 5. Source Term Module

Altenhofen, M.K. and P.W. Eslinger, "Evaluation of Near-Field Thermal Environmental Conditions for a Spent Fuel Repository in Tuff," American Nuclear Society/American Society of Civil Engineers, *Proceedings of the Third International Conference: High-Level Radioactive Waste Management*, April 12-16, 1992, Las Vegas, Nevada, 1:402-409 [1992].

Apted, M.J., "Engineered Barrier System of the Near Field: The 'Little Brother' of Performance Assessment," OECD Nuclear Energy Agency/International Atomic Energy Agency/Commission of the European Communities, *Proceedings of the Symposium on the Safety Assessments for Radioactive Waste Repositories*, October 9-13, 1989, Paris, France, pp. 471-480 [1990].

Bateman, H., "The Solution of a System of Differential Equations Occurring in the Theory of Radioactive Transformation," *Proceedings of the Cambridge Philosophical Society*, 15:473 [1910].

Bazant, Z.P. and L. Cedolin, *Stability of Structures*, New York, Oxford University Press, 1991.

Buscheck, T.A. and J.J. Nitao, "The Analysis of Repository-Heat-Driven Hydrothermal Flow at Yucca Mountain," American Nuclear Society/American Society of Civil Engineers, *Proceedings of the Fourth International Conference: High-Level Radioactive Waste Management*, April 26-30, 1993, Las Vegas, Nevada, 1:847-867 [1993].

Buscheck, T.A., D.G. Wilder, and J.J. Nitao, "Large Scale In-Situ Heater Tests for Hydrothermal Characterization at Yucca Mountain," American Nuclear Society/American Society of Civil Engineers, *Proceedings of the Fourth International Conference: High-Level Radioactive Waste Management*, April 26-30, 1993, Las Vegas, Nevada, 2:1854-1872 [1993].

## 11. References

- Carslaw, H.S. and J.C. Jaeger, *Conduction of Heat in Solids*, Oxford, England, Clarendon Press, 1959.
- Codell, R.B., "Model for Release of Gaseous  $^{14}\text{C}$  from Spent Fuel," American Nuclear Society/American Society of Civil Engineers, *Proceedings of the Forth International Conference: High-Level Radioactive Waste Management*, April 26–30, 1993, Las Vegas, Nevada, 1:22–29 [1993].
- Einzig, R.E. and R. Kohli, "Low-Temperature Rupture Behavior of Zircaloy-Clad Pressurized Water Reactor Spent Fuel Rods under Dry Storage Conditions," *Nuclear Technology*, 67:107–123 [1984].
- Einzig, R.E. and H.C. Buchanan, "Long-Term, Low-Temperature Oxidation of PWR Spent Fuel," Richland, Washington, Westinghouse Hanford Co, WHC-EP-0070, April 1988.
- Einzig, R.E. "Evaluation of the Potential for Spent Fuel Oxidation under Tuff Repository Conditions," Richland, Washington, Westinghouse Hanford Company/Engineering Development Laboratory, HEDL-7452, 1991.
- Einzig, R.E., "Effects of an Oxidizing Atmosphere in a Spent Fuel Packaging Facility," American Nuclear Society, *Proceedings of the Topical Meeting on Nuclear Waste Packaging (FOCUS '91)*, September 29–October 2, 1991, Las Vegas, Nevada, pp. 88–99 [1992].
- Einzig, R.E., S.C. Marschman, and H.C. Buchanan, "Spent-Fuel Dry-Bath Oxidation Testing," *Nuclear Technology*, 94:383–393 [1991].
- Einzig, R.E., *et al.*, "Oxidation of Spent Fuel in Air at 75° and 195°C," American Nuclear Society/American Society of Civil Engineers, *Proceedings of the Third International Conference: High-Level Radioactive Waste Management*, April 12–16, 1992, Las Vegas, Nevada, 2:1449–1457 [1992].
- Farmer, J.C., *et al.*, "Corrosion Models for Performance Assessment of High-Level Radioactive-Waste Containers," *Nuclear Engineering Design*, 129:57–88 [1991].
- Garzarolli, F., *et al.*, "Review of PWR Fuel Rod Waterside Corrosion Behavior," Palo Alto, California, Electric Power Research Institute, EPRI-NP-1472, August 1980. [Prepared by Kraftwerk Union A.G. and Combustion Engineering, Inc.]
- Grambow, B., "Spent Fuel Dissolution and Oxidation: An Evaluation of Literature Data," Stockholm, Sweden, Statens Kärnkraftinspektion (SKI) [Swedish Nuclear Power Inspectorate], SKI Technical Report 89:13, March 1989.
- Henshall, G.A. "Stochastic Models for Predicting Pitting Corrosion Damage of HLRW Containers," American Nuclear Society, *Proceedings of the Topical Meeting on Nuclear Waste Packaging (FOCUS '91)*, September 29–October 2, 1991, Las Vegas, Nevada, pp. 225–232 [1992].
- Kubaschewski, O. and B.E. Hopkins, *Oxidation of Metals and Alloys*, London, England: Butterworth Publishers, 36, 1962.
- Kopp, D. and H. Munzel, "Release of Volatile Carbon-14 Containing Products from Zircaloy," *Journal of Nuclear Materials*, 173:1–6 [1990].
- Johnson, G.L. and D.L. Montan, "Thermal Calculations Pertaining to a Proposed Yucca Mountain Nuclear Waste Repository," Livermore, California, Lawrence Livermore National Laboratory, UCRL-ID-103534, February 1990.
- Lapidus, L., *Digital Computation for Chemical Engineers*, New York, McGraw-Hill, Inc., 1962.
- Longsine, D.E., E.J. Bonano, and C.P. Harlan, "User's Manual for the NEFTRAN Computer Code," U.S. Nuclear Regulatory Commission, NUREG/CR-4766, September 1987. [Prepared by the Sandia National Laboratories.]
- Macdonald, D.D. and M. Urquidi-Macdonald, "Thin-Layer Mixed-Potential Model for the Corrosion of High-Level Nuclear Waste Canisters," *Corrosion*, 46(5):380–390 [1990].
- O'Neal, W.C., *et al.*, "Preclosure Analysis of Conceptual Waste Package Designs for a Nuclear Waste Repository in Tuff," Livermore, California, Lawrence Livermore National Laboratory, UCRL 53595, November 1984. [Prepared for the U.S. Department of Energy.]
- Park, U.S., "Regulatory Overview and Recommendations on a Repository's Release of Carbon-14,"

- San Diego, California, Science Applications International Corporation, January 1992. [Prepared for the U.S. Department of Energy.]
- Pigford, Th.H., P.L. Chambré, and W. Lee, "A Review of Near-Field Mass Transfer in Geologic Disposal Systems," *Radioactive Waste Management and the Nuclear Fuel Cycle* 16(3/4):175-276 [1992].
- Ramirez, A.L. and D.G. Wilder, "Prototype Engineered Barrier System Field Tests," Livermore, California, Lawrence Livermore National Laboratory, UCID-21640, February 1991.
- Roark, R.J. and W.C. Young, *Formulas for Stress and Strain (Fifth Edition)*, New York, McGraw-Hill Book Company, 1975.
- Sagar, B., *et al.*, "SOTEC: A Source Term Code for High-Level Geologic Repositories—User's Manual (Version 1.0)," San Antonio, Texas, Center for Nuclear Waste Regulatory Analyses, CNWRA 92-009, July 1992. [Prepared for the U.S. Nuclear Regulatory Commission.]
- Shoesmith, D.W. and S. Sunder, "The Prediction of Nuclear Fuel (UO<sub>2</sub>) Dissolution Rates under Waste Disposal Conditions," *Journal of Nuclear Materials*, 190:20-35 [1992].
- Smith, H.D. and D.L. Baldwin, "An Investigation of Thermal Release of <sup>14</sup>C from PWR Spent Fuel Cladding," American Nuclear Society, *Proceedings of the Topical Meeting on Nuclear Waste Isolation in the Unsaturated Zone (FOCUS '89)*, September 17-21, 1989, Las Vegas, Nevada, pp. 46-49 [1989].
- Stout, R.B., *et al.*, "Spent Fuel Waste Form Characteristics: Grain and Fragment Size Statistical Dependence for Oxidation Response," American Nuclear Society/American Society of Civil Engineers, *Proceedings of the Second International Conference: High-Level Radioactive Waste Management*, April 28-May 3, 1991, 1:103-111 [1991].
- Tempest, P.A., P.M. Tucker, and J.W. Tyler, "Oxidation of UO<sub>2</sub> Fuel Pellets in Air at 503° and 543°K Studied, Using X-ray Photoelectron Spectroscopy and X-ray Diffraction," *Journal of Nuclear Materials*, 151(3):251-268 [1988].
- Thomas, L.E., O.D. Slagle, and R.E. Einziger, "Nonuniform Oxidation of LWR Spent Fuel in Air," *Journal of Nuclear Materials*, 184:117-126 [1991].
- TRW Environmental Safety Systems Inc., "Initial Summary Report for Repository/Waste Package Advanced Conceptual Design," Las Vegas, Nevada, Document No. B00000000-01717-5705-00015 (Rev. 00), 2 vols., August 29, 1994. [Prepared for the U.S. Department of Energy.]
- U.S. Department of Energy, "Site Characterization Plan, Yucca Mountain Site, Nevada Research and Development Area, Nevada," Nevada Operations Office/Yucca Mountain Project Office, Nevada, DOE/RW-0199, 9 vols., December 1988.
- U.S. Department of Energy, "Integrated Data Base for 1992: U.S. Spent Fuel and Radioactive Waste Inventories, Projections and Characteristics, Office of Civilian Radioactive Waste Management, RW-0006 (Revision 8), October 1992.
- Van Konynenburg, R.A., *et al.*, "Behavior of Carbon-14 in Waste Packages for Spent Fuel in a Repository in Tuff," Livermore, California, Lawrence Livermore National Laboratory, UCRL-90855, November 1984.
- Van Konynenburg, R.A., *et al.*, "Carbon-14 in Waste Packages for Spent Fuel in a Tuff Repository," in Bates, J.K. and W.B. Seefeldt (eds.), *Scientific Basis for Nuclear Waste Management X: Materials Research Society Symposium Proceedings*, 84:185-196 [1987].
- Van Konynenburg, R.A., "Gaseous Release of Carbon-14: Why the High-Level Waste Regulations Should be Changed," American Nuclear Society/American Society of Civil Engineers, *Proceedings of the Second International Conference: High-Level Radioactive Waste Management*, April 28-May 3, 1991, 1:313-319 [1991].
- Walton, J.C., "Effects of Evaporation in Solute Concentration on Presence and Composition of Water in and around the Waste Package at Yucca Mountain," *Waste Management*, 13:293-301 [1993].
- Watson, M. and J. Postlethwaite, "Numerical Simulation of Crevice Corrosion of Stainless Steel

## 11. References

and Nickel Alloys in Chloride Solutions,” *Corrosion*, 46(7):522-530 [1990].

Williford, R.E., “Uncertainties in Container Failure Time Predictions,” in Abrajano, T., Jr. and L.H. Johnson (eds.), *Scientific Basis for Nuclear Waste Management XIV: Materials Research Society Symposium Proceedings*, 212:335-342 [1991].

Wilson, C.N., “Results from NNWSI Series 3 Spent Fuel Dissolution Tests,” Richland, Washington, Battelle Pacific Northwest Laboratories, PNL-7170, June 1990.

Woodley, R.E., R.E. Einziger, and H.C. Buchanan, “Measurement of the Oxidation of Spent Fuel Between 140° and 225°C,” *Nuclear Technology*, 85:74-88 [1989].

### Chapter 6. Disruptive Consequence Analysis

Codell, R.B., *et al.*, “Initial Demonstration of the NRC’s Capability to Conduct a Performance Assessment for a High-Level Waste Repository,” U.S. Nuclear Regulatory Commission, NUREG-1327, May 1992.

Connor, C.B. and B.E. Hill, “Volcanism Research (Chapter 10)” in Sagar, B. (ed.), “NRC High-Level Radioactive Waste Research at CNWRA, January-June 1993,” San Antonio, Texas, Center for Nuclear Waste Regulatory Analyses, CNWRA 93-01S, August 1993. [Prepared for the U.S. Nuclear Regulatory Commission.]

Crisp, J.A., “Rates of Magma Emplacement and Volcanic Output,” *Journal of Volcanology and Geothermal Research*, 20:177-211 [1984].

Crowe, B.M. and F.V. Perry, “Volcanic Probability Calculation for the Yucca Mountain Site: Estimation of Volcanic Rates,” American Nuclear Society, *Proceedings of the Topical Meeting on Nuclear Waste Isolation in the Unsaturated Zone (FOCUS '89)*, September 17-21, 1989, Las Vegas, Nevada, pp. 326-334 [1989].

Crowe, B.M., *et al.*, “Aspects of Potential Magmatic Disruptions of a High-Level Radioactive Waste Repository in Southern Nevada,” *Journal of Geology*, 91:259-276 [1983].

Crowe, B.M., *et al.*, “Recurrence Models of Volcanic Events: Applications to Volcanic Risk

Assessment,” American Nuclear Society/American Society of Civil Engineers, *High-Level Radioactive Waste Management: Proceedings of Third International Conference*, April 12-16, 1992, Las Vegas, Nevada, 2:2344-2355 [1992].

Czarnecki, J.B., “Simulated Effects of Increased Recharge on the Ground-Water Flow System of Yucca Mountain and Vicinity, Nevada-California,” U.S. Geological Survey, Water-Resources Investigations Report, WRI-84-4344, 1985.

DeWispelare, A.R., *et al.*, “Expert Elicitation of Future Climate in the Yucca Mountain Vicinity—Iterative Performance Assessment Phase 2.5,” San Antonio, Texas, Center for Nuclear Waste Regulatory Analyses, CNWRA 93-016, August 1993. [Prepared for the U.S. Nuclear Regulatory Commission.]

Freitas, C.J., R.B. Codell, and N.A. Eisenberg, “SEISMO Version 1.0—A Module for Simulation of Seismo-Mechanical Scenarios, Model Description, and User Guide,” San Antonio, Texas, Center for Nuclear Waste Regulatory Analyses, CNWRA 94-008, June 1994. [Prepared for the U.S. Nuclear Regulatory Commission.]

Ho, C-H., “The Mathematical Model of Volcanism at Yucca Mountain,” State of Nevada Agency for Nuclear Projects/Nuclear Waste Project Office, 1990. [Prepared by the University of Nevada, Las Vegas.]

Ho, C-H., *et al.*, “Eruptive Probability Calculation for the Yucca Mountain Site, USA: Statistical Estimation of Recurrence Rates,” *Bulletin of Volcanology*, 54:50-56 [1991].

Johnson, G.L., and D.L. Montan, “Thermal Calculations Pertaining to a Proposed Yucca Mountain Nuclear Waste Repository,” Livermore, California, Lawrence Livermore National Laboratory, UCRL-ID-103534, February 1990.

Lin, C.S., R.G. Baca, and R. Drake, “VOLCANO Code—A Module for Simulation of Magmatic Scenario Model Description and User Guide,” San Antonio, Texas, Center for Nuclear Waste Regulatory Analyses, CNWRA 93-010. October 1993. [Prepared for the U.S. Nuclear Regulatory Commission.]

Margulies, T., *et al.*, “Probability Analysis of Magma Scenarios for Assessing Geologic Waste

Repository Performance," American Society of Mechanical Engineers, New York, Paper 92-WA/SAF-11, 7 p., 1992. [Presented at the ASME Winter Meeting, November 8-13, 1992, Anaheim, California.]

Nakamura, K., "Volcanoes as Possible Indicators of Tectonic Stress Orientation: Principle and Proposal," *Journal of Volcanology and Geothermal Research*, 2:1-16 [1977].

Sagar, B. and R.W. Janetzke, "Total-System Performance Assessment Computer Code: Description of Executive Module (Version 2.0)," San Antonio, Texas, Center for Nuclear Waste Regulatory Analyses, CNWRA 93-107, August 1993. [Prepared for the U.S. Nuclear Regulatory Commission.]

Sheridan, M.F., "A Monte Carlo Technique to Estimate the Probability of Volcanic Dikes," American Nuclear Society/American Society of Civil Engineers, *High-Level Radioactive Waste Management, Proceedings of Third International Conference*, April 12-16, 1992, Las Vegas, Nevada, 2:2033-2338 [1992].

Smith, E.I., T.R. Feuerbach, and J.E. Faulds. "The Area of Most Recent Volcanism Near Yucca Mountain, Nevada: Implications for Volcanic Risk Assessment," American Society of Civil Engineers/American Nuclear Society, *High-Level Radioactive Waste Management: Proceedings of the International Topical Meeting*, April 8-12, 1990, Las Vegas, Nevada, 1:81-90 [1990].

Trapp, J.S. and P.S. Justus, "Regulatory Requirements to Address Issues Related to Volcanism and Magmatism: Code of Federal Regulations, Title 10, Part 60, Disposal of High-Level Radioactive Wastes in Geological Repositories," American Nuclear Society/American Society of Civil Engineers, *High-Level Radioactive Waste Management, Proceedings of Third International Conference*, April 12-16, 1992, Las Vegas, Nevada, 2:2039-2046 [1992].

URS/John A. Blume & Associates, "Ground Motion Evaluations at Yucca Mountain, Nevada with Applications to Repository Conceptual Design and Siting" Albuquerque, New Mexico, Sandia National Laboratories, SAND85-7104, February 1986. [Prepared for the U.S. Department of Energy.]

U.S. Department of Energy, "Site Characterization Plan Overview, Yucca Mountain Site, Nevada Research and Development Area, Nevada," Nevada Operations Office/Yucca Mountain Project Office, Nevada, DOE/RW-0198, December 1988.

U.S. Department of Energy, "Site Characterization Plan, Yucca Mountain Site, Nevada Research and Development Area, Nevada," Nevada Operations Office/Yucca Mountain Project Office, Nevada, DOE/RW-0199, 9 vols., December 1988b.

U.S. Environmental Protection Agency, "Environmental Standards for the Management of Spent Nuclear Fuel, High-Level and Transuranic Wastes [Final Rule]," *Federal Register*, vol. 50, no. 182, September 19, 1985, pp. 38066 - 38089.

Valentine, G.A., B.M. Crowe, and F.V. Perry, "Physical Processes and Effects of Magmatism in the Yucca Mountain Region," American Nuclear Society/American Society of Civil Engineers, *High-Level Radioactive Waste Management, Proceedings of Third International Conference*, April 12-16, 1992, Las Vegas, Nevada, 2:2014-2024 [1992].

## Chapter 7. Dose Assessment Module

Baes, C.F. III, *et al.*, "A Review and Analysis of Parameters for Assessing Transport of Environmentally Released Radionuclides through Agriculture," Oak Ridge, Tennessee, Oak Ridge National Laboratory, ORNL-5786, September 1984.

Biospheric Model Validation Study, "BIOMOVS II: Progress Report No. 2," Oxon, United Kingdom, INTERA, BIOMOVS II PR2 (Report IE2859-2), May 1992.

Charles, D. and G.M. Smith, "Conversion of Releases from the Geosphere to Estimates of Individual Doses to Man (Version 2)," Oxon, United Kingdom, INTERA, Report IM1802-10, July 1991.

Czarnecki, J.B., "Simulated Water-Level Declines Caused by Withdrawals from Wells J-13 and J-12 Near Yucca Mountain, Nevada," U.S. Geological Survey, Open-File Report 91-478, 1992.

Fisher, R.V. and H.V. Schminke, *Pyroclastic Rock*, New York, Springer-Verlag, Inc., 1984.

## 11. References

- Freeze, R.A. and J.A. Cherry, *Groundwater*, Englewood Cliffs, New Jersey, Prentice Hall, Inc., 1979.
- International Atomic Energy Agency, "Generic Models and Parameters for Assessing the Environmental Transfer of Radionuclides from Routine Releases, Exposures of Critical Groups: Procedures and Data," Vienna, Safety Series No. 57, 1982.
- International Commission on Radiological Protection, "Reference Man: Anatomical, Physiological, and Metabolic Characteristics (Report of the Task Group on Reference Man)," Pergamon Press, Oxford, ICRP Publication 23, 1975.
- International Commission on Radiological Protection, "Recommendations of the ICRP," *Annals of the ICRP*, vol. 1, no. 3 [1977]. [ICRP Publication 26]
- International Commission on Radiological Protection, "Limits for Intakes of Radionuclides by Workers (Part 1)," *Annals of the ICRP*, vol. 2, nos. 3/4 [1979]. [ICRP Publication 30]
- International Commission on Radiological Protection, "Radiation Protection: 1990 Recommendations of the International Commission on Radiological Protection," *Annals of the ICRP*, vol. 21, nos. 1-3, 1990. [ICRP Publication 60]
- Johnson J.R. and M.B. Carver, "A General Model [GENMOD] for Use in Internal Dosimetry," *Health Physics*, 41:341-348 [1981].
- Kennedy, W.E., Jr., and D.L. Strenge, "Residual Radioactive Contamination from Decommissioning, Technical Basis for Translating Contamination Levels to Annual Total Effective Dose Equivalent, Final Report," U.S. Nuclear Regulatory Commission, NUREG/CR-5512, 2 vols., October 1992. [Prepared by the Pacific Northwest Laboratory.]
- Kocher, D.C., "Dose-Rate Conversion Factors for External Exposure to Photons and Electrons," U.S. Nuclear Regulatory Commission, NUREG/CR-1918, August 1981. [Prepared by Oak Ridge National Laboratory.]
- Leigh, C.D., *et al.*, "User's Guide for GENII-S: A Code for Statistical and Deterministic Simulation of Radiation Doses to Humans from Radionuclides in the Environment," Albuquerque, New Mexico, Sandia National Laboratories, SAND91-0561, April 1993.
- Logan, S.E., *et al.*, "Parametric Studies of Radiological Consequences of Basaltic Volcanism," Albuquerque, Sandia National Laboratories, SAND81-2375, April 1982. [Prepared for the U.S. Department of Energy.]
- Mills, L., "Beginning Desert Gardening," University of Nevada Cooperative Extension, 1993.
- Napier, B.A., *et al.*, "GENII: The Hanford Environmental Radiation Dosimetry Software System, Volume 1: Conceptual Representation," Richland, Washington, Pacific Northwest Laboratory, PNL-6584, December 1988a. [Prepared for the U.S. Department of Energy.]
- Napier, B.A., *et al.*, "GENII: The Hanford Environmental Radiation Dosimetry Software System, Volume 2: Users' Manual," Richland, Washington, Pacific Northwest Laboratory, PNL-6584, December 1988b. [Prepared for the U.S. Department of Energy.]
- Nevada Agricultural Statistics Service, "Nevada Agricultural Statistics: 1987-1988," Reno, Nevada, 1988.
- U.S. Code of Federal Regulations*, "Environmental Standards for the Management and Disposal of Spent Nuclear Fuel, High-Level and Transuranic Radioactive Wastes," Part 191, Chapter I, Title 40, "Protection of the Environment."
- U.S. Code of Federal Regulations*, "Standards for Protection Against Radiation," Part 20, Chapter I, Title 10, "Energy."
- U.S. Department of Commerce/Bureau of the Census, "1987 Census of Agriculture, Volume 1: Geographic Area Series, Part 28: Nevada State and County Data," Washington, D.C., AC87-A-28, June 1989.
- U.S. Department of Commerce/National Oceanographic and Atmospheric Administration "STAR Data for Desert Rock Station, Nevada (1986-1990)," Nashville, North Carolina, National Climatic Data Center, 1992.

- U.S. Department of Energy, "Chapter 3, Hydrology," in "Site Characterization Plan, Yucca Mountain Site, Nevada Research and Development Area, Nevada," Office of Civilian Radioactive Waste Management, Nevada Operations Office/ Yucca Mountain Project Office, Nevada, DOE/RW-0199, Vol. II, Part A, December 1988.
- U.S. Environmental Protection Agency, "Environmental Standards for the Management of Spent Nuclear Fuel, High-Level and Transuranic Wastes [Final Rule]," *Federal Register*, vol. 50, no. 182, September 19, 1985, pp. 38066-38089.
- U.S. Environmental Protection Agency, "High-Level and Transuranic Radioactive Wastes: Background Information Document for Final Rule," Washington, D.C., Report 520/1-85-023, August 1985.
- U.S. Environmental Protection Agency, "Limiting Values of Radionuclide Intake and Air Concentration and Dose Conversion Factors for Inhalation, Submersion and Ingestion," Washington, D.C., EPA-520/1-88-020, September 1988.
- U.S. Environmental Protection Agency, "Environmental Radiation Protection Standards for the Management and Disposal of Spent Nuclear Fuel, High-Level and Transuranic Radioactive Wastes [Proposed Rule]," *Federal Register*, vol. 58, no. 26, February 10, 1993, pp. 7924-7936.
- U.S. Nuclear Regulatory Commission, "Calculation of Annual Doses to Man from Routine Releases of Reactor Effluents for the Purpose of Evaluating Compliance with 10 CFR Part 50, Appendix I," Office of Standards Development, Regulatory Guide 1.109, Revision 1, October 1977.
- U.S. Nuclear Regulatory Commission, "Standards for Protection against Radiation [Final Rule]," *Federal Register*, vol. 56, no. 98, May 21, 1991, pp. 23360-23474.
- Chapter 8. Sensitivity and Uncertainty Analysis**
- Baybutt, P., D.C. Cox, and R.E. Kurth, "Methodology for Uncertainty Analysis of Light Water Reactor Meltdown Accident Consequences," Battelle Columbus Laboratories, Letter Report, May 31, 1981. [Prepared for the U.S. Nuclear Regulatory Commission.]
- Bowen, W.M. and C.A. Bennett (eds.), "Statistical Methods for Nuclear Material Management," U.S. Nuclear Regulatory Commission, NUREG/CR-4604, March 1988. [Prepared by Pacific Northwest Laboratories, Richland, Washington.]
- Cochran, W.G., *Sampling Techniques*, New York, John Wiley and Sons, Inc., 1963.
- Codell, R.B., *et al.*, "Initial Demonstration of the NRC's Capability to Conduct a Performance Assessment for a High-Level Waste Repository," U.S. Nuclear Regulatory Commission, NUREG-1327, May 1992.
- Draper, N.R. and H. Smith, *Applied Regression Analysis*, New York, John Wiley and Sons, Inc., 1966.
- Gunst, R.F. and R.L. Mason, *Regression Analysis and Its Application*, New York, Marcel Dekker, Inc., 1980.
- Gureghian, A.B., *et al.*, "Sensitivity and Uncertainty Analyses Applied to One-Dimensional Radionuclide Transport in a Layered Fractured Rock," U.S. Nuclear Regulatory Commission, NUREG/CR-5917, December 1992. [Prepared by the Center for Nuclear Waste Regulatory Analyses.]
- Helton, J.C., "A Retrospective and Prospective Survey of the Monte Carlo Method," *SIAM Review*, 12[1]:1-60 [1970].
- Helton, J.C., *et al.*, "Sensitivity Analysis Techniques and Results for Performance Assessment at the Waste Isolation Pilot Plant," Albuquerque, New Mexico, Sandia National Laboratories, SAND90-7103, March 1991.
- Iman, R.L. and W.J. Conover, "The Use of Rank Transform in Regression," *Technometrics*, 21:499-509 [1979].
- Iman, R.L., J. Davenport, and D. Zeigler, "Latin Hypercube Sampling (Program Users' Guide)," Albuquerque, New Mexico, Sandia National Laboratories, SAND79-1473, January 1980. [Also see Iman and Shortencarier (1984) referenced in Chapter 2.]
- Iman, R.L., and J.C. Helton, "A Comparison of Uncertainty and Sensitivity Analysis Techniques

## 11. References

for Computer Models," U.S. Nuclear Regulatory Commission, NUREG/CR-3904, March 1985.

Intriligator, M.D., *Econometric Models, Techniques, and Applications*, Englewood Cliffs, New Jersey, Prentice-Hall, Inc., 1978.

McKay, M.D., "Interim Report on the Status of Research on Uncertainty Analysis of Computer Models," Los Alamos, New Mexico, Los Alamos National Laboratory, LAUR 92-4299, December 1992. [Prepared for U.S. Nuclear Regulatory Commission.]

Mallows, C.L., "Some Comments on  $C_p$ ," *Technometrics*, 15:661-675 [1973].

Mendenhall, W. and R.L. Schaeffer, *Mathematical Statistics with Applications*, North Scituate, Massachusetts, Duxbury Press, 1973.

Seitz, R.R., *et al.*, "Sample Application of Sensitivity/Uncertainty Analysis Techniques to a Groundwater Transport Problem," Idaho Falls, Idaho, Idaho National Engineering Laboratory, DOE/LLW-108, June 1991. [Prepared by EG&G Idaho, Inc., for the U.S. Department of Energy.]

Sen, A. and M. Srivastava, *Regression Analysis—Theory, Methods, and Applications*, New York, Springer-Verlag, Inc., 1990.

Statistical Sciences, Inc., *S-PLUS: Guide to Statistical and Mathematical Analysis*, Seattle, Washington, MathSoft, Inc., Version 3.1, September 1991. [Computer program.]

Tukey, J.W., *Exploratory Data Analysis*, Reading, Massachusetts, Addison Wesley, 1977.

Walpole, R.E., and R.H. Myers, *Probability and Statistics for Engineers and Scientists*, New York, Macmillan Publishing Co., Inc., 1978.

Wu, Y.T., A.B. Gureghian, and R.B. Codell, "Sensitivity and Uncertainty Analysis Applied to One-Dimensional Transport in a Layered Fractured Rock," San Antonio, Texas, Center for Nuclear Waste Regulatory Analysis, CNWRA92-002, March 1992.

Zimmerman, D.A., *et al.*, "A Review of Techniques for Propagating Data and Parameter Uncertainties in High-Level Radioactive Waste Performance

Assessment Models," U.S. Nuclear Regulatory Commission, NUREG/CR-5393, March 1990.

Zimmerman, D.A., R.T. Hanson, and P.A. Davis, "A Comparison of Parameter Estimation and Sensitivity Analysis Techniques and Their Impact on the Uncertainty in Ground Water Flow Model Predictions," U.S. Nuclear Regulatory Commission, NUREG/CR-5522, May 1991. [Prepared by the Sandia National Laboratories, Gram, Inc., and the U.S. Geological Survey.]

### Chapter 9. Analytical Results

Cranwell, R.M., *et al.*, "Risk Methodology for Geologic Disposal of Radioactive Waste: Scenario Selection Procedure," U.S. Nuclear Regulatory Commission, NUREG/CR-1667, April 1990. [Prepared by the Sandia National Laboratories.]

Helton, J.C., *et al.*, "Sensitivity Analysis Techniques and Results for Performance Assessment at the Waste Isolation Pilot Plant," Albuquerque, New Mexico, Sandia National Laboratories, SAND90-7103, March 1991. [Prepared for the U.S. Department of Energy.]

Longsine, D.E., E.J. Bonano, and C.P. Harlan, "User's Manual for the NEFTRAN Computer Code," U.S. Nuclear Regulatory Commission, NUREG/CR-4766, September 1987. [Prepared by the Sandia National Laboratories.]

Napier, B.A., *et al.*, "GENII: The Hanford Environmental Radiation Dosimetry Software System," Richland, Washington, Pacific Northwest Laboratory, PNL-6584, 3 vols., December 1988. [Prepared for the U.S. Department of Energy.]

Sagar, B., *et al.*, "SOTEC: A Source Term Code for High-Level Geologic Repositories—User's Manual (Version 1.0)," San Antonio, Texas, Center for Nuclear Waste Regulatory Analyses, CNWRA 92-009, July 1992. [Prepared for the U.S. Nuclear Regulatory Commission.]

U.S. Environmental Protection Agency, "Environmental Radiation Protection Standards for the Management and Disposal of Spent Nuclear Fuel, High-Level and Transuranic Radioactive Wastes [Proposed Rule]," *Federal Register*, vol. 58, no. 26, February 10, 1993, pp. 7924-7936.

### Chapter 10. Conclusions and Recommendation

Barnard, R.W., *et al.*, "TSPA: 1991 An Initial Total-System Performance Assessment for Yucca

Mountain", Albuquerque, New Mexico, Sandia National Laboratories, SAND91-2795, September 1992. [Prepared for the U.S. Department of Energy.]

Codell, R.B., *et al.*, "Initial Demonstration of the NRC's Capability to Conduct a Performance Assessment for a High-Level Waste Repository," U.S. Nuclear Regulatory Commission, NUREG-1327, May 1992.

Cranwell, R.M., *et al.*, "Risk Methodology for Geologic Disposal of Radioactive Waste: Scenario Selection Procedure," U.S. Nuclear Regulatory Commission, NUREG/CR-1667, April 1990. [Prepared by the Sandia National Laboratories.]

Eslinger, P.W., *et al.*, "Preliminary Total System Analysis of a Potential High-Level Nuclear Waste Repository at Yucca Mountain," Richland, Washington, Pacific Northwest Laboratory, PNL-8444, January 1993. [Prepared for the U.S. Department of Energy.]

Helton, J.C., *et al.*, "Sensitivity Analysis Techniques and Results for Performance Assessment at the Waste Isolation Pilot Plant," Albuquerque, New Mexico, Sandia National Laboratories, SAND90-7103, March 1991. [Prepared for the U.S. Department of Energy.]

Her Majesty's Inspectorate of Pollution/  
Department of Environment [HMIP/DOE], "A

Trial Assessment of Underground Disposal of Radioactive Wastes Based on Probabilistic Risk Analysis", DOE Report No. DOE/HMIP/RR/92.042, January 1993.

International Commission on Radiological Protection, "Radiation Protection: 1990 Recommendations of the International Commission on Radiological Protection," *Annals of the ICRP*, vol. 21, nos. 1-3, 1990. [ICRP Publication 60]

U.S. Department of Energy, "Site Characterization Plan, Yucca Mountain Site, Nevada Research and Development Area, Nevada," Nevada Operations Office/Yucca Mountain Project Office, Nevada, DOE/RW-0199, 9 vols., December 1988.

U.S. Environmental Protection Agency, "Environmental Radiation Protection Standards for the Management and Disposal of Spent Nuclear Fuel, High-Level and Transuranic Wastes [Proposed Rule]," *Federal Register*, vol. 58, no. 242, December 20, 1993, pp. 66398-66416.

Wu, Y.T., *et al.*, "Sensitivity and Uncertainty Analyses Applied to One-Dimensional Radionuclide Transport in a Layered Fractured Rock, Volume 2: Evaluation of the Limit State Approach," U.S. Nuclear Regulatory Commission, NUREG/CR-5917, December 1992. [Prepared by the Center for Nuclear Waste Regulatory Analyses.]

## APPENDIX A LHS-SAMPLED INPUT PARAMETERS

The following is a list of parameters used by the total-system performance assessment computer code (including its modules) in the Iterative Performance Assessment Phase 2 demonstration. It includes constants that were considered as "global parameters" (see Section 2.1.5). The list does not include parameters or constants internal to a particular computational module. All dimensions are in meters-kilogram-years; open brackets ( [ ] ) are dimensionless parameters.

The parameters sampled for the base case include those parameters listed for the *C14*, *SOTEC*, and *FLOWMOD* modules (described in Section 2.1.3). The parameters sampled for the fully disturbed case are those parameters listed for the *C14*, *FLOWMOD*, *SOTEC*, *VOLCANO*, and *DRILLO* modules. The infiltration rate used for the fully disturbed case was the disturbed infiltration.

<i>Type of Distribution Value (or Range in Value)</i>	<i>Parameter Name</i>	<i>Module</i>	<i>Parameter Description</i>	<i>Basis for Parameter Assignment</i>
CONSTANT 0.0	alpha	C14	gas dispersivity [m <sup>2</sup> /yr]	Assumed
LOGNORMAL 6.5E-17	5.5E-15 AKR(1)	C14	fracture permeability of layer [m <sup>2</sup> ] (Tiva Canyon)	Klavetter and Peters (1986) (+/- one order of magnitude of the reported value)
LOGNORMAL 1.6E-16	1.6E-14 AKR(2)	C14	fracture permeability of layer [m <sup>2</sup> ] (Paintbrush)	Klavetter and Peters (1986) (+/- one order of magnitude of the reported value)
LOGNORMAL 3.24E-17	3.24E-15 AKR(3)	C14	fracture permeability of layer [m <sup>2</sup> ] (Topopah Spring)	Klavetter and Peters (1986) (+/- one order of magnitude of the highest reported value)
LOGNORMAL 9.7E-17	9.7E-15 AKR(4)	C14	fracture permeability of layer [m <sup>2</sup> ] (Calico Hills, vitric)	Klavetter and Peters (1986) (+/- one order of magnitude of the reported value)
LOGNORMAL 9.7E-17	9.7E-15 AKR(5)	C14	fracture permeability of layer [m <sup>2</sup> ] (Calico Hills, zeolitic)	Klavetter and Peters (1986) (+/- one order of magnitude of the reported value)
CONSTANT 0.00014	pork(1)	C14	fracture porosity of layer [ ] (Tiva Canyon)	Klavetter and Peters (1986) (reported value)
CONSTANT 0.000027	pork(2)	C14	fracture porosity of layer [ ] (Paintbush)	Klavetter and Peters (1986) (reported value)

Appendix A

<i>Type of Distribution Value (or Range in Value)</i>	<i>Parameter Name</i>	<i>Module</i>	<i>Parameter Description</i>	<i>Basis for Parameter Assignment</i>
CONSTANT 0.000041	pork(3)	C14	fracture porosity of layer [ ] (Topopah Spring)	Klavetter and Peters (1986) (reported value)
CONSTANT 0.000046	pork(4)	C14	fracture porosity of layer [ ] (Calico Hills, vitric)	Klavetter and Peters (1986) (reported value)
CONSTANT 0.000046	pork(5)	C14	fracture porosity of layer [ ] (Calico Hills, zeolitic)	Klavetter and Peters (1986) (reported value)
UNIFORM 10.0	100. retardk(1)	C14	retardation factor [ ] (Tiva Canyon)	Based on geochemical model presented in Appendix K
UNIFORM 10.0	100. retardk(2)	C14	retardation factor [ ] (Paintbrush)	Based on geochemical model presented in Appendix K
UNIFORM 10.0	100. retardk(3)	C14	retardation factor [ ] (Topopah Spring)	Based on geochemical model presented in Appendix K
UNIFORM 10.0	100. retardk(4)	C14	retardation factor [ ] (Calico Hills, vitric)	Based on geochemical model presented in Appendix K
UNIFORM 10.0	100. retardk(5)	C14	retardation factor [ ] (Calico Hills, zeolitic)	Based on geochemical model presented in Appendix K
LOGNORMAL 3.6E-19	1.2E-18 permm (1)	FLOWMOD	matrix permeability [m <sup>2</sup> ] (Topopah Spring)	Peters et al. (1984) (reported range and correlation length considerations)
LOGNORMAL 3.9E-15	2.0E-14 permm (2)	FLOWMOD	matrix permeability [m <sup>2</sup> ] (Calico Hills, vitric)	Peters et al. (1984) (reported range and correlation length considerations)
LOGNORMAL 1.3E-20	6.7E-19 permm (3)	FLOWMOD	matrix permeability [m <sup>2</sup> ] (Calico Hills, zeolitic)	Peters et al. (1984) (reported range and correlation length considerations)
LOGNORMAL 1.9E-16	9.6E-16 permm (4)	FLOWMOD	matrix permeability [m <sup>2</sup> ] (Prow Pass)	Peters et al. (1984) (reported range and correlation length considerations)
LOGNORMAL 5.1E-1 <sup>o</sup>	1.5E-17 permm (5)	FLOWMOD	matrix permeability [m <sup>2</sup> ] (Upper Crater Flat)	Peters et al. (1984) (reported range and correlation length considerations)

<i>Type of Distribution Value (or Range in Value)</i>	<i>Parameter Name</i>	<i>Module</i>	<i>Parameter Description</i>	<i>Basis for Parameter Assignment</i>	
LOGNORMAL 3.5E-16	4.4E-16	permm (6)	FLOWMOD	matrix permeability [m <sup>2</sup> ] (Bullfrog)	Peters <i>et al.</i> (1984) (reported range and correlation length considerations)
LOGNORMAL 4.1E-18	1.6E-17	permm (7)	FLOWMOD	matrix permeability [m <sup>2</sup> ] (Middle Crater Flat)	Assumed same as Upper Crater Flat
LOGNORMAL 1.1E-16	1.9E-16	permf (1)	FLOWMOD	fracture permeability [m <sup>2</sup> ] (Topopah Spring)	Klavetter and Peters (1986) (reported range and correlation length considerations)
LOGNORMAL 5.6E-16	1.2E-15	permf (2)	FLOWMOD	fracture permeability [m <sup>2</sup> ] (Calico Hills, vitric)	Klavetter and Peters (1986) (+/- 50 percent of reported value and correlation length considerations)
LOGNORMAL 6.2E-16	9.9E-16	permf (3)	FLOWMOD	fracture permeability [m <sup>2</sup> ] (Calico Hills, zeolitic)	Klavetter and Peters (1986) (+/- 50 percent of reported value and correlation length considerations)
LOGNORMAL 3.9E-17	8.1E-17	permf (4)	FLOWMOD	fracture permeability [m <sup>2</sup> ] (Prow Pass)	Klavetter and Peters (1986) (+/- 50 percent of reported value and correlation length considerations)
LOGNORMAL 6.7E-16	9.8E-16	permf (5)	FLOWMOD	fracture permeability [m <sup>2</sup> ] (Upper Crater Flat)	Assumed same as Calico Hills
LOGNORMAL 4.9E-17	6.4E-17	permf (6)	FLOWMOD	fracture permeability [m <sup>2</sup> ] (Bullfrog)	Assumed same as Prow Pass
LOGNORMAL 6.2E-16	9.9E-16	permf (7)	FLOWMOD	fracture permeability [m <sup>2</sup> ] (Middle Crater Flat)	Assumed same as Calico Hills
UNIFORM 0.06	0.16	porm (1)	FLOWMOD	matrix porosity [ ] (Topopah Spring)	Peters <i>et al.</i> (1984) (reported range)
UNIFORM 0.33	0.56	porm (2)	FLOWMOD	matrix porosity [ ] (Calico Hills, vitric)	Peters <i>et al.</i> (1984) (+/- 25 percent of mean)
UNIFORM 0.20	0.33	porm (3)	FLOWMOD	matrix porosity [ ] (Calico Hills, zeolitic)	Peters <i>et al.</i> (1984) (+/- 25 percent of mean)

Appendix A

<i>Type of Distribution Value (or Range in Value)</i>		<i>Parameter Name</i>	<i>Module</i>	<i>Parameter Description</i>	<i>Basis for Parameter Assignment</i>
UNIFORM 0.24	0.40	porm (4)	FLOWMOD	matrix porosity [ ] (Prow Pass)	Peters <i>et al.</i> (1984) (+/- 25 percent of mean)
UNIFORM 0.18	0.30	porm (5)	FLOWMOD	matrix porosity [ ] (Upper Crater Flat)	Peters <i>et al.</i> (1984) (+/- 25 percent of mean)
UNIFORM 0.19	0.32	porm (6)	FLOWMOD	matrix porosity [ ] (Bullfrog)	Peters <i>et al.</i> (1984) (+/- 25 percent of mean)
UNIFORM 0.18	0.30	porm (7)	FLOWMOD	matrix porosity [ ] (Middle Crater Flat)	Assumed same as Upper Crater Flat
CONSTANT 4.1E-5		porf (1)	FLOWMOD	fracture porosity [ ] (Topopah Spring)	Klavetter and Peters (1986)
CONSTANT 4.6E-5		porf (2)	FLOWMOD	fracture porosity [ ] (Calico Hills, vitric)	Klavetter and Peters (1986)
CONSTANT 4.6E-5		porf (3)	FLOWMOD	fracture porosity [ ] (Calico Hills, zeolitic)	Klavetter and Peters (1986)
CONSTANT 1.3E-5		porf (4)	FLOWMOD	fracture porosity [ ] (Prow Pass)	Klavetter and Peters (1986)
CONSTANT 4.6E-5		porf (5)	FLOWMOD	fracture porosity [ ] (Upper Crater Flat)	Assumed same as Calico Hills
CONSTANT 1.3E-5		porf (6)	FLOWMOD	fracture porosity [ ] (Bullfrog)	Assumed same as Prow Pass
CONSTANT 4.6E-5		porf (7)	FLOWMOD	fracture porosity [ ] (Middle Crater Flat)	Assumed same as Calico Hills
UNIFORM 1.4	2.2	betam (1)	FLOWMOD	van Genuchten power term [ ] (Topopah Spring - matrix)	Klavetter and Peters (1986) (+/- 25 percent reported value)
UNIFORM 1.5	4.9	betam (2)	FLOWMOD	van Genuchten power term [ ] (Calico Hills, vitric - matrix)	Klavetter and Peters (1986) (+/- 25 percent of reported value—lower bound replaced with reported low value in Peters <i>et al.</i> (1984))

Type of Distribution Value (or Range in Value)		Parameter Name	Module	Parameter Description	Basis for Parameter Assignment
UNIFORM 1.2	3.3	betam (3)	FLOWMOD	van Genuchten power term [ ] (Calico Hills, zeolitic - matrix)	Klavetter and Peters (1986) (+/- 25 percent of reported value—upper bound replaced with reported high value in Peters <i>et al.</i> (1984))
UNIFORM 2.0	3.4	betam (4)	FLOWMOD	van Genuchten power term [ ] (Prow Pass - matrix)	Klavetter and Peters (1986) (+/- 25 percent of reported value—upper bound replaced with reported high value in Peters <i>et al.</i> (1984))
UNIFORM 1.5	2.4	betam (5)	FLOWMOD	van Genuchten power term [ ] (Upper Crater Flat - matrix)	Peters <i>et al.</i> (1984) (+/- 25 percent of mean)
UNIFORM 2.3	4.2	betam (6)	FLOWMOD	van Genuchten power term [ ] (Bullfrog - matrix)	Peters <i>et al.</i> (1984) (reported range)
UNIFORM 1.5	2.4	betam (7)	FLOWMOD	van Genuchten power term [ ] (Middle Crater Flat - matrix)	Assumed same as Upper Crater Flat
UNIFORM 3.2	5.3	betaf (1)	FLOWMOD	van Genuchten power term [ ] (Topopah Spring - fracture)	Klavetter and Peters (1986) (+/- 25 percent of reported value)
UNIFORM 3.2	5.3	betaf (2)	FLOWMOD	van Genuchten power term [ ] (Calico Hills, vitric - fracture)	Klavetter and Peters (1986) (+/- 25 percent of reported value)
UNIFORM 3.2	5.3	betaf (3)	FLOWMOD	van Genuchten power term [ ] (Calico Hills, zeolitic - frac.)	Klavetter and Peters (1986) (+/- 25 percent of reported value)
UNIFORM 3.2	5.3	betaf (4)	FLOWMOD	van Genuchten power term [ ] (Prow Pass - fracture)	Klavetter and Peters (1986) (+/- 25 percent of reported value)
UNIFORM 3.2	5.3	betaf (5)	FLOWMOD	van Genuchten power term [ ] (Upper Crater Flat - fracture)	Assumed same as Calico Hills
UNIFORM 3.2	5.3	betaf (6)	FLOWMOD	van Genuchten power term [ ] (Bullfrog - fracture)	Assumed same as Prow Pass
UNIFORM 3.2	5.3	betaf (7)	FLOWMOD	van Genuchten power term [ ] (Middle Crater Flat - fracture)	Assumed same as Calico Hills

Appendix A

<i>Type of Distribution Value (or Range in Value)</i>	<i>Parameter Name</i>	<i>Module</i>	<i>Parameter Description</i>	<i>Basis for Parameter Assignment</i>
CONSTANT 0.0026	grad (1)	FLOWMOD	gradient in saturated zone [ ] (Topopah Spring)	Based on elevation of water table at the Yucca Mountain site
CONSTANT 0.0026	grad (2)	FLOWMOD	gradient in saturated zone [ ] (Calico Hills, vitric)	Based on elevation of water table at the Yucca Mountain site
CONSTANT 0.0026	grad (3)	FLOWMOD	gradient in saturated zone [ ] (Calico Hills, zeolitic)	Based on elevation of water table at the Yucca Mountain site
CONSTANT 0.0026	grad (4)	FLOWMOD	gradient in saturated zone [ ] (Prow Pass)	Based on elevation of water table at the Yucca Mountain site
CONSTANT 0.0026	grad (5)	FLOWMOD	gradient in saturated zone [ ] (Upper Crater Flat)	Based on elevation of water table at the Yucca Mountain site
CONSTANT 0.0026	grad (6)	FLOWMOD	gradient in saturated zone [ ] (Bullfrog)	Based on elevation of water table at the Yucca Mountain site
CONSTANT 0.0026	grad (7)	FLOWMOD	gradient in saturated zone [ ] (Middle Crater Flat)	Based on elevation of water table at the Yucca Mountain site
NORMAL 0.3	30.0 dispersion	FLOWMOD	dispersion length [m]	Assumed
LOGUNIFORM 1.0E-4	5.0E-3 infiltration	FLOWMOD	infiltration rate (undisturbed) [m/yr]	Assumed (similar to IPA Phase 1; see Codell <i>et al.</i> (1992))
LOGUNIFORM 5.0E-3	1.0E-2 infiltration (pluvial)	FLOWMOD	infiltration rate [m/yr] (pluvial conditions)	Assumed (similar to IPA Phase 1; see Codell <i>et al.</i> (1992))
LOGUNIFORM 0.045	4.5 kdm (1)	FLOWMOD	Cm K <sub>d</sub> [m <sup>3</sup> /kg] (Topopah Spring)	Codell <i>et al.</i> (1992) (+/- one order of magnitude of the mean of log of retradation factors from IPA Phase 1)
LOGUNIFORM 0.328	32.8 kdm (2)	FLOWMOD	Cm K <sub>d</sub> [m <sup>3</sup> /kg] (Calico Hills, vitric)	Codell <i>et al.</i> (1992) (+/- one order of magnitude of the mean of log of retardation factors from IPA Phase 1)

<i>Type of Distribution Value (or Range in Value)</i>		<i>Parameter Name</i>	<i>Module</i>	<i>Parameter Description</i>	<i>Basis for Parameter Assignment</i>
LOGUNIFORM 0.166	16.6	kdm (3)	FLOWMOD	Cm K <sub>d</sub> [m <sup>3</sup> /kg] (Calico Hills, zeolitic)	Codell <i>et al.</i> (1992) (+/- one order of magnitude of the mean of log of retardation factors from IPA Phase 1)
LOGUNIFORM 0.116	11.6	kdm (4)	FLOWMOD	Cm K <sub>d</sub> [m <sup>3</sup> /kg] (Prow Pass)	Codell <i>et al.</i> (1992) (+/- one order of magnitude of the mean of log of retardation factors from IPA Phase 1)
LOGUNIFORM 0.132	13.2	kdm (5)	FLOWMOD	Cm K <sub>d</sub> [m <sup>3</sup> /kg] (Upper Crater Flat)	Codell <i>et al.</i> (1992) (+/- one order of magnitude of the mean of log of retardation factors from IPA Phase 1)
LOGUNIFORM 0.12	12.0	kdm (6)	FLOWMOD	Cm K <sub>d</sub> [m <sup>3</sup> /kg] (Bullfrog)	Codell <i>et al.</i> (1992) (+/- one order of magnitude of the mean of log of retardation factors from IPA Phase 1)
LOGUNIFORM 0.132	13.2	kdm (7)	FLOWMOD	Cm K <sub>d</sub> [m <sup>3</sup> /kg] (Middle Crater Flat)	Codell <i>et al.</i> (1992) (+/- one order of magnitude of the mean of log of retardation factors from IPA Phase 1)
LOGUNIFORM 2.0E-5	2.0E-3	kdm (15)	FLOWMOD	U K <sub>d</sub> [m <sup>3</sup> /kg] (Topopah Spring)	Meijer (1990) (+/- one order of magnitude of log mean of reported values—Wells UE25a1, G3, and J13)
LOGUNIFORM 0.002	0.2	kdm (16)	FLOWMOD	U K <sub>d</sub> [m <sup>3</sup> /kg] (Calico Hills, vitric)	Meijer (1990) (+/- one order of magnitude of the reported value—Well G3)
LOGUNIFORM 0.0001	0.01	kdm (17)	FLOWMOD	U K <sub>d</sub> [m <sup>3</sup> /kg] (Calico Hills, zeolitic)	Meijer (1990) (+/- one order of magnitude of log mean of reported values—Wells G1 and G2)
CONSTANT 0.0		kdm (18)	FLOWMOD	U K <sub>d</sub> [m <sup>3</sup> /kg] (Prow Pass)	Assumed to be zero
LOGUNIFORM 8.0E-5	8.0E-3	kdm (19)	FLOWMOD	U K <sub>d</sub> [m <sup>3</sup> /kg] (Upper Crater Flat)	Same retardation factor as Calico Hills zeolitic (allowances made for density and porosity)

Appendix A

<i>Type of Distribution Value (or Range in Value)</i>	<i>Parameter Name</i>	<i>Module</i>	<i>Parameter Description</i>	<i>Basis for Parameter Assignment</i>
LOGUNIFORM 0.0002      0.02	kdm (20)	FLOWMOD	U $K_d$ [ $m^3/kg$ ] (Bullfrog)	Meijer (1990) (+/- one order of magnitude of log mean of reported values—Wells G1, J13, and UE25a1)
LOGUNIFORM 8.0E-5      8.0E-3	kdm (21)	FLOWMOD	U $K_d$ [ $m^3/kg$ ] (Middle Crater Flat)	Same retardation factor as Calico Hills zeolitic (allowances made for density and porosity)
LOGUNIFORM 0.081      8.1	kdm (22)	FLOWMOD	Am $K_d$ [ $m^3/kg$ ] (Topopah Spring)	Meijer (1990) (+/- one order of magnitude of log mean of reported values—Wells J13, G3, and UE25a1)
LOGUNIFORM 0.081      8.1	kdm (23)	FLOWMOD	Am $K_d$ [ $m^3/kg$ ] (Calico Hills, vitric)	Assumed same $K_d$ as Topopah Spring
LOGUNIFORM 0.17      17.0	kdm (24)	FLOWMOD	Am $K_d$ [ $m^3/kg$ ] (Calico Hills, zeolitic)	Meijer (1990) (+/- one order of magnitude of the reported value—Well G2)
LOGUNIFORM 0.45      45.0	kdm (25)	FLOWMOD	Am $K_d$ [ $m^3/kg$ ] (Prow Pass)	Meijer (1990) (+/- one order of magnitude of log mean of reported values—Wells G1 and UE25a1)
LOGUNIFORM 0.136      13.6	kdm (26)	FLOWMOD	Am $K_d$ [ $m^3/kg$ ] (Upper Crater Flat)	Same retardation factor as Calico Hills zeolitic (allowances made for density and porosity)
LOGUNIFORM 0.014      1.4	kdm (27)	FLOWMOD	Am $K_d$ [ $m^3/kg$ ] (Bullfrog)	Meijer (1990) (+/- one order of magnitude of log mean of reported values—Wells J13 and UE25a1)
LOGUNIFORM 0.136      13.6	kdm (28)	FLOWMOD	Am $K_d$ [ $m^3/kg$ ] (Middle Crater Flat)	Same retardation factor as Calico Hills zeolitic (allowances made for density and porosity)
LOGUNIFORM 0.00045      0.045	kdm (29)	FLOWMOD	Np $K_d$ [ $m^3/kg$ ] (Topopah Spring)	Meijer (1990) (+/- one order of magnitude of log mean of reported values—Wells G3 and UE25a1)

<i>Type of Distribution Value (or Range in Value)</i>	<i>Parameter Name</i>	<i>Module</i>	<i>Parameter Description</i>	<i>Basis for Parameter Assignment</i>
LOGUNIFORM 0.00045      0.045	kdm (30)	FLOWMOD	Np K <sub>d</sub> [m <sup>3</sup> /kg] (Calico Hills, vitric)	Assumed same K <sub>d</sub> as Topopah Spring
LOGUNIFORM 0.00027      0.027	kdm (31)	FLOWMOD	Np K <sub>d</sub> [m <sup>3</sup> /kg] (Calico Hills, zeolitic)	Meijer (1990) (+/- one order of magnitude of the reported value—Well G2)
LOGUNIFORM 0.00051      0.051	kdm (32)	FLOWMOD	Np K <sub>d</sub> [m <sup>3</sup> /kg] (Prow Pass)	Meijer (1990) (+/- one order of magnitude of log mean of reported values—Wells G1 and UE25a1)
LOGUNIFORM 0.00022      0.022	kdm (33)	FLOWMOD	Np K <sub>d</sub> [m <sup>3</sup> /kg] (Upper Crater Flat)	Same retardation factor as Calico Hills zeolitic (allowances made for density and porosity)
LOGUNIFORM 0.00051      0.051	kdm (34)	FLOWMOD	Np K <sub>d</sub> [m <sup>3</sup> /kg] (Bullfrog)	Assumed same K <sub>d</sub> as Prow Pass
LOGUNIFORM 0.00022      0.022	kdm (35)	FLOWMOD	Np K <sub>d</sub> [m <sup>3</sup> /kg] (Middle Crater Flat)	Same retardation factor as Calico Hills zeolitic (allowances made for density and porosity)
LOGUNIFORM 0.017          1.7	kdm (8)	FLOWMOD	Pu K <sub>d</sub> [m <sup>3</sup> /kg] (Topopah Spring)	Meijer (1990) (+/- one order of magnitude of log mean of reported values—Wells G3, J13, and UE25a1)
LOGUNIFORM 0.017          1.7	kdm (9)	FLOWMOD	Pu K <sub>d</sub> [m <sup>3</sup> /kg] (Calico Hills, vitric)	Assumed same K <sub>d</sub> as Topopah Spring
LOGUNIFORM 0.0066        0.66	kdm (10)	FLOWMOD	Pu K <sub>d</sub> [m <sup>3</sup> /kg] (Calico Hills, zeolitic)	Meijer (1990) (+/- one order of magnitude of the reported value—Well G2)
LOGUNIFORM 0.013          1.3	kdm (11)	FLOWMOD	Pu K <sub>d</sub> [m <sup>3</sup> /kg] (Prow Pass)	Meijer (1990) (+/- one order of magnitude of log mean of reported values—Wells G1 and UE25a1)
LOGUNIFORM 0.0053        0.53	kdm (12)	FLOWMOD	Pu K <sub>d</sub> [m <sup>3</sup> /kg] (Upper Crater Flat)	Same retardation factor as Calico Hills zeolitic (allowances made for density and porosity)

Appendix A

Type of Distribution Value (or Range in Value)		Parameter Name	Module	Parameter Description	Basis for Parameter Assignment
LOGUNIFORM 0.0094	0.94	kdm (13)	FLOWMOD	Pu $K_d$ [ $m^3/kg$ ] (Bullfrog)	Meijer (1990) (+/- one order of magnitude of log mean of reported values—Wells J13 and UE25a1)
LOGUNIFORM 0.0053	0.53	kdm (14)	FLOWMOD	Pu $K_d$ [ $m^3/kg$ ] (Middle Crater Flat)	same retardation factor as Calico Hills zeolitic (allowances made for density and porosity)
LOGUNIFORM 0.0048	0.48	kdm (36)	FLOWMOD	Th $K_d$ [ $m^3/kg$ ] (Topopah Spring)	Codell <i>et al.</i> (1992) (+/- one order of magnitude of mean of log of retardation factors from IPA Phase 1)
LOGUNIFORM 0.034	3.4	kdm (37)	FLOWMOD	Th $K_d$ [ $m^3/kg$ ] (Calico Hills, vitric)	Codell <i>et al.</i> (1992) (+/- one order of magnitude of the mean of log of retardation factors from IPA Phase 1)
LOGUNIFORM 0.017	1.7	kdm (38)	FLOWMOD	Th $K_d$ [ $m^3/kg$ ] (Calico Hills, zeolitic)	Codell <i>et al.</i> (1992) (+/- one order of magnitude of the mean of log of retardation factors from IPA Phase 1)
LOGUNIFORM 0.012	1.2	kdm (39)	FLOWMOD	Th $K_d$ [ $m^3/kg$ ] (Prow Pass)	Codell <i>et al.</i> (1992) (+/- one order of magnitude of the mean of log of retardation factors from IPA Phase 1)
LOGUNIFORM 0.014	1.4	kdm (40)	FLOWMOD	Th $K_d$ [ $m^3/kg$ ] (Upper Crater Flat)	Codell <i>et al.</i> (1992) (+/- one order of magnitude of the mean of log of retardation factors from IPA Phase 1)
LOGUNIFORM 0.013	1.3	kdm(41)	FLOWMOD	Th $K_d$ [ $m^3/kg$ ] (Bullfrog)	Codell <i>et al.</i> (1992) (+/- one order of magnitude of the mean of log of retardation factors from IPA Phase 1)
LOGUNIFORM 0.014	1.4	kdm(42)	FLOWMOD	Th $K_d$ [ $m^3/kg$ ] (Middle Crater Flat)	Codell <i>et al.</i> (1992) (+/- one order of magnitude of the mean of log of retardation factors from IPA Phase 1)
LOGUNIFORM 0.1 <sup>c</sup>	15.0	kdm (43)	FLOWMOD	Ra $K_d$ [ $m^3/kg$ ] (Topopah Spring)	Meijer (1990) (+/- one order of magnitude of the reported value— Well G1)

Type of Distribution Value (or Range in Value)		Parameter Name	Module	Parameter Description	Basis for Parameter Assignment
LOGUNIFORM 0.15	15.0	kdm (44)	FLOWMOD	Ra $K_d$ [ $m^3/kg$ ] (Calico Hills, vitric)	Assumed same $K_d$ as Topopah Spring
LOGUNIFORM 0.15	15.0	kdm (45)	FLOWMOD	Ra $K_d$ [ $m^3/kg$ ] (Calico Hills, zeolitic)	Assumed same $K_d$ as Topopah Spring
LOGUNIFORM 0.15	15.0	kdm(46)	FLOWMOD	Ra $K_d$ [ $m^3/kg$ ] (Prow Pass)	Assumed same $K_d$ as Topopah Spring
LOGUNIFORM 0.12	12.0	kdm (47)	FLOWMOD	Ra $K_d$ [ $m^3/kg$ ] (Upper Crater Flat)	Same retardation factor as Calico Hills zeolitic (allowances made for density and porosity)
LOGUNIFORM 0.5	50.0	kdm (48)	FLOWMOD	Ra $K_d$ [ $m^3/kg$ ] (Bullfrog)	Meijer (1990) (+/- one order of magnitude of log mean of reported values—Well G1)
LOGUNIFORM 0.12	12.0	kdm (49)	FLOWMOD	Ra $K_d$ [ $m^3/kg$ ] (Middle Crater Flat)	Same retardation factor as Calico Hills zeolitic (allowances made for density and porosity)
LOGUNIFORM 0.00068	0.068	kdm (50)	FLOWMOD	Pb $K_d$ [ $m^3/kg$ ] (Topopah Spring)	Codell <i>et al.</i> (1992) (+/- one order of magnitude of the mean of log of retardation factors from IPA Phase 1)
LOGUNIFORM 0.0049	0.49	kdm (51)	FLOWMOD	Pb $K_d$ [ $m^3/kg$ ] (Calico Hills, vitric)	Codell <i>et al.</i> (1992) (+/- one order of magnitude of the mean of log of retardation factors from IPA Phase 1)
LOGUNIFORM 0.0025	0.25	kdm (52)	FLOWMOD	Pb $K_d$ [ $m^3/kg$ ] (Calico Hills, zeolitic)	Codell <i>et al.</i> (1992) (+/- one order of magnitude of the mean of log of retardation factors from IPA Phase 1)
LOGUNIFORM 0.0017	0.17	kdm (53)	FLOWMOD	Pb $K_d$ [ $m^3/kg$ ] (Prow Pass)	Codell <i>et al.</i> (1992) (+/- one order of magnitude of the mean of log of retardation factors from IPA Phase 1)
LOGUNIFORM 0.0020	0.20	kdm (54)	FLOWMOD	Pb $K_d$ [ $m^3/kg$ ] (Upper Crater Flat)	Codell <i>et al.</i> (1992) (+/- one order of magnitude of the mean of log of retardation factors from IPA Phase 1)

Appendix A

<i>Type of Distribution Value (or Range in Value)</i>	<i>Parameter Name</i>	<i>Module</i>	<i>Parameter Description</i>	<i>Basis for Parameter Assignment</i>
LOGUNIFORM 0.0018      0.18	kdm (55)	FLOWMOD	Pb $K_d$ [ $m^3/kg$ ] (Bullfrog)	Codell <i>et al.</i> (1992) (+/- one order of magnitude of the mean of log of retardation factors from IPA Phase 1)
LOGUNIFORM 0.0020      0.20	kdm (56)	FLOWMOD	Pb $K_d$ [ $m^3/kg$ ] (Middle Crater Flat)	Codell <i>et al.</i> (1992) (+/- one order of magnitude of the mean of log of retardation factors from IPA Phase 1)
LOGUNIFORM 0.036      3.6	kdm (57)	FLOWMOD	Cs $K_d$ [ $m^3/kg$ ] (Topopah Spring)	Meijer (1990) (+/- one order of magnitude of log mean of reported values—Wells G1, G3, and UE25a1)
LOGUNIFORM 0.024      2.4	kdm (58)	FLOWMOD	Cs $K_d$ [ $m^3/kg$ ] (Calico Hills, vitric)	Meijer (1990) (+/- one order of magnitude of log mean of reported values in Topopah Spring unit—Well G3)
LOGUNIFORM 2.2      220.	kdm (59)	FLOWMOD	Cs $K_d$ [ $m^3/kg$ ] (Calico Hills, zeolitic)	Meijer (1990) (+/- one order of magnitude of log mean of reported values—Wells G1 and G2)
LOGUNIFORM 0.22      22.0	kdm (60)	FLOWMOD	Cs $K_d$ [ $m^3/kg$ ] (Prow Pass)	Meijer (1990) (+/- one order of magnitude of log mean of reported values—Wells G1, J13, and UE25a1)
LOGUNIFORM 1.76      176.0	kdm (61)	FLOWMOD	Cs $K_d$ [ $m^3/kg$ ] (Upper Crater Flat)	Same retardation factor as Calico Hills zeolitic (allowances made for density and porosity)
LOGUNIFORM 0.32      32.0	kdm (62)	FLOWMOD	Cs $K_d$ [ $m^3/kg$ ] (Bullfrog)	Meijer (1990) (+/- one order of magnitude of log mean of reported values—Wells G1, J13, and UE25a1)
LOGUNIFORM 1.76      176.0	kdm (63)	FLOWMOD	Cs $K_d$ [ $m^3/kg$ ] (Middle Crater Flat)	Same retardation factor as Calico Hills zeolitic (allowances made for density and porosity)
CONSTANT 0.0	kdm (64)	FLOWMOD	I $K_d$ [ $m^3/kg$ ] (Topopah Spring)	Assumed to be zero

<i>Type of Distribution Value (or Range in Value)</i>	<i>Parameter Name</i>	<i>Module</i>	<i>Parameter Description</i>	<i>Basis for Parameter Assignment</i>
CONSTANT 0.0	kdm (65)	FLOWMOD	I K <sub>d</sub> [m <sup>3</sup> /kg] (Calico Hills, vitric)	Assumed to be zero
CONSTANT 0.0	kdm (66)	FLOWMOD	I K <sub>d</sub> [m <sup>3</sup> /kg] (Calico Hills, zeolitic)	Assumed to be zero
CONSTANT 0.0	kdm(67)	FLOWMOD	I K <sub>d</sub> [m <sup>3</sup> /kg] (Prow Pass)	Assumed to be zero
CONSTANT 0.0	kdm(68)	FLOWMOD	I K <sub>d</sub> [m <sup>3</sup> /kg] (Upper Crater Flat)	Assumed to be zero
CONSTANT 0.0	kdm (69)	FLOWMOD	I K <sub>d</sub> [m <sup>3</sup> /kg] (Bullfrog)	Assumed to be zero
CONSTANT 0.0	kdm (70)	FLOWMOD	I K <sub>d</sub> [m <sup>3</sup> /kg] (Middle Crater Flat)	Assumed to be zero
LOGUNIFORM 1.0E-6	1.0E-4 kdm (78)	FLOWMOD	Tc K <sub>d</sub> [m <sup>3</sup> /kg] (Topopah Spring)	Meijer (1990) (+/- one order of magnitude of log mean of reported values—Wells G3 and UE25a1)
CONSTANT 0.0	kdm (79)	FLOWMOD	Tc K <sub>d</sub> [m <sup>3</sup> /kg] (Calico Hills, vitric)	Assumed to be zero
CONSTANT 0.0	kdm (80)	FLOWMOD	Tc K <sub>d</sub> [m <sup>3</sup> /kg] (Calico Hills, zeolitic)	Assumed to be zero
LOGUNIFORM 1.7E-5	1.7E-3 kdm (81)	FLOWMOD	Tc K <sub>d</sub> [m <sup>3</sup> /kg] (Prow Pass)	Meijer (1990) (+/- one order of magnitude of log mean of reported values—Well J13)
CONSTANT 0.0	kdm (82)	FLOWMOD	Tc K <sub>d</sub> [m <sup>3</sup> /kg] (Upper Crater Flat)	Same retardation factor as Calico Hills zeolitic
LOGUNIFORM 0.00042	0.042 kdm (83)	FLOWMOD	Tc K <sub>d</sub> [m <sup>3</sup> /kg] (Bullfrog)	Meijer (1990) (+/- one order of magnitude of the reported value—Well UE25a1)
CONSTANT 0.0	kdm (84)	FLOWMOD	Tc K <sub>d</sub> [m <sup>3</sup> /kg] (Middle Crater Flat)	Same retardation factor as Calico Hills zeolitic

Appendix A

Type of Distribution Value (or Range in Value)		Parameter Name	Module	Parameter Description	Basis for Parameter Assignment
LOGUNIFORM 0.00037	0.037	kdm (99)	FLOWMOD	Ni $K_d$ [ $m^3/kg$ ] (Topopah Spring)	Codell <i>et al.</i> (1992) (+/- one order of magnitude of the mean of log of retardation factors from IPA Phase 1)
LOGUNIFORM 0.0027	0.27	kdm (100)	FLOWMOD	Ni $K_d$ [ $m^3/kg$ ] (Calico Hills, vitric)	Codell <i>et al.</i> (1992) (+/- one order of magnitude of the mean of log of retardation factors from IPA Phase 1)
LOGUNIFORM 0.0014	0.14	kdm (101)	FLOWMOD	Ni $K_d$ [ $m^3/kg$ ] (Calico Hills, zeolitic)	Codell <i>et al.</i> (1992) (+/- one order of magnitude of the mean of log of retardation factors from IPA Phase 1)
LOGUNIFORM 0.0009	0.09	kdm (102)	FLOWMOD	Ni $K_d$ [ $m^3/kg$ ] (Prow Pass)	Codell <i>et al.</i> (1992) (+/- one order of magnitude of the mean of log of retardation factors from IPA Phase 1)
LOGUNIFORM 0.0011	0.11	kdm (103)	FLOWMOD	Ni $K_d$ [ $m^3/kg$ ] (Upper Crater Flat)	Codell <i>et al.</i> (1992) (+/- one order of magnitude of the mean of log of retardation factors from IPA Phase 1)
LOGUNIFORM 0.001	0.1	kdm (104)	FLOWMOD	Ni $K_d$ [ $m^3/kg$ ] (Bullfrog)	Codell <i>et al.</i> (1992) (+/- one order of magnitude of the mean of log of retardation factors from IPA Phase 1)
LOGUNIFORM 0.0011	0.11	kdm (105)	FLOWMOD	Ni $K_d$ [ $m^3/kg$ ] (Middle Crater Flat)	Codell <i>et al.</i> (1992) (+/- one order of magnitude of the mean of log of retardation factors from IPA Phase 1)
CONSTANT 0.0		kdm (106)	FLOWMOD	C $K_d$ [ $m^3/kg$ ] (Topopah Spring)	Assumed to be zero
CONSTANT 0.0		kdm (107)	FLOWMOD	C $K_d$ [ $m^3/kg$ ] (Calico Hills, vitric)	Assumed to be zero
CONSTANT 0.0		kdm (108)	FLOWMOD	C $K_d$ [ $m^3/kg$ ] (Calico Hills, zeolitic)	Assumed to be zero
CONSTANT 0.0		kdm (109)	FLOWMOD	C $K_d$ [ $m^3/kg$ ] (Prow Pass)	Assumed to be zero

<i>Type of Distribution Value (or Range in Value)</i>	<i>Parameter Name</i>	<i>Module</i>	<i>Parameter Description</i>	<i>Basis for Parameter Assignment</i>
CONSTANT 0.0	kdm (110)	FLOWMOD	C $K_d$ [ $m^3/kg$ ] (Upper Crater Flat)	Assumed to be zero
CONSTANT 0.0	kdm (111)	FLOWMOD	C $K_d$ [ $m^3/kg$ ] (Bullfrog)	Assumed to be zero
CONSTANT 0.0	kdm (112)	FLOWMOD	C $K_d$ [ $m^3/kg$ ] (Middle Crater Flat)	Assumed to be zero
LOGUNIFORM 0.00026      0.026	kdm (113)	FLOWMOD	Se $K_d$ [ $m^3/kg$ ] (Topopah Spring)	Meijer (1990) (+/- one order of magnitude of log mean of reported values—Well G3)
LOGUNIFORM 0.0003      0.03	kdm (114)	FLOWMOD	Se $K_d$ [ $m^3/kg$ ] (Calico Hills, vitric)	Meijer (1990) (+/- one order of magnitude of the reported value—Well G3)
LOGUNIFORM 0.00045      0.045	kdm (115)	FLOWMOD	Se $K_d$ [ $m^3/kg$ ] (Calico Hills, zeolitic)	Meijer (1990) (+/- one order of magnitude of log mean of reported values—Wells G1 and G2)
LOGUNIFORM 0.00025      0.025	kdm (116)	FLOWMOD	Se $K_d$ [ $m^3/kg$ ] (Prow Pass)	Meijer (1990) (+/- one order of magnitude of the reported value—Well G1)
LOGUNIFORM 0.00036      0.036	kdm (117)	FLOWMOD	Se $K_d$ [ $m^3/kg$ ] (Upper Crater Flat)	Same retardation factor as Calico Hills zeolitic (allowances made for density and porosity)
LOGUNIFORM 0.0013      0.13	kdm (118)	FLOWMOD	Se $K_d$ [ $m^3/kg$ ] (Bullfrog)	Meijer (1990) (+/- one order of magnitude of log mean of reported values—Well G1)
LOGUNIFORM 0.00036      0.036	kdm (119)	FLOWMOD	Se $K_d$ [ $m^3/kg$ ] (Middle Crater Flat)	Same retardation factor as Calico Hills zeolitic (allowances made for density and porosity)
CONSTANT 0.0	kdm (120)	FLOWMOD	Nb $K_d$ [ $m^3/kg$ ] (Topopah Spring)	Assumed to be zero
CONSTANT 0.0	kdm (121)	FLOWMOD	Nb $K_d$ [ $m^3/kg$ ] (Calico Hills, vitric)	Assumed to be zero

Appendix A

<i>Type of Distribution Value (or Range in Value)</i>	<i>Parameter Name</i>	<i>Module</i>	<i>Parameter Description</i>	<i>Basis for Parameter Assignment</i>
CONSTANT 0.0	kdm (122)	FLOWMOD	Nb $K_d$ [ $m^3/kg$ ] (Calico Hills, zeolitic)	Assumed to be zero
CONSTANT 0.0	kdm (123)	FLOWMOD	Nb $K_d$ [ $m^3/kg$ ] (Prow Pass)	Assumed to be zero
CONSTANT 0.0	kdm (124)	FLOWMOD	Nb $K_d$ [ $m^3/kg$ ] (Upper Crater Flat)	Assumed to be zero
CONSTANT 0.0	kdm (125)	FLOWMOD	Nb $K_d$ [ $m^3/kg$ ] (Bullfrog)	Assumed to be zero
CONSTANT 0.0	kdm (126)	FLOWMOD	Nb $K_d$ [ $m^3/kg$ ] (Middle Crater Flat)	Assumed to be zero
LOGUNIFORM 0.0134      1.34	kdm (71)	FLOWMOD	Sn $K_d$ [ $m^3/kg$ ] (Topopah Spring)	Codell <i>et al.</i> (1992) (+/- one order of magnitude of the mean of log of retardation factors from IPA Phase 1)
LOGUNIFORM 0.097      9.7	kdm (72)	FLOWMOD	Sn $K_d$ [ $m^3/kg$ ] (Calico Hills, vitric)	Codell <i>et al.</i> (1992) (+/- one order of magnitude of the mean of log of retardation factors from IPA Phase 1)
LOGUNIFORM 0.049      4.9	kdm (73)	FLOWMOD	Sn $K_d$ [ $m^3/kg$ ] (Calico Hills, zeolitic)	Codell <i>et al.</i> (1992) (+/- one order of magnitude of the mean of log of retardation factors from IPA Phase 1)
LOGUNIFORM 0.034      3.4	kdm (74)	FLOWMOD	Sn $K_d$ [ $m^3/kg$ ] (Prow Pass)	Codell <i>et al.</i> (1992) (+/- one order of magnitude of the mean of log of retardation factors from IPA Phase 1)
LOGUNIFORM 0.039      3.9	kdm (75)	FLOWMOD	Sn $K_d$ [ $m^3/kg$ ] (Upper Crater Flat)	Codell <i>et al.</i> (1992) (+/- one order of magnitude of the mean of log of retardation factors from IPA Phase 1)
LOGUNIFORM 0.035      3.5	kdm (76)	FLOWMOD	Sn $K_d$ [ $m^3/kg$ ] (Bullfrog)	Codell <i>et al.</i> (1992) (+/- one order of magnitude of the mean of log of retardation factors from IPA Phase 1)

<i>Type of Distribution Value (or Range in Value)</i>	<i>Parameter Name</i>	<i>Module</i>	<i>Parameter Description</i>	<i>Basis for Parameter Assignment</i>
LOGUNIFORM 0.039            3.9	kdm (77)	FLOWMOD	Sn $K_d$ [ $m^3/kg$ ] (Middle Crater Flat)	Codell <i>et al.</i> (1992) (+/- one order of magnitude of the mean of log of retardation factors from IPA Phase 1)
LOGUNIFORM 0.00048        0.048	kdm (85)	FLOWMOD	Zr $K_d$ [ $m^3/kg$ ] (Topopah Spring)	Codell <i>et al.</i> (1992) (+/- one order of magnitude of the mean of log of retardation factors from IPA Phase 1)
LOGUNIFORM 0.0034         0.34	kdm (86)	FLOWMOD	Zr $K_d$ [ $m^3/kg$ ] (Calico Hills, vitric)	Codell <i>et al.</i> (1992) (+/- one order of magnitude of the mean of log of retardation factors from IPA Phase 1)
LOGUNIFORM 0.0017         0.17	kdm (87)	FLOWMOD	Zr $K_d$ [ $m^3/kg$ ] (Calico Hills, zeolitic)	Codell <i>et al.</i> (1992) (+/- one order of magnitude of the mean of log of retardation factors from IPA Phase 1)
LOGUNIFORM 0.0012         0.12	kdm (88)	FLOWMOD	Zr $K_d$ [ $m^3/kg$ ] (Prow Pass)	Codell <i>et al.</i> (1992) (+/- one order of magnitude of the mean of log of retardation factors from IPA Phase 1)
LOGUNIFORM 0.0014         0.14	kdm (89)	FLOWMOD	Zr $K_d$ [ $m^3/kg$ ] (Upper Crater Flat)	Codell <i>et al.</i> (1992) (+/- one order of magnitude of the mean of log of retardation factors from IPA Phase 1)
LOGUNIFORM 0.0013         0.13	kdm (90)	FLOWMOD	Zr $K_d$ [ $m^3/kg$ ] (Bullfrog)	Codell <i>et al.</i> (1992) (+/- one order of magnitude of the mean of log of retardation factors from IPA Phase 1)
LOGUNIFORM 0.0014         0.14	kdm (91)	FLOWMOD	Zr $K_d$ [ $m^3/kg$ ] (Middle Crater Flat)	Codell <i>et al.</i> (1992) (+/- one order of magnitude of the mean of log of retardation factors from IPA Phase 1)
LOGUNIFORM 0.008           0.8	kdm (92)	FLOWMOD	Sr $K_d$ [ $m^3/kg$ ] (Topopah Spring)	Meijer (1990) (+/- one order of magnitude of log mean of reported values—Wells G1, G3, and UE25a1)
LOGUNIFORM 0.0034         0.34	kdm (93)	FLOWMOD	Sr $K_d$ [ $m^3/kg$ ] (Calico Hills, vitric)	Meijer (1990) (+/- one order of magnitude of log mean of reported values in Topopah Spring unit—Well G3)

Appendix A

<i>Type of Distribution Value (or Range in Value)</i>		<i>Parameter Name</i>	<i>Module</i>	<i>Parameter Description</i>	<i>Basis for Parameter Assignment</i>
LOGUNIFORM 0.89	89.0	kdm (94)	FLOWMOD	Sr $K_d$ [ $m^3/kg$ ] (Calico Hills, zeolitic)	Meijer (1990) (+/- one order of magnitude of log mean of reported values—Wells G1 and G2)
LOGUNIFORM 0.045	4.5	kdm (95)	FLOWMOD	Sr $K_d$ [ $m^3/kg$ ] (Prow Pass)	Meijer (1990) (+/- one order of magnitude of log mean of reported values—Wells G1, J13, and UE25a1)
LOGUNIFORM 0.71	71.0	kdm (96)	FLOWMOD	Sr $K_d$ [ $m^3/kg$ ] (Upper Crater Flat)	Same retardation factor as Calico Hills zeolitic (allowances made for density and porosity)
LOGUNIFORM 0.028	2.8	kdm (97)	FLOWMOD	Sr $K_d$ [ $m^3/kg$ ] (Bullfrog)	Meijer (1990) (+/- one order of magnitude of log mean of reported values—Wells G1, J13, and UE25a1)
LOGUNIFORM 0.71	71.0	kdm (98)	FLOWMOD	Sr $K_d$ [ $m^3/kg$ ] (Middle Crater Flat)	Same retardation factor as Calico Hills zeolitic (allowances made for density and porosity)
UNIFORM 3.75E4	3.75E5	areao	FLOWMOD	area of discharge [ $m^2$ ]	Production zone thicknesses from field determinations (see Table 4-9)
UNIFORM 100.	150.	ecorr(1)	SOTEC	baseline corrosion potential [mV]	Estimate based on Macdonald and Urquidi-Macdonald (1990)
UNIFORM -2.	-0.5	ecorr(2)	SOTEC	factor for temperature effect [ ]	Estimate based on Macdonald and Urquidi-Macdonald (1990)
UNIFORM -3.40	-3.	ecorr(3)	SOTEC	factor for temperature effect on ambient potential [ ]	Estimate based on Macdonald and Urquidi-Macdonald (1990)
UNIFORM 100.	300.	ecorr(4)	SOTEC	factor for radiolysis effect [ ]	Estimate based on Macdonald and Urquidi-Macdonald (1990)
UNIFORM 0.001	0.023	ecorr(5)	SOTEC	decay rate for gamma emitters [ $yr^{-1}$ ]	Upper limit based on $^{137}Cs$

<i>Type of Distribution Value (or Range in Value)</i>		<i>Parameter Name</i>	<i>Module</i>	<i>Parameter Description</i>	<i>Basis for Parameter Assignment</i>
UNIFORM 1000.	1500.	ecorr(6)	SOTEC	crevice corrosion potential [mV]	Estimate based on Watson and Postlethwaite (1990)
UNIFORM 1000.	1500.	ecorr(7)	SOTEC	pitting corrosion potential [mV]	Estimate based on Henshall (1991)
LOGUNIFORM 1.E-5	0.001	ecorr(8)	SOTEC	rate for localized corrosion [m/yr]	Assumed
CONSTANT 1.E-7		carbon(1)	SOTEC	thickness of zirconium oxide [m]	Estimate based on Smith and Baldwin (1989)
CONSTANT 1.E-5		carbon(2)	SOTEC	initial radius of UO <sub>2</sub> grain [m]	Estimate based on Einziger and Buchanan (1988)
CONSTANT 1.786E-2		carbon(3)	SOTEC	O <sub>2</sub> concentration outside of particle [kg-mole/m <sup>3</sup> ]	Atmospheric concentration value
CONSTANT 37.		carbon(4)	SOTEC	density of UO <sub>2</sub> [Kg-mole/m <sup>3</sup> ]	Assumed
CONSTANT 5.256E-8		carbon(5)	SOTEC	reference diffusion, inner layer [m <sup>2</sup> /yr]	Fitted value from empirical model presented in Section 5.6.3
CONSTANT 3.942E-7		carbon(6)	SOTEC	reference diffusion, outer layer [m <sup>2</sup> /yr]	Fitted value from empirical model presented in Section 5.6.3
CONSTANT 32.		carbon(7)	SOTEC	activation energy [Kcal/g-mole]	Fitted value from empirical model presented in Section 5.6.3
CONSTANT 473.		carbon(8)	SOTEC	reference temperature [°K]	Assumed
CONSTANT 3.		carbon(9)	SOTEC	moles of UO <sub>2</sub> per mole of O <sub>2</sub> [ ]	Based on stoichiometry assuming U <sub>3</sub> O <sub>8</sub> product
CONSTANT 0.001		carbon(10)	SOTEC	radius of UO <sub>2</sub> fragment [m]	See Einziger and Buchanan (1988)

Appendix A

<i>Type of Distribution Value (or Range in Value)</i>	<i>Parameter Name</i>	<i>Module</i>	<i>Parameter Description</i>	<i>Basis for Parameter Assignment</i>
CONSTANT 6.1E-4	carbon(11)	SOTEC	thickness of cladding [m]	See Smith and Baldwin (1989)
CONSTANT 7.2E-4	carbon(12)	SOTEC	curies <sup>14</sup> C/kg in UO <sub>2</sub> [Ci/kg]	See Park (1992)
CONSTANT 4.89E-4	carbon(13)	SOTEC	curies <sup>14</sup> C/kg in cladding [Ci/kg]	See Park (1992)
CONSTANT 2.48E-5	carbon(14)	SOTEC	curies <sup>14</sup> C/kg in ZrO <sub>2</sub> [Ci/kg]	See Park (1992)
CONSTANT 6.2E-6	carbon(15)	SOTEC	curies <sup>14</sup> C/kg in grain and gap [Ci/kg]	See Park (1992)
LOGUNIFORM 1.0E-5      1.0E-3	forwar(1)	SOTEC	UO <sub>2</sub> alteration rate [1/yr] (repository sub-area No. 1)	Estimate based on Grambow (1989)
LOGUNIFORM 1.0E-5      1.0E-3	forwar(2)	SOTEC	UO <sub>2</sub> alteration rate [1/yr] (repository sub-area No. 2)	Estimate based on Grambow (1989)
LOGUNIFORM 1.0E-5      1.0E-3	forwar(3)	SOTEC	UO <sub>2</sub> alteration rate [1/yr] (repository sub-area No. 3)	Estimate based on Grambow (1989)
LOGUNIFORM 1.0E-5      1.0E-3	forwar(4)	SOTEC	UO <sub>2</sub> alteration rate [1/yr] (repository sub-area No. 4)	Estimate based on Grambow (1989)
LOGUNIFORM 1.0E-5      1.0E-3	forwar(5)	SOTEC	UO <sub>2</sub> alteration rate [1/yr] (repository sub-area No. 5)	Estimate based on Grambow (1989)
LOGUNIFORM 1.0E-5      1.0E-3	forwar(6)	SOTEC	UO <sub>2</sub> alteration rate [1/yr] (repository sub-area No. 6)	Estimate based on Grambow (1989)
LOGUNIFORM 1.0E-5      1.0E-3	forwar(7)	SOTEC	UO <sub>2</sub> alteration rate [1/yr] (repository sub-area No. 7)	Estimate based on Grambow (1989)
UNIFORM 0.0      1.0	warea(1)	SOTEC	fraction of waste packages contacted [ ] (repository sub-area No. 1)	Assumed

<i>Type of Distribution Value (or Range in Value)</i>		<i>Parameter Name</i>	<i>Module</i>	<i>Parameter Description</i>	<i>Basis for Parameter Assignment</i>
UNIFORM 0.0	1.0	warea(2)	SOTEC	fraction of waste packages contacted [ ] (repository sub-area No. 2)	Assumed
UNIFORM 0.0	1.0	warea(3)	SOTEC	fraction of waste packages contacted [ ] (repository sub-area No. 3)	Assumed
UNIFORM 0.0	1.0	warea(4)	SOTEC	fraction of waste packages contacted [ ] (repository sub-area No. 4)	Assumed
UNIFORM 0.0	1.0	warea(5)	SOTEC	fraction of waste packages contacted [ ] (repository sub-area No. 5)	Assumed
UNIFORM 0.0	1.0	warea(6)	SOTEC	fraction of waste packages contacted [ ] (repository sub-area No. 6)	Assumed
UNIFORM 0.0	1.0	warea(7)	SOTEC	fraction of waste packages contacted [ ] (repository sub-area No. 7)	Assumed
UNIFORM 0.08	0.2	rpor(1,1)	SOTEC	porosity in near field [ ] (repository sub-area No. 1)	Assumed (based on crushed tuff)
UNIFORM 0.08	0.2	rpor(2,1)	SOTEC	porosity in near field [ ] (repository sub-area No. 2)	Assumed (based on crushed tuff)
UNIFORM 0.08	0.2	rpor(3,1)	SOTEC	porosity in near field [ ] (repository sub-area No. 3)	Assumed (based on crushed tuff)
UNIFORM 0.08	0.2	rpor(4,1)	SOTEC	porosity in near field [ ] (repository sub-area No. 4)	Assumed (based on crushed tuff)
UNIFORM 0.08	0.2	rpor(5,1)	SOTEC	porosity in near field [ ] (repository sub-area No. 5)	Assumed (based on crushed tuff)
UNIFORM 0.08	0.2	rpor(6,1)	SOTEC	porosity in near field [ ] (repository sub-area No. 6)	Assumed (based on crushed tuff)
UNIFORM 0.08	0.2	rpor(7,1)	SOTEC	porosity in near field [ ] (repository sub-area No. 7)	Assumed (based on crushed tuff)

Appendix A

<i>Type of Distribution Value (or Range in Value)</i>		<i>Parameter Name</i>	<i>Module</i>	<i>Parameter Description</i>	<i>Basis for Parameter Assignment</i>
LOGUNIFORM 5.7E-6	5.7E-3	rdiff(1,1)	SOTEC	diffusion coefficient in near field [m <sup>2</sup> /yr] (layer No. 1)	Assumed
LOGUNIFORM 5.7E-6	5.7E-3	rdiff(1,2)	SOTEC	diffusion coefficient in near field [m <sup>2</sup> /yr] (layer No. 2)	Assumed
LOGUNIFORM 5.7E-6	5.7E-4	rdiff(1,3)	SOTEC	diffusion coefficient in near field [m <sup>2</sup> /yr] (layer No. 3)	Assumed
LOGUNIFORM 5.7E-6	5.7E-4	rdiff(1,4)	SOTEC	diffusion coefficient in near field [m <sup>2</sup> /yr] (layer No. 4)	Assumed
UNIFORM 0.0	1.2	volmax(1)	SOTEC	max. vol. of water in waste package [m <sup>3</sup> ] (repository sub-area No. 1)	Upper limit based on volume of Site Characterization Plan (SCP) containers and fuel (see DOE, 1988a)
UNIFORM 0.0	1.2	volmax(2)	SOTEC	max. vol. of water in waste package [m <sup>3</sup> ] (repository sub-area No. 2)	Upper limit based on volume of SCP containers and fuel (see DOE, 1988a)
UNIFORM 0.0	1.2	volmax(3)	SOTEC	max. vol. of water in waste package [m <sup>3</sup> ] (repository sub-area No. 3)	Upper limit based on volume of SCP containers and fuel (see DOE, 1988a)
UNIFORM 0.0	1.2	volmax(4)	SOTEC	max. vol. of water in waste package [m <sup>3</sup> ] (repository sub-area No. 4)	Upper limit based on volume of SCP containers and fuel (see DOE, 1988a)
UNIFORM 0.0	1.2	volmax(5)	SOTEC	max. vol. of water in waste package [m <sup>3</sup> ] (repository sub-area No. 5)	Upper limit based on volume of SCP containers and fuel (see DOE, 1988a)
UNIFORM 0.0	1.2	volmax(6)	SOTEC	max. vol. of water in waste package [m <sup>3</sup> ] (repository sub-area No. 6)	Upper limit based on volume of SCP containers and fuel (see DOE, 1988a)
UNIFORM 0.0	1.2	volmax(7)	SOTEC	max. vol. of water in waste package [m <sup>3</sup> ] (repository sub-area No. 7)	Upper limit based on volume of SCP containers and fuel (see DOE, 1988a)
LOGNORMAL 2.3	131.2	rde(1)	SOTEC	Cm retardation coefficient [ ]	Assumed (based on crushed tuff)
LOGNORMAL 1.0 <sup>00</sup>	1.325	rde(3)	SOTEC	U retardation coefficient [ ]	Assumed (based on crushed tuff)

<i>Type of Distribution Value (or Range in Value)</i>	<i>Parameter Name</i>	<i>Module</i>	<i>Parameter Description</i>	<i>Basis for Parameter Assignment</i>
LOGNORMAL 2.79      165.4	rde(4)	SOTEC	Am retardation coefficient [ ]	Assumed (based on crushed tuff)
LOGNORMAL 1.008      1.81	rde(5)	SOTEC	Np retardation coefficient [ ]	Assumed (based on crushed tuff)
LOGNORMAL 1.3      33.6	rde(2)	SOTEC	Pu retardation coefficient [ ]	Assumed (based on crushed tuff)
LOGNORMAL 1.76      77.5	rde(6)	SOTEC	Th retardation coefficient [ ]	Assumed (based on crushed tuff)
LOGNORMAL 3.44      245.2	rde(7)	SOTEC	Ra retardation coefficient [ ]	Assumed (based on crushed tuff)
LOGNORMAL 1.39      40.07	rde(8)	SOTEC	Pb retardation coefficient [ ]	Assumed (based on crushed tuff)
LOGNORMAL 1.68      69.4	rde(9)	SOTEC	Cs retardation coefficient [ ]	Assumed (based on crushed tuff)
CONSTANT 1.0	rde(10)	SOTEC	I retardation coefficient [ ]	Assumed (based on crushed tuff)
LOGNORMAL 1.0002      1.016	rde(12)	SOTEC	Tc retardation coefficient [ ]	Assumed (based on crushed tuff)
LOGNORMAL 1.08      8.81	rde(15)	SOTEC	Ni retardation coefficient [ ]	Assumed (based on crushed tuff)
CONSTANT 1.0	rde(16)	SOTEC	C retardation coefficient [ ]	Assumed (based on crushed tuff)
LOGNORMAL 1.007      1.65	rde(17)	SOTEC	Se retardation coefficient [ ]	Assumed (based on crushed tuff)
CONSTANT 1.0	rde(18)	SOTEC	Nb retardation coefficient [ ]	Assumed (based on crushed tuff)

Appendix A

<i>Type of Distribution Value (or Range in Value)</i>	<i>Parameter Name</i>	<i>Module</i>	<i>Parameter Description</i>	<i>Basis for Parameter Assignment</i>
CONSTANT 1.23	rde(11)	SOTEC	Sn retardation coefficient [ ]	Assumed (based on crushed tuff)
CONSTANT 1.39	rde(13)	SOTEC	Zr retardation coefficient [ ]	Assumed (based on crushed tuff)
CONSTANT 1.19	rde(14)	SOTEC	Sr retardation coefficient [ ]	Assumed (based on crushed tuff)
LOGUNIFORM 2.56E-7      5.E-4	sol(1)	SOTEC	Cm solubility [kg/m <sup>3</sup> ]	Assumed
LOGUNIFORM 4.E-8      3.E-5	sol(3)	SOTEC	U solubility [kg/m <sup>3</sup> ]	Assumed
LOGUNIFORM 1.E-6      3.E-4	sol(4)	SOTEC	Am solubility [kg/m <sup>3</sup> ]	Assumed
LOGUNIFORM 1.4E-4      0.0237	sol(5)	SOTEC	Np solubility [kg/m <sup>3</sup> ]	Assumed
LOGUNIFORM 2.E-7      5.E-4	sol(2)	SOTEC	Pu solubility [kg/m <sup>3</sup> ]	Assumed
LOGUNIFORM 2.E-12      1.E-4	sol(6)	SOTEC	Th solubility [kg/m <sup>3</sup> ]	Assumed
LOGUNIFORM 9.E-6      9.E-5	sol(7)	SOTEC	Ra solubility [kg/m <sup>3</sup> ]	Assumed
LOGUNIFORM 2.1E-6      6.3E-4	sol(8)	SOTEC	Pb solubility [kg/m <sup>3</sup> ]	Assumed
CONSTANT 1.0	sol(9)	SOTEC	Cs solubility [kg/m <sup>3</sup> ]	Assumed
CONSTANT 1.0	sol(10)	SOTEC	I solubility [kg/m <sup>3</sup> ]	Assumed

<i>Type of Distribution Value (or Range in Value)</i>	<i>Parameter Name</i>	<i>Module</i>	<i>Parameter Description</i>	<i>Basis for Parameter Assignment</i>
CONSTANT 1.0	sol(12)	SOTEC	Tc solubility [kg/m <sup>3</sup> ]	Assumed
LOGUNIFORM 2.8E-7	1.7E-3 sol(15)	SOTEC	Ni solubility [kg/m <sup>3</sup> ]	Assumed
CONSTANT 1.0	sol(16)	SOTEC	C solubility [kg/m <sup>3</sup> ]	Assumed
CONSTANT 1.0	sol(17)	SOTEC	Se solubility [kg/m <sup>3</sup> ]	Assumed
CONSTANT 1.0	sol(18)	SOTEC	Nb solubility [kg/m <sup>3</sup> ]	Assumed
CONSTANT 5.E-9	sol(11)	SOTEC	Sn solubility [kg/m <sup>3</sup> ]	Assumed
CONSTANT 4.E-9	sol(13)	SOTEC	Zr solubility [kg/m <sup>3</sup> ]	Assumed
CONSTANT 8.E-2	sol(14)	SOTEC	Sr solubility [kg/m <sup>3</sup> ]	Assumed
UNIFORM 0.0	0.4 funnel(1)	SOTEC	fluid capture area of canister [m <sup>2</sup> ] (repository sub-area No. 1)	Upper limit based on twice the cross-sectional area of SCP emplacement hole (see DOE, 1988b)
UNIFORM 0.0	0.4 funnel(2)	SOTEC	fluid capture area of canister [m <sup>2</sup> ] (repository sub-area No. 2)	Upper limit based on twice the cross-sectional area of SCP emplacement hole (see DOE, 1988b)
UNIFORM 0.0	0.4 funnel(3)	SOTEC	fluid capture area of canister [m <sup>2</sup> ] (repository sub-area No. 3)	Upper limit based on twice the cross-sectional area of SCP emplacement hole (see DOE, 1988b)
UNIFORM 0.0	0.4 funnel(4)	SOTEC	fluid capture area of canister [m <sup>2</sup> ] (repository sub-area No. 4)	Upper limit based on twice the cross-sectional area of SCP emplacement hole (see DOE, 1988b)

Appendix A

<i>Type of Distribution Value (or Range in Value)</i>		<i>Parameter Name</i>	<i>Module</i>	<i>Parameter Description</i>	<i>Basis for Parameter Assignment</i>
UNIFORM 0.0	0.4	funnel(5)	SOTEC	fluid capture area of canister [m <sup>2</sup> ] (repository sub-area No. 5)	Upper limit based on twice the cross-sectional area of SCP emplacement hole (see DOE, 1988b)
UNIFORM 0.0	0.4	funnel(6)	SOTEC	fluid capture area of canister [m <sup>2</sup> ] (repository sub-area No. 6)	Upper limit based on twice the cross-sectional area of SCP emplacement hole (see DOE, 1988b)
UNIFORM 0.0	0.4	funnel(7)	SOTEC	fluid capture area of canister [m <sup>2</sup> ] (repository sub-area No. 7)	Upper limit based on twice the cross-sectional area of SCP emplacement hole (see DOE, 1988b)
UNIFORM 0.0	10000.	time	VOLCANO	time of occurrence of volcanic event [yr]	Assumed random over performance period (assumed constant probability)
UNIFORM 0.0	1.0	u1	VOLCANO	probabilities of intrusive magmatism (dike: 0.0-0.9) and extrusive magmatism (cone: 0.9-1.0) [ ]	Assumed
UNIFORM 0.0	1.0	u2	VOLCANO	location scaling factor (dike X <sub>0</sub> /cone X <sub>center</sub> ) [ ]	Assumed random over the simulation area
UNIFORM 0.0	1.0	u3	VOLCANO	location scaling factor (dike Y <sub>0</sub> /cone Y <sub>center</sub> ) [ ]	Assumed random over the simulation area
UNIFORM 0.0	1.0	u4	VOLCANO	dike area scaling factor [ ]	Assumed (see Section 6.5.3.2)
UNIFORM 0.0	1.0	u5	VOLCANO	scaling factor for dike length [ ]	Assumed (see Section 6.5.3.2)
UNIFORM 0.0	1.0	u6	VOLCANO	scaling factor for dike angle [ ]	Assumed (see Section 6.5.3.2)
UNIFORM 0.0	1.0	u7	VOLCANO	scaling factor for radius of magma conduit of cone [ ] (minimum of 25 meters and maximum of 100 meters)	Assumed (see Section 6.5.3.2)

<i>Type of Distribution Value (or Range in Value)</i>		<i>Parameter Name</i>	<i>Module</i>	<i>Parameter Description</i>	<i>Basis for Parameter Assignment</i>
NORMAL 4	27	nbore	DRILLO	total number of boreholes drilled [ ]	Poisson distribution centered around the number of drilling events calculated from U.S. Environmental Protection Agency Appendix B guidance (see EPA, 1993; 58 FR 7936)
UNIFORM 0.02	0.1	radius	DRILLO	radius of borehole [m]	Assumed based on current exploratory drilling practice
UNIFORM 0.0	1.0	hit(1 through 27)	DRILLO	indicator for borehole No. 1 through No. 27 interception of a waste package [ ] (A minimum of 4 and a maximum of 27 hit indicators are used. A hit indicator is sampled separately for each borehole. The number of boreholes is determined by the sampled parameter <i>nbore</i> which ranges from 4 to 27.)	See Section 6.3.4
UNIFORM 100.0	9900.0	Td(1 through 27)	DRILLO	time at which drilling occurs for boreholes No. 1 through No. 27 [yr] (A minimum of 4 and a maximum of 27 hit indicators are used. A hit indicator is sampled separately for each borehole. The number of boreholes is determined by the sampled parameter <i>nbore</i> which ranges from 4 to 27.)	Time of drilling randomly occurs after institutional control (100 years) and before end of performance period (9900 years used as an upper limit to allow at least one time step over the 10,000 year performance period)
UNIFORM 0.0	1.0	Regn(1 through 27)	DRILLO	repository region locator for boreholes No. 1 through No. 27 [ ] (A minimum of 4 and a maximum of 27 region locators are used. A region locator is sampled separately for each borehole. The number of boreholes is determined by the sampled parameter <i>nbore</i> which ranges from 4 to 27.)	Sampled value is compared to fraction of total area of each region to locate the borehole in one of the 7 repository sub-areas: sub-area 1 = 0.00 to 0.06; sub-area 2 = 0.06 to 0.33; sub-area 3 = 0.33 to 0.55; sub-area 4 = 0.55 to 0.68; sub-area 5 = 0.68 to 0.73; sub-area 6 = 0.73 to 0.96; and sub-area 7 = 0.96 to 1.00.

Appendix A

<i>Type of Distribution Value (or Range in Value)</i>	<i>Parameter Name</i>	<i>Module</i>	<i>Parameter Description</i>	<i>Basis for Parameter Assignment</i>
UNIFORM 0.0                      1.0	U	SEISMO	comparitive number to determine whether a representative (they all fail or none fail) waste package is failed or not [ ] (if "U" is less than the failure probability, the representative waste package is assumed to be failed, and thus all the packages are failed)	See Section 6.4.4

**References**

- Codell, R.B., *et al.*, "Initial Demonstration of the NRC's Capability to Conduct a Performance Assessment for a High-Level Waste Repository," U.S. Nuclear Regulatory Commission, NUREG-1327, May 1992.
- Einzigler, R.E. and H.C. Buchanan, "Long-Term, Low-Temperature Oxidation of PWR Spent Fuel," Richland, Washington, Westinghouse Hanford Co, WHC-EP-0070, April 1988.
- Grambow, B., "Spent Fuel Dissolution and Oxidation: An Evaluation of Literature Data," Stockholm, Sweden, Statens Kärnkraftinspektion (SKI) [Swedish Nuclear Power Inspectorate], SKI Technical Report 89:13, March 1989.
- Henshall, G.A., "Stochastic Models for Predicting Pitting Corrosion Damage of HLRW Containers," American Nuclear Society, *Proceedings of the Topical Meeting on Nuclear Waste Packaging (FOCUS '91)*, September 29-October 2, 1991, Las Vegas, Nevada, pp. 225-232 [1992].
- Klavetter, E.A. and R.R. Peters, "Fluid Flow in a Fractured Rock Mass," Albuquerque, New Mexico, Sandia National Laboratories, SAND85-0855, March 1986.
- Macdonald, D.D. and M. Urquidi-Macdonald, "Thin-Layer Mixed-Potential Model for the Corrosion of High-Level Nuclear Waste Canisters," *Corrosion*, 46(5):380-390 [1990].
- Meijer, A., "Yucca Mountain Project Far-Field Sorption Studies and Data Needs," Los Alamos, New Mexico, Los Alamos National Laboratory, LA-11671-MS, September 1990.
- Park, U.S., "Regulatory Overview and Recommendations on a Repository's Release of Carbon-14," San Diego, California, Science Applications International Corporation, January 1992. [Prepared for the U.S. Department of Energy.]
- Peters, R.R., *et al.*, "Fracture and Matrix Hydrologic Characteristics of Tuffaceous Materials from Yucca Mountain, Nye County, Nevada," Albuquerque, New Mexico, Sandia National Laboratories, SAND84-1471, December 1984.
- Smith, H.D. and D.L. Baldwin, "An Investigation of Thermal Release of  $^{14}\text{C}$  from PWR Spent Fuel Cladding," American Nuclear Society, *Proceedings of the Topical Meeting on Nuclear Waste Isolation in the Unsaturated Zone (FOCUS '89)*, September 17-21, 1989, Las Vegas, Nevada, pp. 46-49 [1989].
- U.S. Department of Energy, "Chapter 7, Waste Package," in "Site Characterization Plan, Yucca Mountain Site, Nevada Research and Development Area, Nevada," Nevada Operations Office/Yucca Mountain Project Office, Nevada, DOE/RW-0199, Vol. III, Part A, December 1988a.
- U.S. Department of Energy, "Chapter 6, Conceptual Design of a Repository," in "Site Characterization Plan, Yucca Mountain Site, Nevada Research and Development Area, Nevada," Nevada Operations Office/Yucca Mountain Project Office, Nevada, DOE/RW-0199, Vol. III, Part A, December 1988b.

## Appendix A

U.S. Environmental Protection Agency, "Environmental Radiation Protection Standards for the Management and Disposal of Spent Nuclear Fuel, High-Level and Transuranic Radioactive Wastes [Proposed Rule]," *Federal Register*, vol. 58, no. 26, February 10, 1993, pp. 7924-7936.

Watson, M. and J. Postlethwaite, "Numerical Simulation of Crevice Corrosion of Stainless Steel and Nickel Alloys in Chloride Solutions," *Corrosion*, 46(7):522-530 [1990].

## APPENDIX B HYDROLOGIC AND RADIONUCLIDE TRANSPORT DATA FOR THE GROUND-WATER PATHWAY

### B-1 Introduction

Parametric values for use in hydrologic flow and radionuclide transport models were based, when possible, on information published for the Yucca Mountain site. Hydrologic information was based primarily on Peters *et al.* (1984) and Klavetter and Peters (1986), whereas retardation information was based on Meijer (1990) and Thomas (1987). The following tables present the information used from these sources and the resulting ranges and distributions used in the current analysis:

Table	Information
B-1	Hydrologic information reported from experimental and modeling studies.
B-2—B-5	Sorption information from batch experiments on crushed tuff.
B-6	Parametric values and ranges used to represent the ground-water pathway.
B-7	Values for sorption coefficients ( $K_{ds}$ ).

### B-2 Table Information

Table B-1 presents the hydrologic information from Peters *et al.* (1984) and Klavetter and Peters (1986), as well as parametric values used in modeling studies since the publication of the Peters report and information from the U.S. Department of Energy (DOE) Site Characterization Plan (SCP) (DOE, 1988). To assist the correlation to the Yucca Mountain site, the borehole at the site associated with the information taken from Peters *et al.* is identified. Although the values reported from the various studies should only be interpreted based on the purpose for which the modeling was conducted, the values are presented to provide additional insights on differing interpretations of hydrologic properties

of unsaturated tuff being examined. One obvious conclusion is that more information is available on, and more studies have concentrated on, the repository unit (Topopah Spring), than on other units present at Yucca Mountain.

Tables B-2 through B-5 present the information from Meijer (1990) used to develop the  $K_d$  values for individual hydrogeologic units present at Yucca Mountain (abbreviations used in Tables B-2 and B-3 and throughout the remainder of this appendix are as follows: the prefix *JA* indicates drill hole J-13; the prefix *YM* indicates drill hole UE25a-1; and the other abbreviations in the table are unambiguously labeled). A number of assumptions were used to derive the  $K_d$  values; therefore, a more detailed discussion of the interpretation and of the use of the data is given here. (The applicability of the  $K_d$  approach is not discussed here. See Section 4.4.2 for more information on the applicability of the  $K_d$  approach.)

As discussed in Section 4.2.4, the retardation coefficients for each hydrogeologic unit are calculated using the following equation:

$$R_f = 1.0 + \frac{\rho(1-n)}{\theta} \times K_d, \quad (\text{B-1})$$

where:

$R_f$	=	retardation factor;
$K_d$	=	distribution coefficient;
$\theta$	=	moisture content;
$\rho$	=	grain density; and
$n$	=	porosity.

The values for these parameters are specific to the five hydrogeologic units: Topopah Spring Member of the Paintbrush Tuff (Tpt); Calico Hills nonwelded vitric (CHnv); Calico Hills nonwelded zeolitic (CHnz); Prow Pass Member of the Crater Flat Tuff (Tcp); and Bullfrog Member of the Crater Flat Tuff (Tcb). Experimental values (see Tables B-2 through B-5) were used to determine mean  $K_d$  values for a specific hydrogeologic unit, while, for certain elements and hydrogeologic units without data,  $K_d$  values were assigned,

**Table B-1 Hydrologic Properties for Hydrogeologic Units at the Yucca Mountain Site Reported in Modeling Studies and Experimental Studies (Where appropriate, borehole identification labels are provided after the reference.)**

<b>TIVA CANYON (Welded, Devitrified)</b>								
<b>Matrix Properties:</b>								
<i>Reference</i>	<i>Grain Density (kg/m<sup>3</sup>)</i>	<i>Porosity</i>	<i>Residual Saturation</i>	<i>Saturated Conductivity (m/yr)</i>	<i>Alpha (l/m)</i>	<i>Beta</i>		
Peters <i>et al.</i> (1984) [USW G4]	2490	0.08	0.002	3.1E-4	8.2E-3	1.56		
Peters <i>et al.</i> (1984) [USW GU3]	2480 - 2490	0.09 - 0.15	0.014 - 0.160	2.2E-5 - 8.5E-5	3.9E-3 - 2.3E-2	1.51 - 2.13		
Klavetter and Peters (1986)	2490	0.08	0.002	3.1E-4	8.2E-3	1.56		
Dudley <i>et al.</i> (1988)	2490	0.08	0.002	3.1E-4	8.2E-3	1.56		
<b>Fracture Properties:</b>								
<i>Reference</i>	<i>Fracture Aperture (microns)</i>	<i>Fracture Density (l/m<sup>3</sup>)</i>	<i>Porosity</i>	<i>Residual Saturation</i>	<i>Fracture Conductivity (m/yr)</i>	<i>Bulk Conductivity (m/yr)</i>	<i>Alpha (l/m)</i>	<i>Beta</i>
Klavetter and Peters (1986)	6.7	20	1.4E-4	0.04	1.2E3	0.17	1.28	4.23
Dudley <i>et al.</i> (1988)	6.7	20	1.4E-4	0.04	1.2E3	0.17	1.28	4.23

Table B-1 (continued)

**PAINTBRUSH (Non-welded, Vitric)**

**Matrix Properties:**

<i>Reference</i>	<i>Grain Density (kg/m<sup>3</sup>)</i>	<i>Porosity</i>	<i>Residual Saturation</i>	<i>Saturated Conductivity (m/yr)</i>	<i>Alpha (l/m)</i>	<i>Beta</i>
Peters <i>et al.</i> (1984) [USW G4]	2450	0.65	0.105	75.6	1.6E-2	10.6
Peters <i>et al.</i> (1984) [USW GU3]	2350 - 2440	0.40 - 0.59	0.084 - 0.114	11.0 - 50.4	1.1E-2 - 1.5E-2	2.53 - 8.88
Klavetter and Peters (1986)	2350	0.40	0.100	12.3	1.5E-2	6.87
Dudley <i>et al.</i> (1988)	2350	0.40	0.100	12.3	1.5E-2	6.87

**PAINTBRUSH (Non-welded, Vitric)**

**Fracture Properties:**

<i>Reference</i>	<i>Fracture Aperture (microns)</i>	<i>Fracture Density (l/m<sup>3</sup>)</i>	<i>Porosity</i>	<i>Residual Saturation</i>	<i>Fracture Conductivity (m/yr)</i>	<i>Bulk Conductivity (m/yr)</i>	<i>Alpha (l/m)</i>	<i>Beta</i>
Klavetter and Peters (1986)	27.0	1	2.7E-5	0.04	1.9E4	0.50	1.28	4.23
Dudley <i>et al.</i> (1988)	27.0	1	2.7E-5	0.04	1.9E4	0.50	1.28	4.23

Table B-1 (continued)

TOPOPAH SPRING (Welded, Devitrified)						
<b>Matrix Properties:</b>						
<i>Reference</i>	<i>Grain Density (kg/m<sup>3</sup>)</i>	<i>Porosity</i>	<i>Residual Saturation</i>	<i>Saturated Conductivity (m/yr)</i>	<i>Alpha (l/m)</i>	<i>Beta</i>
Peters <i>et al.</i> (1984) [USW G4]	2470 - 2580	0.06 - 0.16	0.058 - 0.120	4.1E-5 - 1.2E-3	2.6E-3 - 1.2E-2	1.56 - 2.12
Peters <i>et al.</i> (1984) [USW GU3]	2540	0.08	0.008	4.7E-5	1.2E-2	1.49
Klavetter and Peters (1986)	2580	0.11	0.080	6.0E-4	5.7E-3	1.80
Tsang and Pruess (1987)	2580	0.11	0.080	6.0E-4	5.7E-3	1.80
Dudley <i>et al.</i> (1988)	2580	0.11	0.080	6.0E-4	5.7E-3	1.80
Pruess <i>et al.</i> (1990)	2550	0.10	9.6E-4	1.0E-2	7.0E-3	1.80
Nitao and Buscheck (1991)	---	0.20	0.080	6.0E-4	---	---
Barnard and Dockery (1991)	2500 - 2570	0.06 - 0.12	0.0 - 0.15	1.6E-4 - 6.3E-4	4.0E-3 - 0.01	1.49 - 2.00
DOE (1988; Table 3-27)						
Lab data	---	0.04 - 0.33	---	1.1E-4 - 0.2	---	---
Field data	---	---	---	260.	---	---

Table B-1 (continued)

TOPOPAH SPRING (Welded, Devitrified)

Fracture Properties:

Reference	Fracture Aperture (microns)	Fracture Density (1/m <sup>2</sup> )	Porosity	Residual Saturation	Fracture Conductivity (m/yr)	Bulk Conductivity (m/yr)	Alpha (l/m)	Beta
Peters <i>et al.</i> (1984) [USW G4]	6. - 67.	—	—	---	1.1E3 - 1.2E5			
Klavetter and Peters (1986)	4.3 - 5.1	8 - 40	4.1E-5 - 1.8E-4	0.04	5.0E2 - 6.9E2	0.02 - 0.10	1.28	4.23
Tsang and Pruess (1987)	—	—	1.8E-3	0.04	—	5.5	—	4.23
Dudley <i>et al.</i> (1988)	4.3 - 5.1	8 - 40	4.1E-5 - 1.8E-4	0.04	5.0E2 - 6.9E2	0.02 - 0.10	1.28	4.23
Pruess <i>et al.</i> (1990)	64.15	4.5	2.9E-4	---	1.1E5	30.9	---	---
Nitao and Buscheck (1991)	90.	22	—	0.04	2.6E5	---	---	---
Barnard and Dockery (1991)	6. - 20.	5 - 10	3.0E-5	0.04	1.3E3 - 1.3E4	3.8E-2 - 2.5	1.28	4.23

B-5

**Table B-1 (continued)**

<b>CALICO HILLS (Non-Welded, Vitric)</b>								
<b>Matrix Properties:</b>								
<i>Reference</i>	<i>Grain Density (kg/m<sup>3</sup>)</i>	<i>Porosity</i>	<i>Residual Saturation</i>	<i>Saturated Conductivity (m/yr)</i>	<i>Alpha (l/m)</i>	<i>Beta</i>		
Peters <i>et al.</i> (1984) [USW GU3]	2350 - 2370	0.43 - 0.46	0.020 - 0.048	.82 - 9.1	1.0E-2 - 4.4E2	1.50 - 4.20		
Klavetter and Peters (1986)	2370	0.46	0.041	8.5	1.6E-2	3.87		
Dudley <i>et al.</i> (1988)	2370	0.46	0.041	85	1.6E-2	3.87		
<b>CALICO HILLS (Non-Welded, Vitric)</b>								
<b>Fracture Properties:</b>								
<i>Reference</i>	<i>Fracture Aperture (microns)</i>	<i>Fracture Density (l/m<sup>3</sup>)</i>	<i>Porosity</i>	<i>Residual Saturation</i>	<i>Fracture Conductivity (m/yr)</i>	<i>Bulk Conductivity (m/yr)</i>	<i>Alpha (l/m)</i>	<i>Beta</i>
Peters <i>et al.</i> (1984) [USW G4]	22	---	---	---	1.4E4	---	---	---
Klavetter and Peters (1986)	15.5	3	4.6E-5	0.04	6.3E3	0.29	1.28	4.23
Dudley <i>et al.</i> (1988)	15.5	3	4.6E-5	0.04	6.3E3	0.29	1.28	4.23

Table B-1 (continued)

CALICO HILLS (Non-Welded, Zeolitic)

Matrix Properties:

Reference	Grain Density (kg/m <sup>3</sup> )	Porosity	Residual Saturation	Saturated Conductivity (m/yr)	Alpha (l/m)	Beta
Peters <i>et al.</i> (1984) [USW G4]	2230 - 2380	0.22 - 0.30	0.037 - 0.215	7.6E-7 - 5.0E-3	6.0E-4 - 6.0E3	1.46 - 3.32
Klavetter and Peters (1986)	2230	0.28	0.110	6.3E-4	3.1E-3	1.60
Dudley <i>et al.</i> (1988)	2230	0.28	0.110	6.3E-4	3.1E-3	1.60
Barnard (1991)	2280 - 2320	0.23 - 0.36	0.0 - 0.15	2.2E-4 - 6.3E-4	2.0E-3 - 5.0E-3	1.37 - 1.65
DOE (1988; Table 3-27)						
Lab data	---	0.20 - 0.34	---	1.5E-3 - 0.11	---	---
Field data	---	---	---	180.	---	---

CALICO HILLS (Non-Welded, Zeolitic)

Fracture Properties:

Reference	Fracture Aperture (microns)	Fracture Density (l/m <sup>3</sup> )	Porosity	Residual Saturation	Fracture Conductivity (m/yr)	Bulk Conductivity (m/yr)	Alpha (l/m)	Beta
Peters <i>et al.</i> (1984) [USW G4]	6 - 31	---	---	---	9.8E2 - 2.5E4			
Klavetter and Peters (1986)	15.5	3	4.6E-5	0.04	6.3E3	0.29	1.28	4.23
Dudley <i>et al.</i> (1988)	15.5	3	4.6E-5	0.04	6.3E3	0.29	1.28	4.23
Barnard and Dockery (1991)	6.0	3	1.8E-5	0.04	9.4E2	0.02	1.28	4.23

Table B-1 (continued)

## PROW PASS (Welded, Devitrified)

## Matrix Properties:

Reference	Grain Density (kg/m <sup>3</sup> )	Porosity	Residual Saturation	Saturated Conductivity (m/yr)	Alpha (1/m)	Beta
Peters <i>et al.</i> (1984) [USW G4]	2590	0.24	0.066	5.0E-2 - 4.4E-1	1.4E-2	2.64
Peters <i>et al.</i> (1984) [USW GU3]	2570 - 2580	0.32 - 0.39	0.018 - 0.066	4.1E-2 - 2.2E-1	1.4E-2 - 3.1E-2	2.96 - 3.44
Klavetter and Peters (1986)	2590	0.24	0.066	0.14	1.4E-2	2.64
Dudley <i>et al.</i> (1988)	2590	0.24	0.066	0.14	1.4E-2	2.64
Barnard and Dockery (1991)	2590	0.25	0.05	0.06 - 1.6	1.0E-2	2.7
DOE (1988; Table 3-27)						
Lab data	---	0.10 - 0.30	---	2.2E-4 - 0.36	---	---
Field data	---	---	---	36.0 - 5.3E2	---	---

## Fracture Properties:

Reference	Fracture Aperture (microns)	Fracture Density (1/m <sup>3</sup> )	Porosity	Residual Saturation	Fracture Conductivity (m/yr)	Bulk Conductivity (m/yr)	Alpha (1/m)	Beta
Klavetter and Peters (1986)	4.16	3	1.3E-5	0.04	4.4E2	0.02	1.28	4.23
Dudley <i>et al.</i> (1988)	4.16	3	1.3E-5	0.04	4.4E2	5.7E-3	1.28	4.23
Barnard and Dockery (1991)	20.	3	6.0E-5	0.04	1.3E4	0.8	1.28	4.23

Table B-1 (continued)

Matrix Properties:

Reference	Grain Density (kg/m <sup>3</sup> )	Porosity	Residual Saturation	Saturated Conductivity (m/yr)	Alpha (l/m)	Beta
<b>UPPER CRATER FLAT (Non-Welded, Zeolitic)</b>						
Peters <i>et al.</i> (1984) [USW G4]	2240 - 2290	0.19 - 0.29	0.135 - 0.322	6.3E-4 - 1.4E-2	3.2E-3 - 4.5E-3	1.87 - 2.02
<b>BULLFROG (Welded, Devitrified)</b>						
Peters (1984) [USW G4]	2620 -2630	0.24 - 0.27	0.056 -0.061	7.2E-2 - 2.0E-1	1.1E-2 - 2.9E-2	2.26 - 4.15
DOE (1988; Table 3-27)						
Lab data	---	0.17 - 0.34	---	1.1E-2 - 0.36	---	---
Field data	---	---	---	2.2 - 8.4E2	---	---
<b>TRAM (Non-Welded)</b>						
DOE (1988; Table 3-27)						
Lab data	---	0.18 - 0.26	---	1.5E-3 - 0.15	---	---
Field data	---	---	---	2.5E-3 - 2.9E2	---	---

B-9

**Table B-3 Average Sorption Ratios (Distribution Coefficients) from Batch Sorption Experiments on Crushed Tuff for Strontium, Cesium, Barium, Radium, Cerium, and Europium (after Meijer, 1990) (The sorption ratio in parentheses represents the standard deviation of the mean.)**

Unit	Sample	Depth (ft)	Sorption Ratios (ml/g)					
			Sr	Cs	Ba	Ra	Ce	Eu
Tiva Canyon (Tpc)	JA-8	606	270 (5)	2700 (400)	435 (15)			2100 (300)
	YM-5	251	280 (80)	5800 (800)	1100 (200)		450,000 (240,000)	2,300,000 (40,000)
Pah Canyon (Tpp)	G2-547	547	265 (10)	13,300 (1500)	3490 (30)			340 (30)
	G2-723	723	290 (40)	4100 (600)	3500 (400)			> 10,000
	GU3-433	433	45 (9)	630 (20)	810 (100)			100 (14)
Topopah Spring (Tpt)	YM-22	848	53 (4)	290 (30)	900 (30)		1270 (40)	1390 (110)
	GU3-1203	1203	42 (1)	350 (30)	640 (40)			190 (2)
	G1-1292	1292	200 (6)	430 (28)	2100 (300)	1500 (100)	66 (8)	140 (14)
	GU3-1301	1301	28 (4)	160 (40)	570 (60)			45 (12)
	YM-30	1264	260 (80)	855 (5)	3400 (1500)		230,000 (100,000)	160,000 (50,000)
	JA-18	1420	17,000 (3000)	16,000 (1000)	38,000 (18,000)		2800 (1400)	1400 (200)
Calico Hills, tuffaceous beds (Tht)	G1-1436	1436	36,000 (3000)	7800 (500)	150,000 (24,000)		59,000 (7000)	30,000 (2000)
	G2-1952	1952	2200 (400)	63,300 (1100)	25,000 (4000)			89 (14)
Prow Pass (Tpc)	G1-1854	1854	60,000 (14,000)	13,000 (2000)	45,000 (7000)		15,000	
	YM-45	1930	195 (14)	520 (90)	1200 (100)		730 (100)	1600 (200)
	G1-1883	1883	22 (0.2)	187 (3)	183 (12)		1420 (20)	
	YM-46	2002	190 (60)	840 (6)	14,000 (6000)		310,000 (110,000)	307,000 (110,000)
	G1-1982	1982	55 (4)	1120 (110)	700 (50)		560 (40)	970 (150)
	YM-48	2114	2100 (400)	9000 (4000)	18,000 (6000)		1400 (500)	2200 (500)
	YM-49	2221	3200 (300)	36,000 (3000)	42,000 (8000)		550 (100)	1200 (100)
	JA-26	1995	95 (35)	1500 (600)	800 (300)			

Table B-3 (continued)

Unit	Sample	Depth (ft)	Sorption Ratios (ml/g)					
			Sr	Cs	Ba	Ra	Ce	Eu
bedded tuff (bt)	YM-38	1504	17,000 (2000)	13,000 (2000)	100,000 (10,000)		760 (140)	1600 (200)
	YM-42	1824	3900 (600)	17,000 (1000)	94,000 (14,000)		49,900 (7000)	52,000 (4000)
Bullfrog (Tcb)	JA-28	2001	94 (20)	1640 (210)	820 (50)			2100(1000)
	G1-2233	2233	48,000 (3000)	13,500 (800)	250,000 (30,000)		1400 (300)	900 (200)
	G1-2289	2289	7300 (500)	37,000 (13,000)	66,000 (9000)	46,000 (20,000)		797 (10)
	YM-54	2491	62 (12)	180 (40)	400 (150)		150 (40)	470 (40)
	G1-2333	2333	180 (20)	1400 (130)	1500 (200)			2300 (400)
	G1-2363	2363	64 (3)	470 (40)	235 (9)	540 (60)		730 (50)
	G1-2410	2410	169 (1)	1250 (50)	1780			440 (80)
	JA-32	2533	57 (3)	123 (4)	380 (30)		82 (14)	90 (20)
G1-2476	2476	41 (1)	700 (40)	385 (11)			3200 (100)	
Tram (Tct)	G1-2698	2698	42,000 (3000)	7700 (400)	63,000 (5000)		240 (30)	200 (30)
	G1-2840	2840	860 (1)	2200 (200)	2070 (70)			4900 (400)
	G1-2854	2854	94 (1)	1080 (120)	1000 (50)			1300 (200)
	G1-2901	2901	68 (1)	1290 (110)	1600 (200)		42,000 (3000)	160,000 (50,000)
	G1-3116	3116	2400 (17)	6600 (500)	12,000 (4000)		100 (10)	760 (60)
	JA-37	3497	287 (14)	610 (40)	760 (150)			6000 (800)
older tuffs (Tl)	G1-3658	3658	13,000 (0)	4950 (50)	13,500 (500)		1000 (200)	530 (40)
bedded tuff (Tba)	G2-3933	3923	240 (60)	2500 (1000)	1700 (500)			1500 (700)

B-11

NUREG-1464

Appendix B

Table B-3 (continued)

Unit	Sample	Depth (ft)	Sorption Ratios (ml/g)					
			Sr	Cs	Ba	Ra	Ce	Eu
bedded tuff (bt)	YM-38	1504	17,000 (2000)	13,000 (2000)	100,000 (10,000)		760 (140)	1600 (200)
	YM-42	1824	3900 (600)	17,000 (1000)	94,000 (14,000)		49,900 (7000)	52,000 (4000)
Bullfrog (Tcb)	JA-28	2001	94 (20)	1640 (210)	820 (50)			2100(1000)
	G1-2233	2233	48,000 (3000)	13,500 (800)	250,000 (30,000)		1400 (300)	900 (200)
	G1-2289	2289	7300 (500)	37,000 (13,000)	66,000 (9000)	46,000 (20,000)		797 (10)
	YM-54	2491	62 (12)	180 (40)	400 (150)		150 (40)	470 (40)
	G1-2333	2333	180 (20)	1400 (130)	1500 (200)			2300 (400)
	G1-2363	2363	64 (3)	470 (40)	235 (9)	540 (60)		730 (50)
	G1-2410	2410	169 (1)	1250 (50)	1780			440 (80)
	JA-32	2533	57 (3)	123 (4)	380 (30)		82 (14)	90 (20)
G1-2476	2476	41 (1)	700 (40)	385 (11)			3200 (100)	
Tram (Tct)	G1-2698	2698	42,000 (3000)	7700 (400)	63,000 (5000)		240 (30)	200 (30)
	G1-2840	2840	860 (1)	2200 (200)	2070 (70)			4900 (400)
	G1-2854	2854	94 (1)	1080 (120)	1000 (50)			1300 (200)
	G1-2901	2901	68 (1)	1290 (110)	1600 (200)		42,000 (3000)	160,000 (50,000)
	G1-3116	3116	2400 (17)	6600 (500)	12,000 (4000)		100 (10)	760 (60)
	JA-37	3497	287 (14)	610 (40)	760 (150)			6000 (800)
older tuffs (TI)	G1-3658	3658	13,000 (0)	4950 (50)	13,500 (500)		1000 (200)	530 (40)
bedded tuff (Tba)	G2-3933	3923	240 (60)	2500 (1000)	1700 (500)			1500 (700)

**Table B-4 Average (De)Sorption Ratios (Distribution Coefficients) from Batch Sorption Experiments on Crushed Tuff for Strontium, Cesium, Barium, Radium, Cerium, and Europium (after Meijer, 1990) (The sorption ratio in parentheses represents the standard deviation of the mean.)**

Unit	Sample	Depth (ft)	(De)Sorption Ratios (ml/g)				
			Sr	Cs	Ba	Ce	Eu
Tiva Canyon (Tpc)	JA-8	606	311 (3)	4600 (400)	480 (50)		10,000 (3000)
	YM-5	251	320 (30)	8900 (600)	1200 (120)	31,000 (30,000)	36,000 (14,000)
Pah Canyon (Tpp)	G2-547	547	210 (10)	8700 (550)	2900 (200)		1700 (600)
	G2-723	723	330 (4)	4300 (4)	4200 (10)		> 10,000
	GU3-433	433	40 (10)	520 (20)	460 (20)		140 (10)
Topopah Spring (Tpt)	YM-22	848	59 (2)	365 (7)	830 (100)	6500 (800)	3500 (200)
	GU3-1203	1203	47 (1)	340 (10)	720 (30)		650 (50)
	G1-1292	1292	120 (5)	510 (20)	1500 (100)	600 (200)	600 (70)
	GU3-1301	1301	80 (20)	185 (20)	675 (60)		100 (20)
	YM-30	1264	210 (30)	1500 (100)	3100 (600)	170,000 (15,000)	11,000 (700)
	JA-18	1420	15,000 (2000)	17,500 (700)	280,000 (50,000)	1600 (500)	2400 (300)
Calico Hills, tuffaceous beds (Tht)	G1-1436	1436	87,000 (12,000)	24,000 (2000)	340,000 (90,000)	6700 (600)	5300 (600)
	G2-1952	1952	4200 (200)	46,000 (1400)	40,000 (1000)		1600 (200)
	YM-38	1540	22,000	13,000	260,000	2600	7300
	YM-42	1842	4100 (1000)	21,000 (2000)	90,000	44,000 (5000)	64,000 (3000)
older tuffs (Tl)	G1-3658	3658	12,000 (3000)	12,000 (2000)	10,000 (4000)	9000 (4000)	9000 (3000)
Prow Pass (Tpc)	G1-1854	1854	72,000 (13,000)	14,000 (2000)	150,000 (40,000)		4800 (700)
	YM-45	1930	210 (20)	620 (110)	1310 (60)	5800 (600)	7300 (900)
	G1-1883	1883	59 (1)	430 (4)	440 (10)	2200 (100)	1350 (50)
	YM-46	2002	260 (20)	1800 (300)	210,000 (3000)	300,000 (50,000)	31,000 (2000)
	G1-1982	1982	322 (8)	2300 (200)	2780 (120)	7000 (800)	6370 (130)
	YM-48	2114	2700 (200)	27,000 (4000)	34,000 (7000)	128,000 (300)	8100 (1200)
	YM-49	2221	4400 (100)	39,000 (1000)	65,000 (7000)	1040 (40)	2100 (500)
	JA-26	1995	39 (3)	1580 (90)	450 (13)		2900 (200)

B-13

NUREG-1464

Appendix B

Table B-4 (continued)

Unit	Sample	Depth (ft)	(De)Sorption Ratios (ml/g)				
			Sr	Cs	Ba	Ce	Eu
Bullfrog (Tcb)	JA-28	2001	114 (3)	2400 (100)	1160 (20)		12,300 (500)
	G1-2233	2233	90,000 (40,000)	23,000 (6000)	240,000 (80,000)	20,000 (13,000)	5000 (2000)
	YM-54	2491	97 (9)	310 (20)	660 (20)	1000 (200)	1840 (110)
	G1-2333	2333	140 (13)	1230 (100)	1460 (130)		9900 (1200)
	G1-2363	2363	150 (6)	1200 (30)	820 (20)	130,000 (6000)	6100 (200)
	G1-2410	2410	140 (14)	1120 (100)	1760 (150)		6000 (3000)
	JA-32	2533	53 (3)	175 (11)	490 (40)	530 (120)	850 (130)
	G1-2476	2476	200 (40)	1520 (0)			
Tram (Tct)	G1-2698	2698	210,000 (50,000)	17,000 (1100)	190,000 (80,000)	2000 (400)	
	G1-2840	2840	1540 (4)	2300 (130)	2500 (200)		9000 (1100)
	G1-2854	2854	96 (1)	1160 (20)	1330 (0)		5000 (200)
	G1-2901	2901	67 (1)	1380 (30)	1980 (30)	39,000 (1000)	210,000 (50,000)
	G1-3116	3116	24,000 (13,000)	11,000 (3000)	160,000 (80,000)	3000 (1000)	8000 (3000)
	JA-37	3497	312 (9)	850 (50)	920 (40)		11,000 (2000)
bedded tuff (Tba)	G2-3933	3933	140 (20)	1400 (350)	1100 (200)		3000 (1100)

**Table B-5 Average (De)Sorption Ratios (Distribution Coefficients) from Batch Sorption Experiments on Crushed Tuff for Americium, Plutonium, Uranium, Technetium, and Neptunium (after Meijer, 1990) (The sorption ratio in parentheses represents the standard deviation of the mean.)**

Unit	Sample	Depth (ft)	(De)Sorption Ratios (ml/g)				
			Am	Pu	U	Tc	Np
Pah Canyon (Tpp)	G2-547	547	17,000 (1400)	1200 (170)			
	G2-723	723	2.8x10 <sup>6</sup> (26,000)	>4700			
	GU3-433	433	9300 (1780)	920 (40)			
Topopah Spring (Tpt)	YM-22	848	2500 (400)	1330 (140)	5 (2)	1.2 (0.3)	33 (5)
	GU3-1203	1203	1300 (200)	920 (15)		0	
	G1-1292	1292					
	GU3-1301	1301	2500 (600)	1300 (460)			
	JA-18	1420	1100 (300)	350 (140)	9.4 (1.4)		
Calico Hills, tuffaceous beds (Tht)	G2-1952	1952	5800 (1100)	350 (45)			15 (2)
	YM-38	1540	7100 (1200)	1600 (300)	4.8 (1.0)		24 (2)
Prow Pass (Tcp)	G1-1883	1883	7200 (900)	890 (60)			36 (10)
	G1-1982	1982			4.1		
	YM-48	2114				1.6 (0.2)	
	YM-49	2221	3400 (400)	720 (90)		2.0 (0.3)	12 (4)
Bullfrog (Tcb)	G1-2233	2233			8 (2)		
	YM-54	2491	550 (80)	720 (40)	12 (8)		
	JA-32	2533	2200 (600)		8 (2)		
	G1-2476	2476			1.5 (0.2)		
Tram (Tct)	G1-3116	3116			1.7 (0.3)		
	JA-37	3497	32,000 (10,000)	1400 (300)	9.9 (0.4)		170 (50)
bedded tuff (Tba)	G2-3933	3933	12,000 (410)	530 (130)		0	

B-15

NUREG-1464

Appendix B

based on chemical similarity to other measurements. When  $K_d$  values could still not be assigned,  $K_d$  values were taken from the Iterative Performance Assessment (IPA) Phase 1 report (see Codell *et al.*, 1992; p. 56). In the sensitivity analysis (described in Chapter 8), the IPA Phase 2 effort assumed that the distribution of  $K_d$  values was log-uniform. For such a distribution, the sampling procedure used required setting the upper and lower bounds of the parameter range. The upper and lower bounds of the distribution were crudely estimated to be plus or minus one order of magnitude about the mean (the support for this assignment was derived from DOE's 1988 SCP, where the range of  $K_d$  values for Sr and Cs varies over two orders of magnitude for different locations in drill hole G1). A mean  $K_d$  value was derived from the Meijer (1990) and Thomas (1987) data by averaging the logs of the reported experimental values. The mean  $K_d$  values, thus calculated, are as follows for the following hydrogeologic units:

Element	$K_d$ ( $m^3/kg$ )				
	Tpt	CHnv	CHnz	Tcp	Tcb
Am	.810	.810	1.7	4.5	.140
Pu	.170	.170	.066	.130	.094
U	.0002	.020	.001	0.0	.002
Se	.0026	.003	.0045	.0025	.013
Tc	.000013	0.0	0.0	.00017	.0042
Np	.0045	.0045	.0027	.0051	.0051
Sr	.08	.034	8.9	.450	.280
Cs	.36	.24	22.0	2.2	3.2
Ba	1.2	.6	61.0	3.9	1.1
Ra	1.5	1.5	1.5	1.5	5.0
Th	.470				.340
Sn				.230	.660

The experimental  $K_d$  values taken from Meijer (1990) and Thomas (1987) were determined using crushed tuff from various drill holes and water, from Well J-13, which was "spiked" with a particular radionuclide. A brief description of the

procedure and information used to derive the mean  $K_d$  values is presented below:

**Am** The  $K_d$  in the Topopah Spring unit (Tpt) is a log average of the values from experiments using crushed tuff recovered from drill holes J-13, G-3, and UE25a-1. The  $K_d$  in the Calico Hills nonwelded vitric unit (CHnv) is estimated to be the same as the Topopah Spring. Glassy units should have low sorption capability. The single value reported from the experiment using crushed tuff from drill hole G-2 is assumed to represent the mean value of the  $K_d$  in the Calico Hills nonwelded zeolitic unit (CHnz). For the Prow Pass unit (Tcp), the  $K_d$  is again the log average of the values from wells G1 and UE25a-1. The  $K_d$  in the Bullfrog unit (Tcb) is the log average of the values from experiments using crushed tuff recovered from drill holes J-13 and UE25a-1.

**Pu** The  $K_d$  in the Topopah Spring unit is the log average of the values from experiments using crushed tuff recovered from drill holes UE25a-1, G-3, and J-13. The  $K_d$  in the Calico Hills nonwelded vitric is estimated to be the same as the Topopah Spring unit. The single value reported from the experiment using crushed tuff from drill hole G-2 is assumed to represent the mean value of the  $K_d$  for the Calico Hills nonwelded zeolitic unit. The Prow Pass unit  $K_d$  is the log average of the values from experiments using crushed tuff recovered from drill holes G-1 and UE25a-1. The Bullfrog unit  $K_d$  is the log average of the values from experiments using crushed tuff recovered from drill holes J-13 and UE25a-1.

**U** The  $K_d$  in the Topopah Spring unit is the log average of the values from experiments using crushed tuff recovered from drill holes UE25a-1, G-3, and J-13. The single value reported from the experiment used crushed tuff recovered from drill hole G-3 is assumed to represent the  $K_d$  in the Calico Hills nonwelded vitric unit. Figures B-1 through B-4 from the SCP (see DOE, 198c) illustrate where the zeolitic beds are located. The  $K_d$  value in the Calico Hills nonwelded

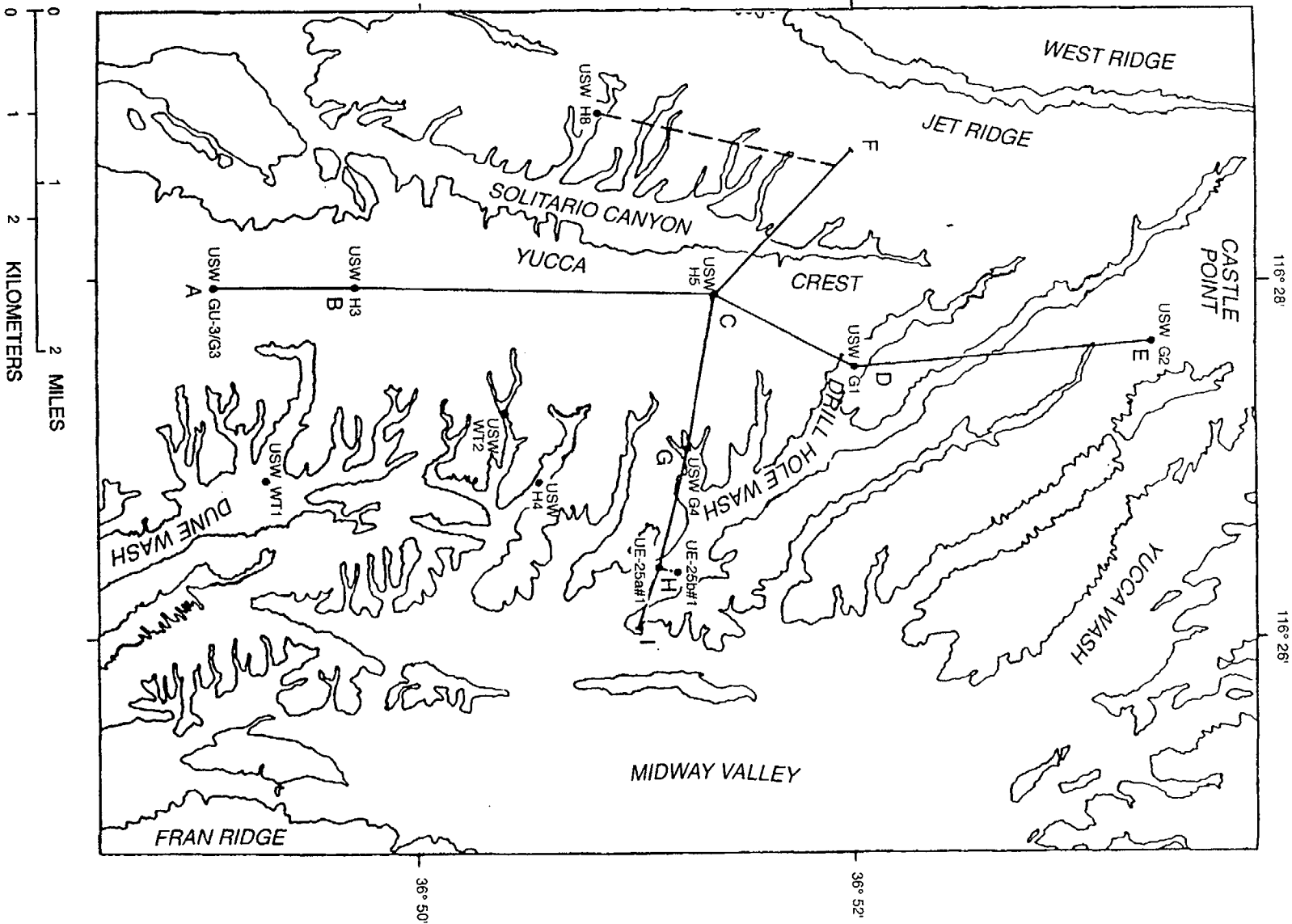


**Figure B-1** Location map for the zeolitic cross-sections in Figures B-2, B-3, and B-4 (This figure and the stratigraphy shown in Figures B-2 and B-4 are based on Scott and Bonk (1984). Taken from DOE (1988, p. 4-22).)

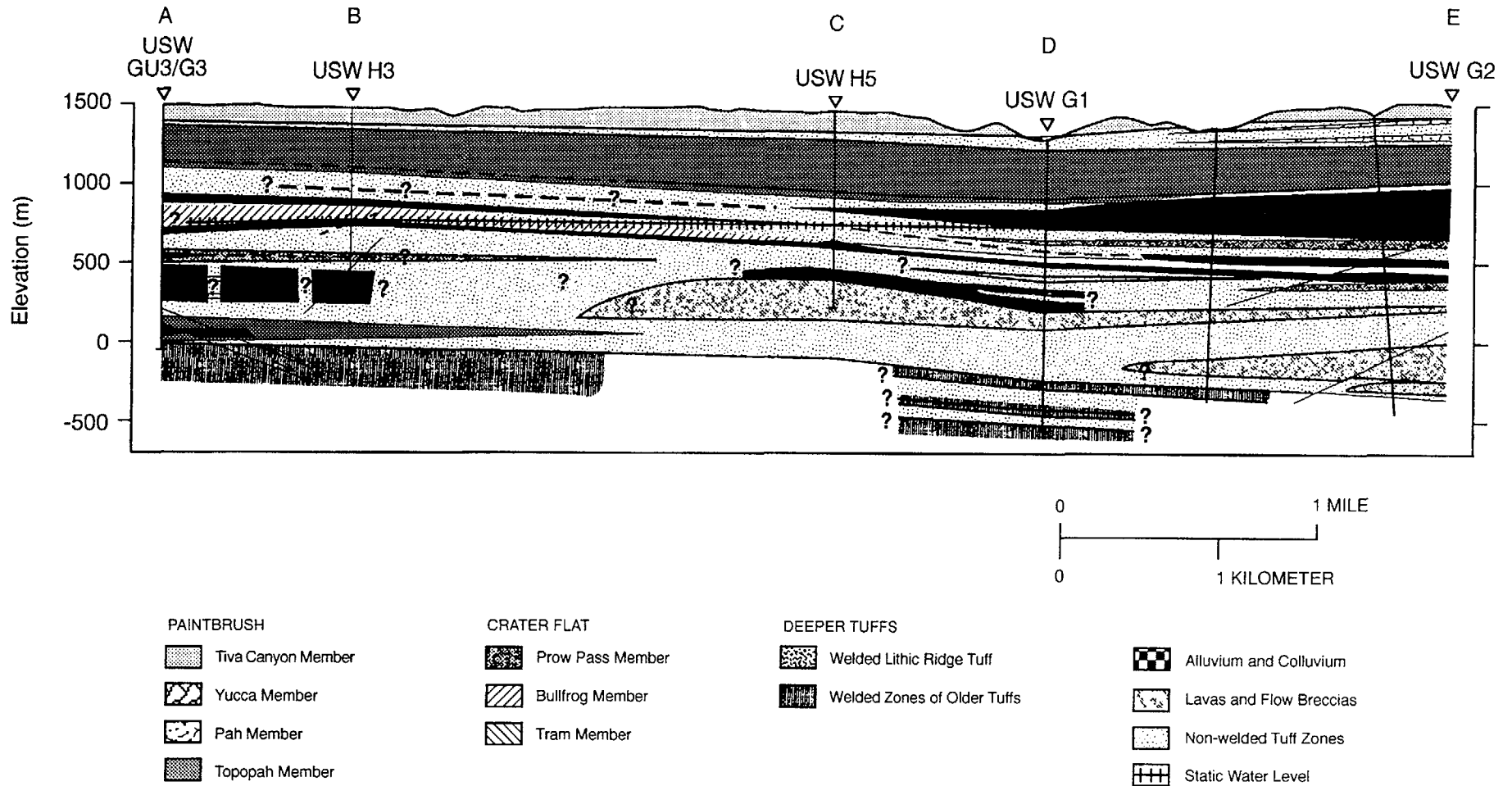


**Figure B-2 Major zeolitic distributions (Bish and Vaniman, 1985), north-south cross-section, shown as a dark pattern overlying the stratigraphic cross-section of Scott and Bonk (1984) (Location of cross-section is shown on Figure B-1. The subhorizontal barred line indicates the water table as inferred from static water levels in the drill holes. Taken from DOE (1988, p. 4-24)**

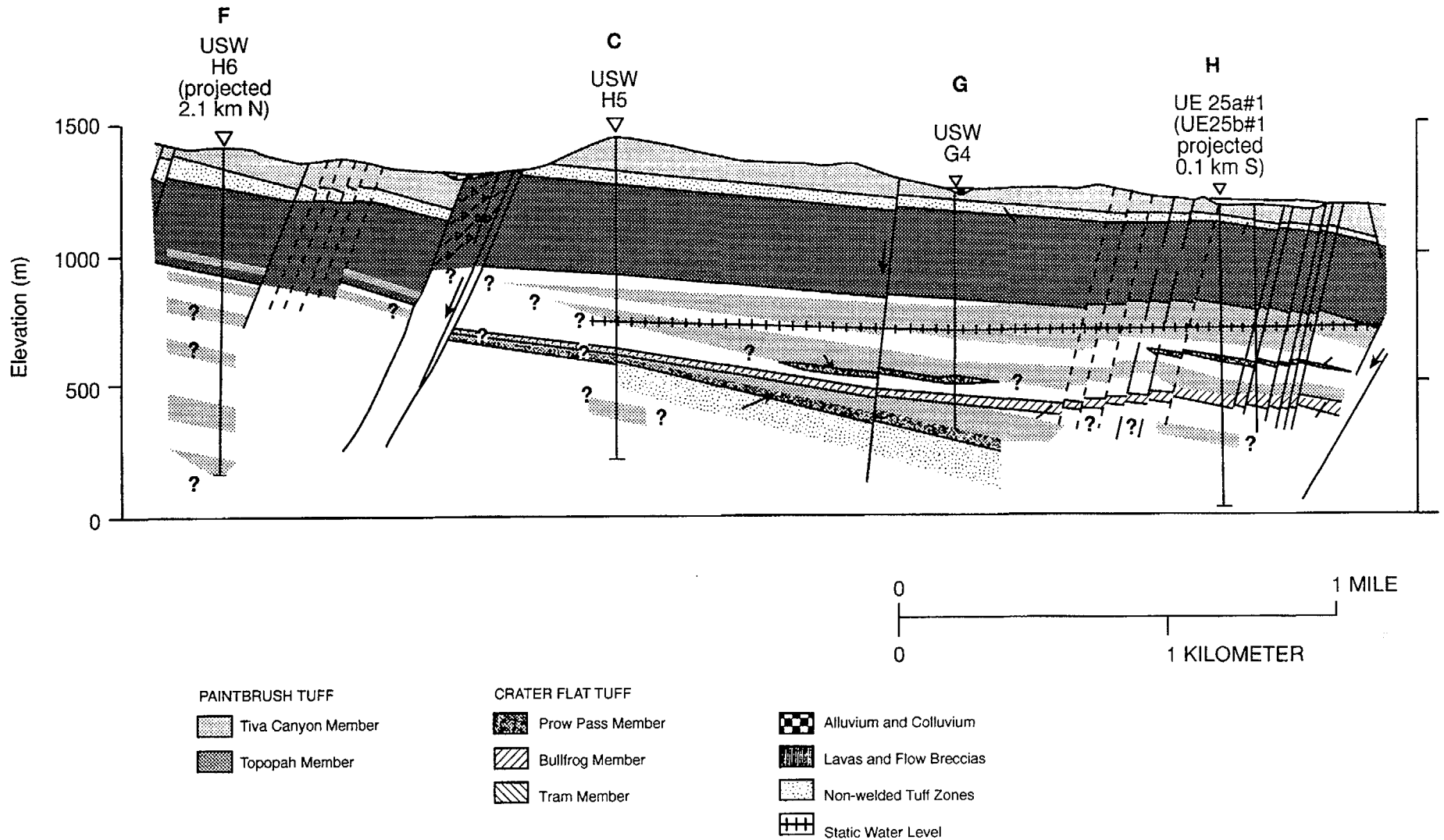


**Figure B-3 Major clinoptilolite-mordenite distributions (Bish and Vaniman, 1985), northwest-southeast cross-section** (Location of cross-section is shown on Figure B-1. Information on drill hole USW H-5 below 760 meters is from Bentley *et al.* (1983) and information on the central part of the drill hole USW H-6 is from Craig *et al.* (1983). Taken from DOE (1988, p. 4-25).)

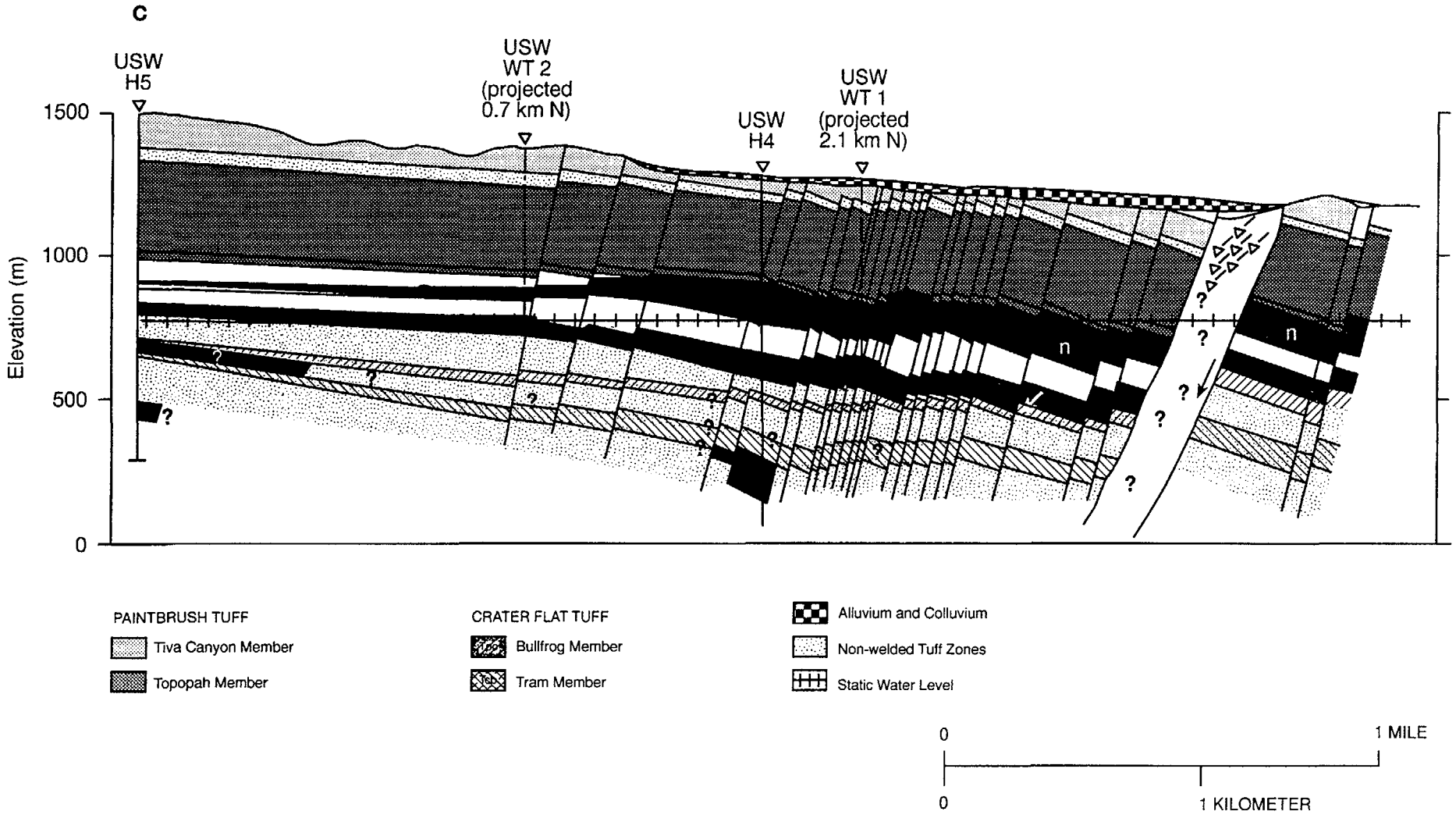


**Figure B-4 Major zeolite distributions (Bish and Vaniman, 1985), center to southeast cross-section as depicted in Figure B-1 (Taken from DOE (1988, p. 4-?)**

zeolitic unit is a log average of the values from experiments using crushed tuff recovered from drill holes G-1 and G-2. The  $K_d$  in the Prow Pass unit is assumed to be zero, even though no data are available. The  $K_d$  in the Bullfrog unit is the log average of the values from experiments using crushed tuff recovered from drill holes G-1, J-13, and UE25a-1.

*Se* The  $K_d$  in the Topopah Spring unit is the log average of the values from experiments using crushed tuff recovered from drill hole G-3. The single value reported from the experiment used crushed tuff recovered from drill hole G-3 is assumed to represent the mean value of the  $K_d$  in the Calico Hills nonwelded vitric unit. The  $K_d$  value in the Calico Hills nonwelded zeolitic unit is the average of the values from experiments using crushed tuff recovered from drill holes G-1 and G-2. The single value reported from the experiment used crushed tuff recovered from drill hole G-1 is assumed to represent the  $K_d$  in the Prow Pass unit. The  $K_d$  in the Bullfrog unit is the log average of the values from experiments using crushed tuff recovered from drill hole G-1.

*Tc* The  $K_d$  in the Topopah Spring unit is the log average of the values from experiments using crushed tuff recovered from drill holes UE25a-1 and G-3. In the absence of information, the  $K_d$ s in the Calico Hills units are assumed to be zero. The  $K_d$  in the Prow Pass unit is the log average of the values from experiments using crushed tuff recovered from drill hole J-13. The single value from the experiment used crushed tuff recovered from drill hole UE25a-1 is assumed to represent the mean of the  $K_d$  in the Bullfrog unit.

*Np* The  $K_d$  in the Topopah Spring unit is a log average of the values from experiments using crushed tuff recovered from drill holes G-3 and UE25a-1. The  $K_d$  in the Calico Hills nonwelded vitric unit is estimated to be the same as the Topopah Spring unit. The single value reported from the experiment using crushed tuff from drill hole G-2 is assumed to represent the mean value of the  $K_d$  in the Calico Hills non-

welded zeolitic unit is assumed to represent the mean. For the Prow Pass unit, the  $K_d$  is the log average of the values from experiments using crushed tuff recovered from drill holes G1 and UE25a-1. The  $K_d$  in the Bullfrog unit is assumed to be the same as the value in the Prow Pass unit.

*Sr* The  $K_d$  in the Topopah Spring unit is a log average of the values from experiments using crushed tuff recovered from drill holes G-3, G-1, and UE25a-1. The  $K_d$  in the Calico Hills nonwelded vitric unit is based on the log average of the values from well G-3 for the Topopah Spring unit. The  $K_d$  value in the Calico Hills nonwelded zeolitic unit is the log average of the values from experiments using crushed tuff recovered from drill holes G-1 and G-2. For the Prow Pass unit, the  $K_d$  is the log average of the values from experiments using crushed tuff recovered from drill holes G1, J-13, and UE25a-1. For the Bullfrog unit, the  $K_d$  is the log average of the values from experiments using crushed tuff recovered from drill holes G1, J-13, and UE25a-1.

*Cs* The  $K_d$  in the Topopah Spring unit is a log average of the values from experiments using crushed tuff recovered from drill holes G-3, G-1, and UE25a-1. The  $K_d$  in the Calico Hills nonwelded vitric unit is based on the log average of the values from experiments using crushed tuff recovered from drill hole G-3 for the Topopah Spring unit. The  $K_d$  value in the Calico Hills nonwelded zeolitic unit is the log average of the values from experiments using crushed tuff recovered from drill holes G-1 and G-2. For the Prow Pass unit, the  $K_d$  is the log average of the values from experiments using crushed tuff recovered from drill holes G1, J-13, and UE25a-1. For the Bullfrog unit, the  $K_d$  is the log average of the values from experiments using crushed tuff recovered from drill holes G1, J-13, and UE25a-1.

*Ba* The  $K_d$  in the Topopah Spring unit is a log average of the values from experiments using crushed tuff recovered from drill holes G-3, G-1, and UE25a-1. The  $K_d$  in the Calico Hills nonwelded vitric unit is based on the log average of the values from

experiments using crushed tuff recovered from drill hole G-3, for the Topopah Spring unit. The  $K_d$  value in the Calico Hills nonwelded zeolitic unit is the log average of the values from experiments using crushed tuff recovered from drill holes G-1 and G-2. For the Prow Pass unit, the  $K_d$  is the log average of the values from experiments using crushed tuff recovered from drill holes G1, J-13, and UE25a-1. For the Bullfrog unit, the  $K_d$  is the log average of the values from experiments using crushed tuff recovered from drill holes G1, J-13, and UE25a-1.

- Ra** The single value from the experiment used crushed tuff recovered from drill hole G-1 is assumed to represent the mean of the  $K_d$  for the Topopah Spring unit. The  $K_d$ s for the Calico Hills and Prow Pass units are assumed to be the same as the value used for the Topopah Spring unit. The  $K_d$  for the Bullfrog unit is the log average of the values from experiments using crushed tuff recovered from drill hole G-1.
- Th** The  $K_d$  values are taken from Thomas (1987) from experiments using crushed tuff recovered from drill hole G-1.
- Sn** The  $K_d$  values are taken from Thomas (1987) from experiments using crushed tuff recovered from drill hole G-1.

The  $K_d$  in the fractures is assumed to be zero, because of the conceptualization that flow will be fast relative to the rates of the sorption reactions. This is the same approach as proposed in DOE's 1988 SCP.

Table B-6 presents the distributions and the ranges used for representing the hydrologic parameters of the ground-water pathway. Table B-7 presents the  $K_d$  values used for each of the elements and hydrogeologic units used in the analysis. Section 4.2.3 and Appendix A provide additional information on the approaches and sources of information used to derive the various hydrologic and transport parameters used in the IPA Phase 2 analysis.

### B-3 References

- Barnard, R.W. and H.A. Dockery (eds.), "Technical Summary of the Performance Assessment Computational Exercises for 1990 (PACE-90)—Volume 1: 'Nominal Configuration' Hydrogeologic Parameters and Computational Results," Sandia National Laboratories, SAND90-2726, June 1992. [Prepared for the U.S. Department of Energy.]
- Bentley, C.B., J.H. Robison, and R.W. Spengler, "Geohydrologic Data for Test Well USW H-5, Yucca Mountain Area, Nye County, Nevada," U.S. Geological Survey, Open File Report 83-853, 1983.
- Bish, D.L., and D.T. Vaniman, "Mineralogic Summary of Yucca Mountain, Nevada," Los Alamos, New Mexico, Los Alamos National Laboratory, LA-10543-MS, October 1985.
- Codell, R.B., *et al.*, "Initial Demonstration of the NRC's Capability to Conduct a Performance Assessment for a High-Level Waste Repository," U.S. Nuclear Regulatory Commission, NUREG-1327, May 1992.
- Craig, R.W., *et al.*, "Geohydrologic Data for Test Well USW H-6, Yucca Mountain Area, Nye County, Nevada," U.S. Geological Survey, Open File Report 83-856, 1983.
- Dudley, A.L., *et al.*, "Total System Performance Assessment Code (TOSPAC), Volume 1: Physical and Mathematical Bases," Albuquerque, New Mexico, Sandia National Laboratories, SAND85-0002, December 1988.
- Klavetter, E.A. and R.R. Peters, "Fluid Flow in a Fractured Rock Mass," Albuquerque, New Mexico, Sandia National Laboratories, SAND85-0855, March 1986.
- Meijer, A., "Yucca Mountain Project Far-Field Sorption Studies and Data Needs," Los Alamos, New Mexico, Los Alamos National Laboratory, LA-11671-MS, March 1990. [Prepared for the U.S. Department of Energy.]
- Nitao, J.J. and T.A. Buscheck, "Infiltration of a Liquid Front in an Unsaturated, Fractured Porous Media," *Water Resources Research*, 27(8):2099-2112 [1991].
- Peters, R.R., *et al.*, "Fracture and Matrix Hydrologic Characteristics of Tuffaceous Materials from

Yucca Mountain, Nye County, Nevada," Albuquerque, New Mexico, Sandia National Laboratories, SAND84-1471, December 1984.

Pruess, K., J.S.Y. Wang, and Y.W. Tsang, "On Thermohydrologic Conditions Near High-Level Nuclear Wastes Emplaced in Partially Saturated Fractured Tuff 1. Simulation Studies With Explicit Consideration of Fracture Effects," *Water Resources Research*, 26(6):1235-1248 [1990].

Scott, R.B. and J. Bonk, "Preliminary Geologic Map of Yucca Mountain, Nye County, Nevada, with Geologic Sections," U.S. Geological Survey, Open File Report 84-494, 1984.

Thomas, K., "Summary of Sorption Measurements Performed with Yucca Mountain, Nevada, Tuff Samples and Water from Well J-13," Los Alamos, New Mexico, Los Alamos National Laboratory, LA-10960-MS, March 1987.

Tsang, Y.W. and K. Pruess, "A Study of Thermally Induced Convection Near a High-Level Nuclear Waste Repository in Partially Saturated Fractured Tuff," *Water Resources Research*, 23(10):1958-1966 [1987].

U.S. Department of Energy, "Site Characterization Plan Overview, Yucca Mountain Site, Nevada Research and Development Area, Nevada," Office of Civilian Radioactive Waste Management, DOE/RW-0198, December 1988.

Table B-6 Hydrogeologic parameteric values and ranges used for the ground-water pathway

<i>Distribution</i>	<i>Range</i>		<i>Description</i>
<b><i>Porosity of Matrix</i></b>			
uniform	.06 - .16		Topopah Spring, welded
uniform	.33 - .56		Calico Hills, non-welded vitric
uniform	.20 - .33		Calico Hills, non-welded zeolitic
uniform	.24 - .40		Prow Pass, welded
uniform	.18 - .30		Upper and Middle Crater Flat, non-welded
uniform	.19 - .32		Bullfrog, welded
<b><i>Saturated Conductivity (mm/yr) and Permeability [m<sup>2</sup>] of Matrix</i></b>			
lognormal	0.11 - 36.	[3.6E-19 - 1.2E-18]	Topopah Spring, welded
lognormal	1.2E2 - 6.1E3	[3.9E-15 - 2.0E-14]	Calico Hills, non-welded vitric
lognormal	0.004 - .20	[1.3E-20 - 6.7E-19]	Calico Hills, non-welded zeolitic
lognormal	58. - 300.	[1.9E-16 - 9.6E-16]	Prow Pass, welded
lognormal	1.6 - 4.6	[5.1E-18 - 1.5E-17]	Upper Crater Flat, non-welded
lognormal	110. - 140.	[3.5E-16 - 4.4E-16]	Bullfrog, welded
lognormal	1.3 - 4.8	[4.1E-18 - 1.6E-17]	Middle Crater Flat, non-welded
<b><i>van Genuchten Alpha Parameter, for Matrix (1/m)</i></b>			
constant	.006		Topopah Spring, welded
constant	.016		Calico Hills, non-welded vitric
constant	.003		Calico Hills, non-welded zeolitic
constant	.014		Prow Pass, welded
constant	.004		Upper and Middle Crater Flat, non-welded
constant	.02		Bullfrog, welded
<b><i>van Genuchten Beta Parameter, for Matrix</i></b>			
uniform	1.4 - 2.2		Topopah Spring, welded
uniform	1.5 - 4.9		Calico Hills, non-welded vitric
uniform	1.2 - 3.3		Calico Hills, non-welded zeolitic
uniform	2.0 - 3.4		Prow Pass, welded
uniform	1.5 - 2.4		Upper and Middle Crater Flat, non-welded
uniform	2.3 - 4.2		Bullfrog, welded
<b><i>Grain Density for Matrix (kg/m<sup>3</sup>)</i></b>			
constant	2580		Topopah Spring, welded
constant	2370		Calico Hills, non-welded vitric
constant	2230		Calico Hills, non-welded zeolitic
constant	2590		Prow Pass, welded
constant	2270		Upper and Middle Crater Flat, non-welded
constant	2630		Bullfrog, welded

Table B-6 (continued)

<i>Distribution</i>	<i>Range</i>		<i>Description</i>
<b><i>Porosity of Fracture</i></b>			
constant	4.1E-5		Topopah Spring, welded
constant	4.6E-5		Calico Hills, non-welded vitric
constant	4.6E-5		Calico Hills, non-welded zeolitic
constant	1.3E-5		Prow Pass, welded
constant	4.6E-5		Upper and Middle Crater Flat, non-welded
constant	1.3E-5		Bullfrog, welded
<b><i>Saturated Conductivity (mm/yr) and Permeability [m<sup>2</sup>] of Fractures</i></b>			
lognormal	34. - 59.	[1.1E-16 - 1.9E-16]	Topopah Spring, welded
lognormal	170. - 370.	[5.6E-16 - 1.2E-15]	Calico Hills, non-welded vitric
lognormal	190. - 310.	[6.2E-16 - 9.9E-16]	Calico Hills, non-welded zeolitic
lognormal	12. - 25.	[3.9E-17 - 8.1E-17]	Prow Pass, welded
lognormal	210. - 300.	[6.7E-16 - 9.8E-16]	Upper and Middle Crater Flat, non-welded <sup>1</sup>
lognormal	15. - 20.	[4.9E-17 - 6.4E-17]	Bullfrog, welded <sup>2</sup>
<b><i>van Genuchten Alpha Parameter, for Fracture (1/m)</i></b>			
constant	1.3		Topopah Spring, welded
constant	1.3		Calico Hills, non-welded vitric
constant	1.3		Calico Hills, non-welded zeolitic
constant	1.3		Prow Pass, welded
constant	1.3		Upper and Middle Crater Flat, non-welded
constant	1.3		Bullfrog, welded
<b><i>van Genuchten Beta Parameter, for Fracture</i></b>			
uniform	3.2 - 5.3		Topopah Spring, welded
uniform	3.2 - 5.3		Calico Hills, non-welded vitric
uniform	3.2 - 5.3		Calico Hills, non-welded zeolitic
uniform	3.2 - 5.3		Prow Pass, welded
uniform	3.2 - 5.3		Upper and Middle Crater Flat, non-welded
uniform	3.2 - 5.3		Bullfrog, welded
<b><i>Infiltration Rate (mm/yr)</i></b>			
loguniform	0.1 - 5.0		base case
loguniform	5.0 - 10.		pluvial case
<b><i>Dispersivity (m)</i></b>			
normal	.3 - 30.		dispersivity for all units
<b><i>Discharge Area (m<sup>2</sup>)</i></b>			
uniform	3.75E4 - 3.75E5		discharge area for all regions

<sup>1</sup>Values are representative of Calico Hills.<sup>2</sup>Values are representative of Prow Pass.

**Table B-7 Matrix  $K_d$  Values (in cubic meters per kilogram) for Selected Radionuclides for the Hydrogeologic Units of Interest**  
 (Suggested ranges are assumed to +/- one order of magnitude, a loguniform distribution is assumed for all. Where no values are present, a  $K_d$  of zero is assumed. Values in parentheses are derived from Codell *et al.*, 1992.)

Element	Hydrogeologic Unit					
	Topopah Spring	Calico Hills		Prow Pass	Upper and Middle Crater Flat <sup>1</sup>	Bullfrog
		vitric	zeolitic			
Cm	(0.45)	(3.28)	(1.66)	(1.16)	(1.32)	(1.20)
Pu	0.17	0.17	0.066	0.13	0.053	0.094
U	0.0002	0.02	0.001	---	0.0008	0.002
Am	0.81	0.81	1.7	4.5	1.36	0.14
Np	0.0045	0.0045	0.0027	0.0051	0.0022	0.0051
Th	(0.048)	(0.34)	(0.17)	(0.12)	(0.14)	(0.13)
Ra	1.5	1.5	1.5	1.5	1.2	5.0
Pb	(0.0068)	(0.049)	(0.025)	(0.017)	(0.020)	(0.018)
Cs	0.36	0.24	22.0	2.2	17.6	3.2
I	---	---	---	---	---	---
Sn	(0.134)	(0.97)	(0.49)	(0.34)	(0.39)	(0.35)
Tc	0.00001	---	---	0.00017	---	0.0042
Zr	(0.0048)	(0.034)	(0.017)	(0.012)	(0.014)	(0.013)
Sr	0.08	0.034	8.9	0.45	7.1	0.28
Ni	(0.0037)	(0.027)	(0.014)	(0.009)	(0.011)	(0.010)
C	---	---	---	---	---	---
Se	0.0026	0.003	0.0045	0.0025	0.0036	0.013
Nb	---	---	---	---	---	---

<sup>1</sup>Values determined are based on Calico Hills zeolitic values, and allowances are made for differences in porosity and density.